

IN-1404



1658  
UC - 80

527  
12-22

MASTER

SEMISCALE BLOWDOWN AND EMERGENCY CORE COOLING  
(ECC) PROJECT TEST REPORT -- TESTS 803 THROUGH 820

H. W. Heiselmann D. J. Olson J. F. Whitbeck



IDAHO NUCLEAR CORPORATION  
NATIONAL REACTOR TESTING STATION  
IDAHO FALLS, IDAHO

Date Published—October 1970

U. S. ATOMIC ENERGY COMMISSION

DISTRIBUTION OF THIS DOCUMENT IS UNLIMITED

## **DISCLAIMER**

**This report was prepared as an account of work sponsored by an agency of the United States Government. Neither the United States Government nor any agency Thereof, nor any of their employees, makes any warranty, express or implied, or assumes any legal liability or responsibility for the accuracy, completeness, or usefulness of any information, apparatus, product, or process disclosed, or represents that its use would not infringe privately owned rights. Reference herein to any specific commercial product, process, or service by trade name, trademark, manufacturer, or otherwise does not necessarily constitute or imply its endorsement, recommendation, or favoring by the United States Government or any agency thereof. The views and opinions of authors expressed herein do not necessarily state or reflect those of the United States Government or any agency thereof.**

## **DISCLAIMER**

**Portions of this document may be illegible in electronic image products. Images are produced from the best available original document.**

Printed in the United States of America  
Available from  
Clearinghouse for Federal Scientific and Technical Information  
National Bureau of Standards, U. S. Department of Commerce  
Springfield, Virginia 22151  
Price: Printed Copy \$3.00; Microfiche \$0.65

#### LEGAL NOTICE

This report was prepared as an account of Government sponsored work. Neither the United States, nor the Commission, nor any person acting on behalf of the Commission:

A. Makes any warranty or representation, express or implied, with respect to the accuracy, completeness, or usefulness of the information contained in this report, or that the use of any information, apparatus, method, or process disclosed in this report may not infringe privately owned rights; or

B. Assumes any liabilities with respect to the use of, or for damages resulting from the use of any information, apparatus, method, or process disclosed in this report.

As used in the above, "person acting on behalf of the Commission" includes any employee or contractor of the Commission, or employee of such contractor, to the extent that such employee or contractor of the Commission, or employee of such contractor prepares, disseminates, or provides access to, any information pursuant to his employment or contract with the Commission, or his employment with such contractor.

IN-1404

Reactor Technology  
TID-4500

**LEGAL NOTICE**

This report was prepared as an account of work sponsored by the United States Government. Neither the United States nor the United States Atomic Energy Commission, nor any of their employees, nor any of their contractors, subcontractors, or their employees, makes any warranty, express or implied, or assumes any legal liability or responsibility for the accuracy, completeness or usefulness of any information, apparatus, product or process disclosed, or represents that its use would not infringe privately owned rights.

**SEMISCALE BLOWDOWN AND EMERGENCY CORE COOLING (ECC) PROJECT  
TEST REPORT -- TESTS 803 THROUGH 820**

BY

H. W. Heiselmann  
D. J. Olson  
J. F. Whitbeck

**IDAHO NUCLEAR CORPORATION**

A Jointly Owned Subsidiary of

AEROJET GENERAL CORPORATION  
ALLIED CHEMICAL CORPORATION  
PHILLIPS PETROLEUM COMPANY



Date Published — October 1970

**PREPARED FOR THE U.S. ATOMIC ENERGY COMMISSION  
IDAHO OPERATIONS OFFICE  
UNDER CONTRACT NO. AT(10-1)-1230**

**DISTRIBUTION OF THIS DOCUMENT IS UNLIMITED**

## ABSTRACT

This document reports a portion of the results of the Semiscale Blowdown and Emergency Core Cooling (ECC) Project tests conducted at the National Reactor Testing Station as part of the Water Reactor Safety Program of the Atomic Energy Commission. The purpose of the Semiscale Blowdown and Emergency Core Cooling Project is to provide the experimental data base required for development and assessment of analytical models for predicting the thermal hydraulic behavior occurring in a large PWR during a loss-of-coolant accident (LOCA).

The results reported in this document were obtained from decompression experiments on a circulating loop connected to a simulated reactor vessel (without internals) that constitute an extension of previous decompression tests with only a vessel. All tests were initiated from isothermal fluid conditions. Reported are pressure, temperature, strain, momentum flux, thrust, and limited flow and density information for various break sizes, configurations, and initial conditions. The amount of water remaining, blowdown time, and indications of the thermodynamic processes are also reported.

## SUMMARY

This report presents the results from 21 tests performed to investigate the hydraulic phenomena occurring during rapid decompression of a simulated PWR reactor system. The system for these tests (800 series), which included an empty vessel with one operating loop, represents an extension of previous systems with only a vessel (700 series). Phenomena of particular interest for model development included: decompression rates, hydraulic loading during subcooled and saturated blowdown, mass flow rates, phase separation, and water remaining in the system after blowdown. Fifteen of the tests were performed with a single-ended break configuration and six were performed with a double-ended break configuration. Break size, location, and configuration and initial fluid temperature were the test variables.

The addition of a loop to the vessel reduced the amount of water remaining in the system compared with the "vessel-only" tests to the extent that only the smallest breaks (2%) resulted in significant water remaining in the system. Results from tests in which different break configurations (both single-ended and double-ended) were used indicate that the reduction in residual water is independent of the blowdown configuration and is due solely to the addition of the primary loop. Blowdown time appears to be primarily a function of the ratio of initial fluid mass in the system to the break area. Thus, the addition of the primary loop and its components increased the blowdown time (compared to that of the vessel-only tests) according to the increase in system volume. Little difference in blowdown time was noted between top and bottom breaks.

The subcooled decompression was found to be almost isentropic; thus, an isentropic decompression from initial conditions could be used to estimate the pressure at which the saturated portion of the blowdown starts. The limited density data available indicate that the enthalpy at the vessel outlet nozzle increased for a top break. However, the enthalpy at the inlet nozzle is essentially constant for an inlet line rupture. This difference is attributed to phase separation; however, insufficient data are available for further evaluation.

The subcooled decompression for the semiscale loop causes substantial pressure differences across loop components such as the steam generator. Component loads during the saturated portion of blowdown result primarily from thermal expansion and thrust forces.

## CONTENTS

ABSTRACT .....	ii
SUMMARY .....	iii
I. INTRODUCTION .....	1
II. OBJECTIVES .....	2
III. EXPERIMENTAL APPARATUS AND OPERATION .....	3
1. TEST APPARATUS .....	3
2. TEST PROCEDURE .....	6
IV. INITIAL TEST CONDITIONS AND VARIABLES .....	7
V. EVALUATION OF TEST RESULTS .....	10
1. BLOWDOWN TIME .....	10
2. WATER REMAINING IN THE SYSTEM AFTER BLOWDOWN .....	11
3. FLUID DEPRESSURIZATION .....	13
4. FLUID BEHAVIOR .....	18
4.1 Stagnation Locations .....	18
4.2 Flow Rates .....	20
5. THERMODYNAMIC PROCESS .....	24
6. THRUST .....	30
7. PIPING STRAINS .....	33
VI. CONCLUSIONS .....	34
VII. REFERENCES .....	36
APPENDIX A -- DESCRIPTION OF THE FACILITY AND THE DATA ACQUISITION AND PROCESSING SYS- TEM FOR TESTS 803 THROUGH 820 OF THE SEMISCALE BLOWDOWN AND EMERGENCY CORE COOLING (ECC) PROJECT .....	37
A- I. INTRODUCTION .....	39
A- II. TEST CONFIGURATION .....	40
1. SYSTEM LAYOUT .....	40
2. SUSPENSION SYSTEM .....	43
3. STEAM GENERATOR .....	46

4. PRIMARY COOLANT PUMP .....	48
5. VESSEL .....	48
6. BLOWDOWN NOZZLE .....	51
7. PRESSURIZER .....	53
 A-III. SYSTEM HYDRAULIC PARAMETERS .....	 54
1. PRESSURE DROP .....	54
2. SYSTEM VOLUME DISTRIBUTION .....	54
 A-IV. DATA ACQUISITION AND PROCESSING SYSTEM .....	 56
1. DETECTORS .....	56
2. DETECTOR PATCH FACILITIES .....	56
3. SIGNAL CONDITIONING .....	57
4. DATA RECORDING .....	57
5. DATA PROCESSING .....	58
 APPENDIX B -- SEMISCALE DATA -- 800 SERIES TESTS 803 THROUGH 820 .....	 59
 B- I. INTRODUCTION .....	 61
 B- II. DISCUSSION OF DATA .....	 63
1. PRESSURE .....	63
2. TEMPERATURE .....	64
3. DENSITY .....	64
4. THRUST .....	64
5. MOMENTUM FLUX AND FLOW RATE .....	65
 B-III. PRESENTATION OF DATA .....	 66

## FIGURES

1. Semiscale single-ended break configuration .....	4
2. Semiscale double-ended break configuration .....	5
3. Blowdown time versus system fluid weight-to-break-area ratio .....	11

4. Residual water in vessel for various system configurations and break sizes . . . . .	12
5. Subcooled decompression pressures, 10% break . . . . .	14
6. Subcooled decompression pressures, 100% break . . . . .	14
7. Pressure, temperature, and strain during saturated blowdown for a 10% top break . . . . .	15
8. Comparison of pressure, temperature, and strain at the vessel outlet nozzle for various size top breaks and an initial coolant temperature of 584°F. . . . .	16
9. Comparison of pressure, temperature, and strain at the vessel outlet nozzle for various size top breaks and an initial coolant temperature of 540°F. . . . .	17
10. System flow rates during Test 819 for a top double-ended break of 10% total break area . . . . .	21
11. System flow rates during Test 819-2 for a top double-ended break of 30% total break area . . . . .	22
12. System flow rates during Test 817 for a single-ended bottom blowdown of 100% total break area . . . . .	23
13. Mass velocity as a function of vessel pressure. . . . .	24
14. Thermodynamic process of the subcooled decompression, initial temperature of 540°F . . . . .	25
15. Thermodynamic process of the subcooled decompression, initial temperature of 584°F . . . . .	26
16. Comparison of fluid state at vessel outlet nozzle for various size top breaks . . . . .	27
17. Comparison of fluid state at two locations for a 100% bottom break . . . . .	28
18. Comparison of reactor vessel outlet and hot leg fluid state during a 30% double-ended top break . . . . .	28
19. Comparison of reactor vessel outlet and hot leg fluid state during a 10% double-ended top break . . . . .	29
20. Comparison of reactor vessel outlet nozzle and hot leg fluid state during a 200% double-ended top break . . . . .	29
21. Thrust at the start of saturated blowdown for various break sizes . . . . .	31

22. Comparison of calculated and measured thrust for Test 818-1 . . . . .	32
A-1. Single-loop semiscale configuration . . . . .	41
A-2. Double-ended break configuration . . . . .	42
A-3. Semiscale vessel mounting . . . . .	44
A-4. Pipe hanger locations -- plan . . . . .	45
A-5. Pipe hanger locations -- elevation . . . . .	46
A-6. Steam generator . . . . .	47
A-7. Vessel . . . . .	49
A-8. Single-loop semiscale vessel . . . . .	50
A-9. Blowdown nozzle . . . . .	52

#### TABLES

I. Initial Test Conditions for Tests 801 Through 820 . . . . .	8
II. Thermocouple Temperature Breakaway Sequence . . . . .	19
III. Comparison of Calculated and Measured Maximum Circumferential Strains . . . . .	33
A-I. Pressure Drop Across Semiscale Components . . . . .	54
A-II. Semiscale System Volume Distribution . . . . .	55
B-I. Tabulation of Data . . . . .	62

**SEMISCALE BLOWDOWN AND EMERGENCY CORE COOLING (ECC)**  
**PROJECT TEST REPORT -- TEST 803 THROUGH 820**

**I. INTRODUCTION**

The Semiscale Blowdown and Emergency Core Cooling (ECC) Project[1] is an experimental project to investigate the hydraulic, thermodynamic, and mechanical behavior of a pressurized water reactor (PWR) system during a loss-of-coolant accident (LOCA). Specifically, the purpose of the project is to obtain experimental data for use in assessing the capability of analytical models to predict the response of the semiscale system to a simulated accident. The models, if experimentally verified, may be used with greater confidence and understanding to evaluate the LOCA for a large pressurized water reactor.

Previous investigations in the semiscale blowdown project were: (a) the 500 test series performed with a Bettis Flask,(b) the 600 series with a modified Bettis Flask, and (c) the 700 series in the LOFT semiscale vessel. These blowdown tests were primarily intended to provide subcooled and saturated blowdown information with the simplest possible systems[2].

The 800 test series is a series of experiments with an increasingly complex test configuration. For the first group of tests in this series (Tests 801 through 820), a piping loop containing a circulating pump, pressurizer, and steam generator has been added to connect the vessel inlet and outlet nozzles. The data from this group of tests are contained in this report. In subsequent tests of the 800 series, an electrically heated core will be installed in the reactor vessel, and emergency core cooling will be simulated.

## II. OBJECTIVES

The initial 800 series tests were the first tests with an operating primary loop and were conducted from an initially isothermal fluid condition.

The objectives for these isothermal tests were to:

- (1) Obtain reference information on system and coolant response to pipe ruptures of varying size under test conditions that are relatively uncomplicated in comparison to those planned for future tests
- (2) Obtain pressure data throughout the loop for the subcooled portion of blowdown
- (3) Determine the effect of initial coolant circulation on blowdown behavior
- (4) Determine whether a double-ended break geometry significantly affects the amount of water remaining
- (5) Determine the thrust loads developed during blowdown
- (6) Obtain an indication of strains induced in the piping as a result of decompression and cooling during blowdown

### III. EXPERIMENTAL APPARATUS AND OPERATION

The following section describes the experimental hardware and the test procedure.

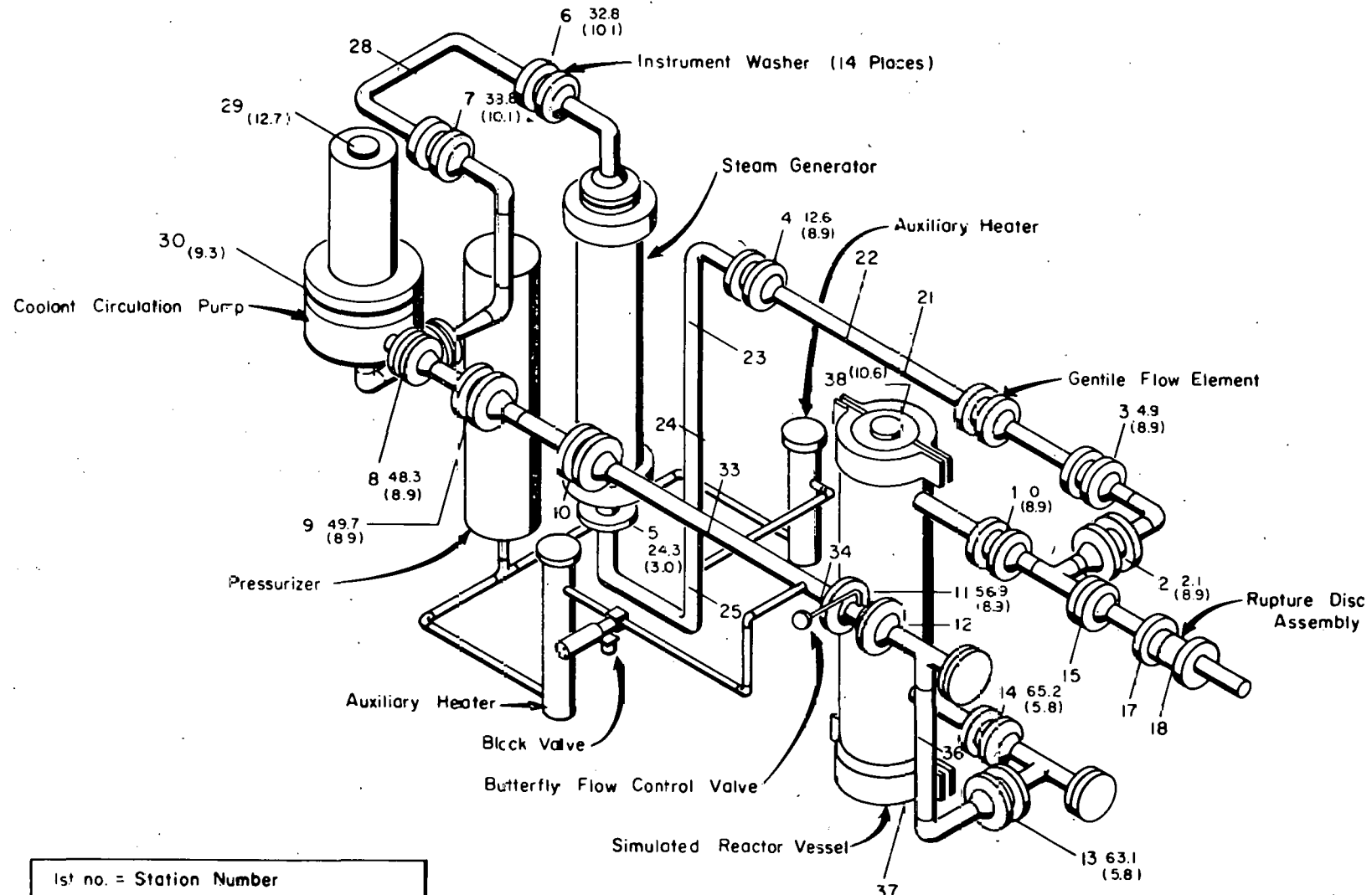
#### 1. TEST APPARATUS

The test equipment used for these experiments consists of a simulated single-loop reactor system containing a reactor vessel (without internals), steam generator, pump, control valve, and piping. An isometric drawing of the basic system is shown in Figure 1. This configuration was used for Tests 803 through 817. It was then modified to the configuration shown in Figure 2 to provide a double-ended break. This arrangement was used for Tests 818 through 820-1[a].

A more detailed description of the system, providing such features as nodal volumes, pressure drops, and pump characteristics may be found in Appendix A. A brief description of the instrumentation system and data processing equipment is also provided in Appendix A.

---

[a] In those cases in which a test was repeated, the repeated tests are designated by a numeral following the base test number. For example, Tests 818-1 and 818-2 are the first and second repeats of Test 818.



1st no. = Station Number  
2nd no. = Distance from Station 1 (feet)  
3rd no. = ( ) Elevation (feet)

INC = A = 14619

Fig. 1 Semiscale single-ended break configuration.

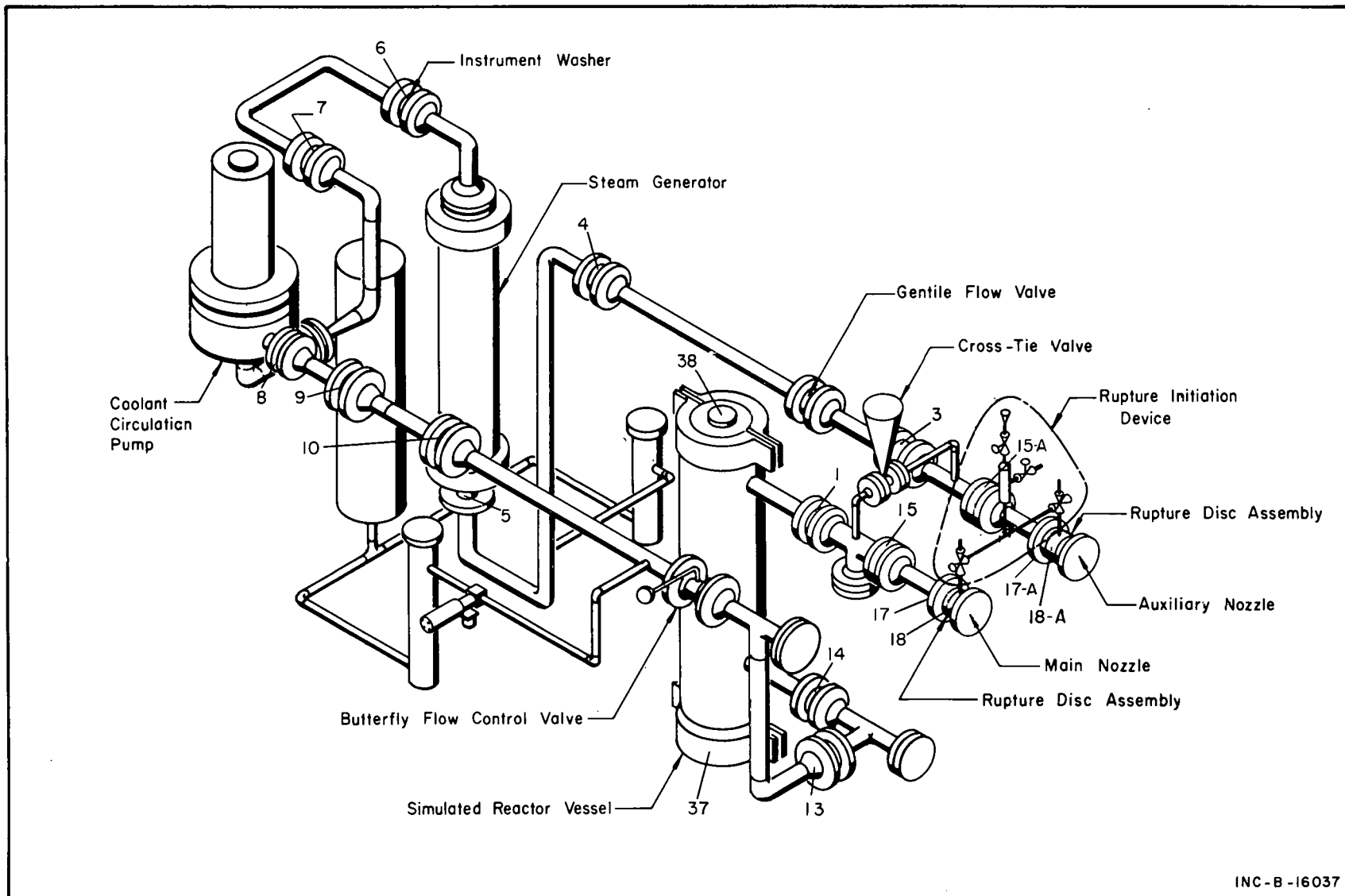


Fig. 2 Semiscale double-ended break configuration.

## 2. TEST PROCEDURE

The test procedure consisted of filling the system with demineralized water and heating the system to the desired test temperature by use of the auxiliary heaters. Coolant circulation through the auxiliary heaters and around the loop was provided by the coolant circulation pump. The pressurizer heaters were used to maintain system pressure at the desired value. The system flow rate was set at about 330 gal/min for all tests by the control valve. After the test temperature and pressure were obtained the auxiliary heaters were shut off and the block valve in the heater circulation line was closed leaving the pressurizer connected only to the hot leg. All single-ended break tests (Tests 803 through 817) were initiated by overpressurizing the cavity between the two rupture discs (Figure 9, Appendix A). The pump was shut off 0.5 sec after rupture by a signal from a breakwire placed across the rupture disc.

A different procedure was used in the double-ended break series. The cross-tie valve just upstream from the two break nozzles in Figure 2 was open during warmup to permit circulation of coolant around the system. Prior to blowdown this valve was closed and the primary pump was stopped. Hence all tests with this configuration were initiated when the coolant was at static conditions. Rupture was achieved by simultaneously venting the cavity between each set of rupture discs.

#### IV. INITIAL TEST CONDITIONS AND VARIABLES

Twenty-three tests were performed: 17 with a single-ended break configuration (Figure 1) and 6 with the double-ended break configuration (Figure 2). In the first two tests with a single-ended break configuration no data were obtained because of premature rupture and leakage. Table I lists the total number of tests and the conditions from which they were initiated. All tests were initiated at a nominal system pressure of 2300 psig. The variables consisted of break size, break location, initial coolant temperature, number of break locations, and initial flow rate.

A double-ended break was not achieved for all tests in the double-ended break series because simultaneous venting of the cavities between the rupture discs was not achieved. Three attempts were required before simultaneous [a] ruptures were achieved in both rupture assemblies for a double-ended break test. The first successful simultaneous ruptures were achieved in Test 818-2. The previous attempts (Tests 818 and 818-1) resulted in opening of only the line connected to the reactor vessel nozzle and hence resulted in a total break area of 15%. In Test 820, a rupture disc was installed only in the line from the steam generator to obtain data for a break initiated at that location. Comparative data on the three breaks (vessel nozzle, steam generator line, and the combination of both the vessel nozzle and the steam generator line) possible with the double-ended break configuration are thus provided by Tests 818-1, 820, and 818-2 for the 15% break case. Simultaneous rupture was achieved for the 10% test (Test 819) and the 200% test (Test 820-1) without difficulty.

---

[a] The ruptures of both assemblies were separated by no more than 4 msec.

TABLE I  
INITIAL TEST CONDITIONS FOR TESTS 801 THROUGH 820

Test	Break Location	Break Size [a] (%)	Initial Conditions			Comment
			Pressure (psig)	Temperature (°F)	Flow Rate (gal/min)	
801	Top	2	1900	540		Leak developed, no data.
802	Top	10				Premature rupture, no data.
803	Top	10	2320	540	323	
804	Top	2	2300	542	326	
805	Top	10	2300	540	330	
806	Top	30	2310	540	323	
807	Top	30	2300	545	0	
808	Top	100	2290	525	324	
809	Top	30	2305	585	327	
810	Top	100	2300	584	340	
811	Top	10	2315	584	352	
812	Top	?	2300	581	321	
813	Top	30	2310	583	327	
814	Top	100	2300	582	327	
815	Top	10	2300	584	327	
816	Bottom	100	2290	584	321	
817	Bottom	100	2300	585	335	

TABLE I (Contd.)

INITIAL TEST CONDITIONS FOR TESTS 801 THROUGH 820

Test	Break Location	Break Size [a]	Initial Conditions			Comment
			Pressure (psig)	Temperature (°F)	Flow Rate (gal/min)	
818	Top	15	2290	582	0	Orifice on vessel nozzle and steam generator line 15% each. Steam generator line did not rupture.
818-1	Top	15	2310	585	0	
818-2	Top	30 (15 each)	2320	583	0	
819	Top	10 (5 each)	2280	583	0	
820	Top	15	2350	583	0	Rupture disc installed in steam generator line only.
820-1	Top	200 (100 each)	2250	588	0	

[a] The break size is expressed as a percent of the cross-sectional area of the five-inch double extra strong pipe ( $100\% = 0.09 \text{ ft}^2$ ). For double-ended breaks the combined break size is given with the size of each break in parentheses.

## V. EVALUATION OF TEST RESULTS

The results of 21 tests are summarized in this section. During these tests primary emphasis was directed toward obtaining information on the sub-cooled pressure relaxation around the loop, the fluid pressure-temperature conditions at various locations in the system, and the effect of primary coolant loop on the amount of water remaining in the vessel after the tests. For most tests, eight to ten pressure measurements and five to eight fluid temperature measurements were obtained. In addition to these measurements, measurements of piping strain, momentum flux, and thrust were obtained. Attempts to measure component acceleration and displacement were generally unsuccessful because the system had been designed for a high natural frequency and the resulting stiffness did not permit sufficient displacement for reliable measurements. Limited density measurements were available for the last eight tests, and thus flow rates could be calculated from momentum flux. Density measurements (in conjunction with temperature) also permit determination of the thermodynamic process at the measurement location.

The following subsections provide a general appraisal of the test results. Specific data, including break size, pressure, temperature, thrust, momentum flux, density, and flow are presented in Appendix B.

### 1. BLOWDOWN TIME

The previous test series (700 series) demonstrated that the blowdown time (time from rupture to zero nozzle pressure) is nearly a linear function of the ratio of system volume to break area. To provide a comparison with the previous test results that were obtained without a loop connected to the vessel, the blowdown time has been plotted as a function of the ratio of initial fluid weight to break area. The data shown in Figure 3 for the 800 series tests are for blowdown at two temperatures (540 and 584°F), for single- and double-ended break configurations, and for a break size ranging from 2 to 200% of the loop piping flow area. The end of blowdown was estimated by reviewing pressure, thrust, and drag disc data; however, the approximate time that the slope of the pressure trace reached zero was the primary means of establishing the blowdown time. The data scatter in Figure 3 is in part due to the inaccuracy in reading the point of zero slope. Comparison of the data from the 800 test series with that from the 700 test series in which the vessel volume and hence weight of initial fluid was slightly less than half of the volume and weight for the 800 test series shows the results to be in good agreement.

The blowdown time appears to deviate slightly from a linear relationship with the fluid weight-to-break-area ratio. However, a rough "rule of thumb" that can be obtained from Figure 3 is that the blowdown time in seconds is about 1/8 to 1/10 of the weight-to-break-area ratio (in the units shown on Figure 3). Thus, a large PWR that undergoes decompression due to a large break such that a fluid weight-to-break-area ratio of 425 lb/in.<sup>2</sup> results would be expected to have a blowdown time of about 42 to 52 seconds. For small breaks, on the order of 0.5 ft<sup>2</sup>, the blowdown time would be on the order of 12 minutes. This type of extrapolation presumes that the presence of a core does not alter the blowdown time significantly.

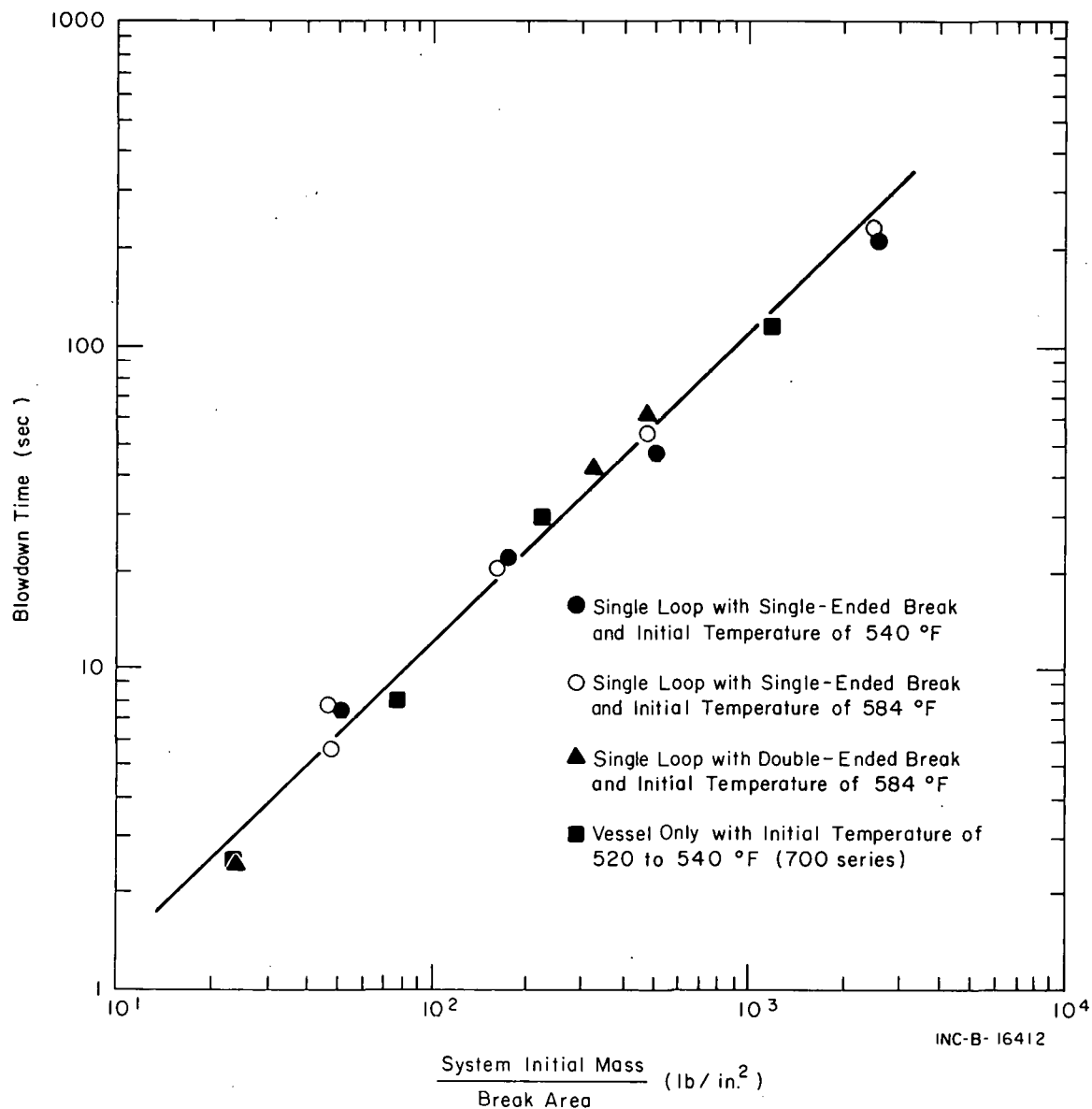


Fig. 3 Blowdown time versus system fluid weight-to-break-area ratio.

## 2. WATER REMAINING IN THE SYSTEM AFTER BLOWDOWN

Tests conducted with the Bettis Flask (500 and 600 series) and the reactor vessel without piping (700 series) showed that the amount of water remaining in the vessel was a function of break size and vessel internal geometry[2]. For those tests substantial amounts of fluid (up to 50% of the initial fluid) remained in the vessel (without internals) subjected to a top nozzle break. As evidenced in Figure 4, the current series of tests with a circulating loop attached to the vessel and a blowdown tee configuration has exhibited considerably different results. Only very small breaks (2% of pipe area) resulted

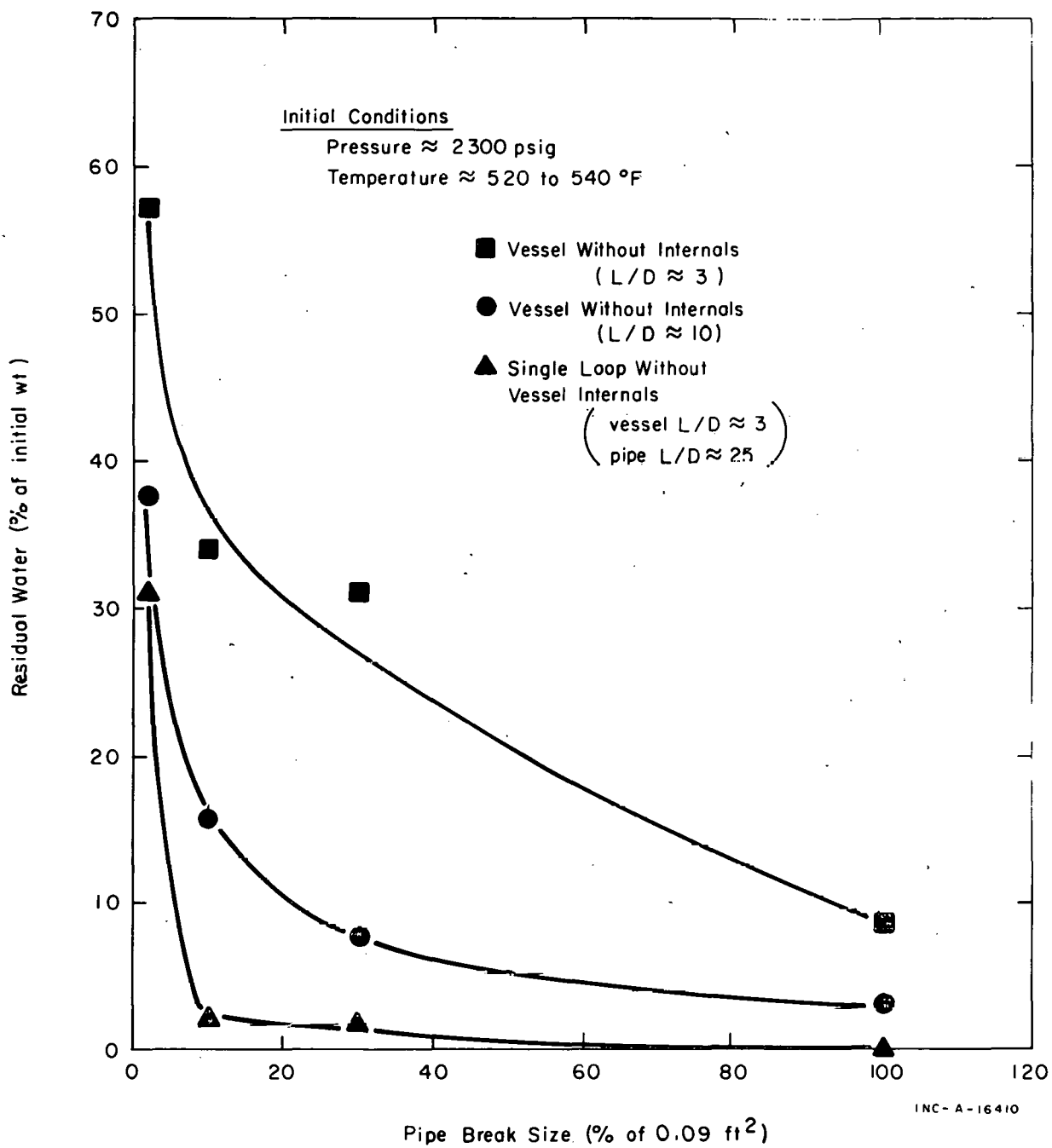


Fig. 4 Residual water in vessel for various system configurations and break sizes.

in significant residual water (25 to 32% of the initial amount). For break sizes of 10 and 30% the water remaining was usually less than 2% of the initial amount and no water remained for any of the 100% breaks.

A double-ended break configuration was installed (Tests 818 through 820-1) to determine whether flow from the vessel past the tee at the vessel outlet would result in fluid being drawn from the rest of the system. The only double-ended break test for which water remained was Test 819 (10%) in which about 2% of the initial amount was collected. The conclusion reached from the double-ended break tests is that the tee configuration does not influence the amount of

water remaining after blowdown and that the lack of water was due solely to the addition of the primary loop.

### 3. FLUID DEPRESSURIZATION

Following rupture, the pressure relaxes around the system until the fluid reaches the saturated fluid condition. This process is shown on Figures 5 and 6 for 10 and 100% top breaks, respectively. The initial drop in pressure at the vessel outlet is the result of the rupture disc yielding. This drop is followed immediately by the large drop due to rupture. The magnitude of the initial decompression wave is greatest for the larger break size. The wave is immediately dissipated upon entering the vessel and therefore does not appear at the vessel inlet. Similar damping occurs by the time the wave passes through the steam generator.

The time required for the decompression wave to reach other locations can be computed by assuming that the wave travels at sonic velocity (3480 ft/sec at 2300 psi and 540°F and 3100 ft/sec at 2300 psi and 584°F). Thus, the pressure wave noted at the vessel outlet nozzle is the result of yielding and rupture that occurred about 1.4 msec earlier. The decompression of the system at different times can produce large pressure differences across components as seen in Figures 5 and 6. For example, steam generators for large PWR's which have an average tube length of over 60 feet would be subjected to large differential pressures for a considerable time during the acoustic decompression period.

The saturated portion of blowdown starts at the end of the subcooled decompression and consists of the initial transition period during which the flow direction becomes established and the remaining period during which flow fluctuation is minor. Pressure and temperature data indicate that the fluid is at or very near saturation conditions throughout blowdown. (The agreement of the measured pressure and temperature with the saturation pressure and temperature is within the measurement capability.) Typical pressure and temperature behavior is shown in Figure 7. Saturation conditions are indicated and agreement of measured pressures with the saturation pressure obtained from fluid temperatures is within less than 50 psi. The deviations that occur toward the end of blowdown are the result of the sensitivity of the pressure detectors to the large temperature change that occurred.

The failure of certain temperatures (Figure 7) to decrease all the way to a final saturation condition of 205°F is assumed to be caused by a loss of flow (cooling) and by voiding in the vicinity of the detector so that the detector receives thermal radiation from the wall. Strain changes occurring at various system locations on the outside of the piping also are shown. The maximum strain change occurs well into the blowdown and is primarily thermal in origin. The eventual return toward initial strain values is due to temperature equilibration within the pipe.

A comparison of these three variables -- temperature, pressure, and strain at the reactor vessel outlet nozzle -- for various break sizes and an initial

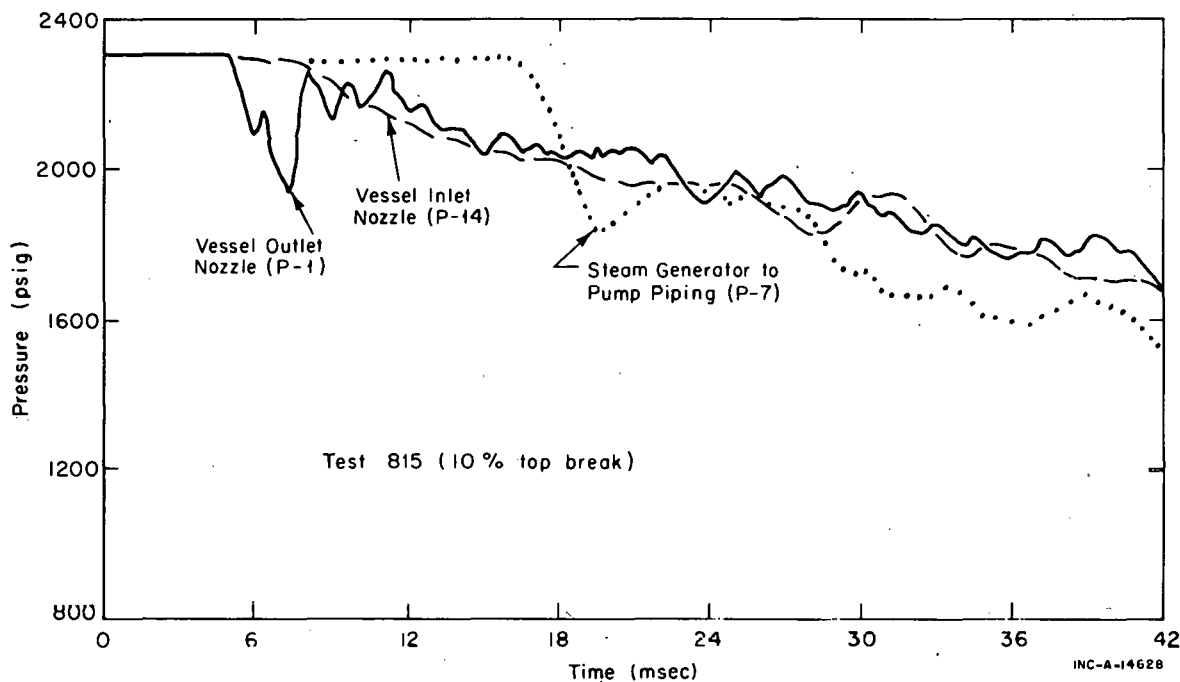


Fig. 5 Subcooled decompression pressures, 10% break.

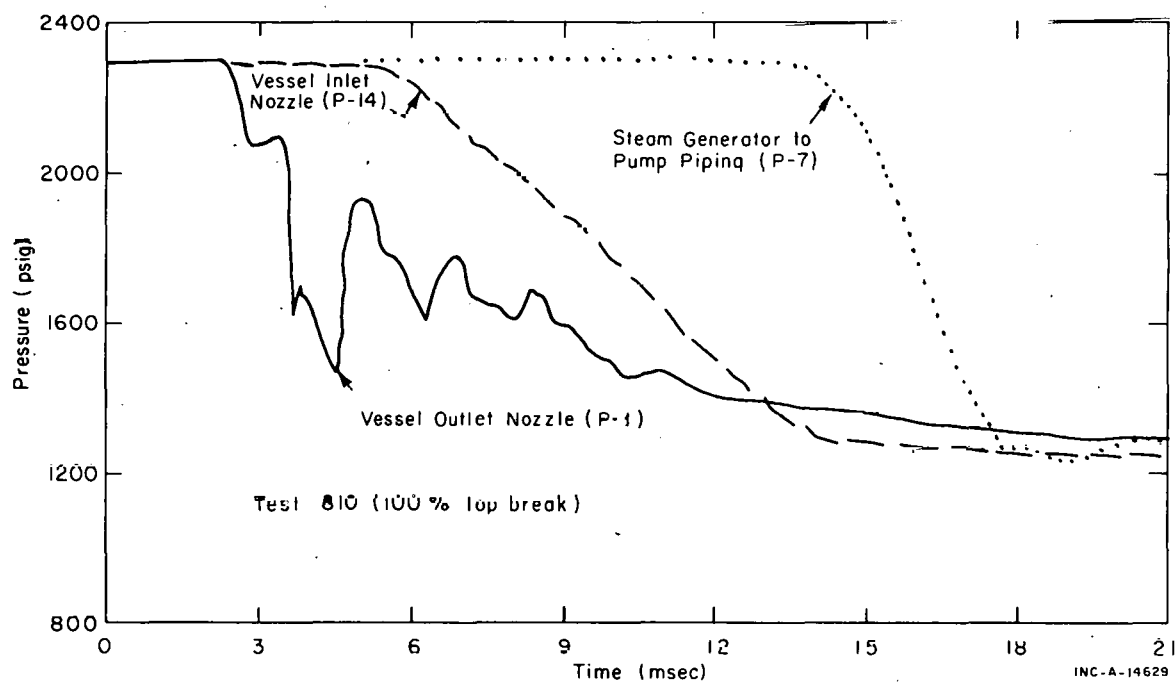


Fig. 6 Subcooled decompression pressures, 100% break.

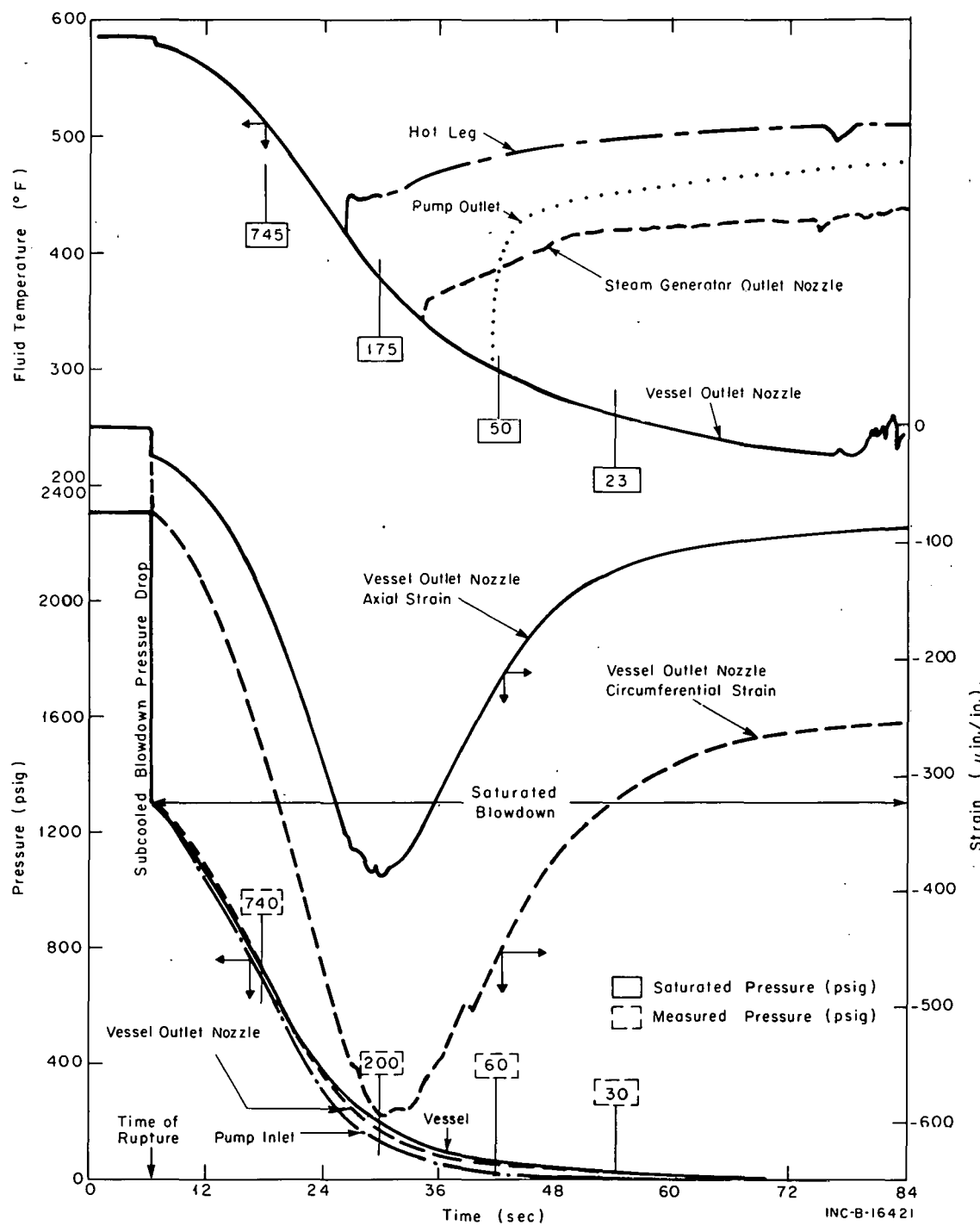


Fig. 7 Pressure, temperature, and strain during saturated blowdown for a 10% top break.

fluid temperature of 584°F is given in Figure 8. From this figure, the pressure at the end of subcooled blowdown is seen to be essentially independent of break size. The maximum piping circumferential strains (except for the 2% case) are also independent of break size. Figure 9 is a similar comparison for an initial temperature of 540°F. Comparison of Figures 8 and 9 shows the following: The temperature and strain behavior are nearly the same for both initial temperatures. The lower initial temperature is reflected in a lower pressure at the

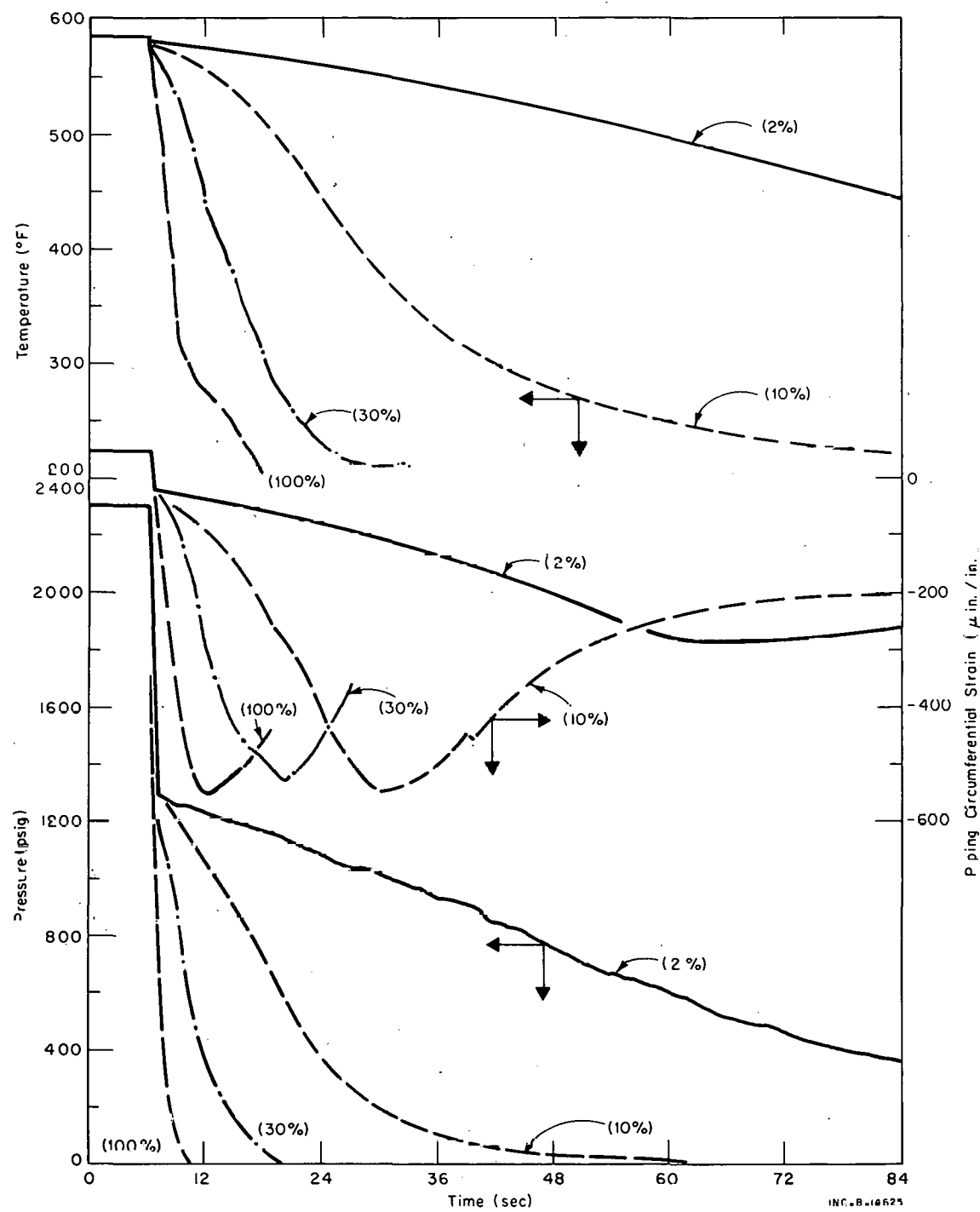


Fig. 8 Comparison of pressure, temperature, and strain at the vessel outlet nozzle for various size top breaks and an initial coolant temperature of 584°F.

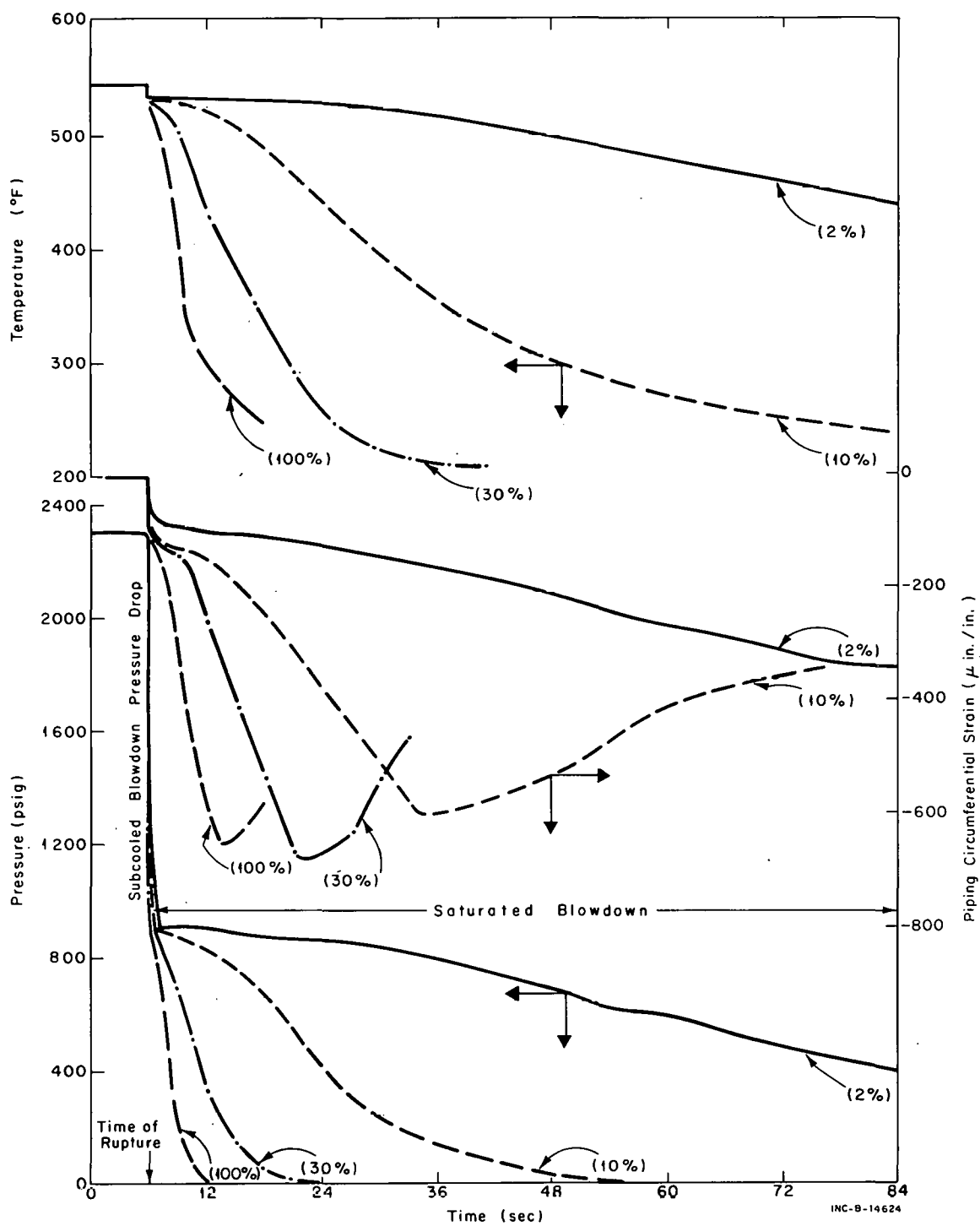


Fig. 9 Comparison of pressure, temperature, and strain at the vessel outlet nozzle for various size top breaks and an initial coolant temperature of 540°F.

end of subcooled blowdown. The pressure for the smaller breaks is maintained somewhat longer after the end of subcooled blowdown for lower initial temperatures; as a result, blowdown is approximately the same for both initial temperatures.

Two 100% bottom-break tests (Tests 816 and 817) were performed and the pressure and temperature at the vessel nozzles were compared with similar measurements obtained during a 100% top break test. No apparent difference was found in the pressure or temperature information between top and bottom break tests.

#### 4. FLUID BEHAVIOR

Fluid behavior is discussed in terms of stagnation locations and flow rate during blowdown.

##### 4.1 Stagnation Locations

Thermocouples measuring fluid temperature exhibit an erratic behavior or a rapid increase in temperature late in the blowdown as shown in Figure 7. This behavior, referred to as temperature breakaway, is believed to occur when the thermocouples are surrounded by a high quality mixture that permits the thermocouples to receive radiation from the high temperature wall and when insufficient flow is present to maintain the thermocouple at fluid temperature.

The sequence of temperature breakaway is given in Table II by station number. The sequence is that observed during the majority of the tests. The thermocouple at the vessel outlet nozzle did not normally indicate temperature breakaway until very late in the blowdown. The 10 and 30% break tests show a different sequence of breakaway than that for the 100% break tests and this behavior is independent of the break configuration. Two possible explanations of these data are:

- (1) Disregarding locations close to the break (because of higher void fraction) the stagnation point is near the point indicating the first breakaway and succeeding breakaways occur as the void region increases.
- (2) The high quality front recedes from the break indicating that the stations that exhibited breakaway later in the sequence are nearest the stagnation location.

TABLE II  
THERMOCOUPLE TEMPERATURE BREAKAWAY SEQUENCE

	<u>Break Size (%)</u>	<u>Order of Station<sup>[a]</sup></u>
Single-Ended Breaks	10	2 or 5, 6, 14, 15
	30	2 or 5, 15, 6, 9, 10
	100	9, 10 or 6, 5, 2
Double-Ended Breaks	10	3, 5, 9
	30	5, 6, 9
	200	10, 9, 6, 5

[a] From first to last.

The latter view is least likely in view of the sequence given for 100% break data and the fact that the temperature at Station 1 never shows a breakaway within the time that the data were recorded; however, it is supported by limited flow data for the smaller break sizes. In almost every case the thermocouples at the vessel inlet and outlet were the last to exhibit temperature breakaway indicating that the vessel is the last component to empty.

Initial water temperature for all tests was uniform throughout the system. Temperature uniformity (within measurement accuracy) was exhibited as temperatures decreased during blowdown for all except the 100% break tests in which a deviation as great as 25°F has been noted. The largest temperature difference during blowdown occurred across the control valve, which is the component providing the highest system resistance and largest pressure difference. In all cases in which the fluid temperature difference is apparent across the control valve, the temperature drop is in the same direction as the expected pressure drop (downstream toward vessel inlet).

Generally, the fluid between the pump and control valve exhibits the highest temperature throughout the 100% break tests, indicating that the general location of the stagnation point is between these two components. An exception was noted for the double-ended test (Test 820-1) in which the fluid temperature upstream from the pump (Station 6) was sometimes greater than that downstream from the pump (Station 9 or 10). In addition, a temperature drop across the steam generator in the direction from Station 6 to Station 5 existed throughout blowdown. Interpretation of data for this test indicates that the flow stagnation point was initially between the pump and control valve, then between the pump and steam generator, and finally again between the pump and control valve.

In summary, the primary flow stagnation point (as indicated by temperature breakaway) in the test system for the 100% breaks is between the pump and control valve. For the smaller break sizes the temperature data indicate that

the first determinable stagnation point is at or near the steam generator inlet. Other stagnation points may have existed in the system prior to the time indicated by the thermocouples.

#### 4.2 Flow Rates

Momentum flux ( $\rho v^2$ ) was measured during nearly all tests by drag discs. This quantity provided the only direct indication of flow from the system in tests prior to Test 816. For tests subsequent to Test 816, data from a single density detector were also available. Data from this detector were used in interpreting the drag disc data in terms of mass flow rates. Typical momentum flux data are provided in Appendix B.

The rate at which fluid passes from the system is the controlling variable in the isothermal blowdown tests. The flow data available provide information on critical flow at high mass velocities. Choking occurs at the exit plane or restricting orifice.

Flow rate as a function of time is given in Figures 10 and 11 for 10 and 30% breaks with the double-ended break configuration. In each case a larger flow oscillation was noted in the hot-leg line than at the vessel outlet and the flow rate was slightly higher in the hot leg throughout most of the test. The total mass ejected from each nozzle was calculated for the 10 and 30% break area tests. For both tests the division was about 35% through the vessel nozzle and the remainder through the hot leg. In terms of system volume this division corresponds to an average stagnation point between the control valve and the reactor vessel inlet and does not agree with the interpretation of the temperature data discussed in Section 4.1. Hot-leg flow data for the 200% break test are not available to provide a similar comparison.

The leak flow during the 100% bottom break test (Test 817) was determined by using the density data obtained at the inlet nozzle in conjunction with the data from the drag disc at Station 13 (the only density measurement obtained for this test was at the vessel inlet nozzle). The flows, computed on this basis and shown in Figure 12, show that 85% of the mass ejected passed through the vessel inlet nozzle indicating a flow division near the pump inlet. If the actual density in the cold leg was lower than at the vessel outlet, the division may have occurred in the cold leg as indicated by the temperature data.

The flow rate information given in Figures 10, 11, and 12 were computed from the data obtained from the drag disc and density detector. Numerical integration of the flow rate curves provided an estimate of the total mass ejected from the system. A comparison of these calculations with the 524 pounds of initial fluid results in the following errors: -17.6% for Test 819, -1.9% for Test 818-2, and +12% for Test 817.

Mass velocity at the exit plane or orifice as a function of reactor vessel pressure is compared in Figure 13 with the values predicted by Moody[3] for an ideal nozzle at the same values of stagnation pressure and enthalpy. For these comparisons critical flow is assumed to exist because the orifice pressure ratio is less than 0.25 over the range indicated. The ideal nozzle prediction when corrected by multiplying by the sharp-edged orifice discharge coefficient (0.62) is in close agreement with the test data obtained when an orifice was used to

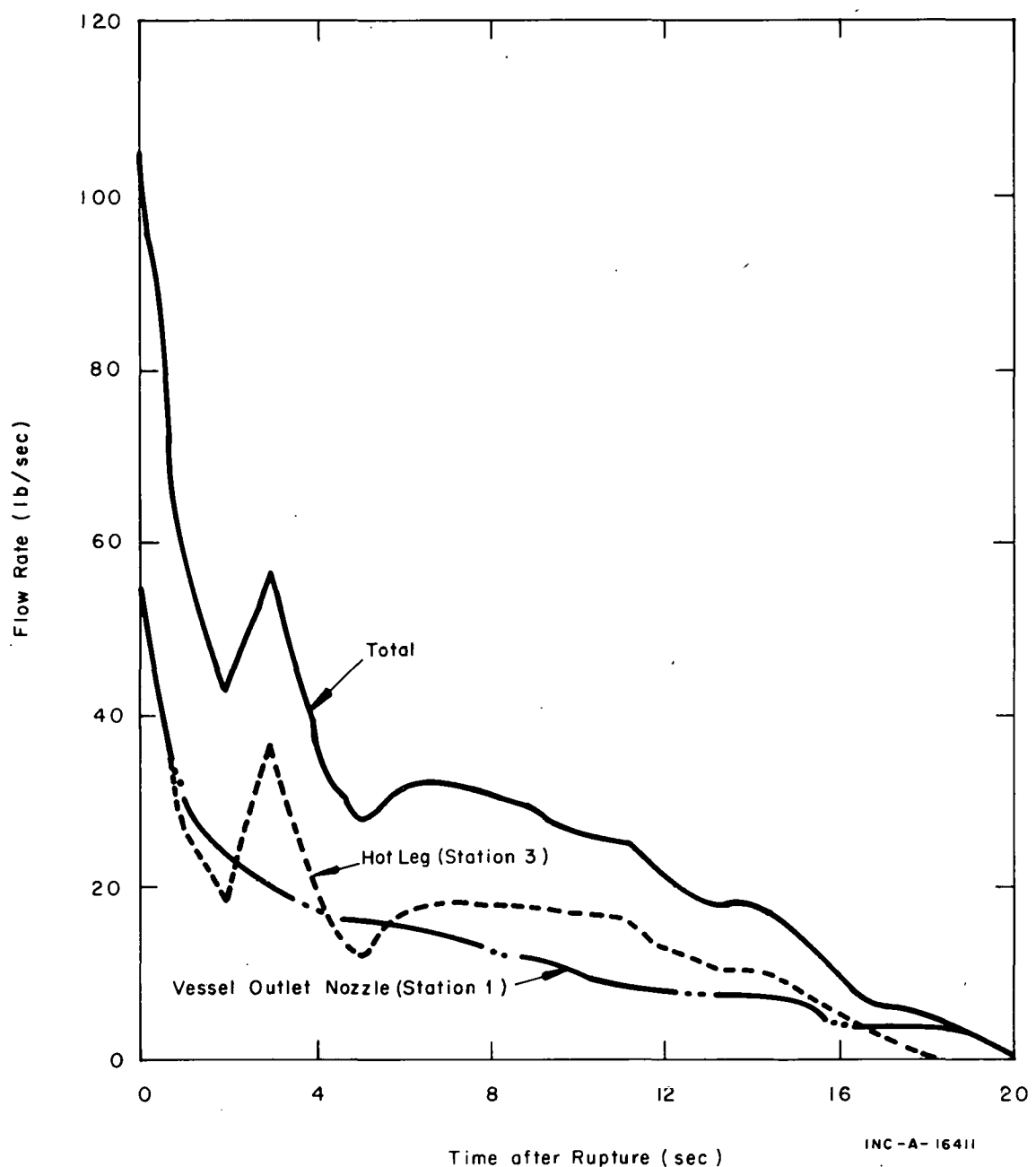


Fig. 10 System flow rates during Test 819 for a top double-ended break of 10% total break area.

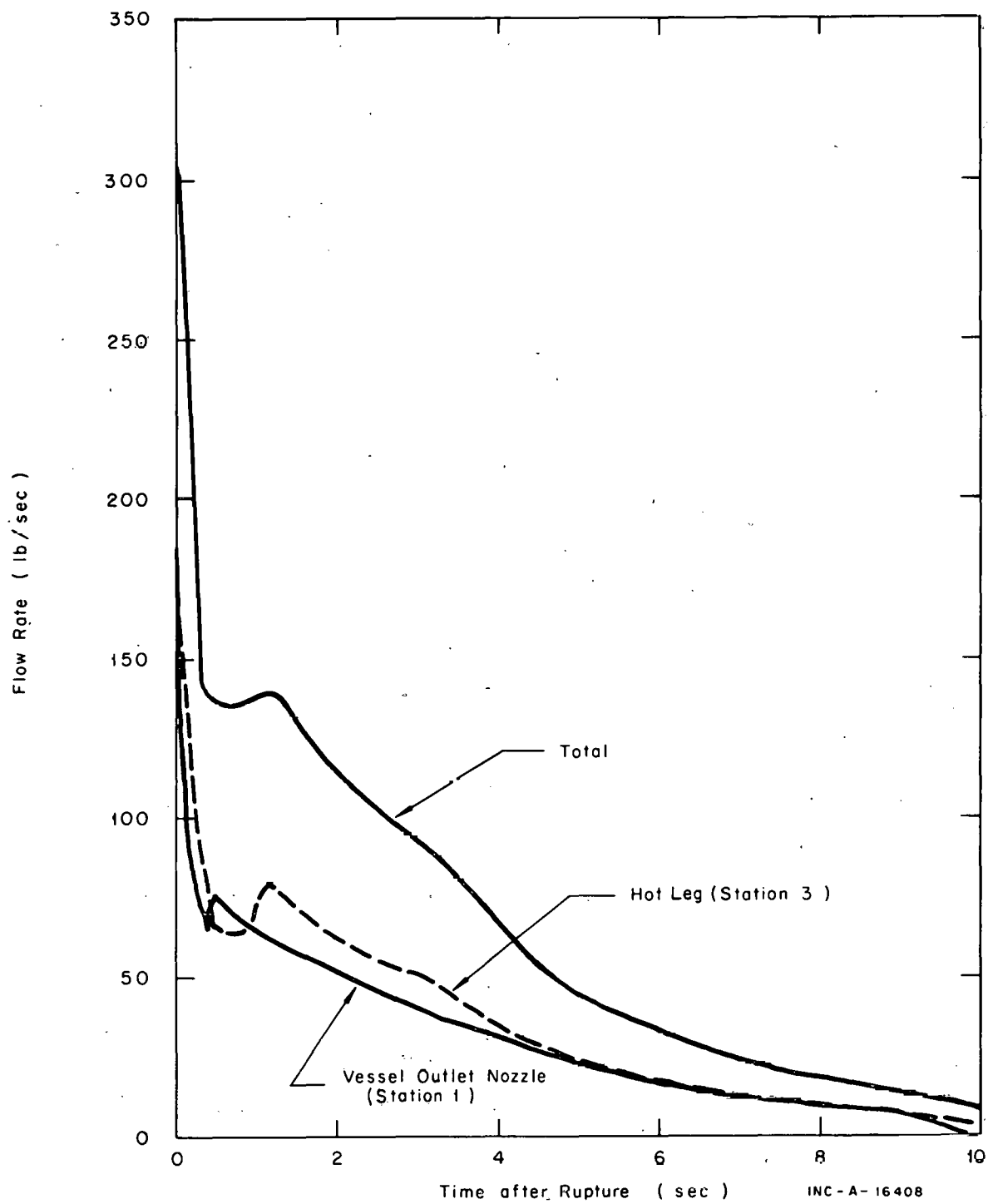


Fig. 11 System flow rates during Test 819-2 for a top double-ended break of 30% total break area.

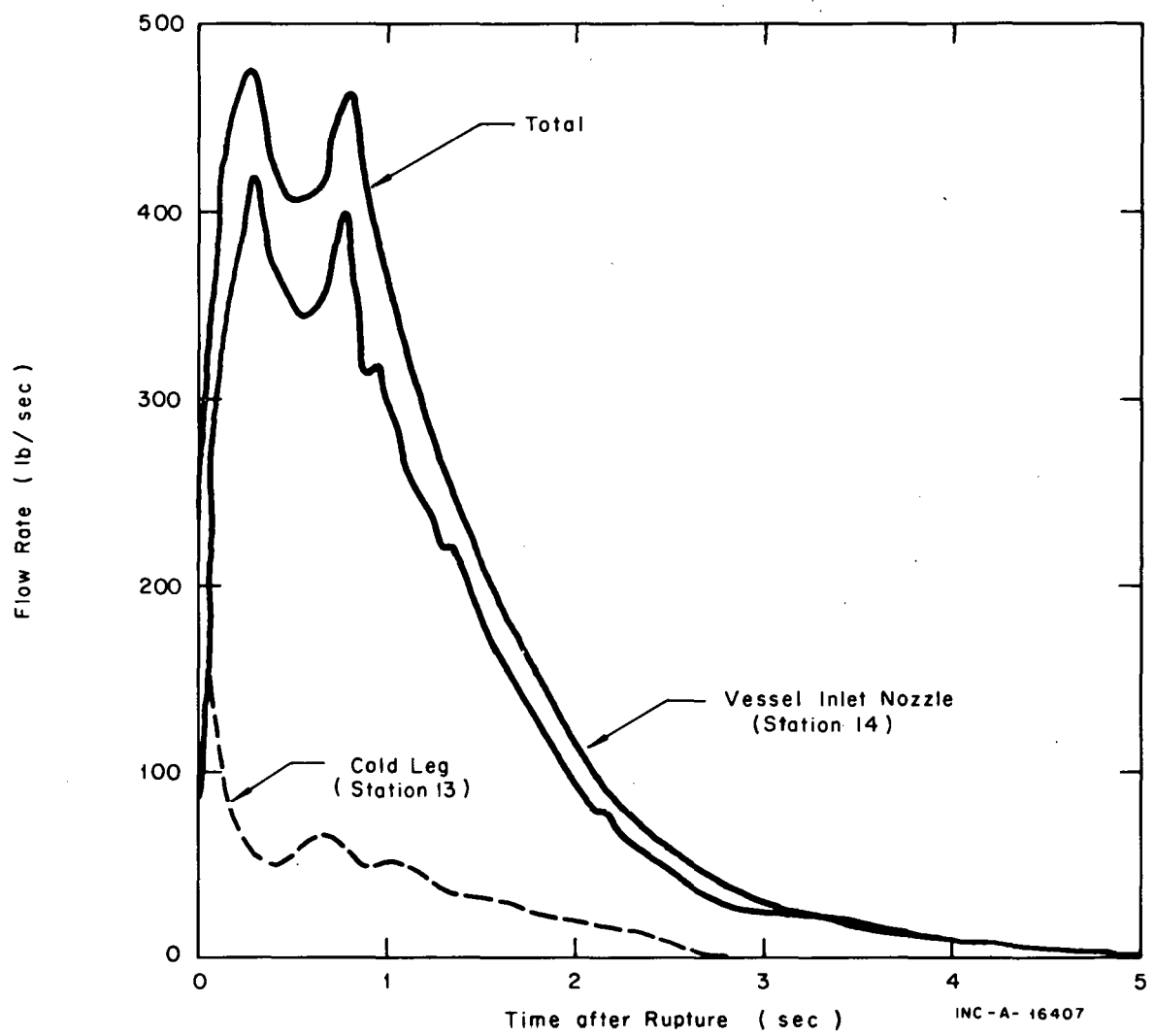


Fig. 12 System flow rates during Test 817 for a single-ended bottom blowdown of 100% total break area.

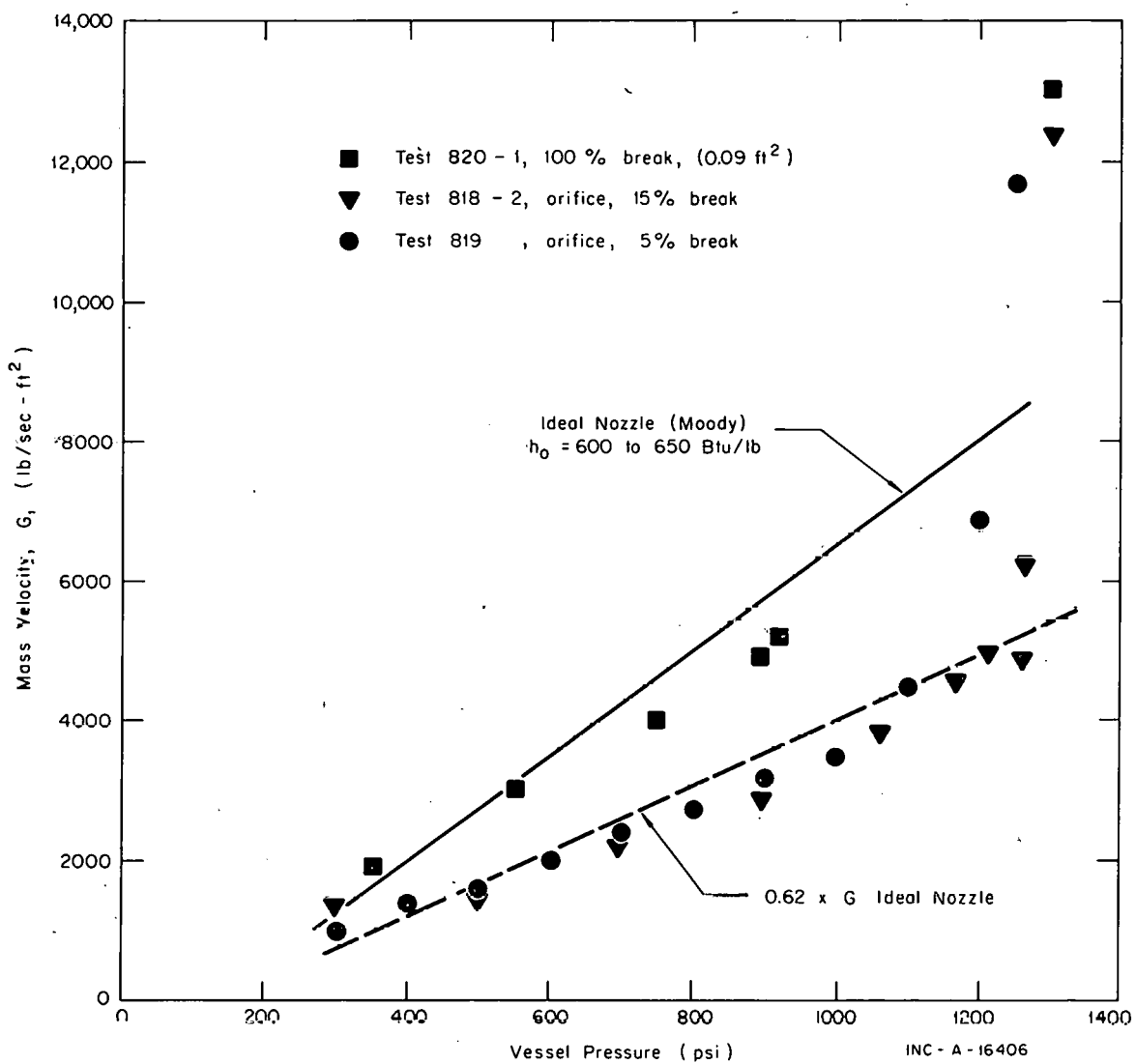


Fig. 13 MASS VELOCITY as a function of VESSEL PRESSURE.

limit the break area. Also shown in Figure 13 are the data obtained for a 100% break (Test 820-1) which produced flow much closer to the ideal nozzle flow.

The maximum break size (100%) resulted in the maximum initial mass velocity ( $G \sim 13,000$  lb/sec-ft $^2$ ); however, other tests with orifice sizes of 5 and 15% of the pipe area produced values almost as high. After the initial surge the mass velocity for all orificed flows dropped to a value of  $G \sim 5,000$  lb/sec-ft $^2$ .

## 5. THERMODYNAMIC PROCESS

In any process in which an exchange or transfer of energy occurs within a system, the system behavior may be viewed in terms of some of the conventional thermodynamic processes. The series of tests covered in this report was conducted without heat addition (no core installed) or heat removal from the fluid except between the fluid and system boundary material and thus provides

good reference information for comparison with future results from tests in which core heat is simulated.

The subcooled decompression process is nearly isentropic as can be seen by comparing the fluid temperature drop (about 6°F) and the final pressure at the end of the subcooled blowdown with values obtained from the assumed process. The processes are displayed in Figure 14 and 15 for initial temperatures of 540 and 584°F, respectively. By assuming isentropicity, the fluid state at the start of the saturated portion of blowdown can be determined.

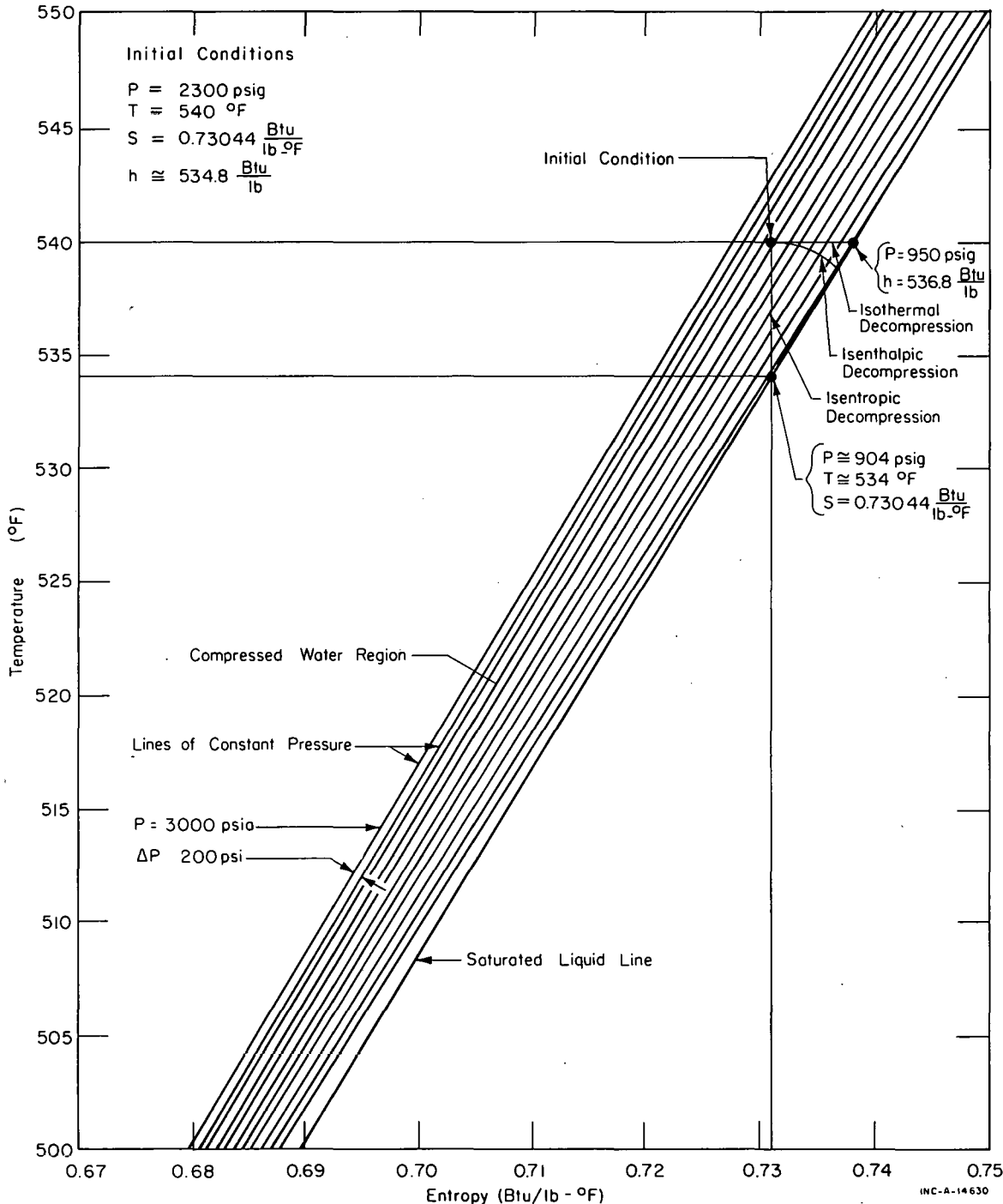


Fig. 14 Thermodynamic process of the subcooled decompression, initial temperature of 540°F.

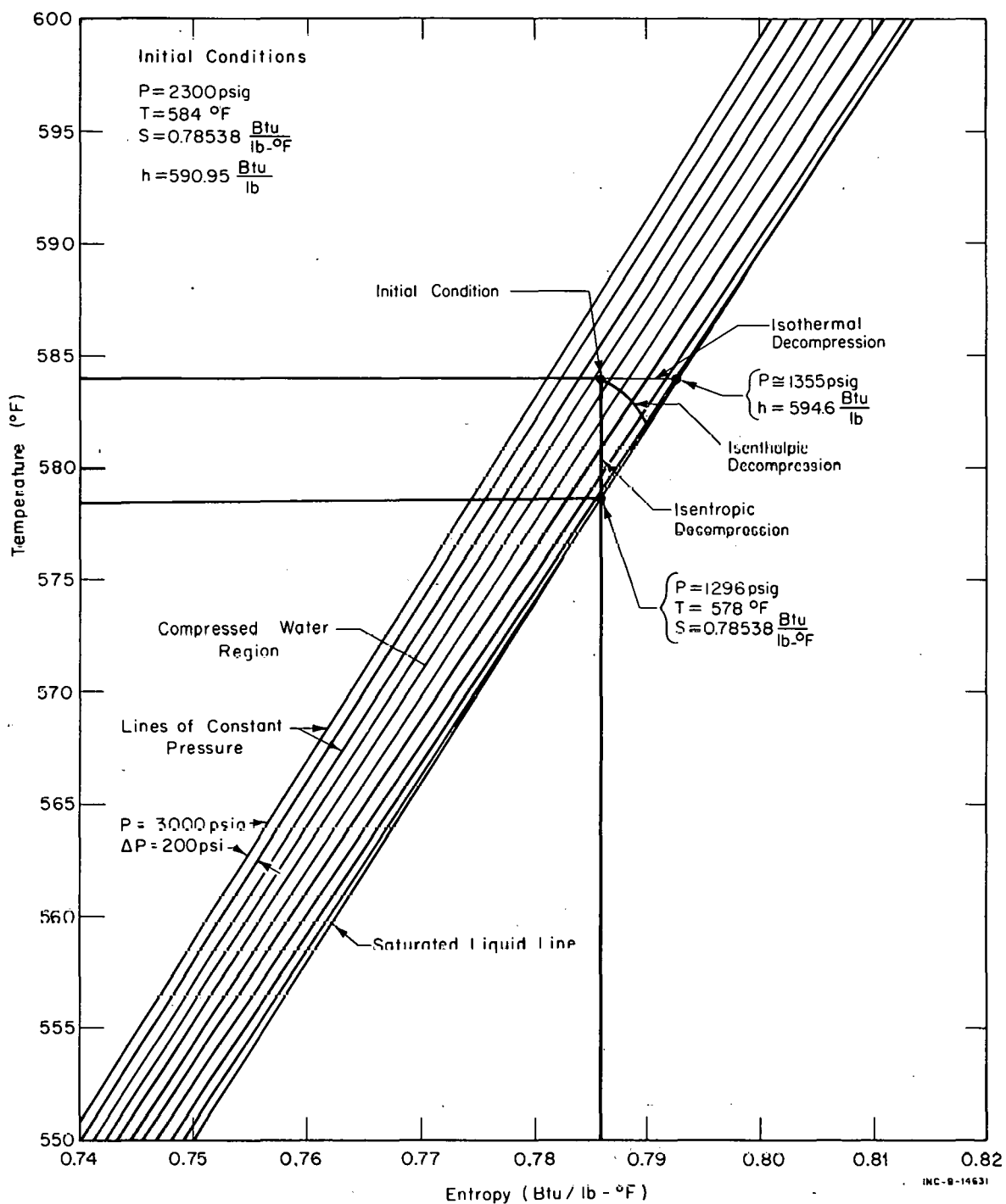


Fig. 15 Thermodynamic process of the subcooled decompression, initial temperature of 584°F.

The process evaluations during the saturated blowdown are limited to those locations where density was measured. Density was determined by gamma attenuation across the piping and hence is an average value. The majority of the density data are available only for the double-ended break series, and then only two measurements for each test were obtained, generally one at the reactor vessel outlet and one in the hot leg. For top breaks, the fluid at the vessel outlet nozzle initially followed an isenthalpic process, then increased in enthalpy. In contrast to this behavior, the fluid at the reactor inlet nozzle for

a bottom break followed an isenthalpic process throughout most of the blowdown. If the assumption is made that the fluid in the vessel during either the top or bottom blowdown remains at its initial enthalpy, the enthalpy increase noted at the reactor vessel outlet nozzle during a top break is attributable to phase separation, the quality at the outlet nozzle being about twice that in the vessel. Figure 16 indicates the process at the vessel outlet nozzle for different size top breaks.

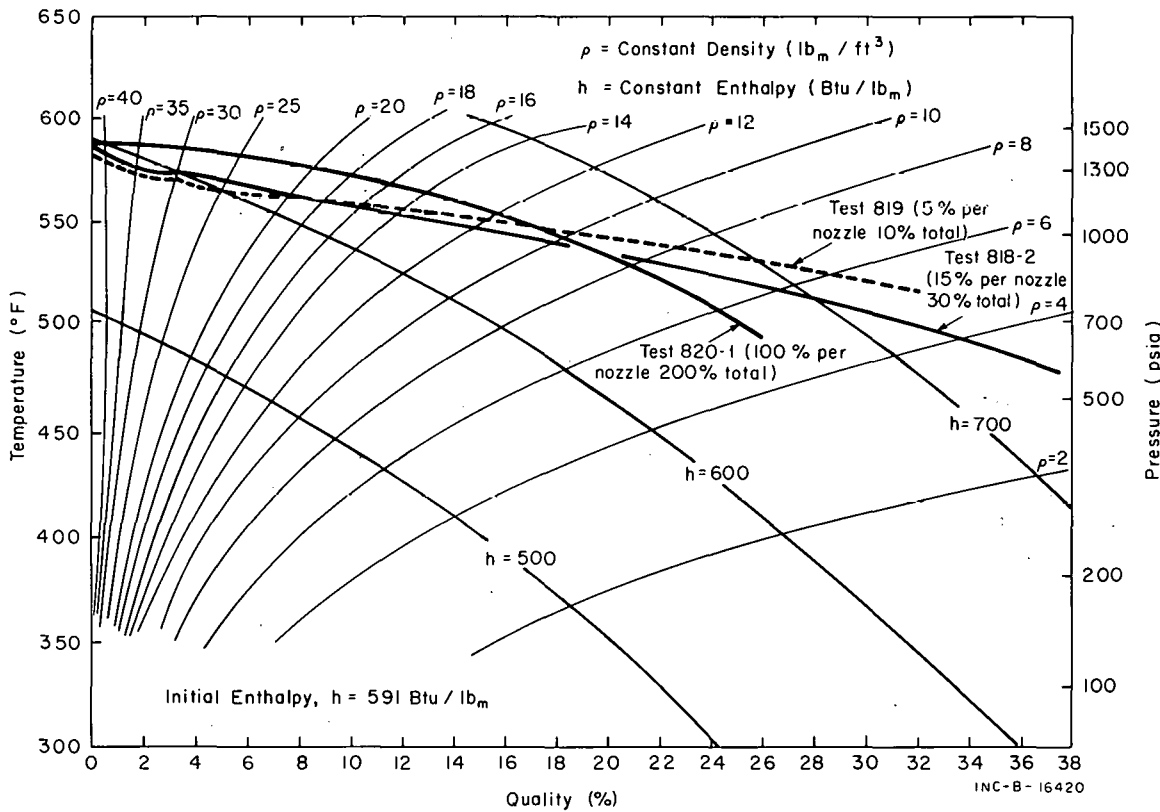


Fig. 16 Comparison of fluid state at vessel outlet nozzle for various size top breaks.

During the bottom break test the enthalpy in the common discharge line was considerably greater than that at the vessel inlet nozzle indicating that the cold leg fluid quality was higher than that at the vessel inlet shown in Figure 17.

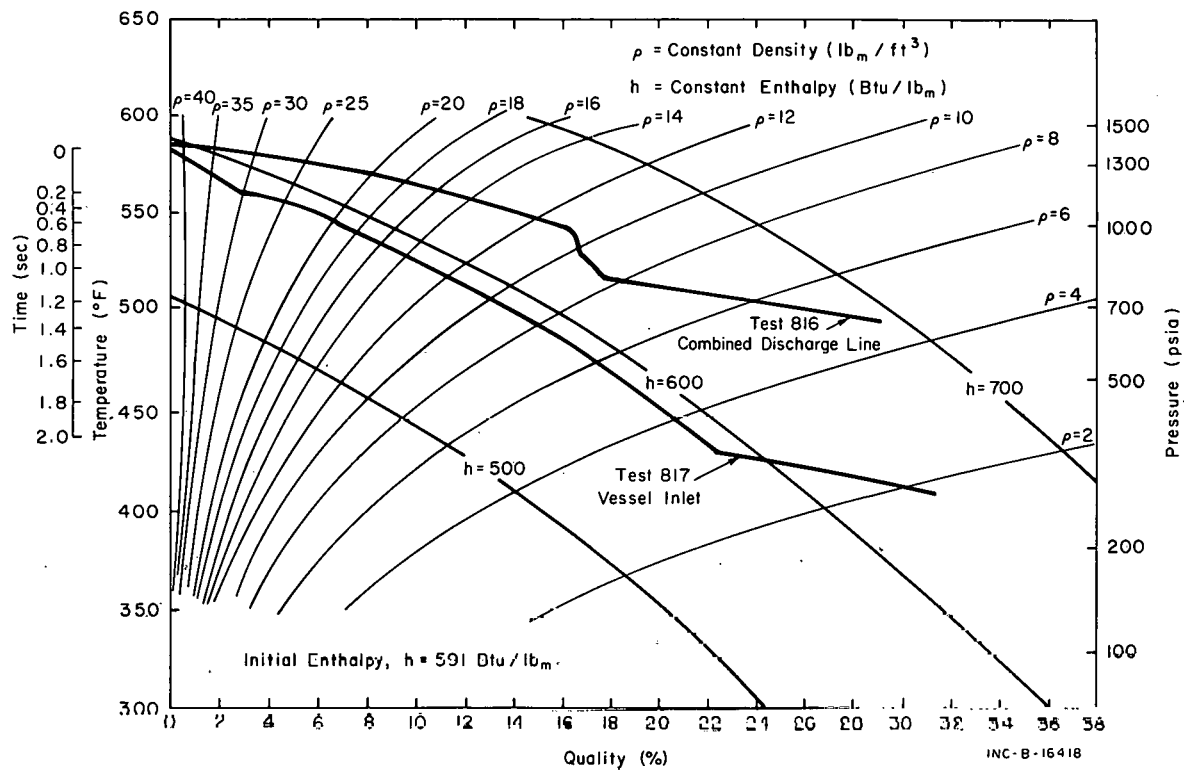


Fig. 17 Comparison of fluid state at two locations for a 100% bottom break.

Figures 18, 19, and 20 provide comparisons of the fluid condition at the vessel outlet nozzle and the cold leg for the double-ended (top) break tests. Both the 10 and 30% breaks indicate a change in the location of highest quality and a sharp shift in the hot leg quality. The shift is thought to be due to the fluid from the auxiliary heater and pressurizer reaching the measurement station. This behavior is not noted during the 200% break test.

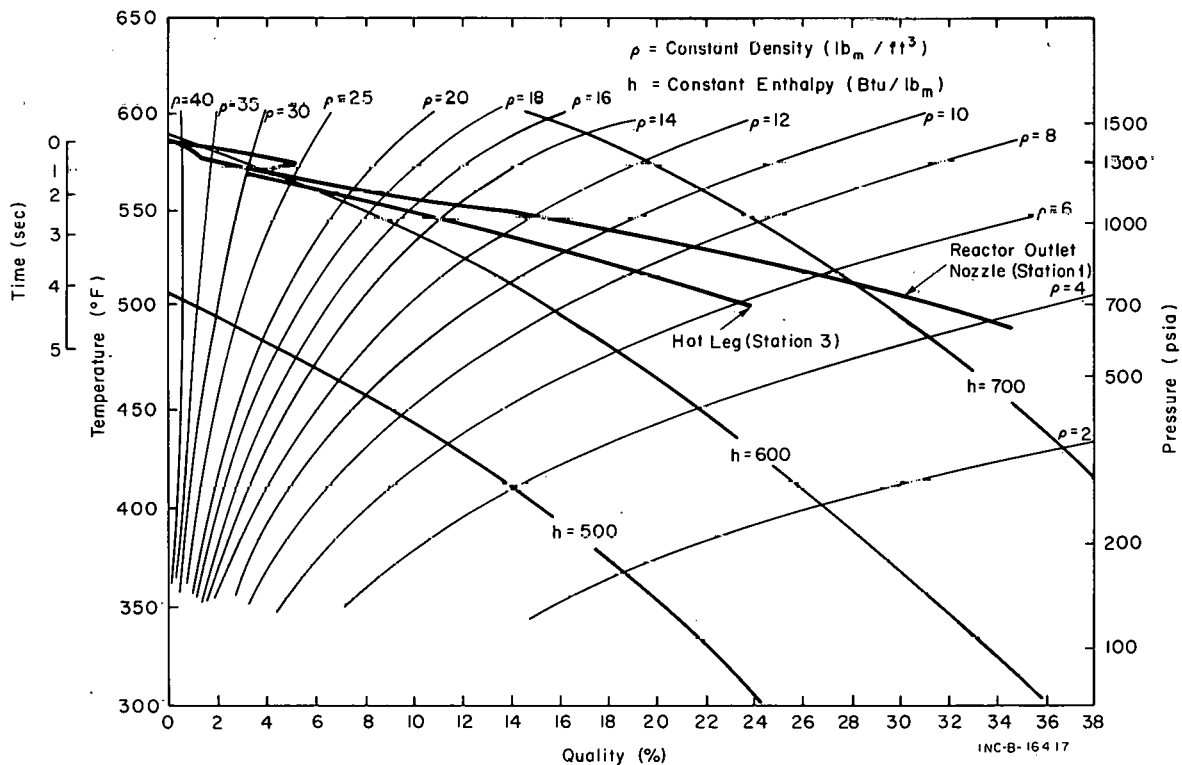


Fig. 18 Comparison of reactor vessel outlet and hot leg fluid state during a 30% double-ended top break.

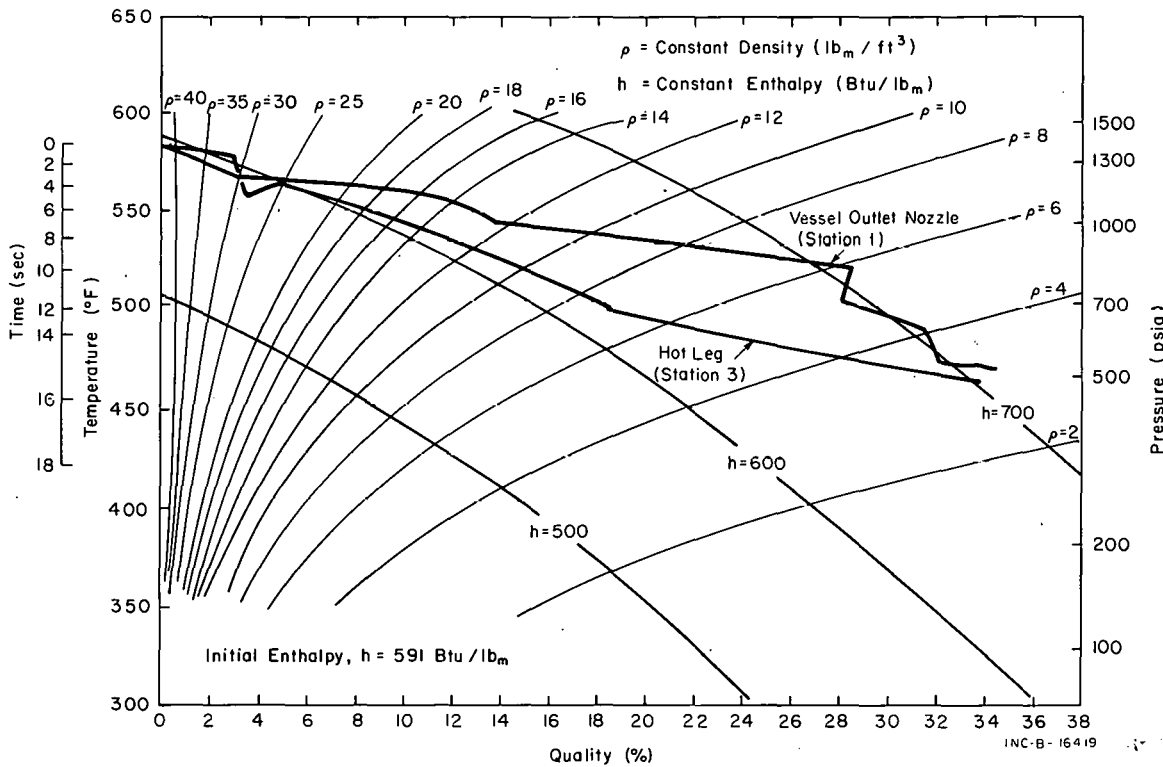


Fig. 19 Comparison of reactor vessel outlet and hot leg fluid state during a 10% double-ended top break.

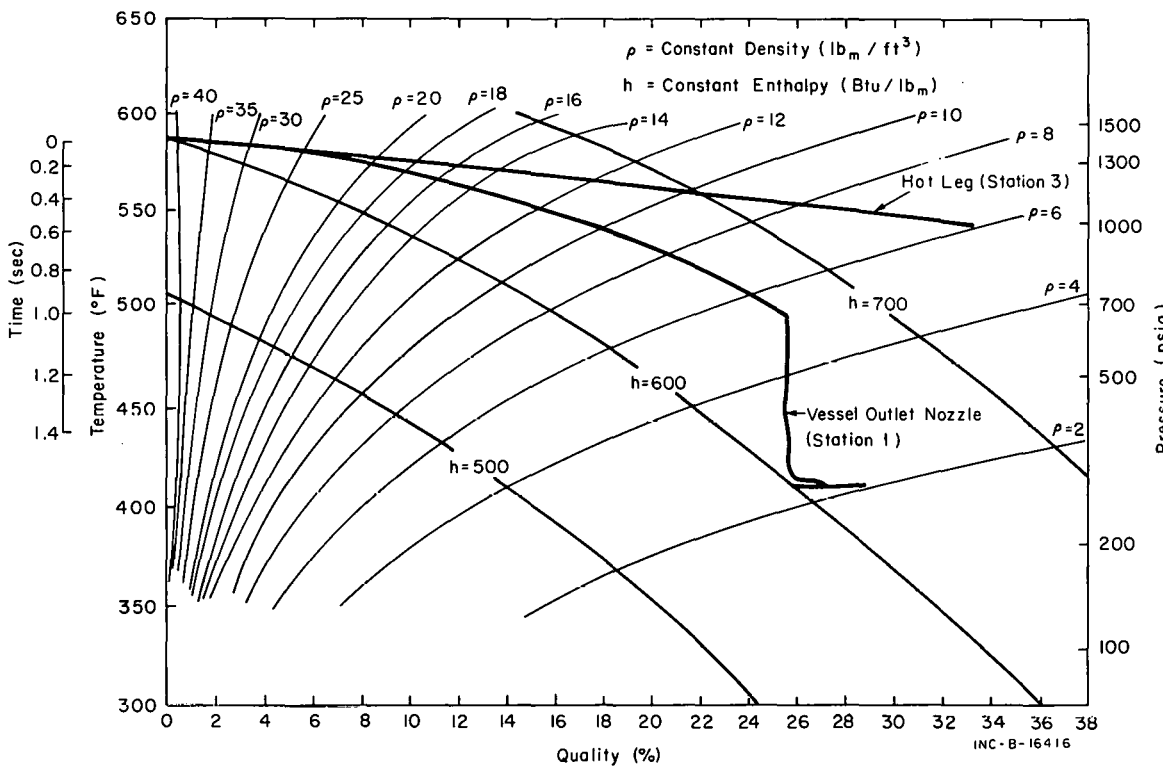


Fig. 20 Comparison of reactor vessel outlet nozzle and hot leg fluid state during a 200% double-ended top break.

## 6. THRUST

Horizontal reaction forces due to the expulsion of fluid from the system can result in high loads on the piping sections. The semiscale blowdown tests have shown that the thrust is initially large and of very short duration. The thrust data for the subcooled portion of blowdown are masked by a ringing of the system due to the sudden application of loads. As a result, separation of the response of the system from the applied force is difficult. The subcooled thrust data are included in Appendix B.

The pressure at the end of the subcooled decompression is about 1300 psi for all tests with an initial temperature of 584°F. The thrust load at this time is given in Figure 21 as a function of break size. Also shown for reference is a curve of pressure (1300 psi) times break area. The deviation is caused by pressure downstream of the orifice. The empirical equation

$$T = (P_v - P_e) A_b + P_e (A_p - A_b) \quad (1)$$

where

$P_v$  = vessel pressure

$P_e$  = pressure downstream of the orifice

$A_p$  = pipe area

$A_b$  = break area

has previously been shown to describe the thrust reasonably well for an orificed system[1]. Previous studies have also shown that  $P \times A$  may be used when no restriction is provided[1]. Equation (1) is only applicable to the thrust forces during saturated blowdown and to only the semiscale system. Although use of the normal thrust equation that is more generally applicable is preferred, lack of data prevents extensive use of the normal thrust equation during the blowdown. Test 818-1, a test with the double-ended break configuration in which only the vessel nozzle ruptured, provides data for a limited evaluation. The thrust equation is

$$T = \frac{w}{g} v_e + P_e A_e \quad (2)$$

where

$w$  = mass flow rate

$g$  = gravitational constant

$v$  = fluid velocity.

The subscript applies to the exit condition. This equation can be modified to the form

$$T = \left( \frac{G^2}{\rho_e g} + P_e \right) A_e \quad (3)$$

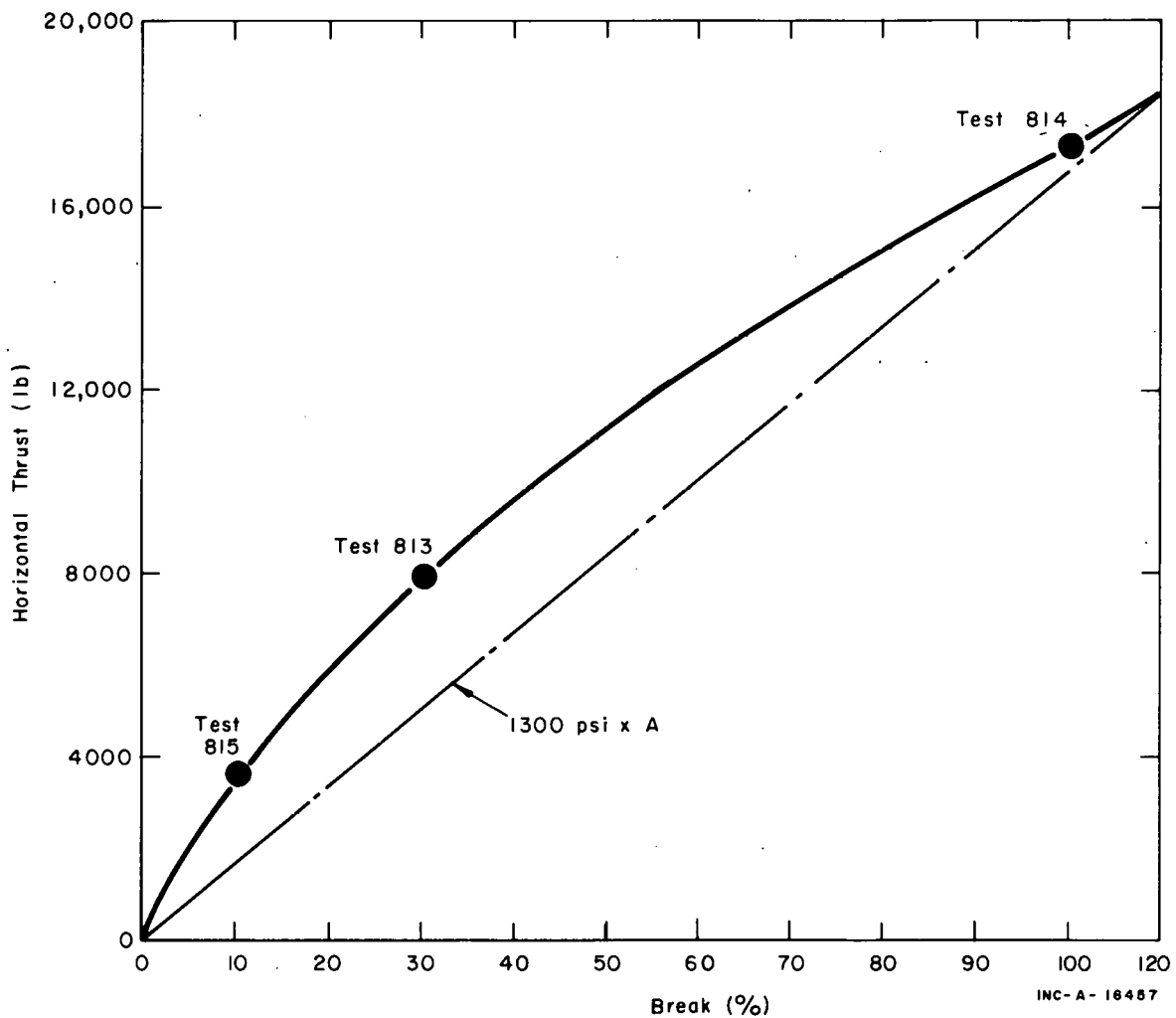


Fig. 21 Thrust at the start of saturated blowdown for various break sizes.

where

$G$  = mass velocity

$\rho$  = fluid density.

From the momentum equation, the following relation can be obtained for Station 1 and the exit

$$P_1 A_1 + \frac{G^2}{\rho_1 g} A_1 = P_e A_e + \frac{G^2}{\rho_e g} A_e . \quad (4)$$

Since  $A_e = A_1$ , the resultant thrust load can be computed from

$$T = \left[ \frac{G_1^2}{\rho_1 g} + P_1 \right] A_1 \quad (5)$$

if the losses are small. For use in evaluating the available data, the preceding equation must be modified to reflect the losses, especially across the orifice. Use

of the static pressure data at Station 18 and the enthalpy of the fluid permits an estimate of the total pressure loss and calculation of thrust. The results, shown in Figure 22, agree quite well with the thrust measured for the first few seconds of blowdown (before shifts in experimental measurements due to drift and system temperature changes become significant). Much better agreement would be expected for a full size break for which an estimate of total pressure loss across an orifice is not required. Also shown in Figure 22 is the thrust computed from the pressure-area relation of Equation (1) through use of the pressure at Station 18 for  $P_e$ .

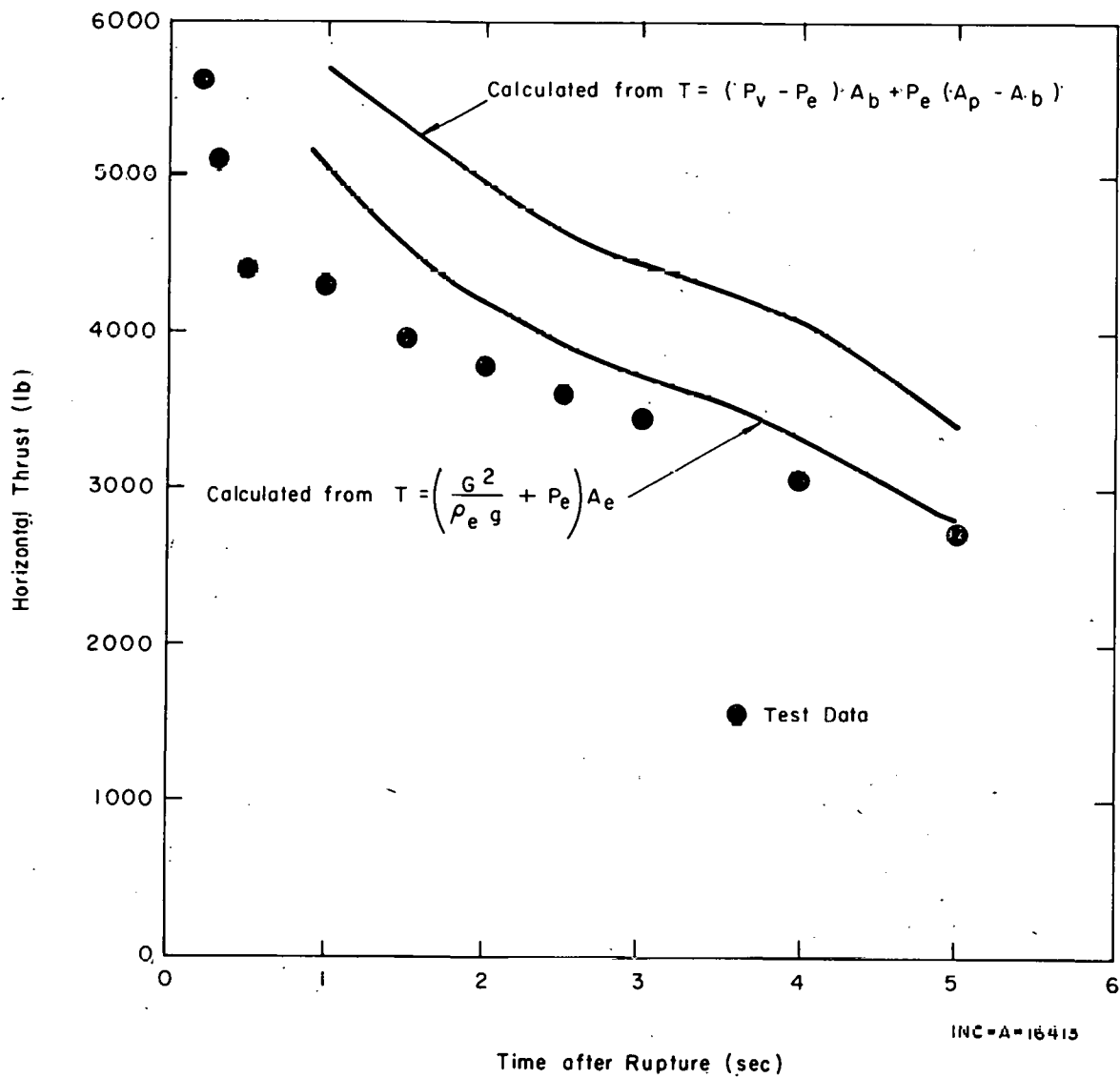


Fig. 22 Comparison of calculated and measured thrust for Test 818-1.

## 7. PIPING STRAINS

Piping strains on the outside walls of the pipe were measured at several locations in the system. The variation during blowdown is shown in Figure 7 for a 10% break. A comparison of the circumferential strain at the vessel outlet nozzle for four different break sizes is given in Figures 8 and 9. The strain change that was recorded at the end of the subcooled blowdown was checked against that predicted by the thick-wall cylinder hoop strain equation. Calculated values were found to exceed the measured values by less than 10%.

The maximum strains measured near the end of the saturated portion of blowdown are the greatest near the rupture location and occur in the circumferential direction. Axial strains are between 60 to 80% of the circumferential strain measured at the same location. The principal strains had nearly the same magnitudes and directions as the circumferential strains.

The major portion of the strains are thermally induced. The temperature gradient in the reactor vessel outlet was determined for a number of tests and used to compute circumferential strain. The comparison of calculated and measured strains is given in Table III. Agreement was within 7% in all cases except that of the small break. Small breaks do not cause as large temperature gradients as the larger breaks and hence errors in the initial temperature distribution and strain measurements can cause significant errors in the results for the small breaks. The large deviation for the 2% case shown on Table III is attributed to the errors in the temperature distribution and strain measurements.

TABLE III

COMPARISON OF CALCULATED AND MEASURED MAXIMUM CIRCUMFERENTIAL STRAINS

Test	Test Conditions			Calculated Strain ( $\mu$ in./in.)	Measured Strain ( $\mu$ in./in.)	Deviation From Measured (%)
	Break Size (%)	Temperature (°F)	Pressure (psig)			
808	100	525	2290	687 <sup>[a]</sup>	640	6.8
809	30	585	2305	595	560	5.9
812	2	584	2300	236	295	-27.5
814	100	584	2300	637	610	4.2
815	10	584	2300	618	590	4.5

[a] Yield strain at test conditions is about 800  $\mu$ in./in.

## VI. CONCLUSIONS

The 800 series test results provide a significant increase in the experimental data base available for development and assessment of analytical models for predicting the decompression behavior of large PWR's in the event of a loss-of-coolant accident. The addition of the loop to the previous vessel-only system has provided a means of obtaining information on subcooled pressure differences that can be used for assessment of appropriate computer codes. In addition, the hydraulic behavior of the system during saturated blowdown has been investigated for a more complex system; however, the unavailability of good fluid measurements throughout the system limits the usefulness of these data for quantifying processes such as phase separation and two-phase pressure drops. As is apparent from the text, the required fluid measurement techniques are, of necessity, being developed and checked out in conjunction with the decompression experiments. The development of devices capable of measuring momentum and density in the decompression environment will in itself represent a significant accomplishment for the overall semiscale project.

The following specific conclusions are drawn from the results presented in previous portions of this report.

- (1) The blowdown time for vessel-with-loop tests increased over that obtained during vessel-only blowdown tests in proportion to the increase in initial fluid mass in the system. The blowdown time for the double-ended break configuration did not differ from that of a single-ended break of the same total break area.
- (2) The addition of a loop to the vessel resulted in no residual water following blowdown except for the very small break case (2% of the pipe area), and in this case the amount was reduced from that observed in the vessel-only blowdowns. Tests with both the blowdown tee configuration and a double ended break configuration produced similar results verifying that the residual water was not dependent on break configuration.
- (3) The position of the first decompression front can be computed accurately by using the isentropic sonic velocity. The initial wave is largest in magnitude and decays rapidly as the distance from the rupture is increased. Application of the results to large PWR's indicates that large pressure differences can occur during subcooled blowdown as a result of the time for various sections of the system to decompress.
- (4) In terms of thermodynamic processes, the subcooled decompression is nearly isentropic. Hence, the fluid state at the start of the saturated portion of blowdown can be determined on the basis of isentropic assumptions.
- (5) The stagnation point appears to shift from the vicinity of the steam generator outlet to the cold leg for full size breaks.

- (6) The thrust calculated from measured fluid properties during saturated blowdown agrees well with the measured thrust.
- (7) The maximum piping strains are thermally induced and occur late in the blowdown. The direction of the principal strain is circumferential.

## VII. REFERENCES

1. H. D. Curet et al, Semiscale Blowdown and ECC, IDO-17258C (April 1969).
2. G. F. Brockett, H. D. Curet, H. W. Heiselmann, Experimental Investigations of Reactor System Blowdown, IN-1348 (September 1970).
3. F. J. Moody, "Maximum Flow Rate of a Single Component, Two-Phase Mixture", ASME Paper No. 64 - 41 T-35 (May 22, 1964).

## APPENDIX A

DESCRIPTION OF THE FACILITY AND THE DATA ACQUISITION AND  
PROCESSING SYSTEM FOR TESTS 803 THROUGH 820 OF THE SEMISCALE  
BLOWDOWN AND EMERGENCY CORE COOLING (ECC) PROJECT

THIS PAGE  
WAS INTENTIONALLY  
LEFT BLANK

## APPENDIX A

### DESCRIPTION OF THE FACILITY AND THE DATA ACQUISITION AND PROCESSING SYSTEM FOR TESTS 803 THROUGH 820 OF THE SEMISCALE BLOWDOWN AND EMERGENCY CORE COOLING (ECC) PROJECT

#### A-I. INTRODUCTION

This appendix presents sufficient information on the test configuration and instrumentation used in single-loop semiscale blowdown Tests 803 through 820 that the reader reviewing or analyzing the data presented in the body of the report will have ready access to the information needed to facilitate understanding of the test results.

## A-II. TEST CONFIGURATION

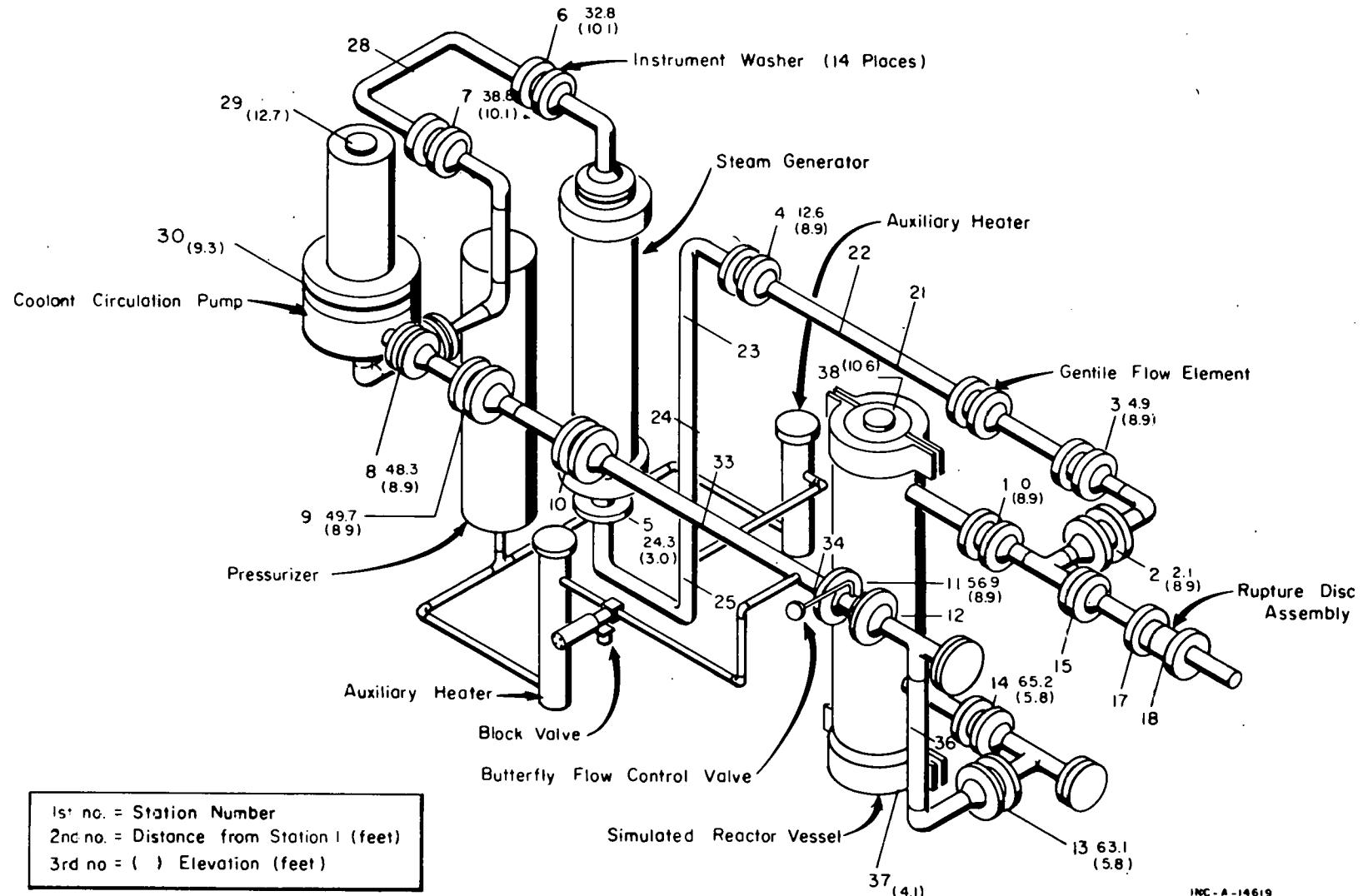
The equipment used in Tests 803 through 820 of the Semiscale Blowdown and Emergency Core Cooling (ECC) Project is described in this section. For this group of tests the system consisted of a single operating loop and a vessel devoid of internals. Both single- and double-ended break tests were performed.

### 1. SYSTEM LAYOUT

The general layout of the major components and interconnecting piping is shown in Figure A-1. This figure indicates the various instrumentation stations located throughout the primary coolant circulation loop. These stations start with Station 1 located at the discharge (top) nozzle of the vessel. The additional numbers listed to identify the stations are the distance, in feet, downstream from Station 1 and the elevation, in feet, from the test cell floor. For example: Station 6, having designations 6, 32.8, and (10.1), is 32.8 feet downstream from Station 1 and is at an elevation of 10.1 feet above the test cell floor.

All piping in the main loop, except the transition pieces at the coolant circulating pump, is constructed of five-inch double-extra-strong, A-106 carbon steel. The transition pieces are carbon steel but are of reduced pipe size to accommodate connections to the pump.

Modification of this basic system for Tests 818 through 820 to permit study of the effect of the double-ended break configuration is shown in Figure A-2.



INC-A-14619

Fig. A-1 Single-loop semiscale configuration.

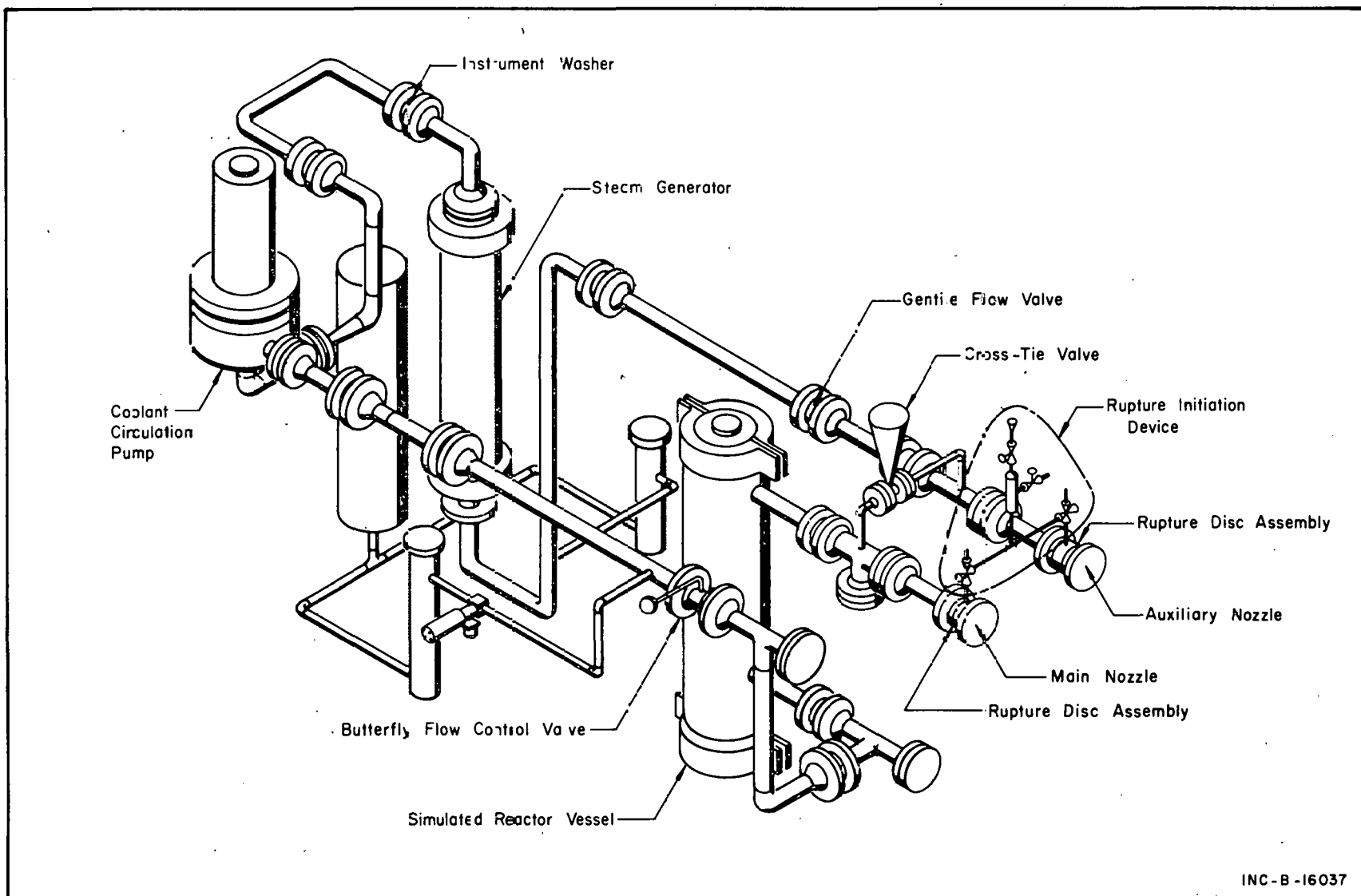


Fig. A-2 Double-ended break configuration.

## 2. SUSPENSION SYSTEM

The vessel is mounted in the test cell as shown in Figure A-3. Six load cells (each having two readout systems) are incorporated into the trunnion supports for measurement of vertical and horizontal thrust forces during blowdown. Figure A-3 also shows a restraining trolley on the blowdown nozzle that prevents excessive movement of the blowdown nozzle during decompression.

The primary coolant piping is supported on flexible pipe hangers as shown on Figures A-4 and A-5. The steam generator is supported on a pedestal as shown in Figure A-5. Additional support for the piping is provided by the support trolley at the blowdown nozzle and the pipe attached to the reactor vessel and pump.

The primary pump rests on a steel platform but is not bolted down. Thus, the pump is free to slide as necessary to prevent excessive stress loads that might be caused by pipe expansion during heatup of the system.

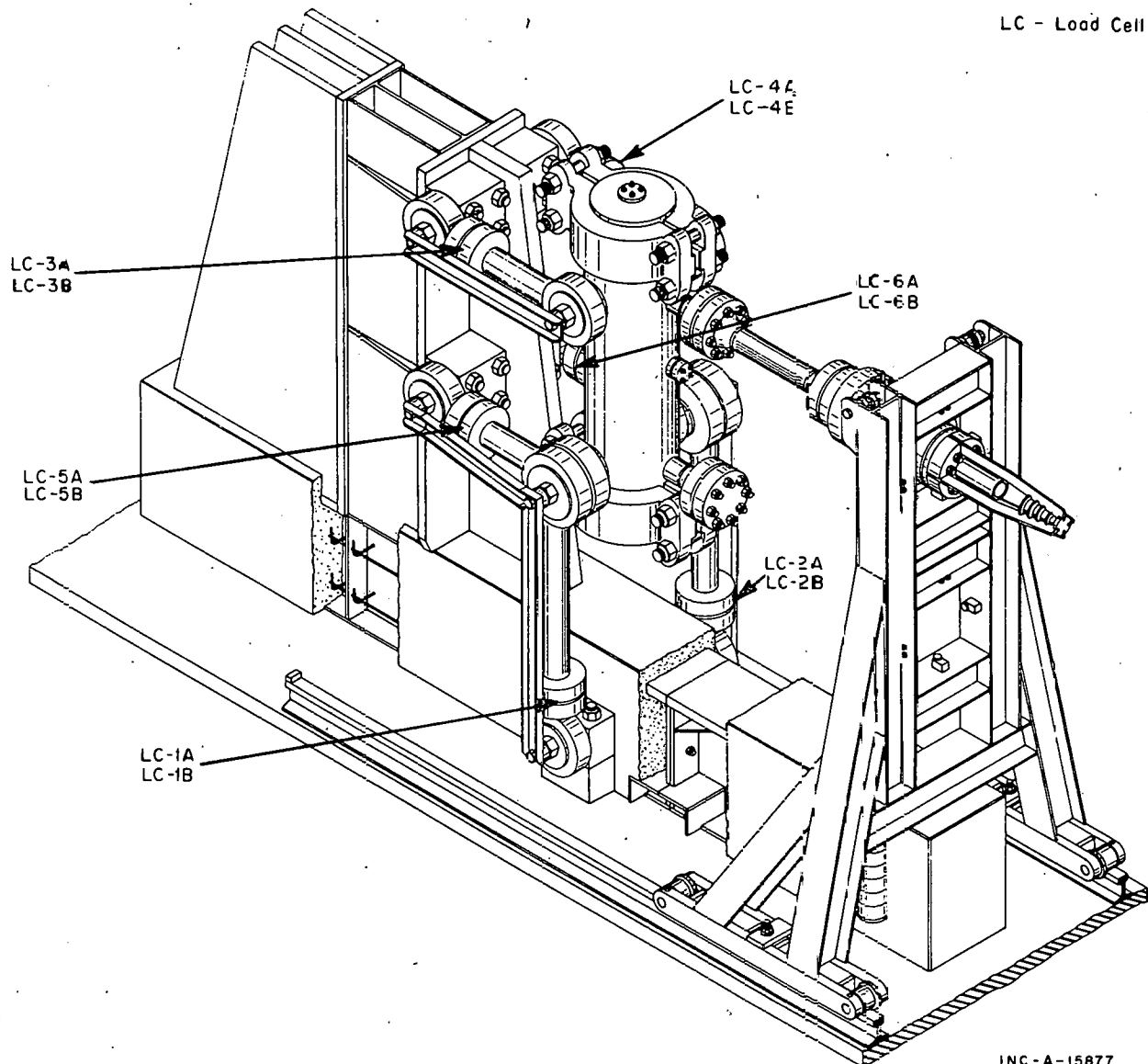


Fig. A-3 Semiscale vessel mounting.

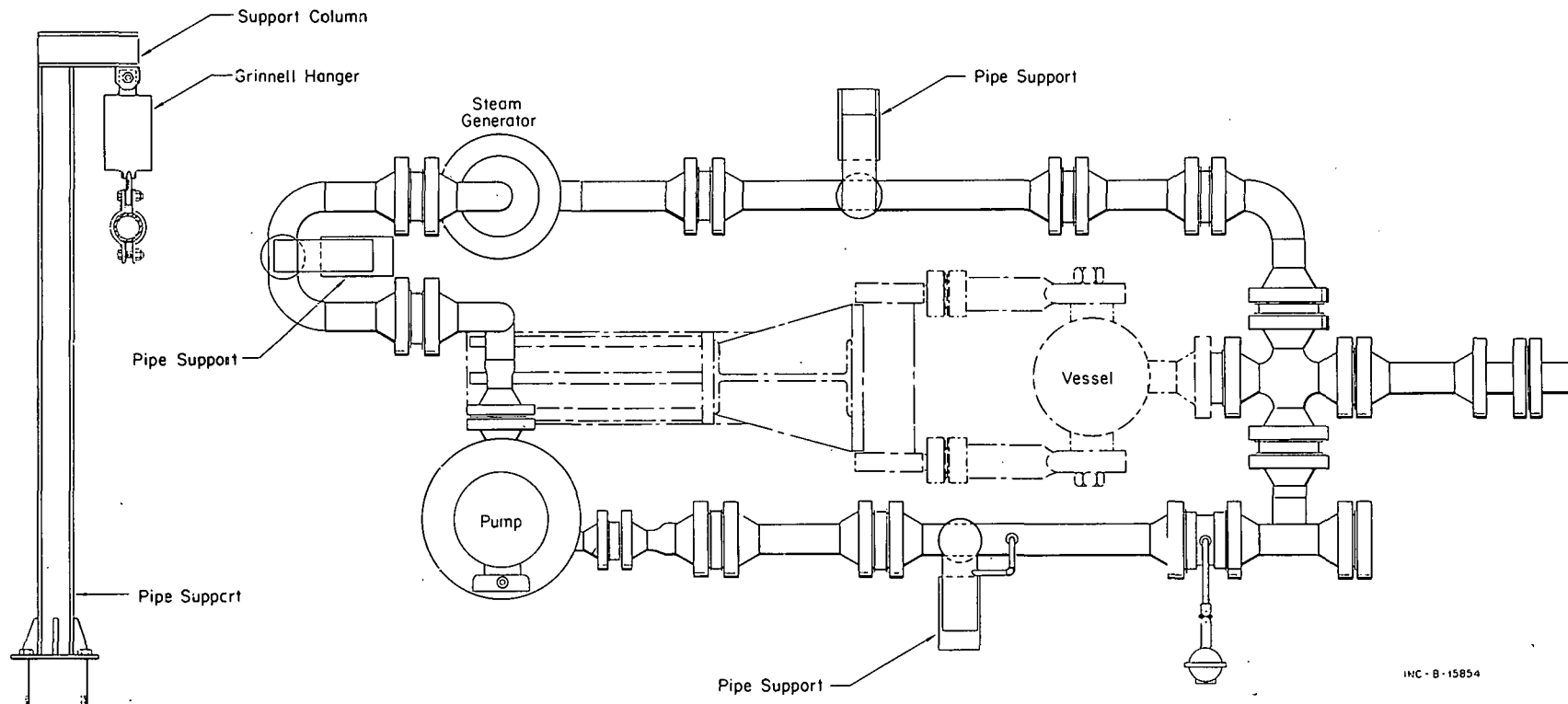


Fig. A-4 Pipe hanger locations -- plan.

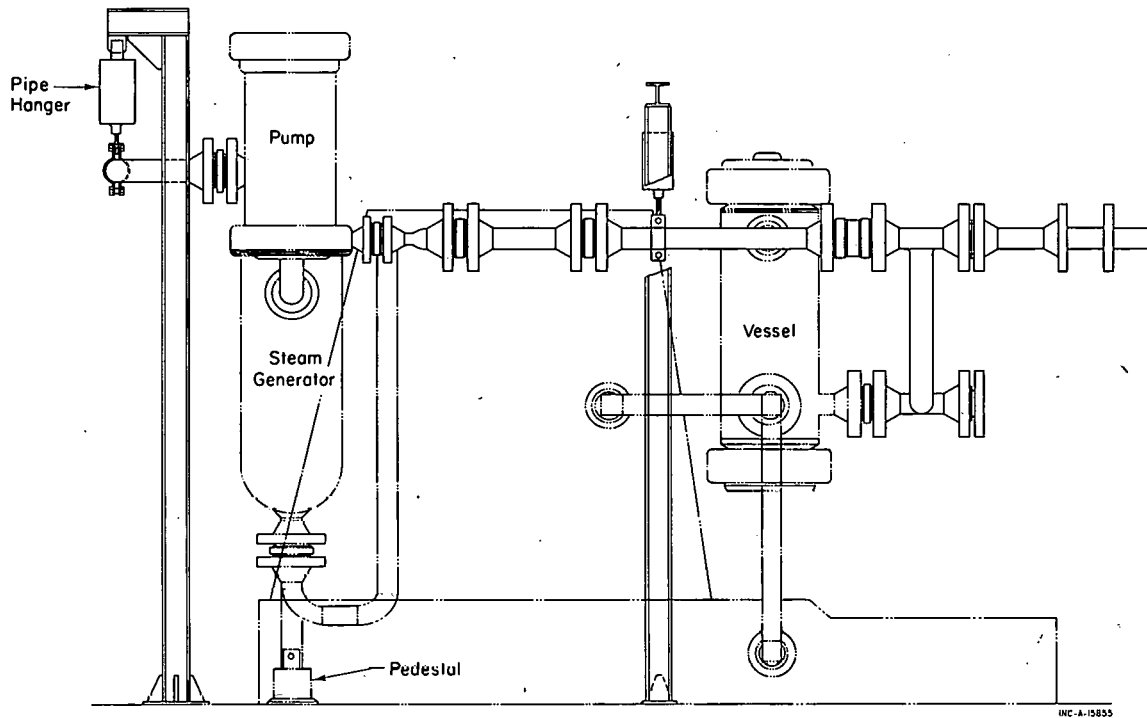


Fig. A-5 Pipe hanger locations -- elevation.

### 3. STEAM GENERATOR

A cutaway isometric of the steam generator is shown in Figure A-6. Primary coolant flows into the lower plenum, upwards through forty-three, 3/4-in.-OD, 12-gauge tubes, 33-1/4-inches long (between tube sheets), into the upper plenum, and out the exit nozzle. No provision was made to pressurize the steam generated from the secondary coolant; therefore, the secondary side of the steam generator operates only at atmospheric pressure. These tests did not require the use of the secondary system because no core heat was added and all tests were initiated from isothermal conditions.

The volume distribution within the steam generator is as follows:

<u>Component</u>	<u>Volume (ft<sup>3</sup>)</u>
Inlet nozzle and lower plenum	0.47
Tube volume	0.20
Upper plenum and outlet nozzle	<u>0.47</u>
Total	1.14

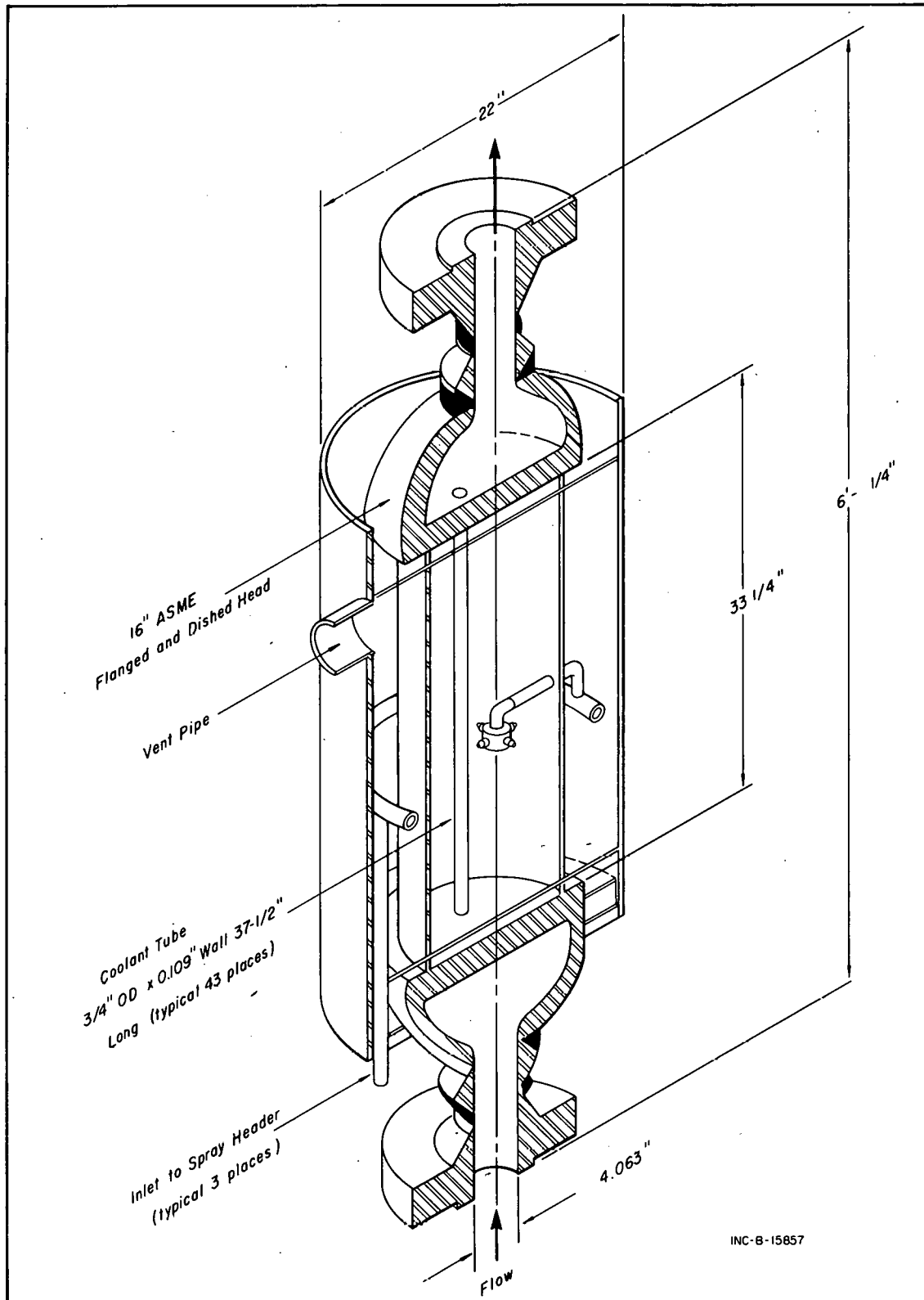


Fig. A-6 Steam generator.

#### 4. PRIMARY COOLANT PUMP

The primary coolant pump is a canned rotor-type pump with a bottom vertical inlet and a top horizontal outlet. The pump is rated for a nominal flow of 300 gal/min at a total head of 150 feet of water when operated at 3550 rpm. The inertia of the moving parts is  $3.5 \text{ lb-ft}^2$ . The internal volume of the pump including inlet and outlet nozzles is  $0.25 \text{ ft}^3$ .

#### 5. VESSEL

The vessel, which is made from Type 316 stainless steel, is shown in the isometric cutaway view of Figure A-7. Station numbers for instrumentation are shown in Figure A-8. The liquid volume of the empty vessel, including the inlet and outlet nozzles, is  $6.40 \text{ ft}^3$ .

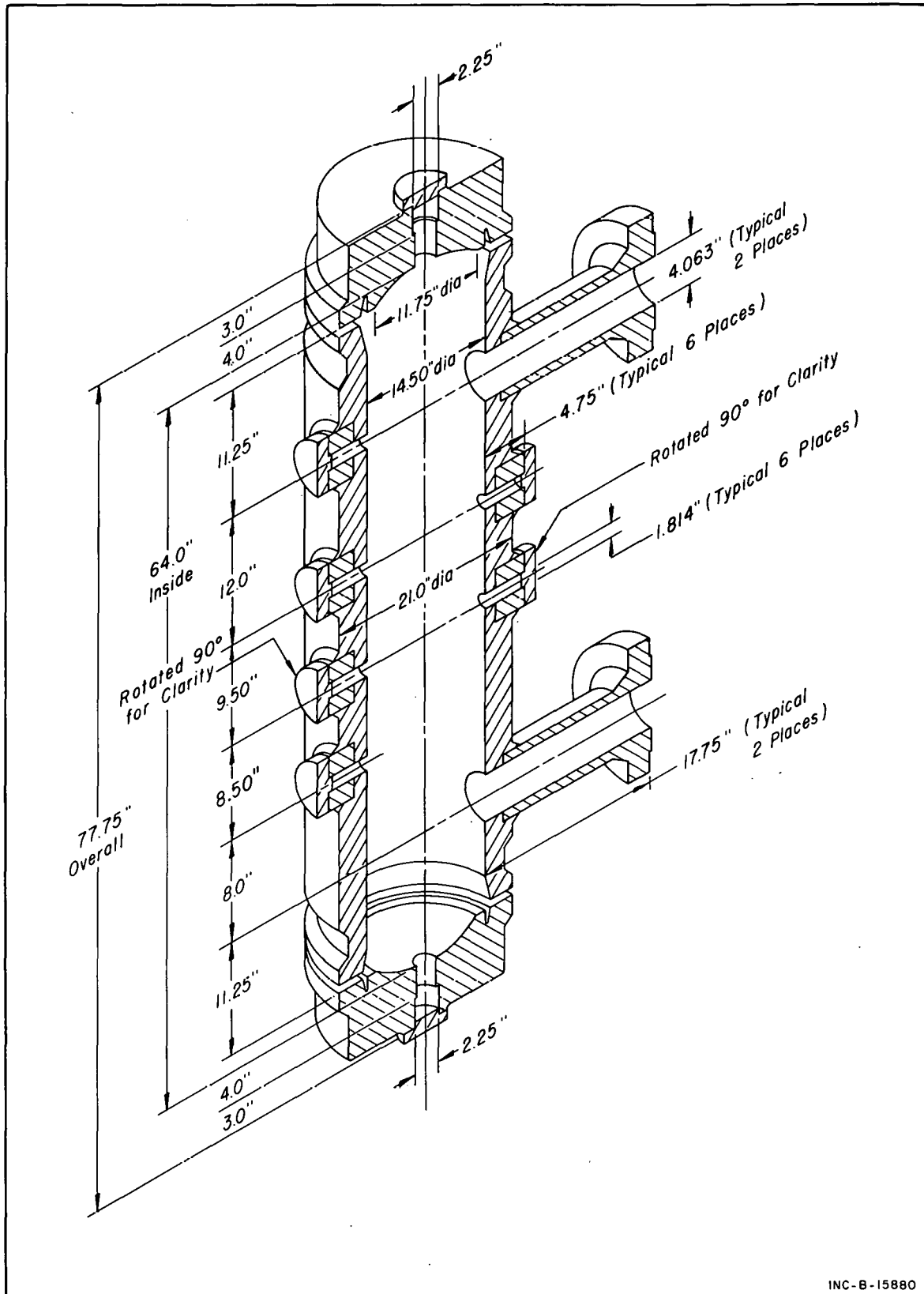
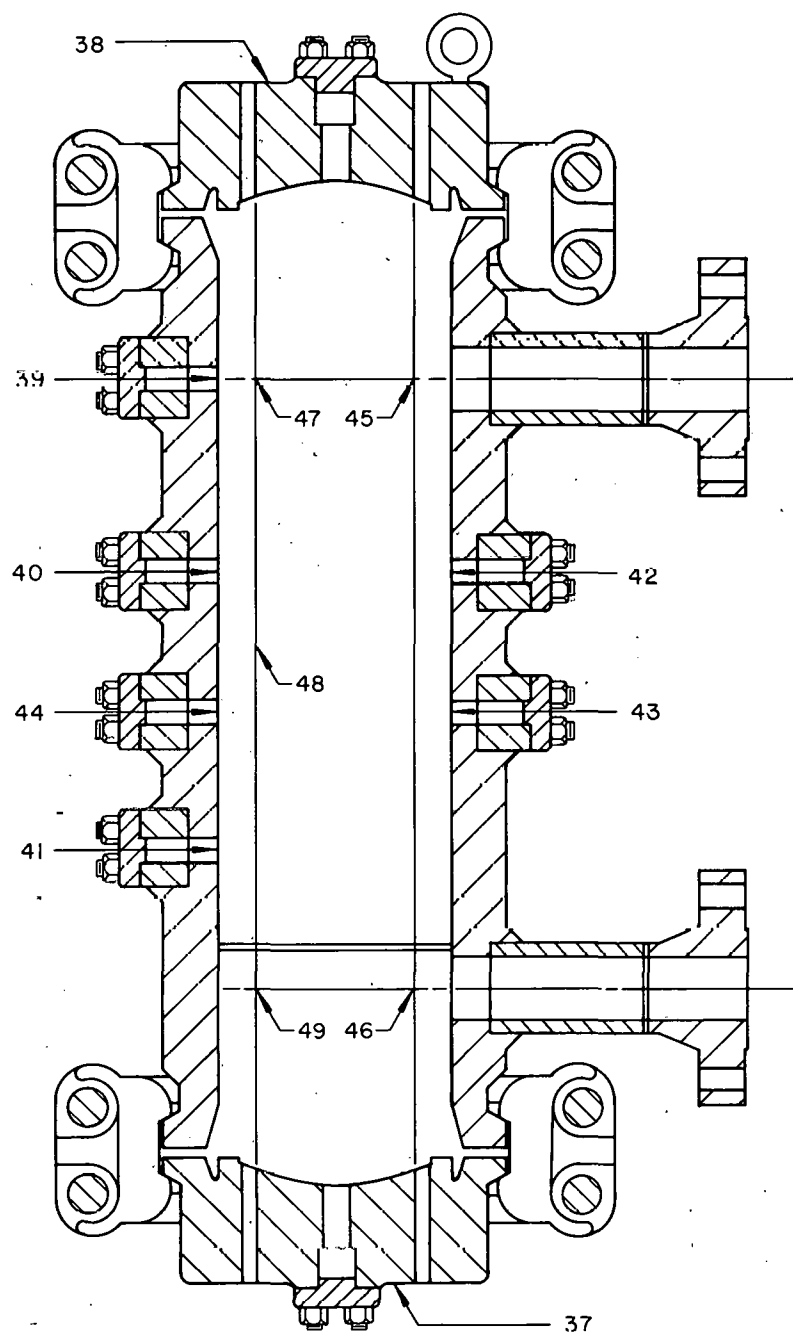


Fig. A-7 Vessel.



INC-B-15859

Fig. A-8 Single-loop semiscale vessel.

## 6. BLOWDOWN NOZZLE

The configuration and dimensions of the blowdown nozzle for the single-ended break tests are shown in Figure A-9. In some tests, extra instrument washers (Component 2) are installed between the tee (Component 3) and the extension spool (Component 4). Instrument washers may also be installed between Components 4 and 5. Depending on the type of test, the orifice plate (Component 5) can be changed to simulate the desired break size or left out completely to provide a 100% opening.

The modification for the double-ended break tests made use of a second nozzle assembly similar to the one depicted in Figure A-9, except that no nozzle spindle (Component 7) was mounted downstream from the rupture disc assembly (Component 6).

Initiation of the rupture during a test is accomplished by use of two rupture discs as shown in Figure A-9, Component 6. These discs are designed to rupture at a pressure less than the primary coolant system pressure. A buffer pressure between the discs can be controlled to subsequently control the pressure and time at which rupture occurs.

When the primary system reaches operating conditions, rupture can be initiated in two ways: (1) by overpressurizing the downstream disc causing it to break and allowing the system pressure to rupture the upstream disc, or (2) by relieving the pressure between the two discs thereby allowing the primary system pressure to rupture first the upstream then the downstream disc.

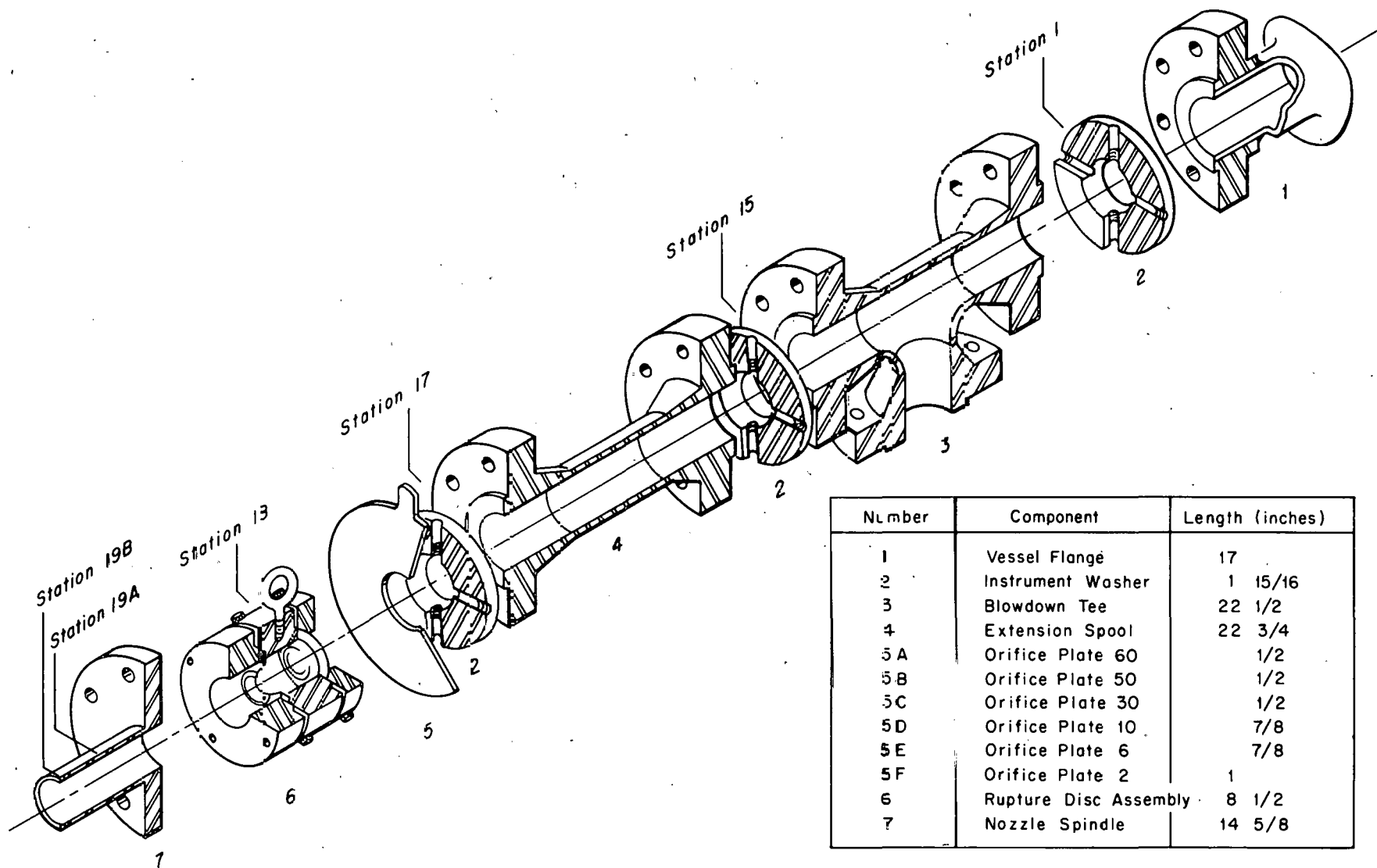


Fig. A-9 Blowdown nozzle.

INC-A-15847

## 7. PRESSURIZER

The pressurizer is an electrically heated vessel connected to the hot leg piping (between the vessel and the steam generator) of the primary system through an auxiliary heater as shown in Figure A-1. This auxiliary heater and the second auxiliary heater, also shown in Figure A-1, are used to increase the system temperature to the desired initial conditions. These heaters are turned off and the block valve connected to the cold leg is closed prior to initiation of the blowdown. The semiscale pressurizer operates in a manner similar to its counterpart in a large pressurized water reactor in that the water in the pressurizer is heated sufficiently to maintain a steam dome at the pressure desired in the primary system. The pressurizer volume is 1.61 ft<sup>3</sup>.

### A-III. SYSTEM HYDRAULIC PARAMETERS

The usual approach to the analysis of a pressurized water reactor system is to break the system into nodes or volume regions and to use the steady state pressure drop throughout the system to initialize the analysis. For the convenience of those readers who may be performing analysis based on the Semiscale Blowdown and Emergency Core Cooling (ECC) Project test results, the system pressure drop at steady state conditions and the volume distribution are included.

#### 1. PRESSURE DROP

During normal operation at 2300 psig, 585°F, and at a flow of 330 gal/min the system pressure drops are as given in Table A-I.

TABLE A-I  
PRESSURE DROP ACROSS SEMISCALE COMPONENTS

Instrument Station	Component	$\Delta P$ (psi)
9 to 14	Cold leg (pump to vessel)	32.0
14 to 1	Vessel	1.2
1 to 5	Hot leg (vessel to steam generator)	1.0
5 to 6	Steam Generator	2.5
6 to 31	Pipe (steam generator to pump)	<u>0.4</u>
Total		37.1

[a] Instrument stations are identified in Figure A-1.

#### 2. SYSTEM VOLUME DISTRIBUTION

The system volume distribution is as given in Table A-II.

TABLE A-II  
SEMISCALE SYSTEM VOLUME DISTRIBUTION

Instrument Station	Component	Volume (ft <sup>3</sup> )
8 to 14	Cold Leg Pipe	1.42
14 to 1	Vessel	6.40
1 to 5	Hot Leg Pipe	2.22
5 to 27	Steam Generator	1.14
27 to 31	Pipe (steam generator to pump)	1.21
31 to 8	Primary Pump	0.25
	Pressurizer	1.61
	Pressurizer Piping	<u>0.15</u>
Total		14.40

[a] Instrumentation stations are identified in Figure A-1.

## A-IV. DATA ACQUISITION AND PROCESSING SYSTEM

The instrumentation system is designed for versatility and to accommodate rapid changes in measurements that may be required by the various tests. In general, the test equipment and instrumentation system was assembled to acquire transient and steady state information regarding hydrodynamic, mechanical, and thermal phenomena that occur during blowdown.

### 1. DETECTORS

Depending on the particular test being conducted, detectors of various types are installed at locations throughout the system. If the measurement of a particular phenomena is crucial to the evaluation of the test results, multiple detectors may be used at some locations to assure that data will not be lost because of a single failure. Multiple detectors at a specific location also provide a check on the accuracy and response of the detectors, the acquisition system, and the data processing techniques.

Typical test measurements employ the following types of detectors:

Measurement	Detector	Designation
Fluid pressure	both strain gage and crystal	P-
Fluid temperature	thermocouples of various types	TF- or TC
Metal temperature	thermocouples of various types	TM- or TC
Pump coastdown	back EMF meter	PCV- or PMC
Thrust	load cells (of strain gage type)	LC-
Acceleration	both crystal and impedance type	AC-
Mass velocity	drag disc type and turbinemeters	V-
Density	gamma attenuation device	D- or XD-
Displacement	potentiometers	M-
Strain	strain gages of various types	S- or SG
Flow direction	various devices	FD

### 2. DETECTOR PATCH FACILITIES

A termination point for signal cabling, referred to as the detector patch panel, serves as an interface between the detector wiring from the test cell and the signal cabling from the signal conditioning equipment. All instrumentation cabling, with the exception of the thermocouple cabling, terminates at the detector patch panel. The detector patch panel is designed to facilitate continuity of cable shields through the patch and to maintain electrical isolation

in order to keep electrical noise to a minimum. Thermocouple patch panels are installed at various locations on the test equipment to reduce the length of thermocouple cabling.

### 3. SIGNAL CONDITIONING

The signal conditioning equipment consists of low-level amplifiers, strain gage completion networks and power supplies, attenuation networks, thermocouple reference junctions, and the equipment necessary to record, monitor, and calibrate data channels. Signal cables from the detector patch panel are terminated at appropriate conditioning equipment.

Cabling from the signal conditioning equipment, with the exception of that from the charge amplifiers and attenuator networks, and all remaining signal cabling from the detector patch panel are terminated at the low-level input patch panel. The low-level input patch panel allows channel changes and provides system versatility by providing convenient detector-amplifier pairing to form the various instrumentation channels.

Requirements for amplifiers to accommodate accelerometers and pressure transducers of the piezoelectric crystal type are fulfilled by electrostatic charge amplifiers. The charge amplifiers provide charge-to-voltage conversion and voltage gain. The gain is adjustable in discrete steps in order to avoid the uncertainties associated with continuously adjustable gains. The outputs of the charge amplifiers are routed to attenuator networks to increase the number of gain changes. Five modes of signal conditioning are accommodated:

- (1) Voltage gains at bandwidths of dc to 100 Hz
- (2) Voltage gains at bandwidths of dc to 1 kHz
- (3) Voltage gains at bandwidths from dc to 20 kHz with high-common-mode rejection
- (4) Voltage gains at bandwidths from 300 Hz to 250 kHz
- (5) Signals not requiring gain.

A patching facility, termed the low-level output patch panel, is provided between the data recording equipment and the signal conditioning equipment to route and channel the conditioned data signals conveniently. All signal outputs and all data recording inputs terminate at the low-level input patch panel for convenient pairing.

### 4. DATA RECORDING

Recording equipment used in the blowdown tests consists of nine 14-channel, high performance, magnetic tape recorders and one 18-channel oscillographic recorder. For data recording, the magnetic tape recorders are operated

in the frequency modulation mode at 60 in./sec producing a dc to 20 kHz frequency response with an overall record, store, and reproduce accuracy within  $\pm 1\%$  of full scale. The tape recorders can also be operated in the direct mode to produce a 0.3 to 250 kHz frequency response with an amplitude accuracy to within about  $\pm 15\%$  of full scale.

The oscillographic recorder is used as a diagnostic tool during system assembly and to provide a readily available record of pertinent data immediately after a test.

## 5. DATA PROCESSING

The semiscale analog data that are recorded on magnetic tapes are converted to the digital domain through use of a data processing computer that serves as an interface between the analog acquisition systems and a digital computer. This interface is designed to:

- (1) Input, convert, and format data acquired on analog magnetic tape for further processing by the digital computer
- (2) Establish a time reference for data required from any single test or experiment
- (3) Display the reduced data values in the form of listings or plots as functions of an independent variable (for example time).

The data processing computer, through use of an X-Y plotter, is capable of producing preliminary plots for most of the test data. Prior to submittal to the digital computer for processing, the data can be edited, linearized, smoothed, filtered, sorted, averaged, or differenced.

Although much of the data involving a single variable can be plotted with the X-Y plotter, processing involving the use of two or more variables requires the use of the digital computer. The test data are digitized by the digital computer to provide data plots that are useful from an engineering analysis standpoint (for example, plots involving time on a logarithmic scale and dimensionless parameters).

**APPENDIX B**

**SEMISCALE DATA -- 800 SERIES TESTS 803 THROUGH 820**

THIS PAGE  
WAS INTENTIONALLY  
LEFT BLANK

## APPENDIX B

### SEMISCALE DATA -- 800 SERIES TESTS 803 THROUGH 820

#### B-I. INTRODUCTION

The bulk of the data contained in this appendix are pressure and temperature data as functions of time. Where available, thrust, density, and momentum flux are also given.

All tests were reviewed and those providing the best composite of data in each break size category were selected. A tabulation of the data given in this appendix is provided in Table B-I for reference.

TABLE B-I

## TABULATION OF DATA

Total Break Size %	Test	Break Configuration	Initial Conditions			Station Locations for Measurements <sup>[t]</sup>						Comments	
			Pressure (psig)	Temperature (°F)	Flow Rate (gpm)	Pressure		Temperature	Horizontal Thrust		Momentum Flux (lb <sup>2</sup> )	Density	
						Short Term	Long Term		Short Term	Long Term			
2	812	Top Single	2300	584	324	1, 39, 14 2, 7	1	14 5					
10	811	Top Single	235	584	352	18, 15, 1, 39, 14 3, 4, 7	1	15, 14, 10, 9 2, 5, 6	3A, 4A	3A, 4A			
	819	Top Double	2250	583	0	18, 15, 1, 39, 14, 9 18A, 15A, 3, 5, 6, 7	1 3	1, 14, 9 5, 6			1 3	1 3[c]	5% break in vessel line, 5% break in hot leg.
30	813	Top Single	2310	583	327	18, 17, 1, 39, 14 3, 4, 7	1	15, 1A, 10	3A, 1A	3A, 4A	1 2		
	818-2	Top Double	2320	583	0	18, 15, 1, 39, 14, 9 18A, 15A, 3, 5, 6, 7	1 3	1, 14, 9 5, 6			1 3	1 3[c]	15% break in vessel line, 15% break in hot leg.
100	810	Top Single	2300	584	340	18, 17, 15, 1, 14 2, 4, 7	1 7	15, 9 2, 5, 6	3A, 4A	3A, 4A	1 2		
	816	Bottom Single	2250	584	321	18, 15, 13 14, 39, 1, 3	7 14	9 1A, 5, 6			17, 13 14[d]	17 14[d]	
15	818-1	Top Double	2320	585	0	18, 1, 39, 40, 14, 9 5, 7	1, 9 7	1, 9 5, 6		3A, 4A	1	1	Hot leg rupture disc failed to rupture; 15% break in vessel line only.
15	820	Top Double	2350	583	0	1, 39, 37, 14, 13 18A, 15A, 3, 5, 6, 7	1, 39, 9 3, 5, 7	38, 37, 9 5, 6			13 3	13 3[c]	Rupture in hot leg only.
200	820-1	Top Double	2250	588	0	18, 1, 39, 14, 9 3, 5, 6, 7	1, 14 3	9 5, 6				1 3	100% break in vessel line, 100% break in hot leg.

[a] Break size is expressed as percent of primary coolant pipe flow area ( $0.09 \text{ ft}^2$ ). Restriction was obtained by use of a sharp-edged orifice upstream of rupture disc assembly.

[b] Numbers appearing under data columns represent station numbers within the system except for thrust where the numbers designate external load cells (Appendix A). The station numbers are arranged in sequential order of distance from break location first through vessel and up cold leg, followed by along the hot leg. For the only bottom break test (Test 816), stations are reported up cold leg, followed by through the vessel, and along hot leg.

[c] Flow rate, mass velocity, and mass integration included.

[d] Data at Station 14 obtained from Test 817.

## B-II. DISCUSSION OF DATA

The major categories of data are discussed in the following sections with respect to accuracy and correction methods that have been applied.

### 1. PRESSURE

The pressure data falls in two categories: short term, which covers the subcooled decompression, and long term, which includes the entire test period. All pressure data were initialized to the known pressure in the system prior to blowdown. The reference pressure was determined by a Heise gage connected to the vessel. Each pressure was initialized to this value (with allowance made for system pressure drop). The large temperature change that occurs during blowdown frequently causes a drift in the strain gage pressure transducers and as a result the raw data do not always go to zero. To account for this drift, the shift has been assumed to be linear and the raw data have been corrected accordingly.

Because of thermal sensitivity, the error of the strain gage pressure transducers, as specified by the manufacturers, is 0.04% of full scale per °F where full scale is 3000 psig. Therefore, the maximum error for subcooled blowdown associated with the maximum temperature change of 6°F would be 7 psig if the instrument responded to the full temperature change.

During the saturated portion of blowdown in which the fluid temperature change can approach 400°F, the maximum error can be as great as 480 psig. Generally, however, the measured uncorrected long term pressure error does not exceed 250 psig and the uncorrected error is less than 100 psig for about 75% of the data.

All pressure data except that from Stations 18 and 18A in the rupture disc cavity start at nearly the same pressure. The pressure behavior in the region between the rupture discs can be used to determine a time when rupture is achieved by the overpressure technique. The pressure in this region increases until the outer disc ruptures at about 1200 psi. The pressure then drops to nearly zero, then suddenly increases as the inner disc ruptures and flow is established.

When the underpressure technique is used (all tests after Test 817) the cavity is vented; hence, the pressure between the discs decreases until rupture of the inner disc is achieved. When the inner disc ruptures a pressure spike occurs and is succeeded by rupture of the outer disc. The pressure then drops and rises rapidly as flow is established.

In some cases the long term plots show an undershoot in pressure at the end of the subcooled blowdown. This undershoot has been found to be a characteristic of the data processing system and does not indicate fluid behavior.

## 2. TEMPERATURE

All tests were initiated with an isothermal system; hence, the differences in initial temperature are due to instrument error. Where necessary, the temperature data presented in this report have been initialized to a reference temperature so that all temperatures start from the same value.

Prior to initialization, a variation as great as about 30°F was noted in the data; this variation is about 5% of full scale and is typical of uncalibrated thermocouples. Much of this error is removed by initializing the temperatures; the temperatures reported are considered to be accurate to within  $\pm 4^{\circ}\text{F}$ .

Blowdown of the system results in a final fluid temperature of about 205°F which corresponds to saturation conditions at the 4700-foot elevation of the National Reactor Testing Station. Most fluid temperatures never reached this value during the recorded interval but deviate or merely level out at a higher value because of voiding in the region of the thermocouple when the velocity is low or nonexistent. Such voiding allows the thermocouple to be influenced by radiation from the wall.

## 3. DENSITY

Density is measured by gamma attenuation techniques. The known density of the water represents the initial condition and the final density of the air or vapor is assumed to be zero. Very little drift is associated with this instrument and thus no drift correction has been applied.

The density measurements have a specified accuracy to within  $\pm 5\%$  of full scale.

The gamma attenuation method used to obtain the density measurements utilized a cesium-137 source. The beam diameter is about 0.75 inch,

## 4. THRUST

Piping expansion during warmup preloads the load cells; thus only the dynamic data recorded are used. Since the temperature drops during blowdown the thrust data frequently do not return to the initial load but continue to change after blowdown is complete. No corrections have been applied to the thrust data contained herein. The load cells have an accuracy to within  $\pm 200$  pounds.

The horizontal thrust is measured by two load cells (LC-3 and -4) connected through links to trunnions on the vessel such that they are on the same plane as the top blowdown nozzle. Thus, to obtain the total measured thrust, the output from both load cells must be combined.

Occasionally the initial impulse provides a momentary load exceeding the range of the data tape which accounts for the clipped data noted on some of the thrust figures.

The short term thrust data have large load fluctuations with a superimposed frequency of about 80 Hz that is apparently caused by the system response to the sudden loading.

In using the long term thrust data, consideration must be given to the distortion due to a shift in the pipe load resulting from the temperature change of the system and the instrument drift. The greater distortions occur for the smaller break tests that produce longer blowdown times.

### 5. MOMENTUM FLUX AND FLOW RATE

All momentum flux and flow rate data have been initialized to values existing at the start of the test and, where necessary, a drift correction has been applied to ensure that the flux is zero at the end of the test.

The detectors have been calibrated in water and air and were found to have only a minor difference in output for the two media. The accuracy for the tests varies because of ranging. Generally, low flows result in considerably less accuracy than the higher flows. Although no means of determining the absolute accuracy under the two-phase flow condition exist, the errors appear to vary between  $\pm 10\%$  for the larger breaks (30% and larger) and  $\pm 20\%$  for the smaller breaks. These error bands are based on computations of the total weight of fluid discharged from the system for those tests from which sufficient density measurements are available. The output has been filtered to remove frequencies above 10 Hz.

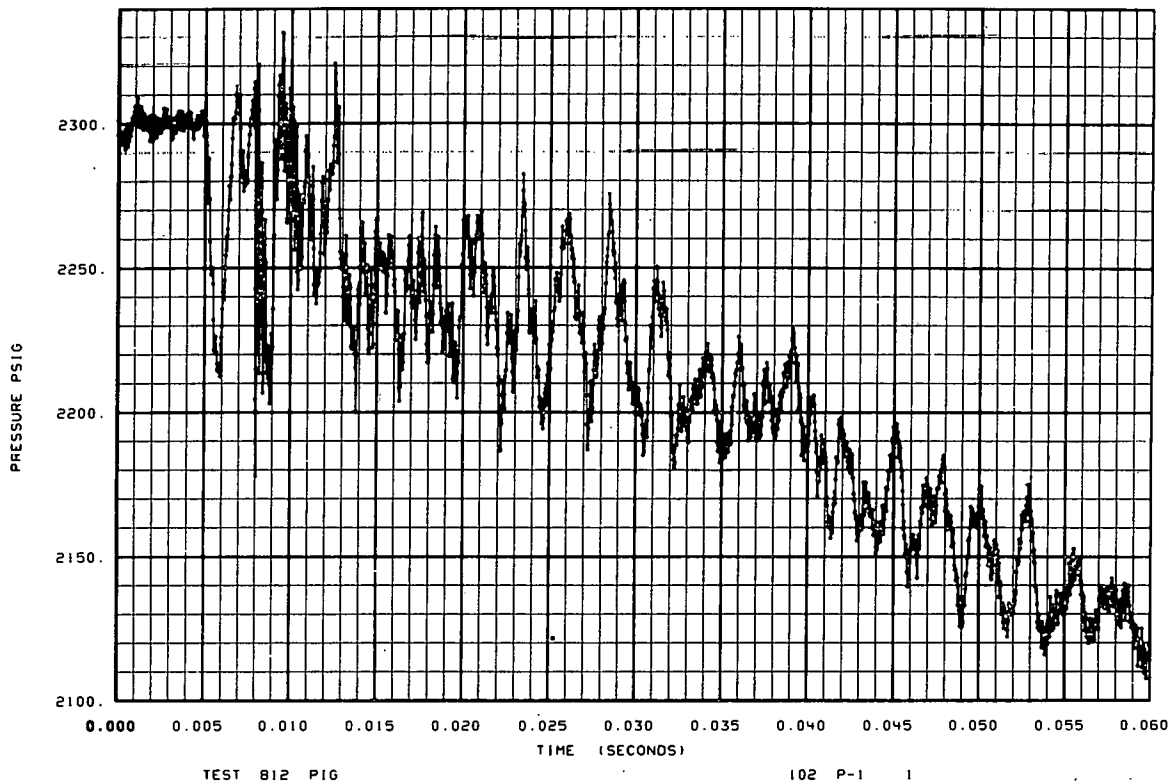
Momentum flux is obtained from drag disc flow meters. The output of these detectors is obtained from strain gages located on the beam, and although thermally compensated, drift results from the large temperature change that occurs during blowdown. This drift is frequently significant compared with the flow obtained for the small break tests. The use of larger targets to obtain a greater output signal with available instruments was impossible because the high initial impulse would over-stress the beam. In addition, the signal obtained for small break tests is frequently of the same order as the noise in the data acquisition system and thus no usable data are available for 2% and some 10% break tests.

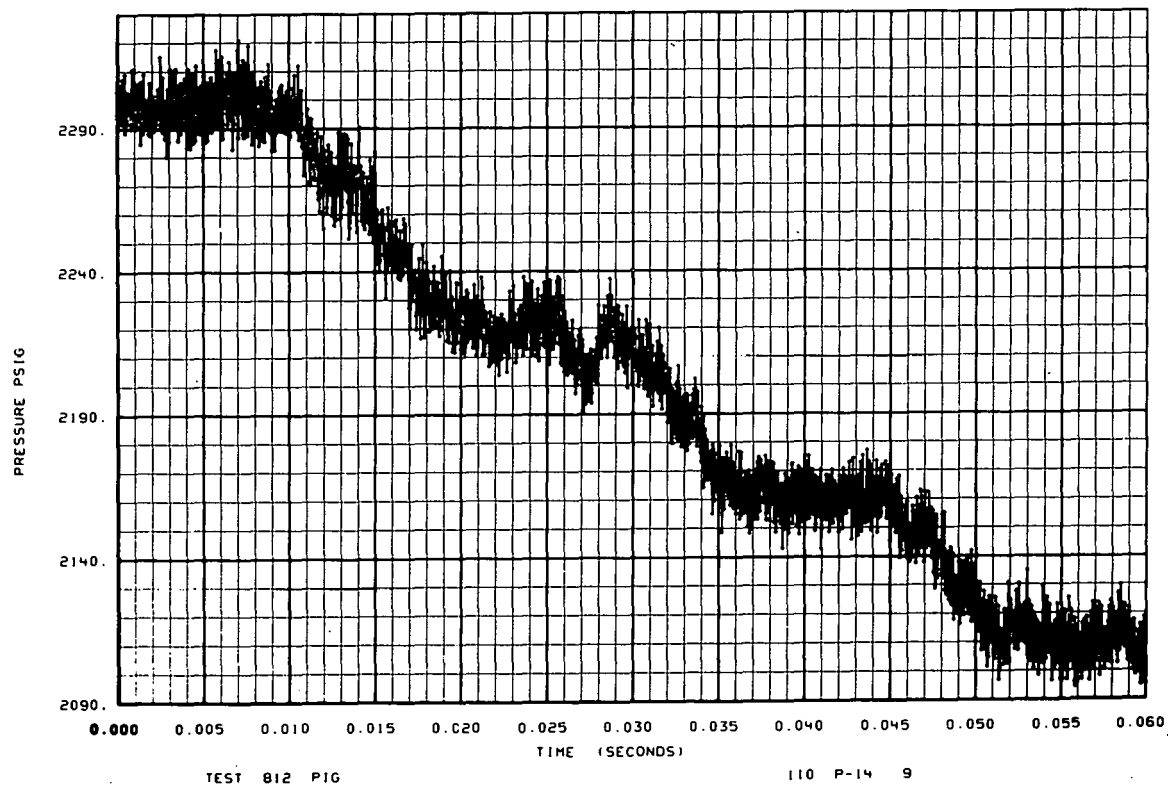
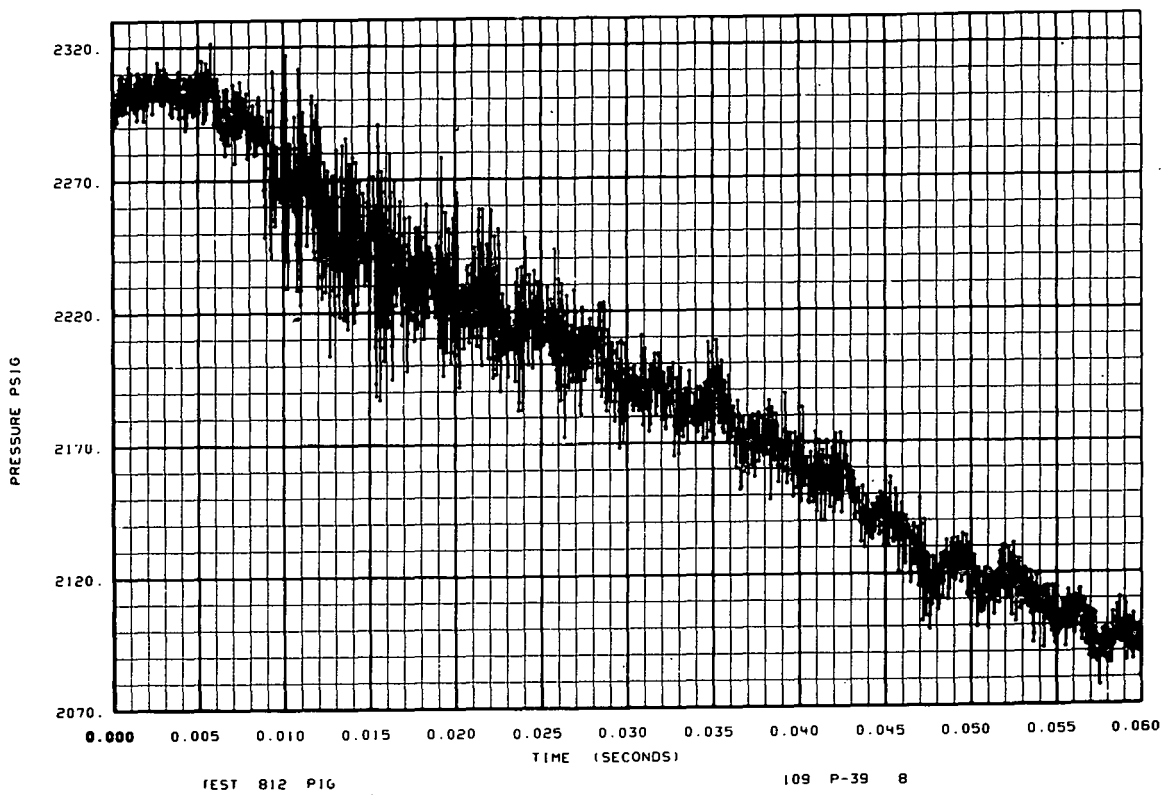
To remove much of the noise from the drag disc data, the data have been filtered. As a result, the initial spikes do not appear in the data. The filtering is particularly evident in the data from the 100% break tests.

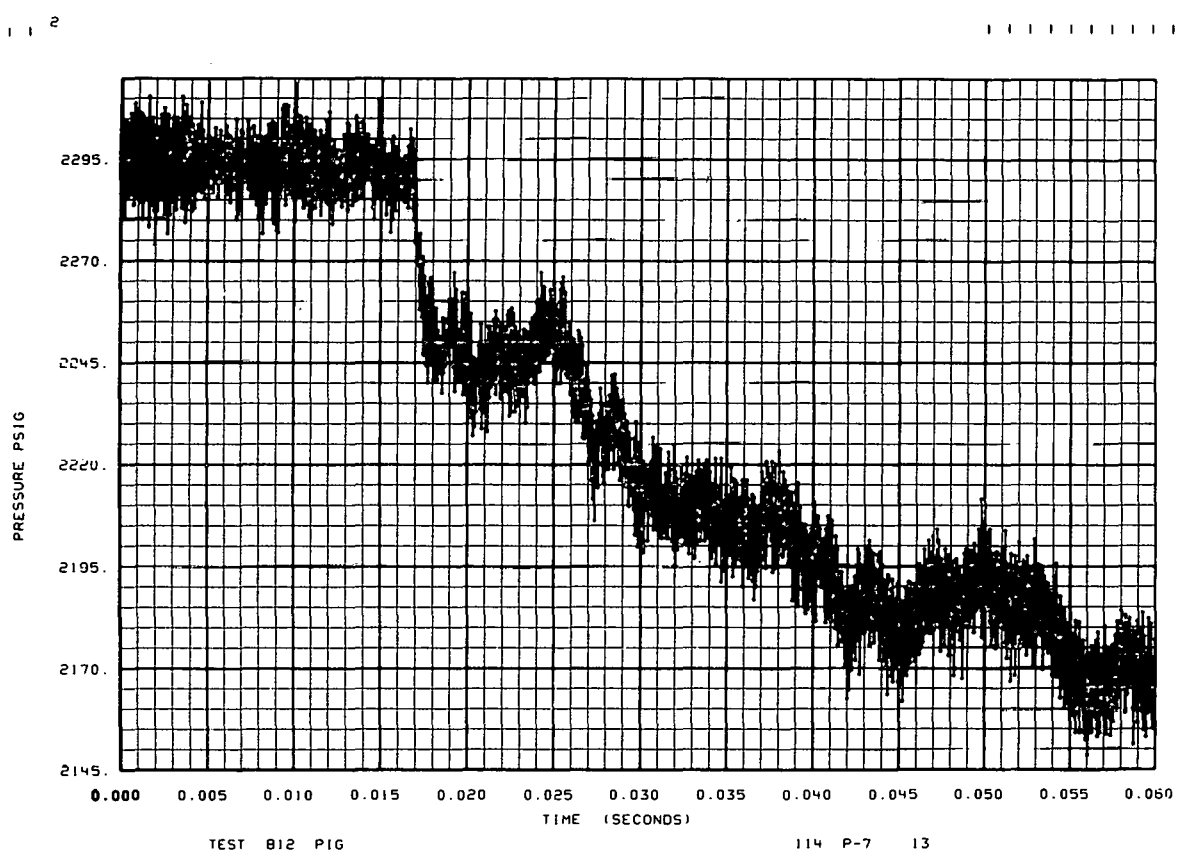
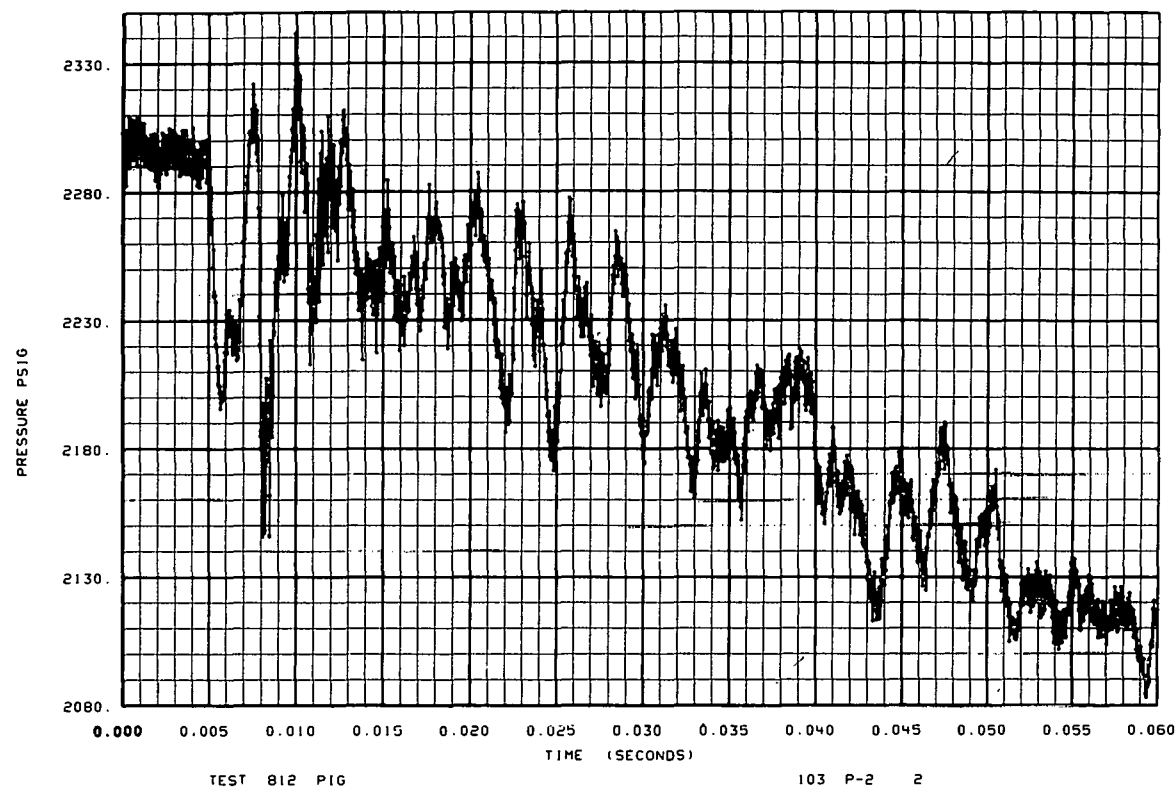
Where sufficient data are available to estimate the total mass flow from the system, such information is included. The curves labeled "mass ejected" are an integration of the flow past the station indicated. Any mass accrued prior to rupture should be deducted from the total because it is the result of failure to obtain an initial reference of zero in the data reduction program.

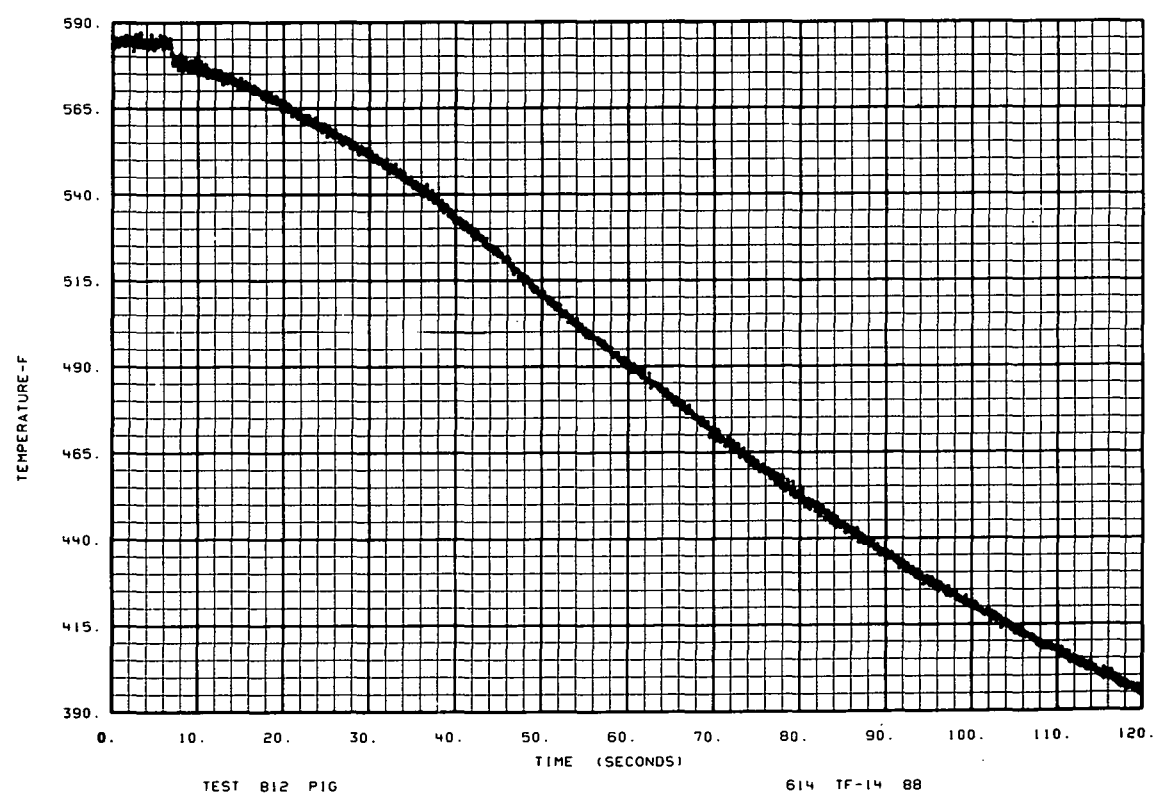
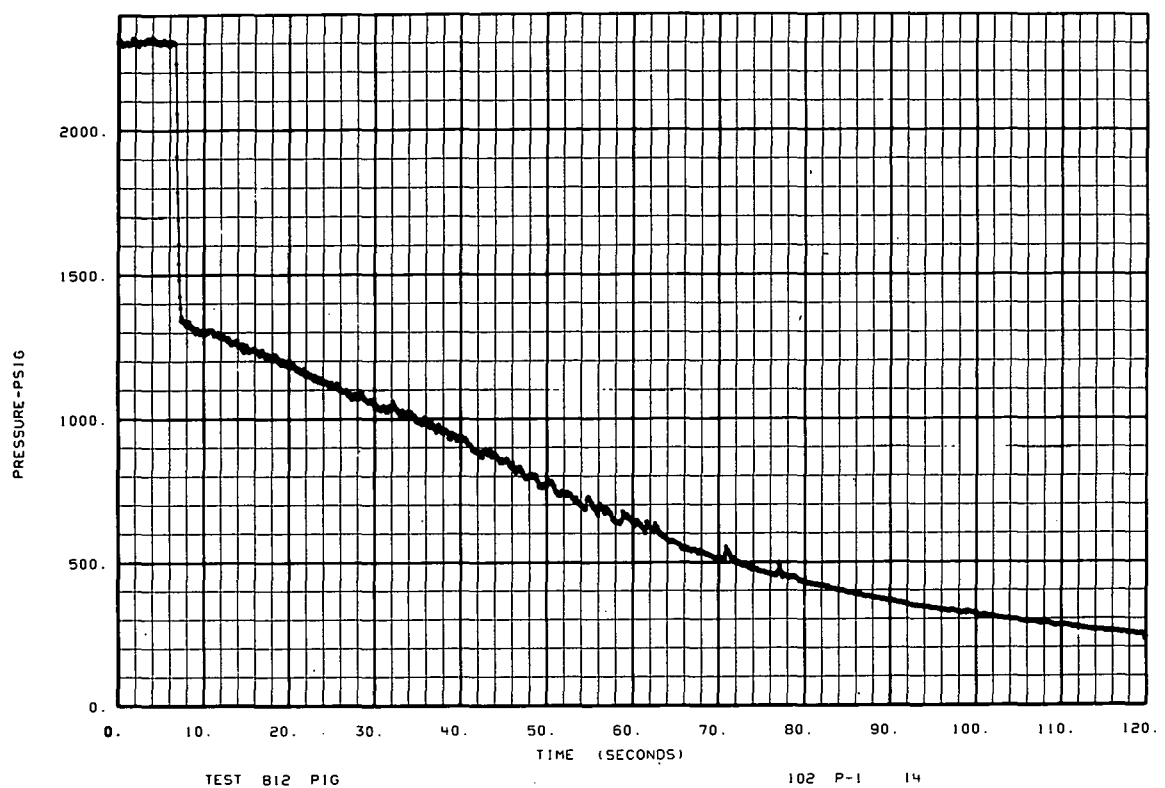
### B-III. PRESENTATION OF DATA

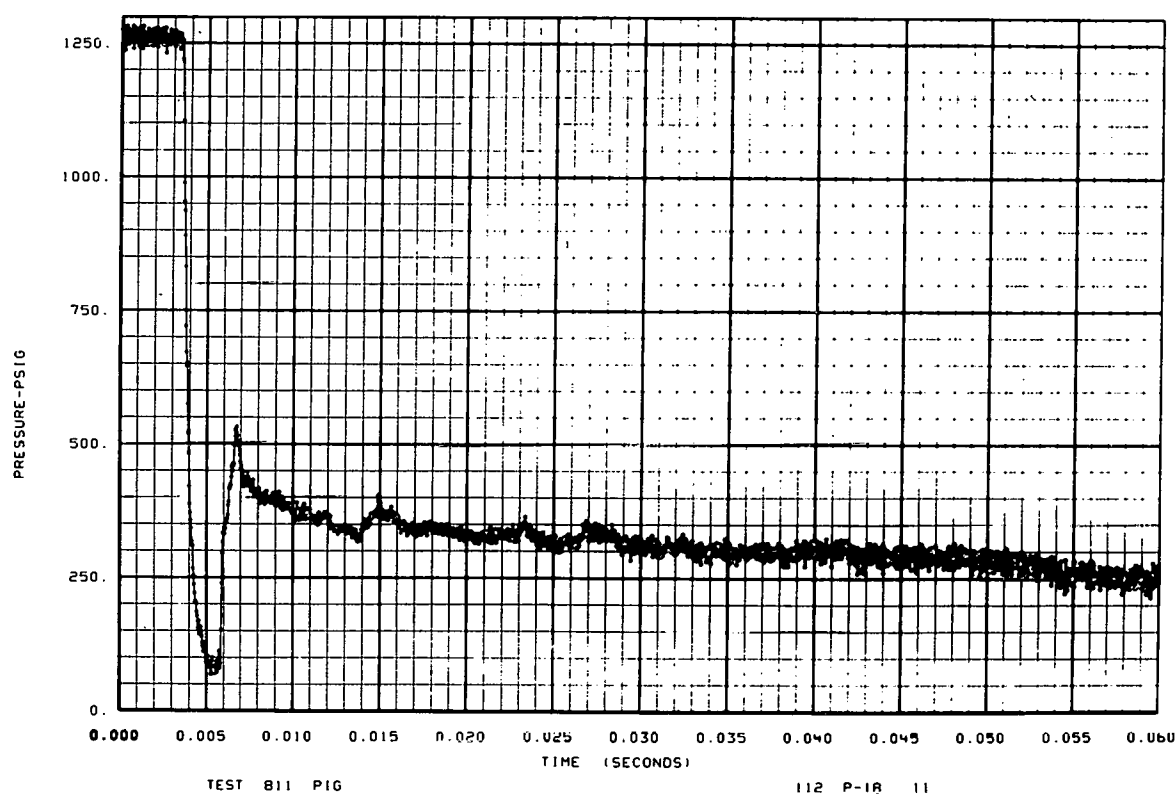
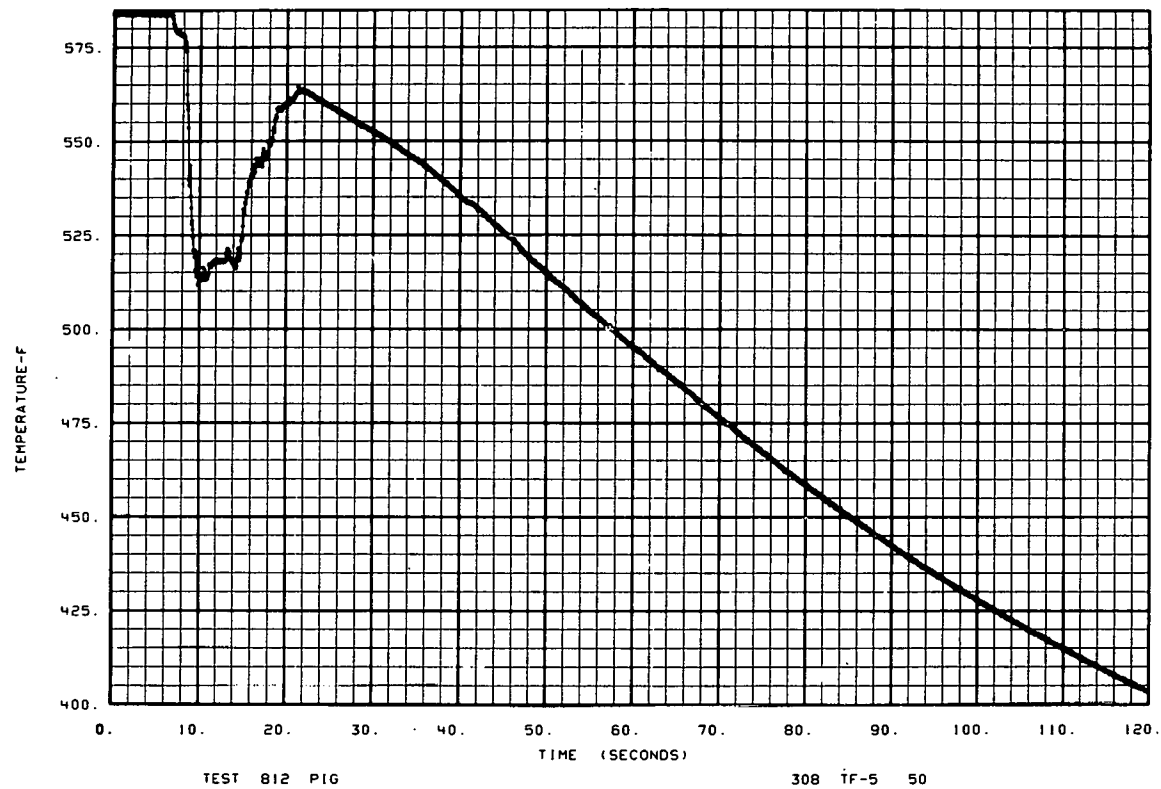
The curves contained in this appendix were obtained from digitization of the analog tapes and thus represent actual test data except for the corrections previously discussed. All plots consist of 2000 digital points regardless of the time covered by the plot. The curves were reproduced from micro-film obtained from a data processing program.

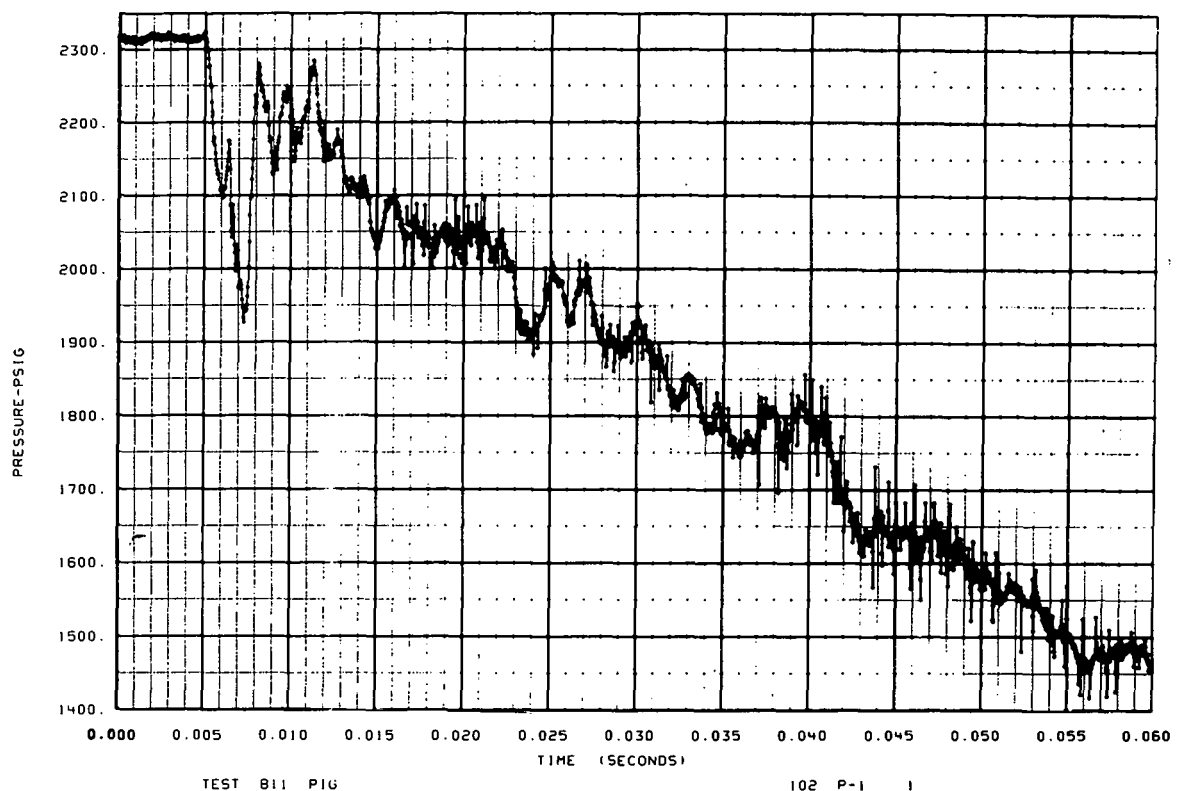
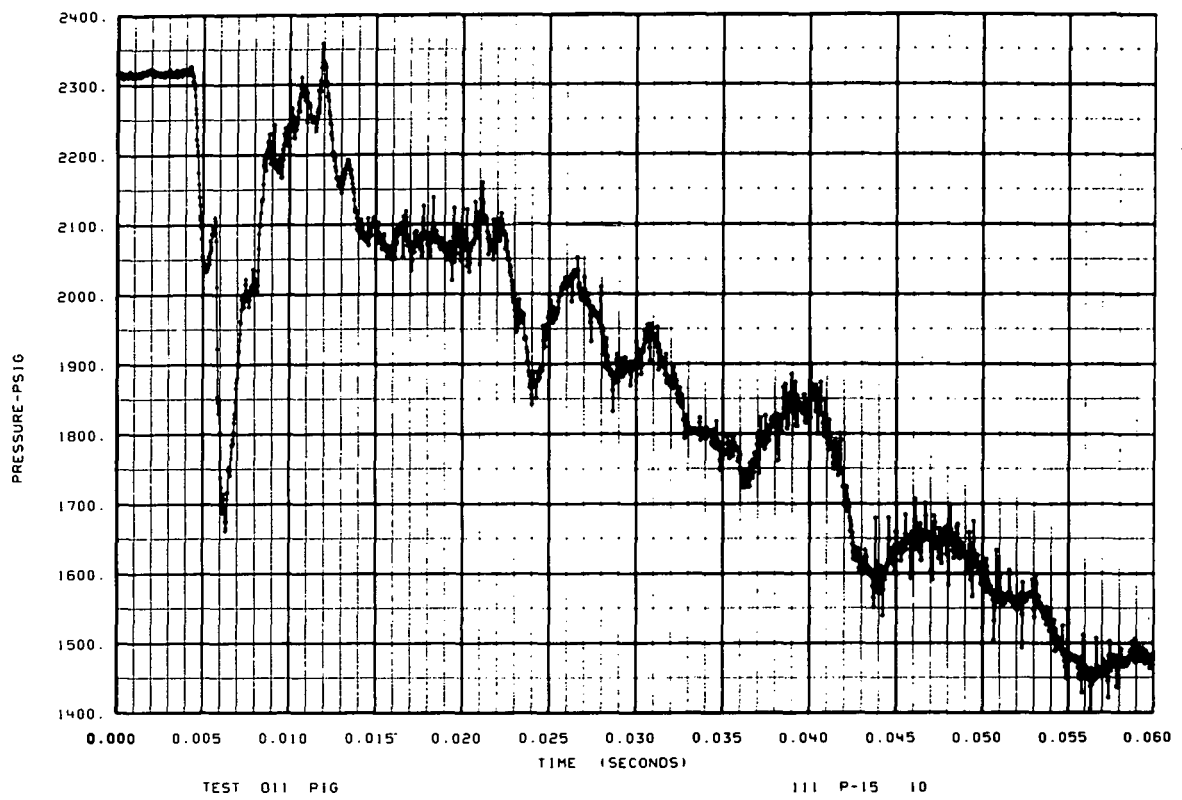


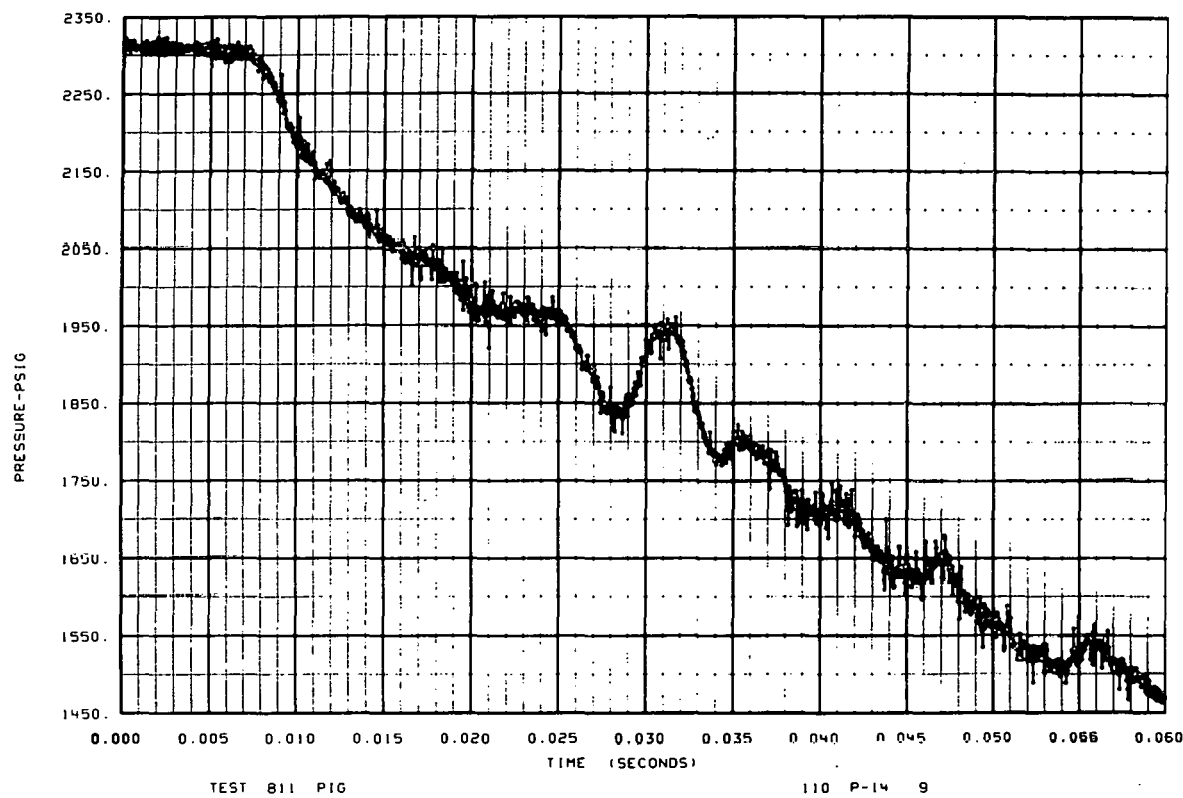
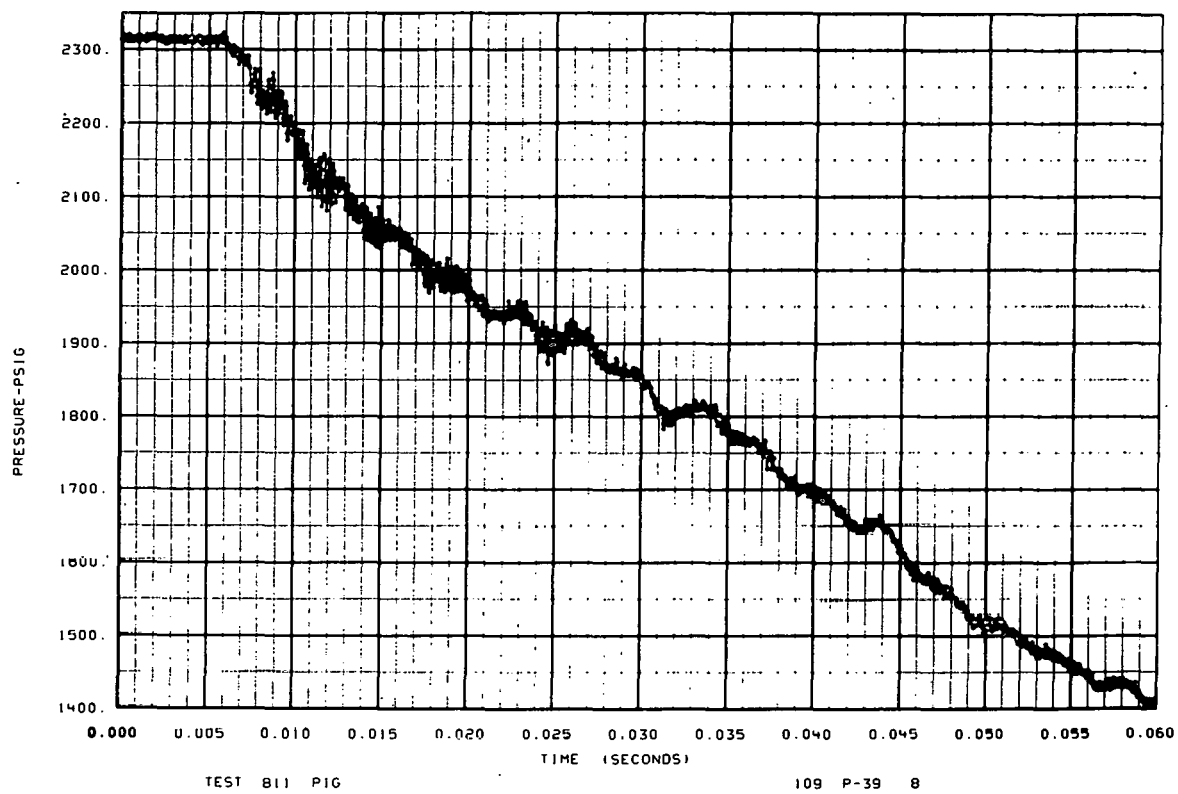


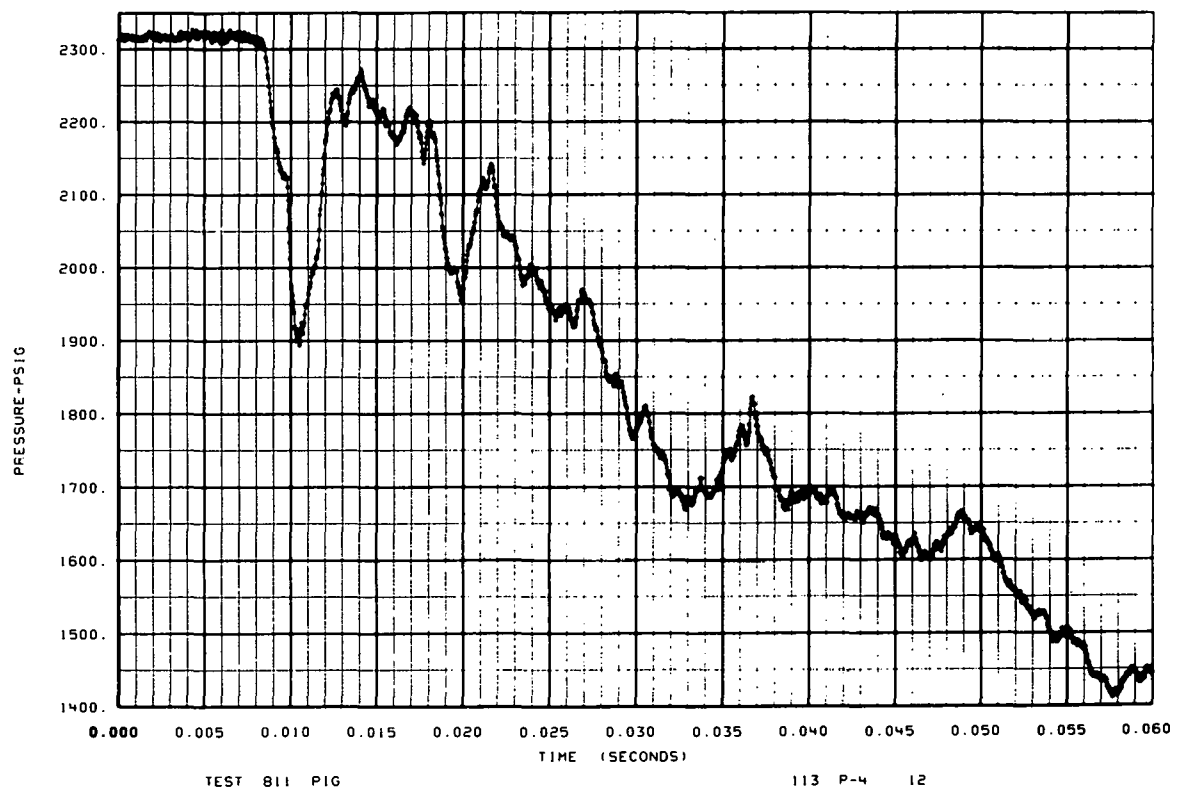
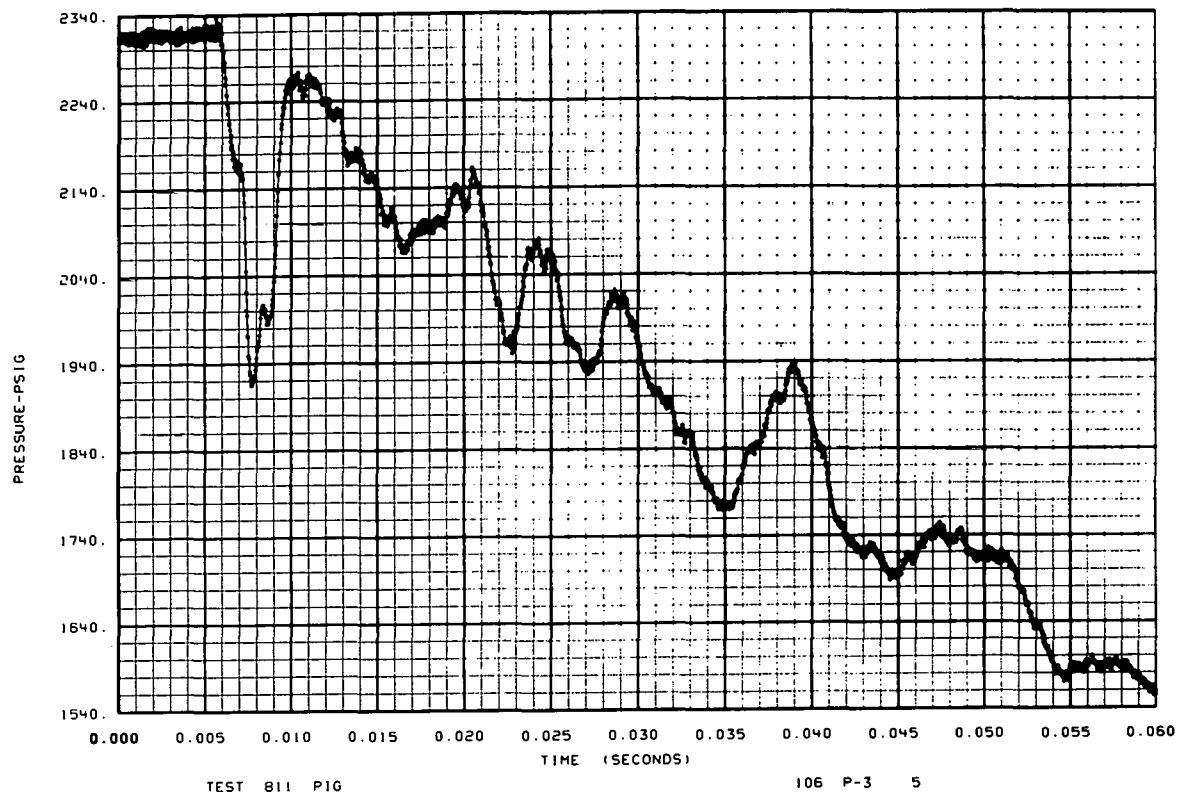


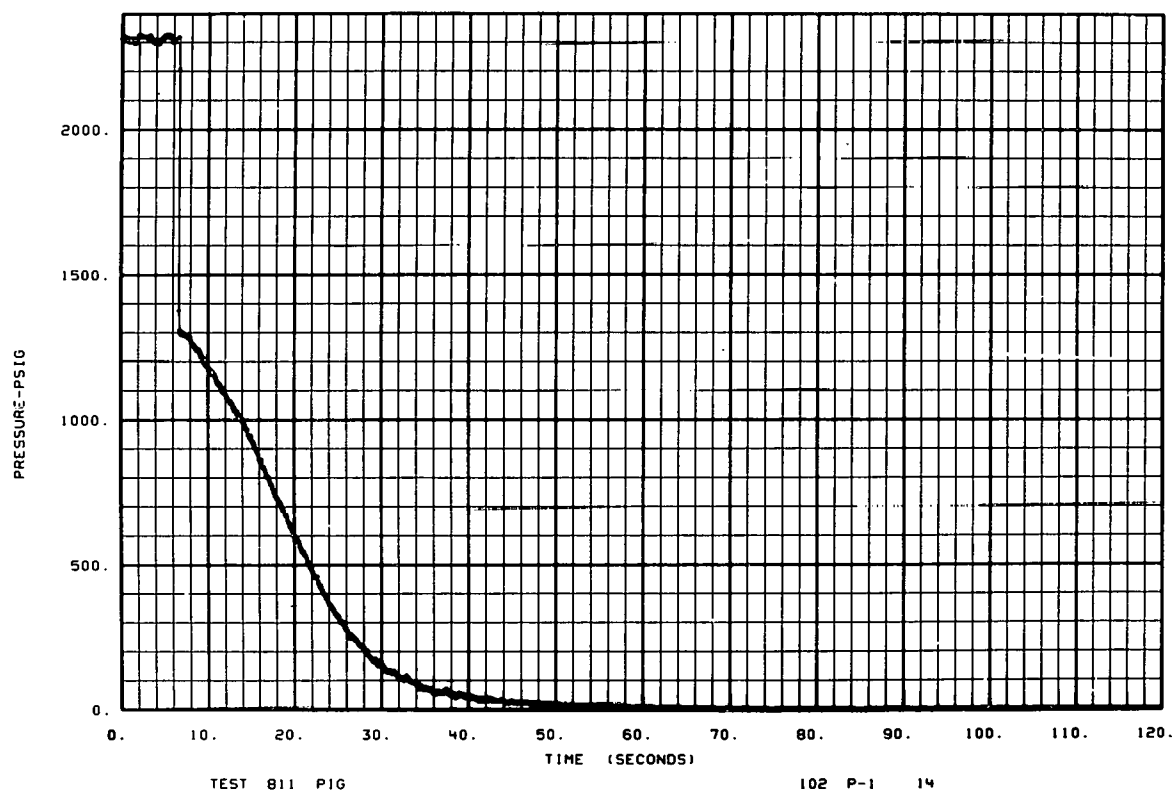
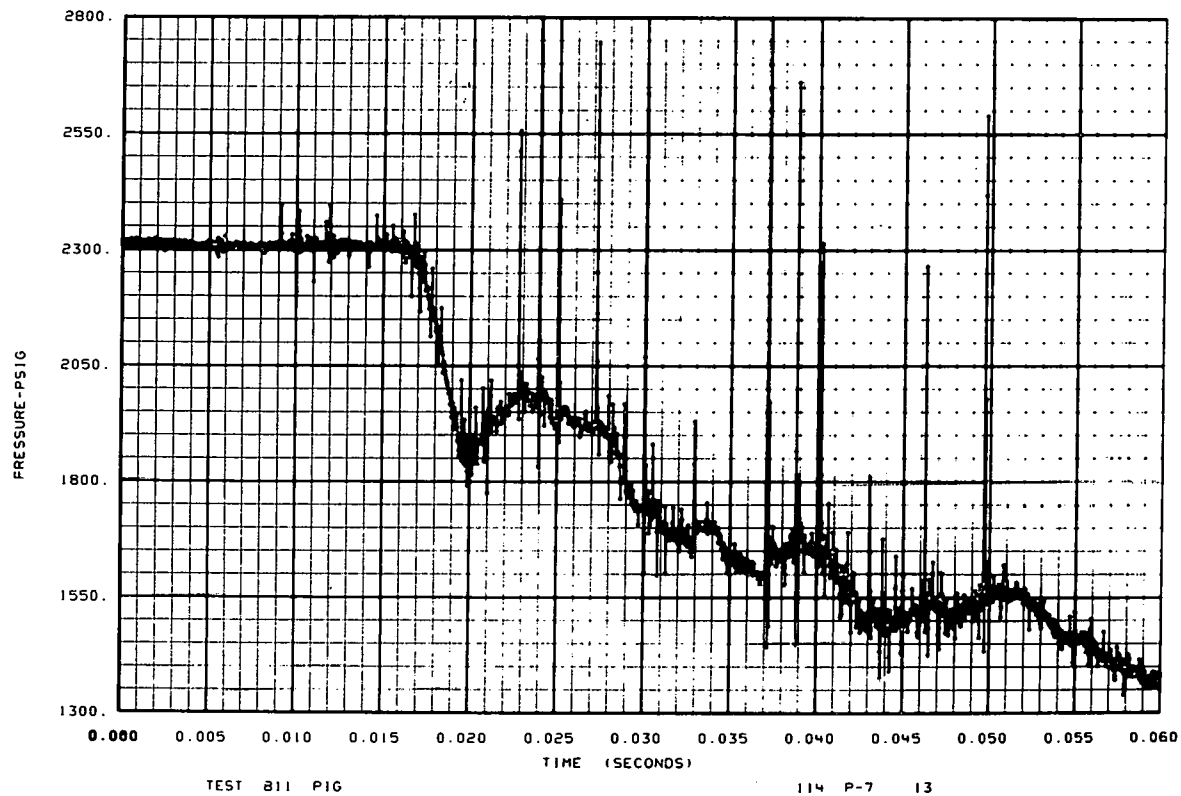


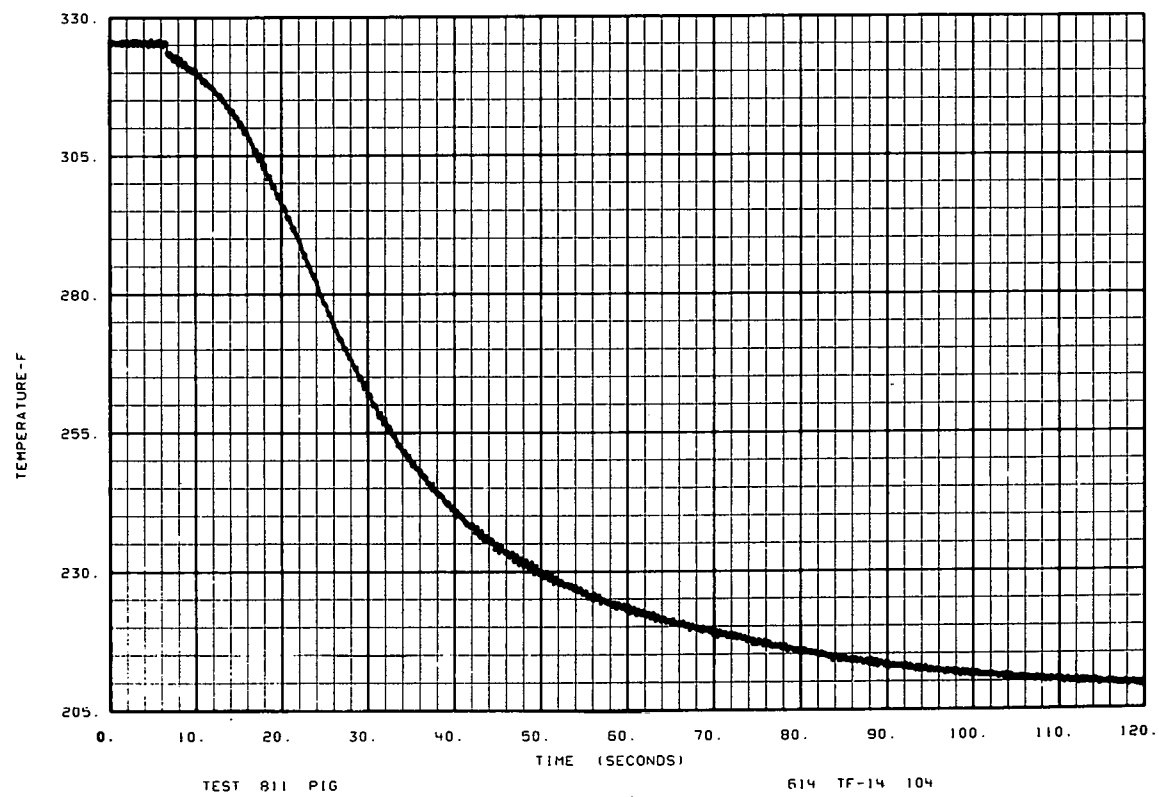
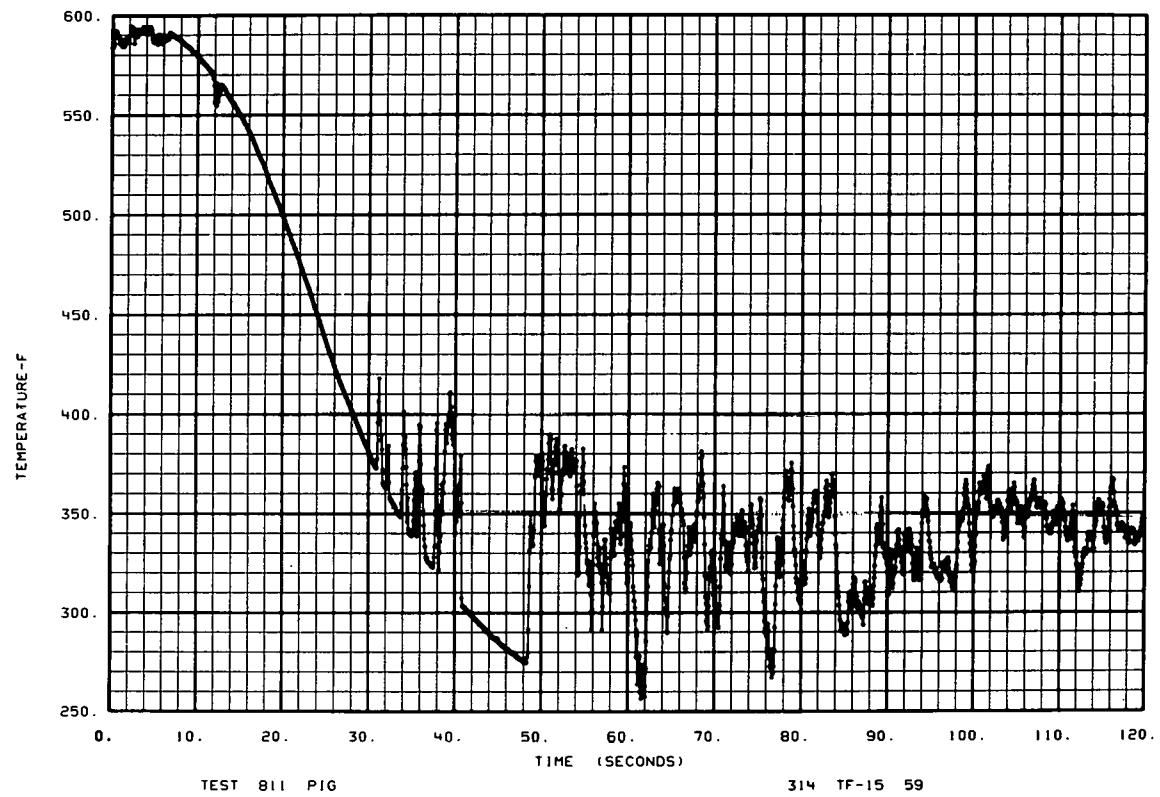


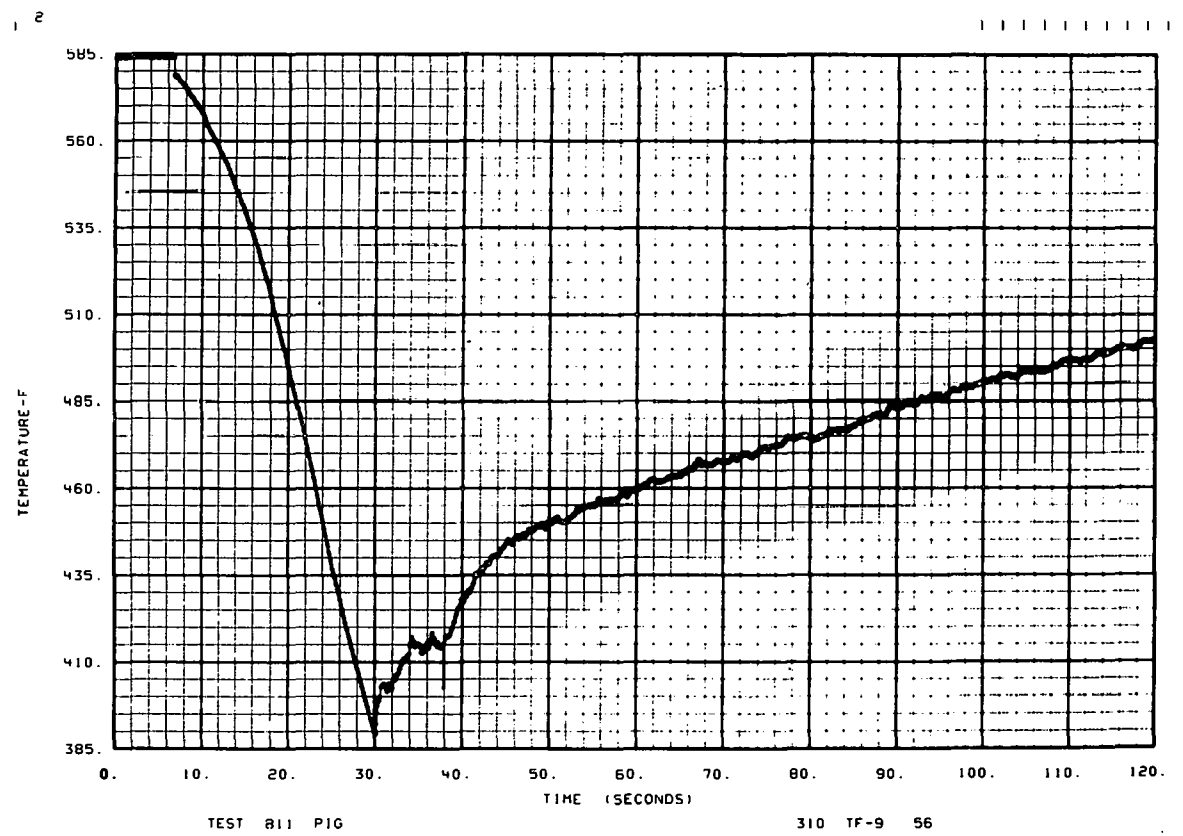
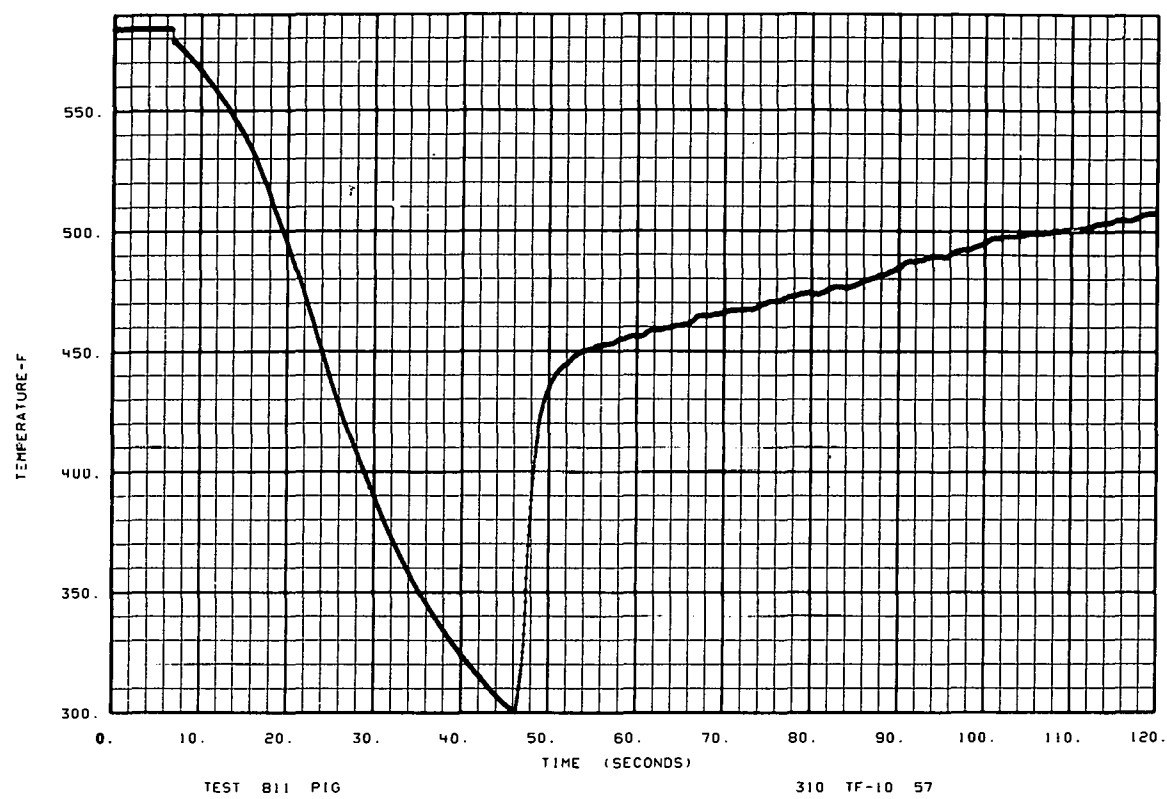


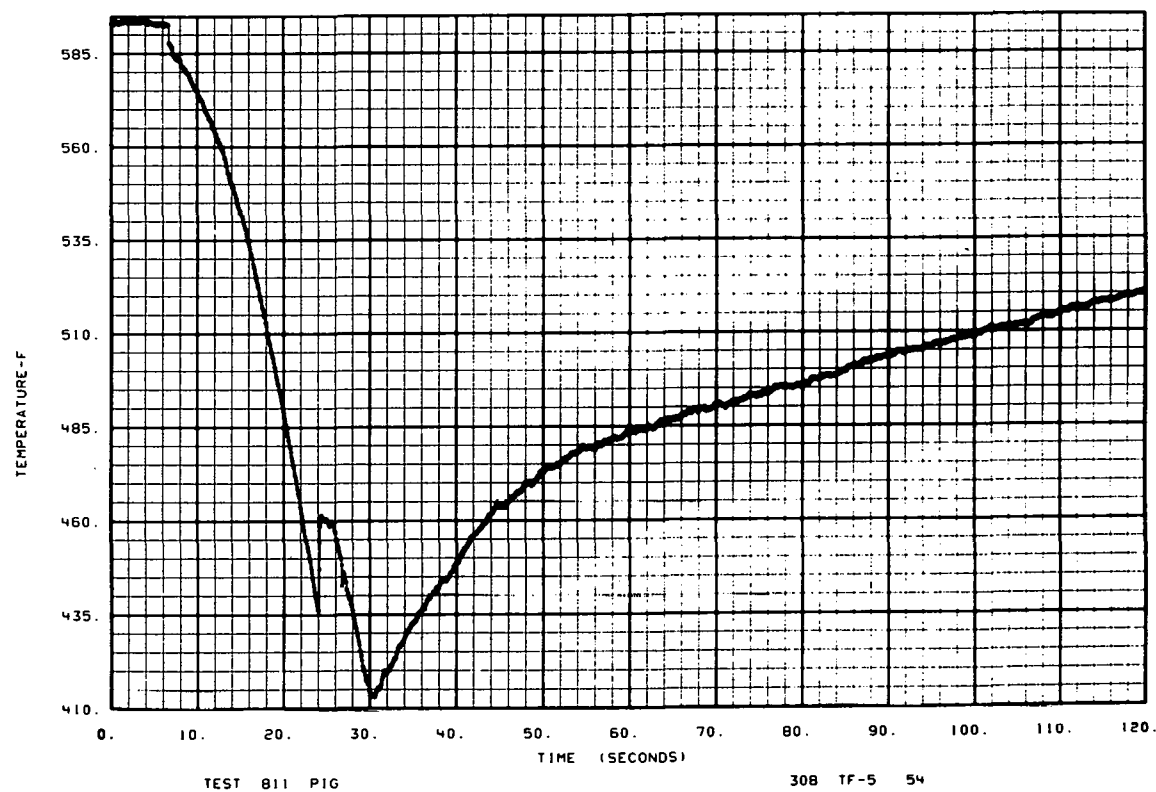
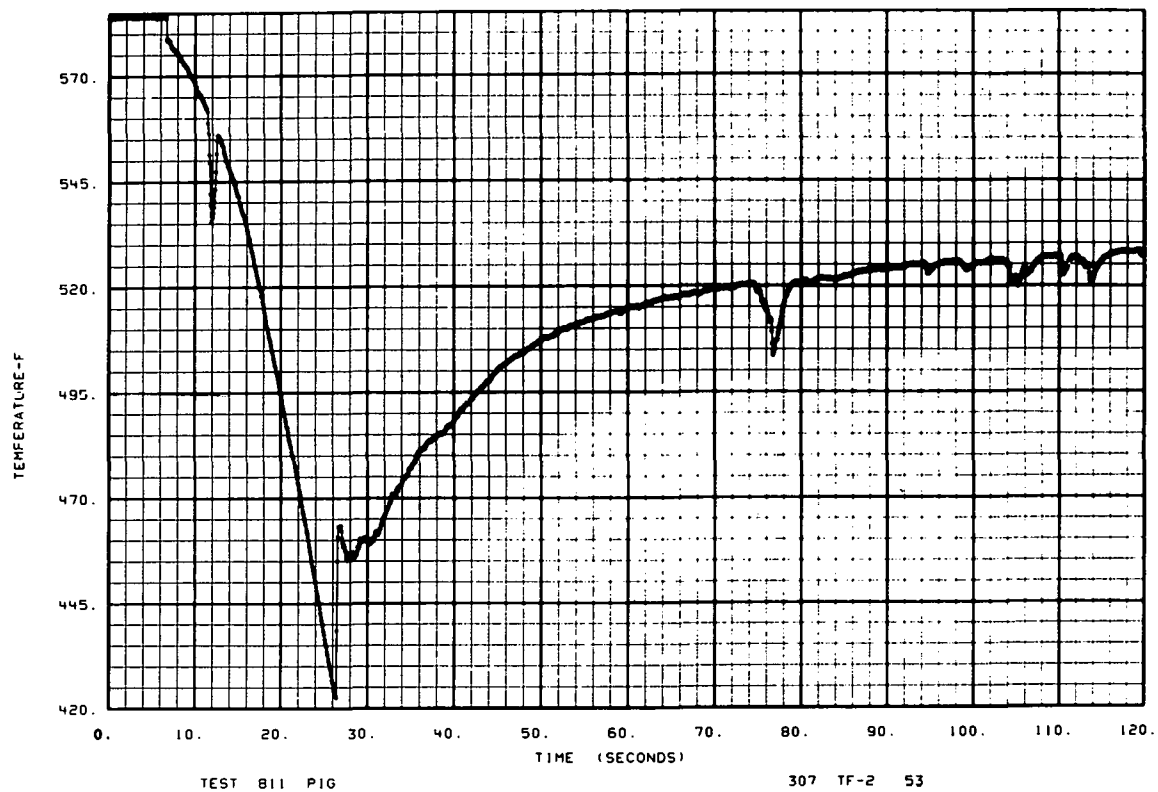


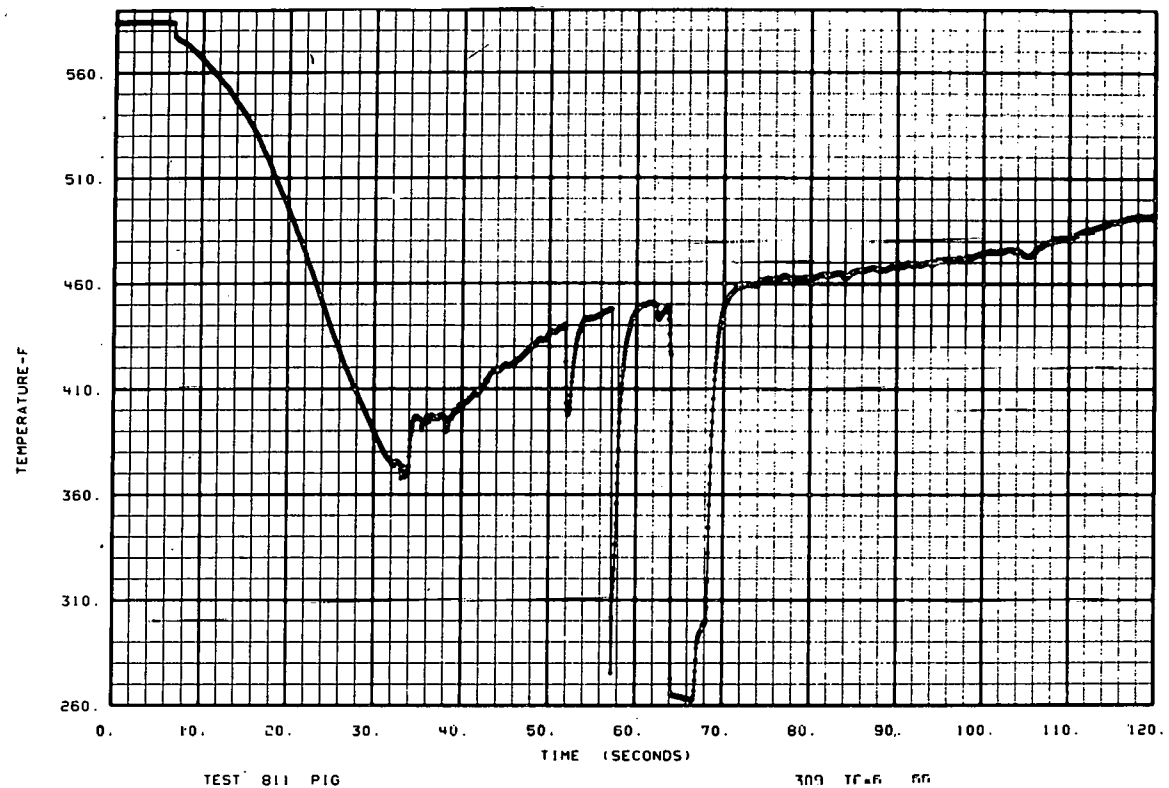


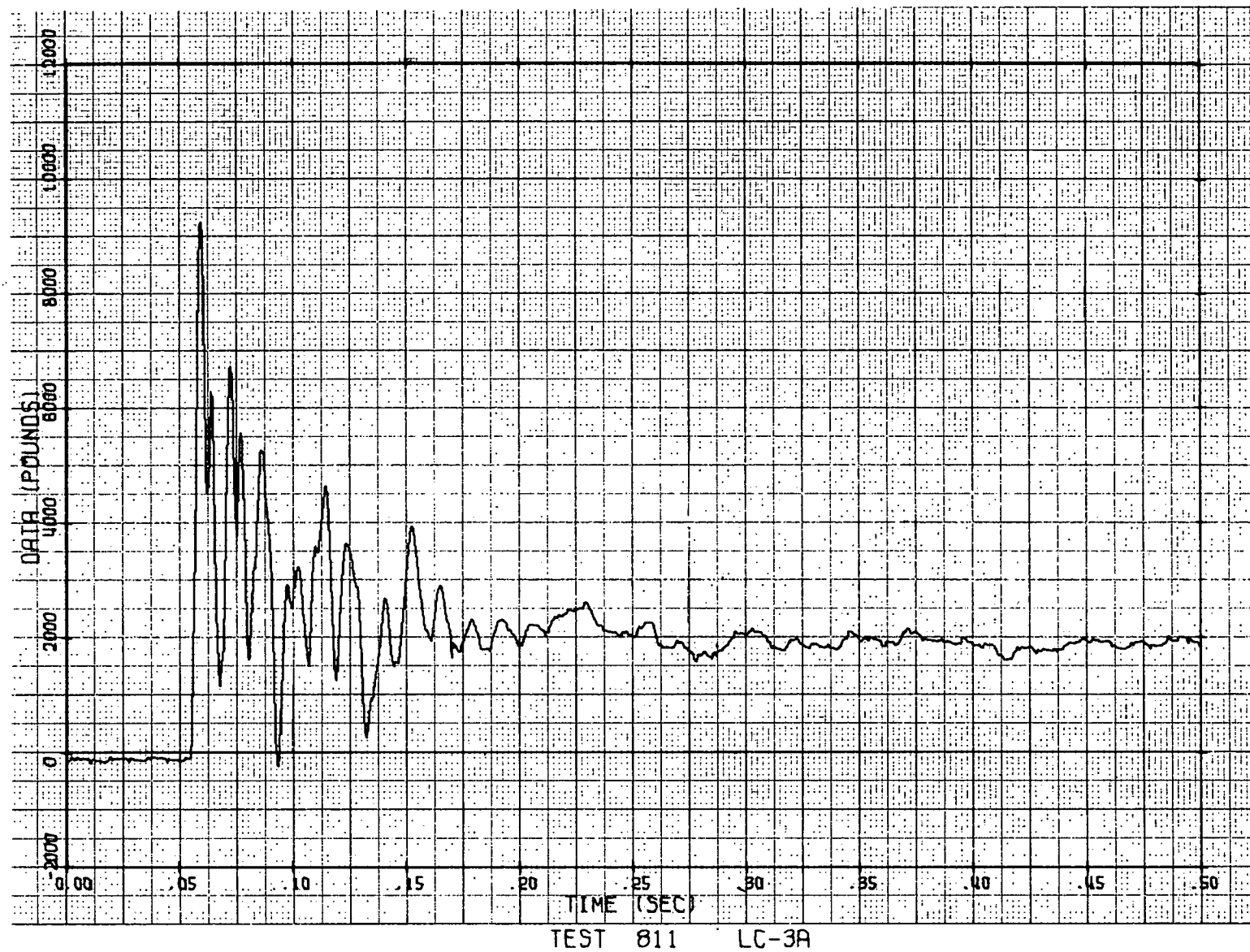


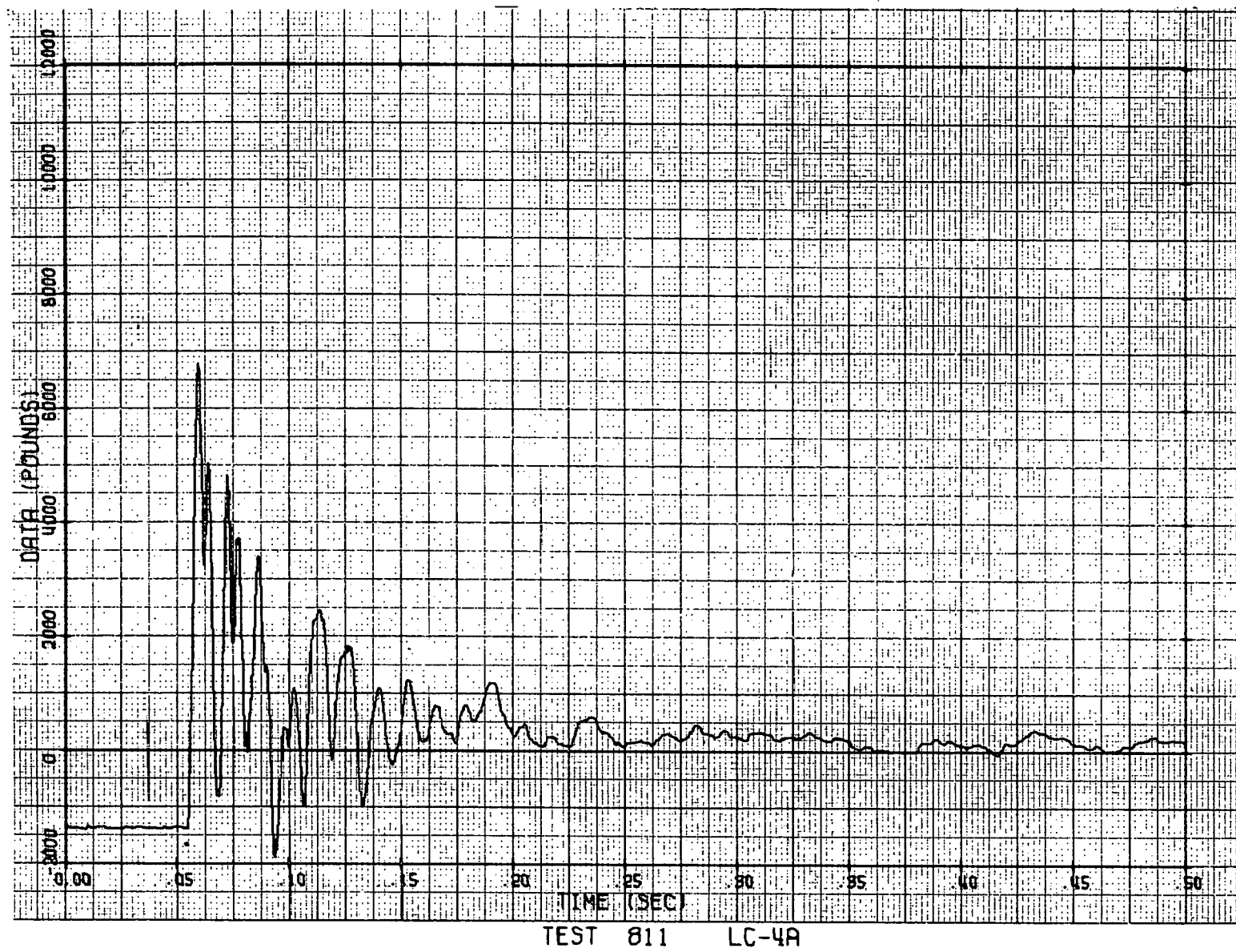


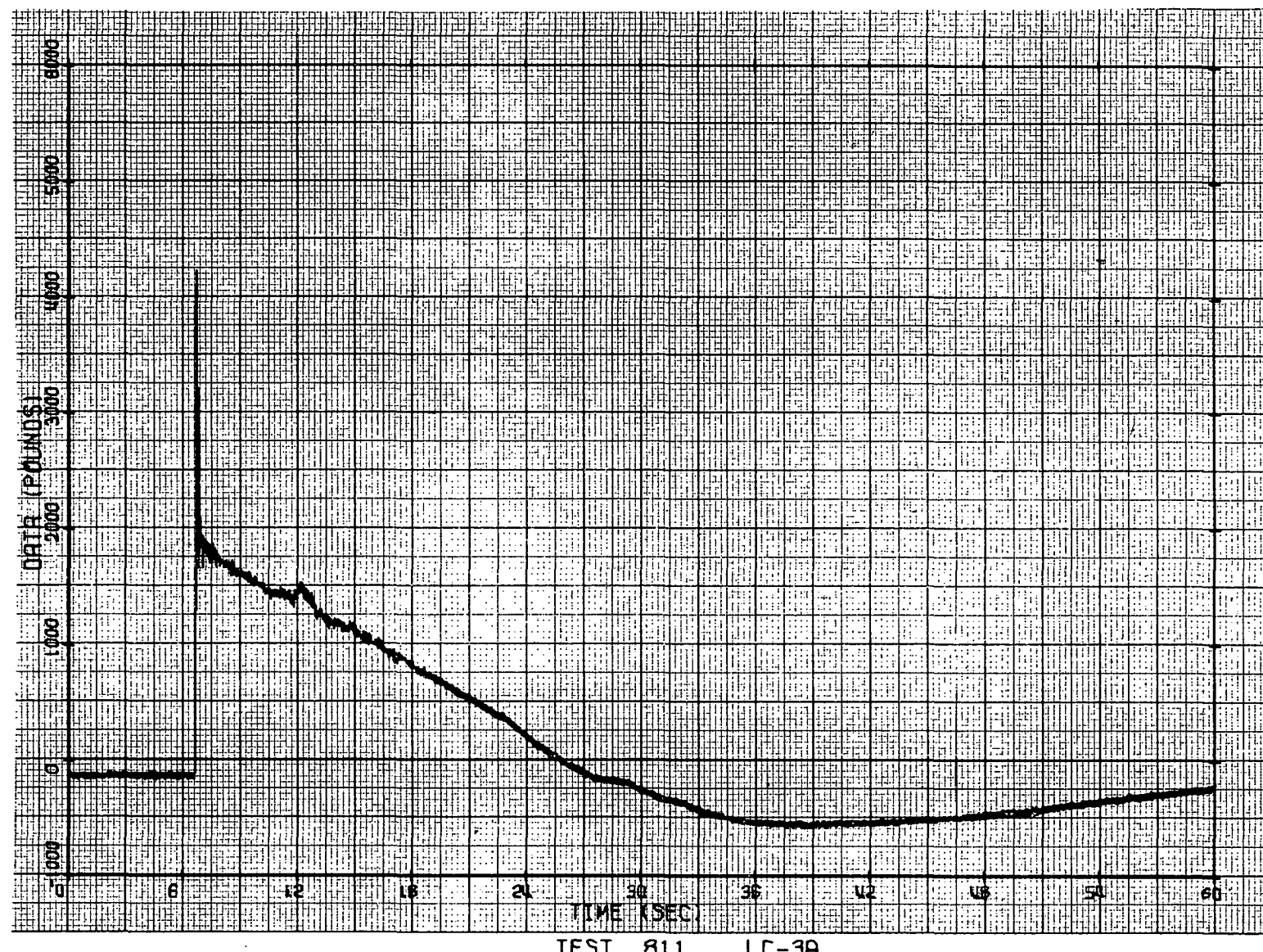




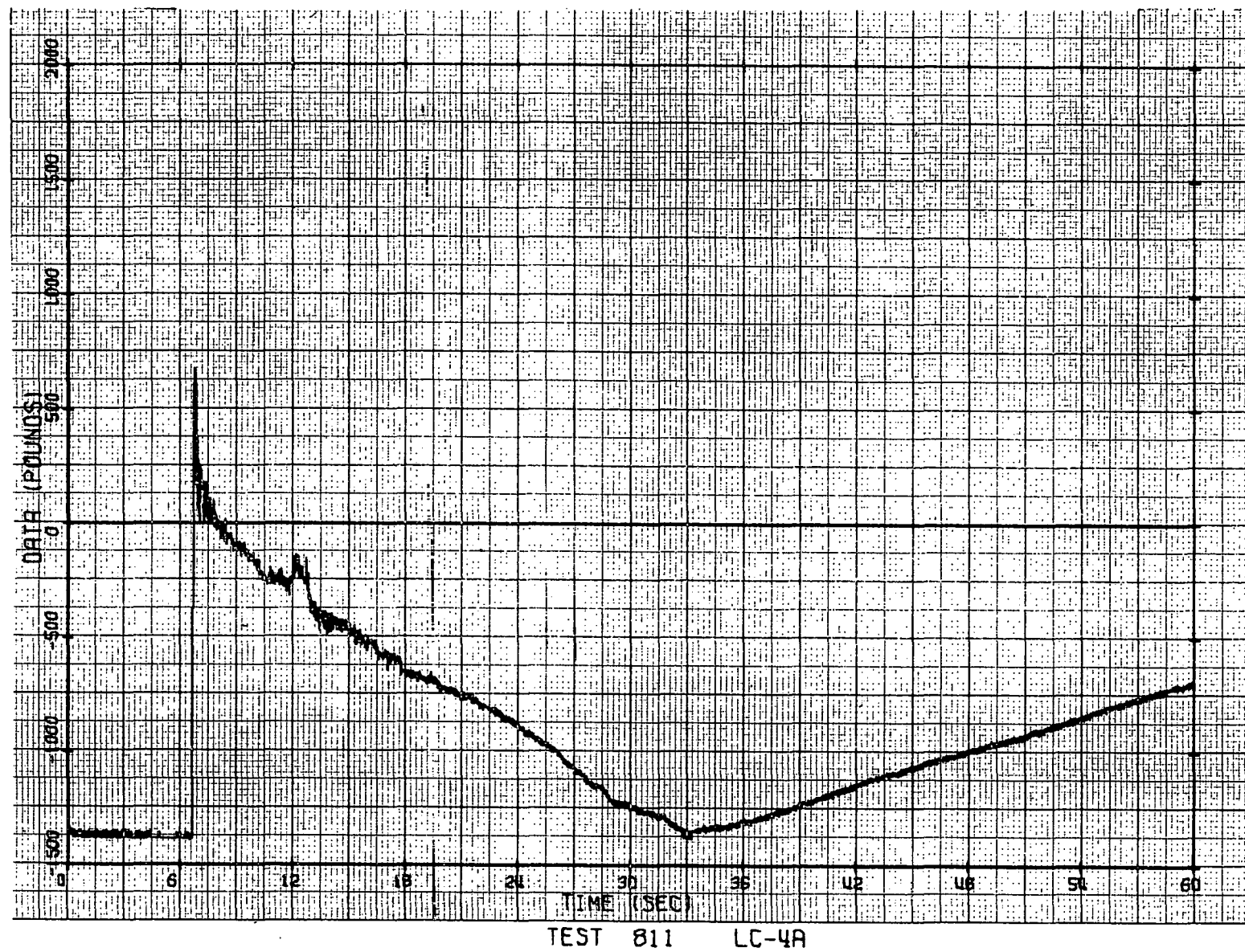


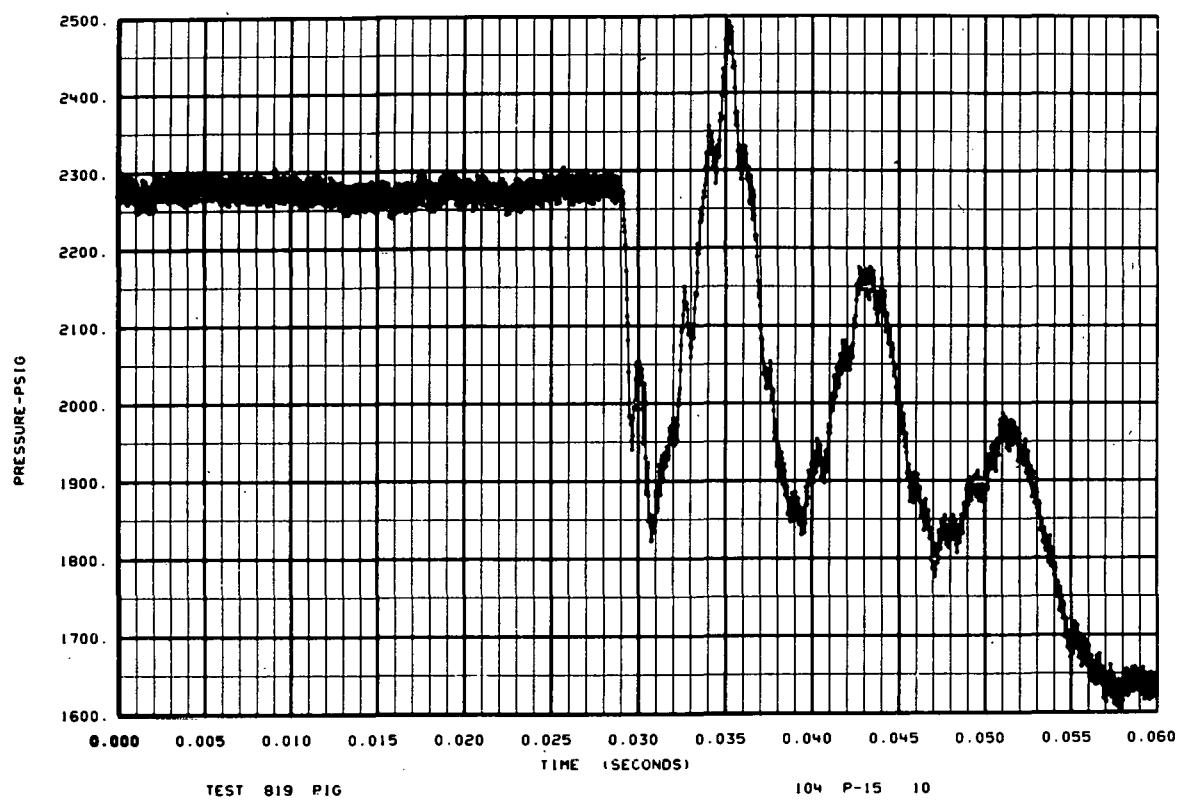
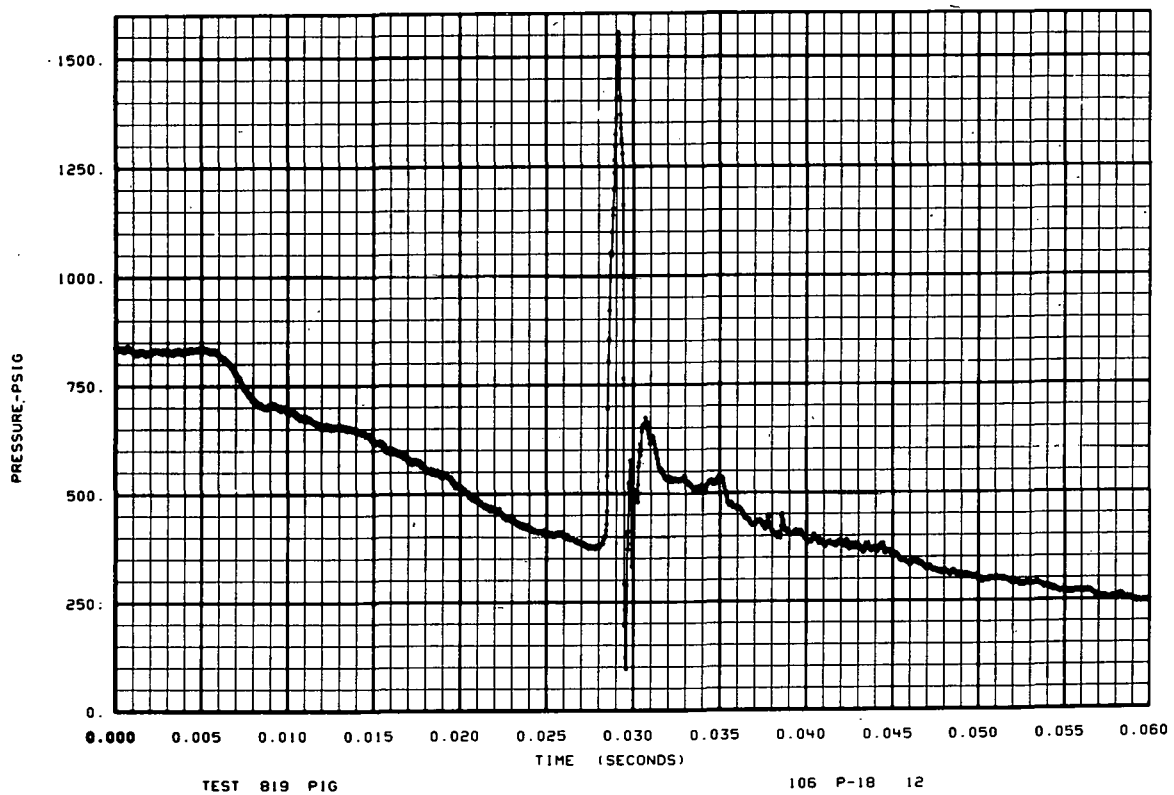


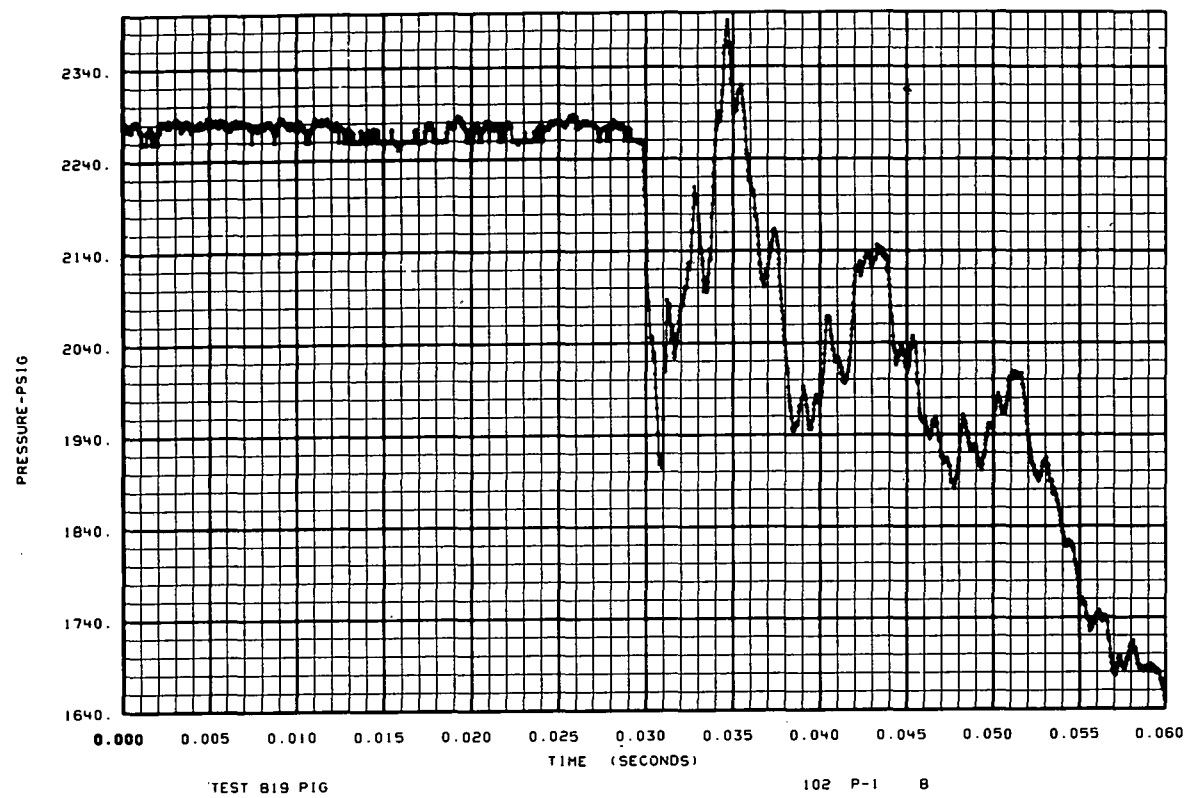


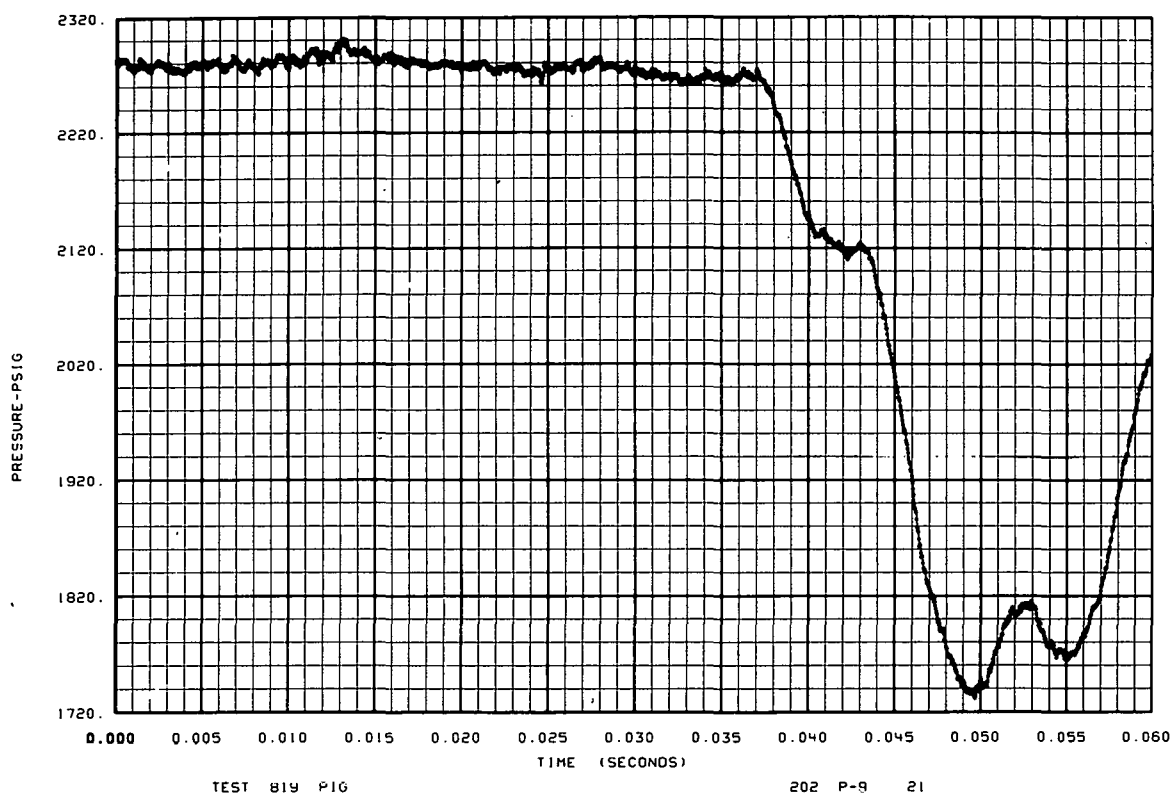
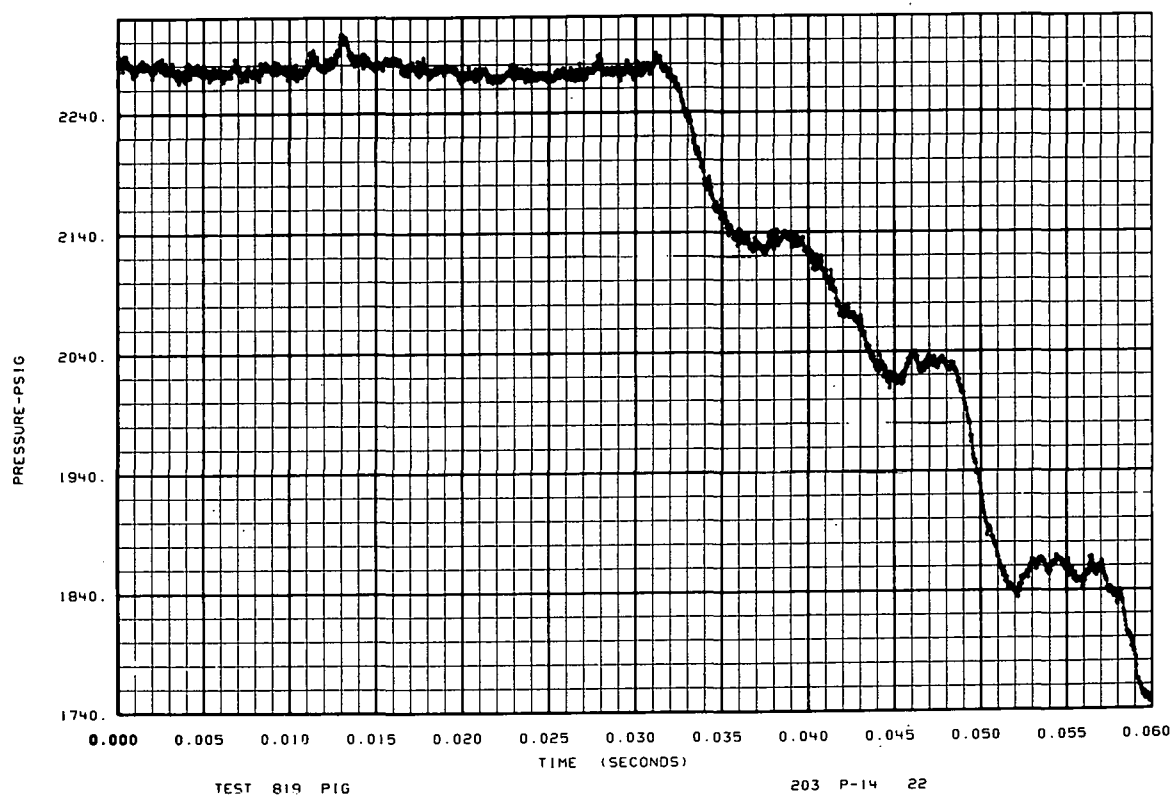


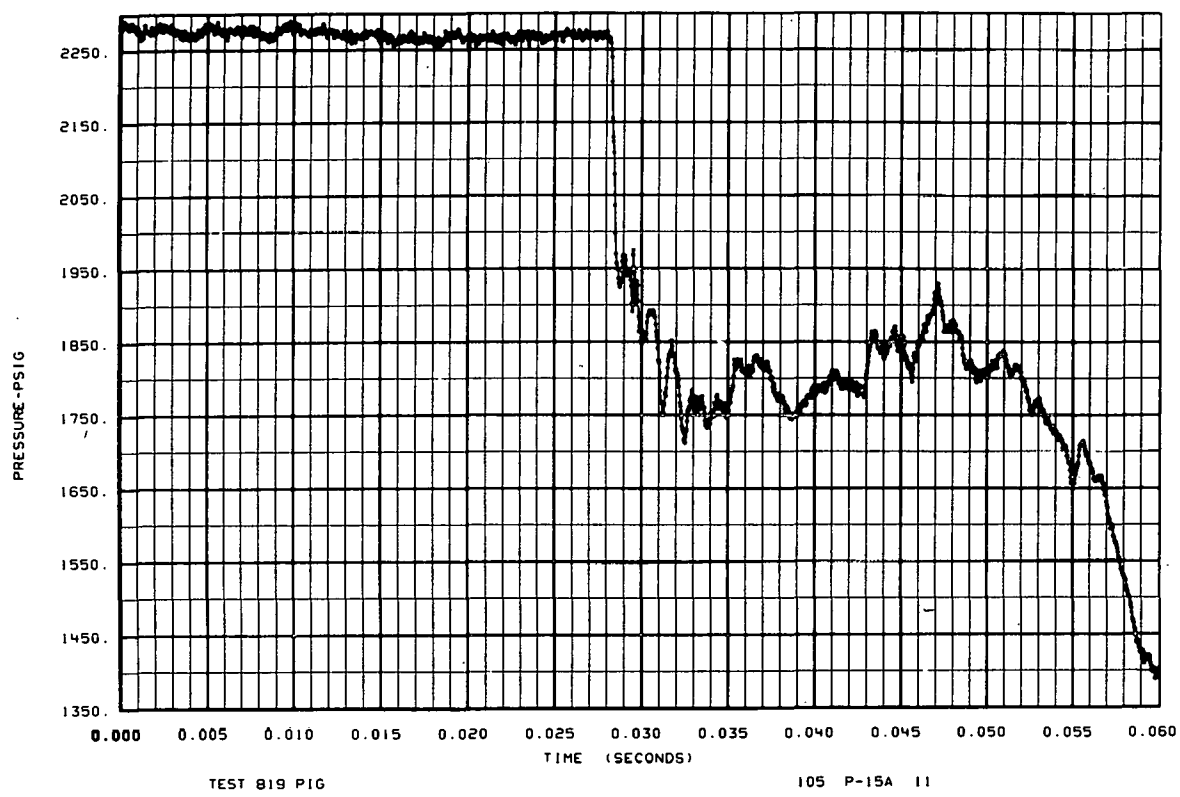
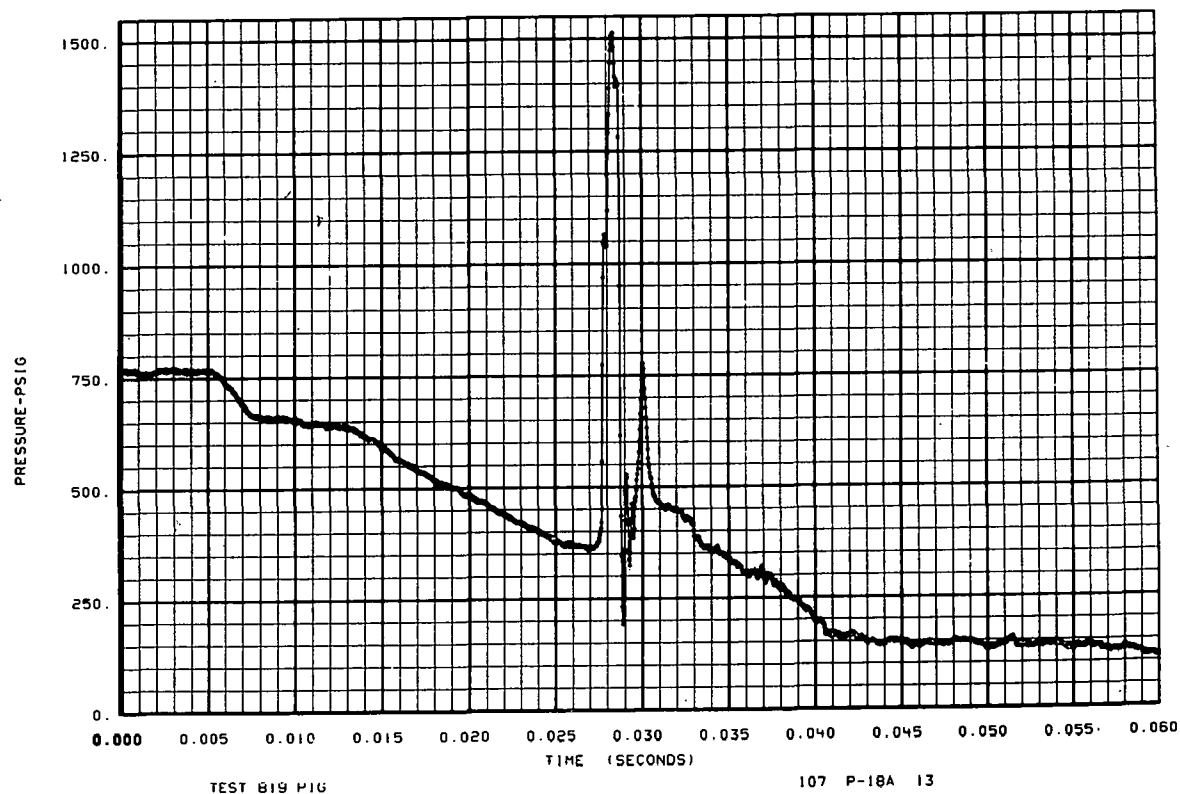
TEST 811 LC-3A

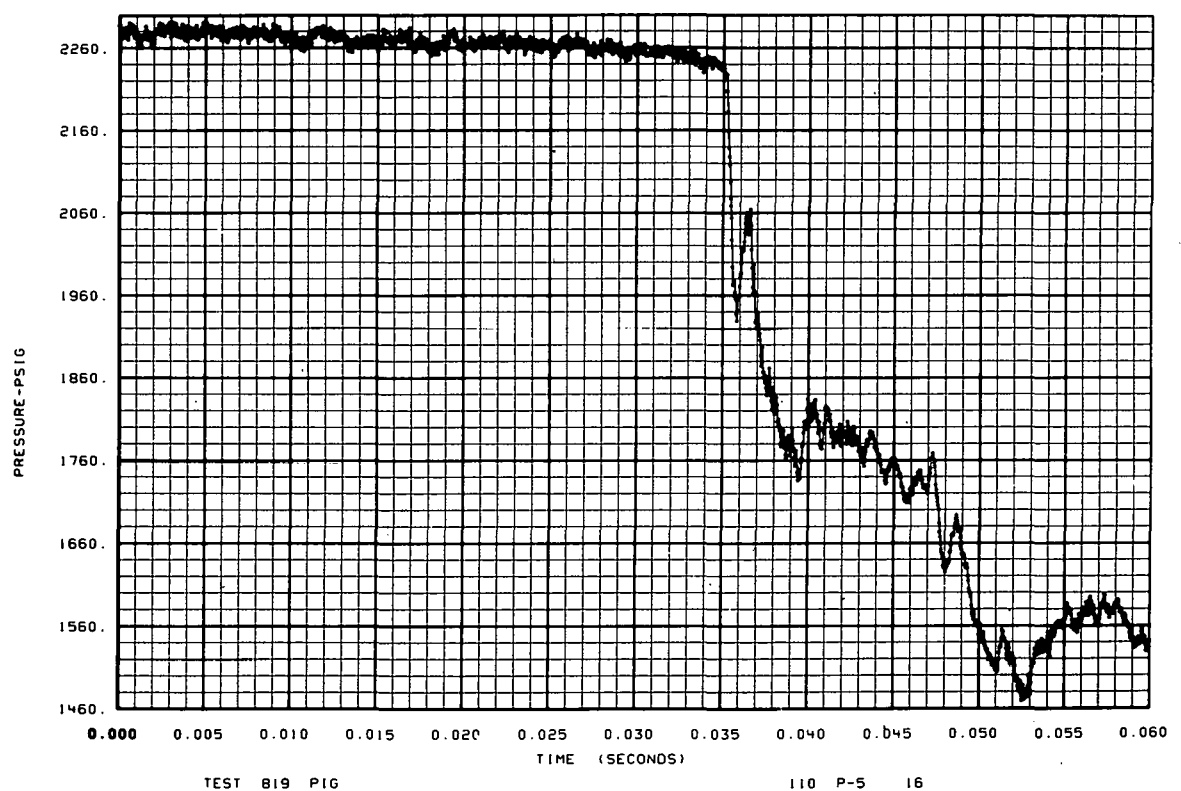
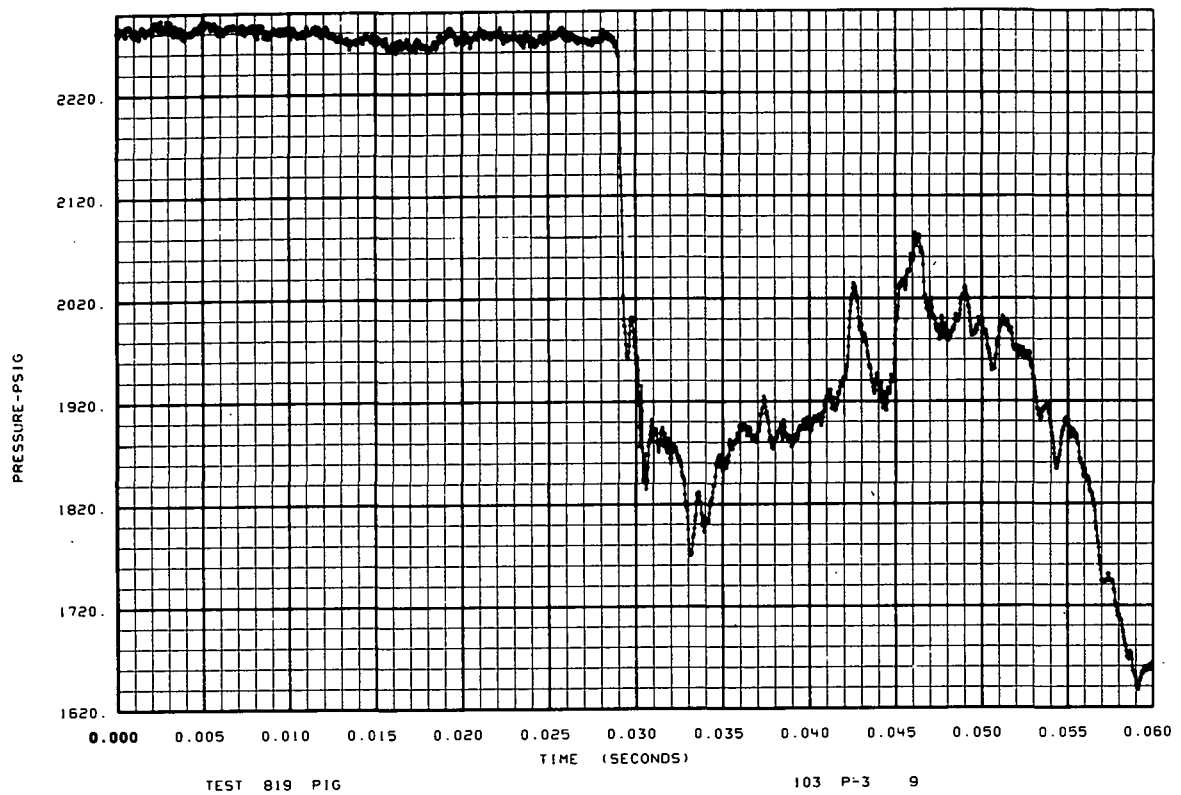


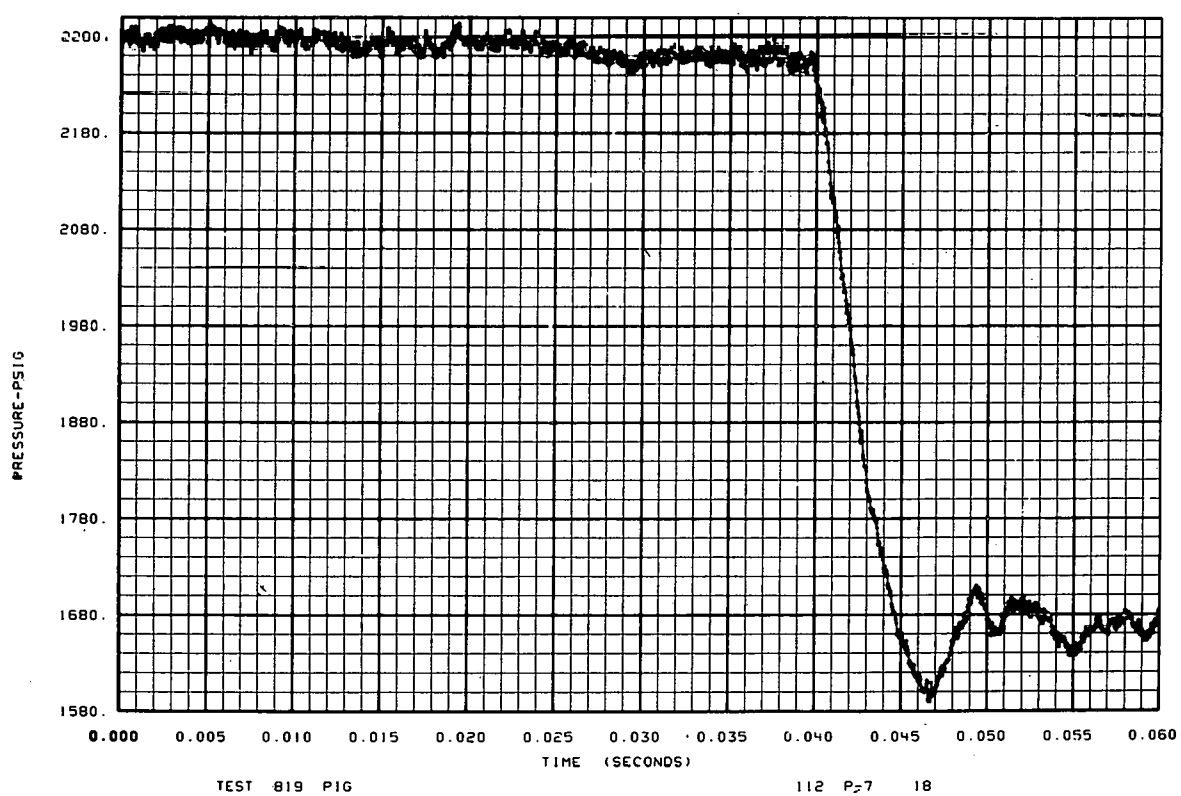
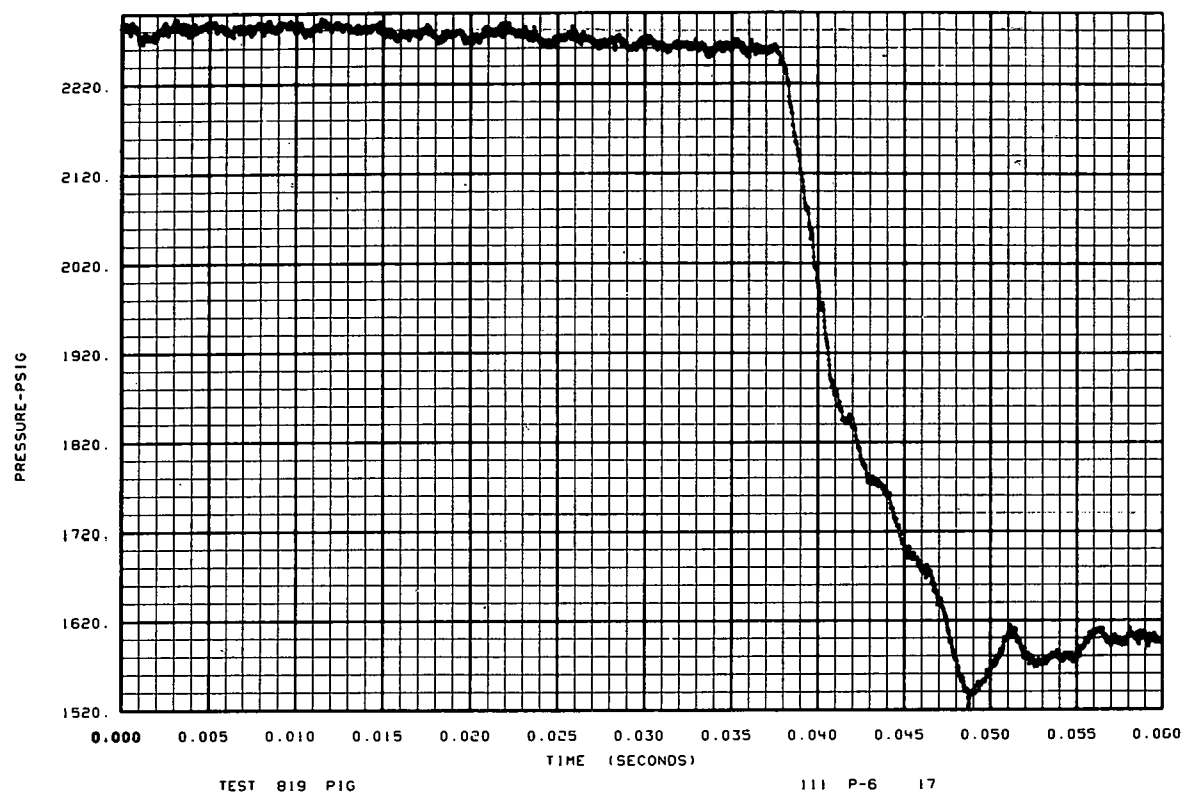


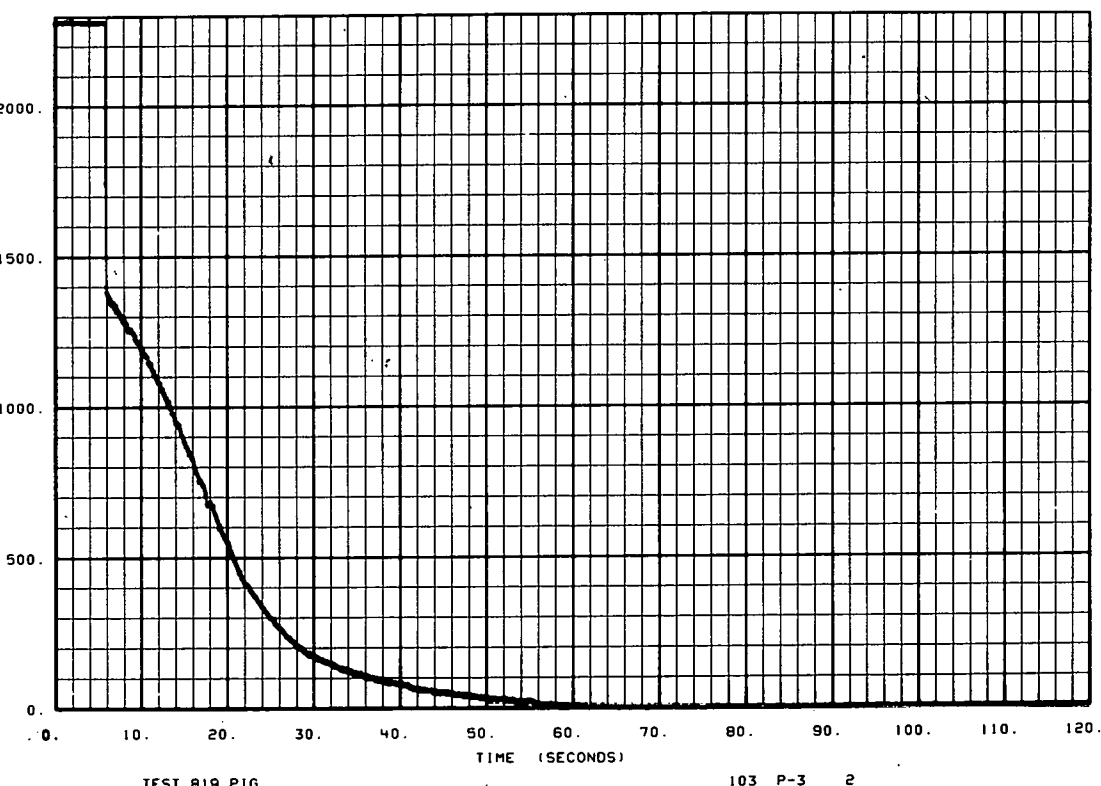
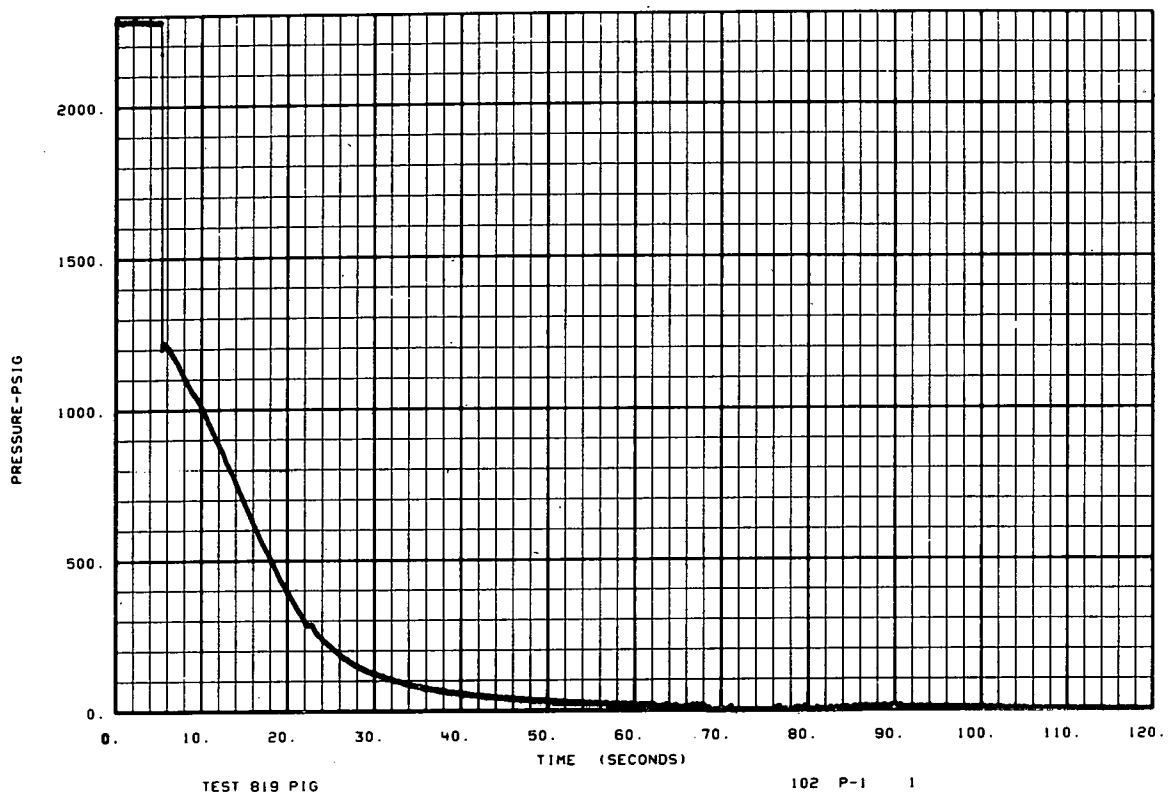


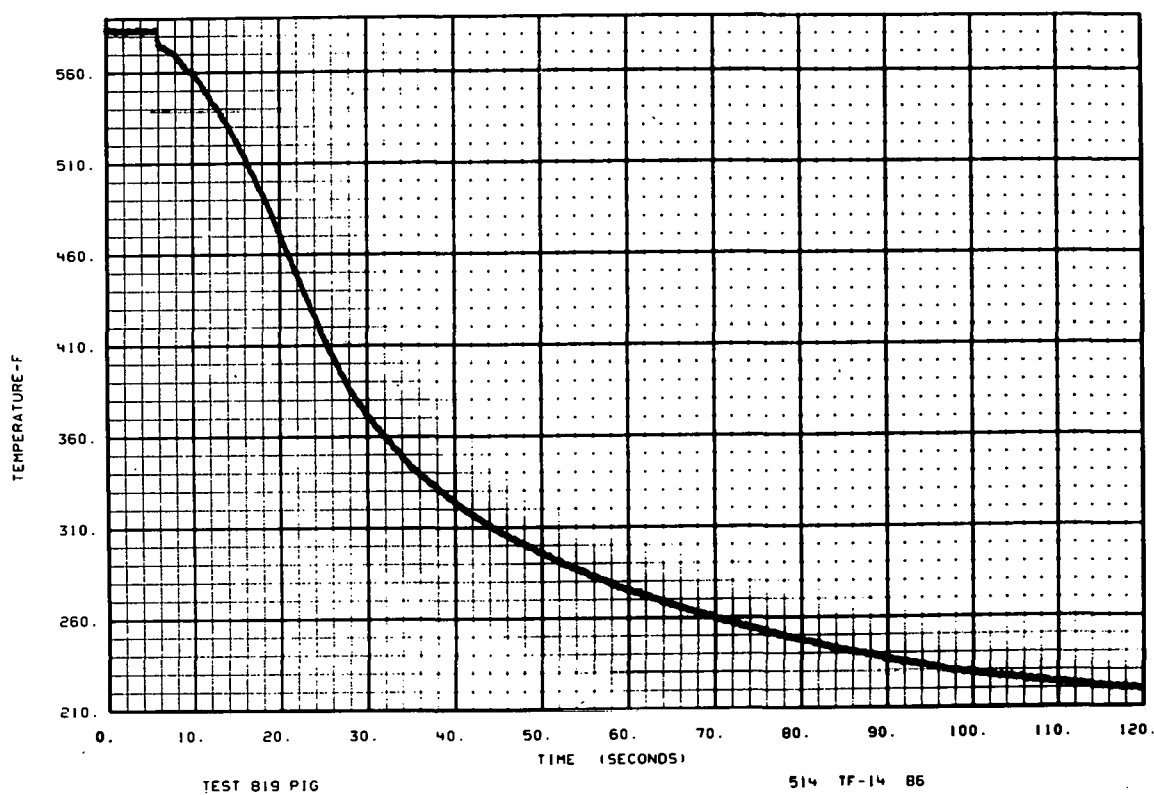
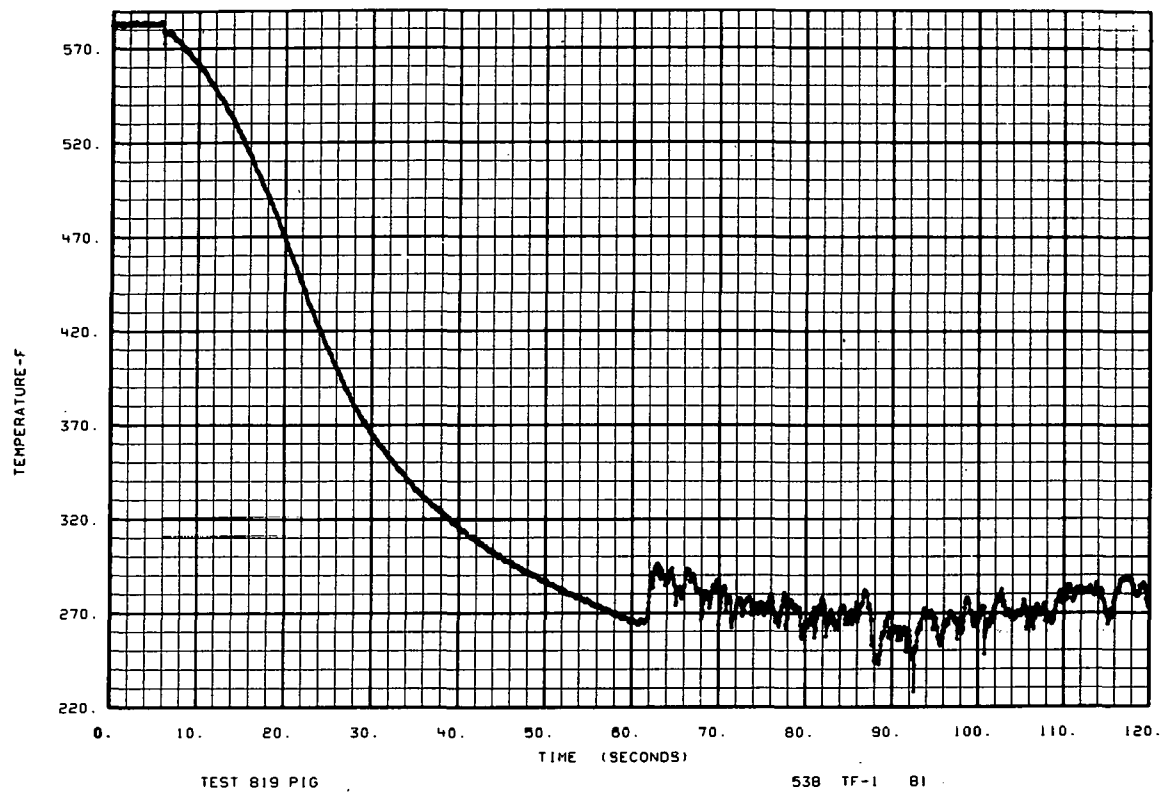


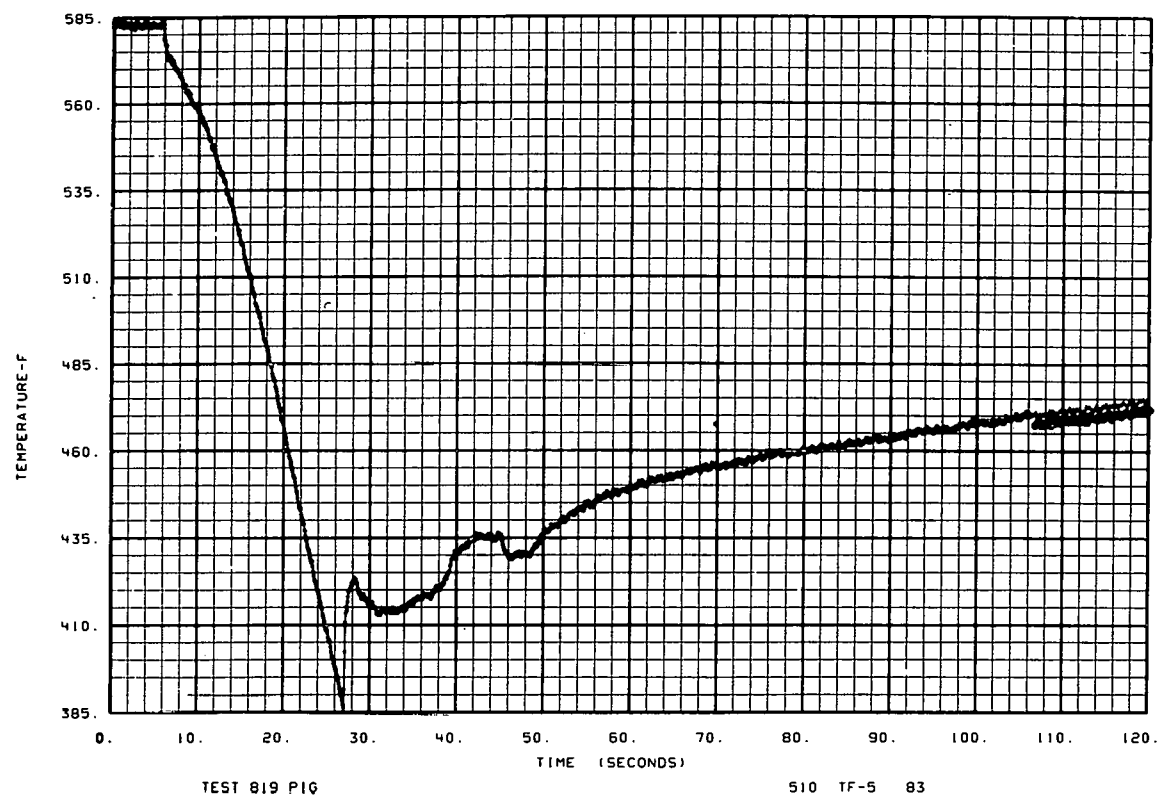
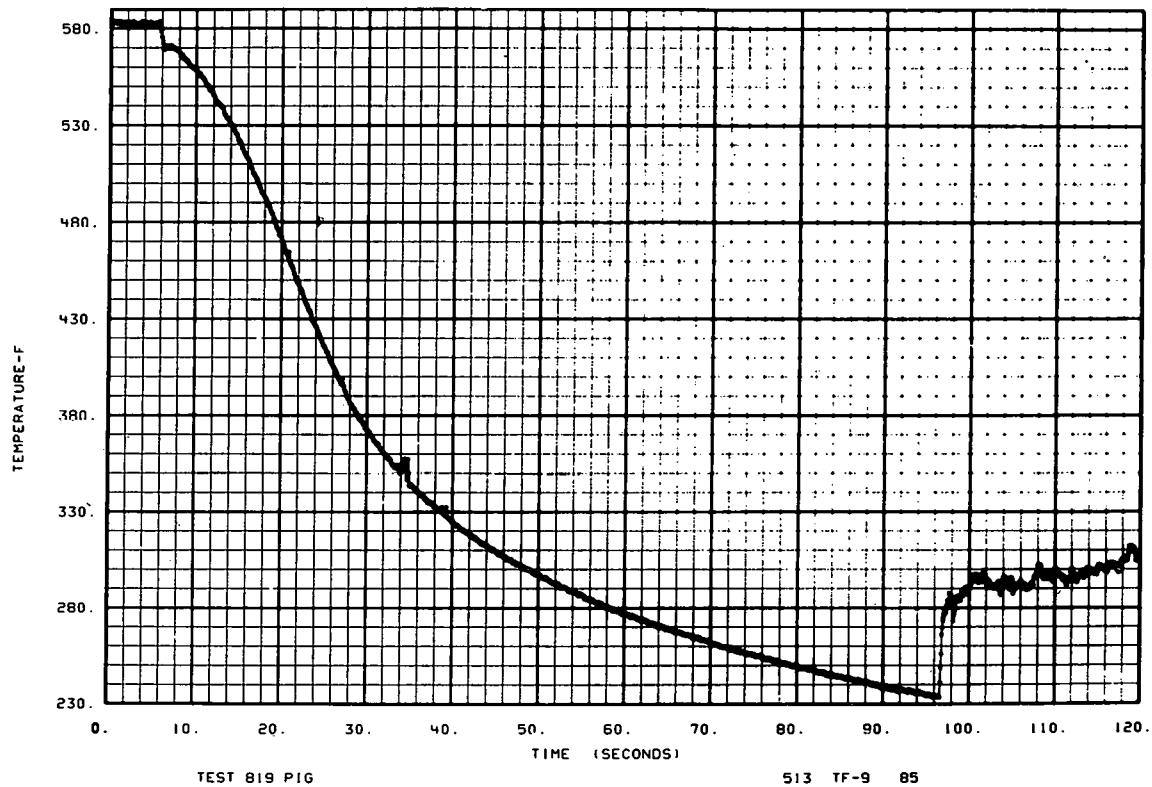


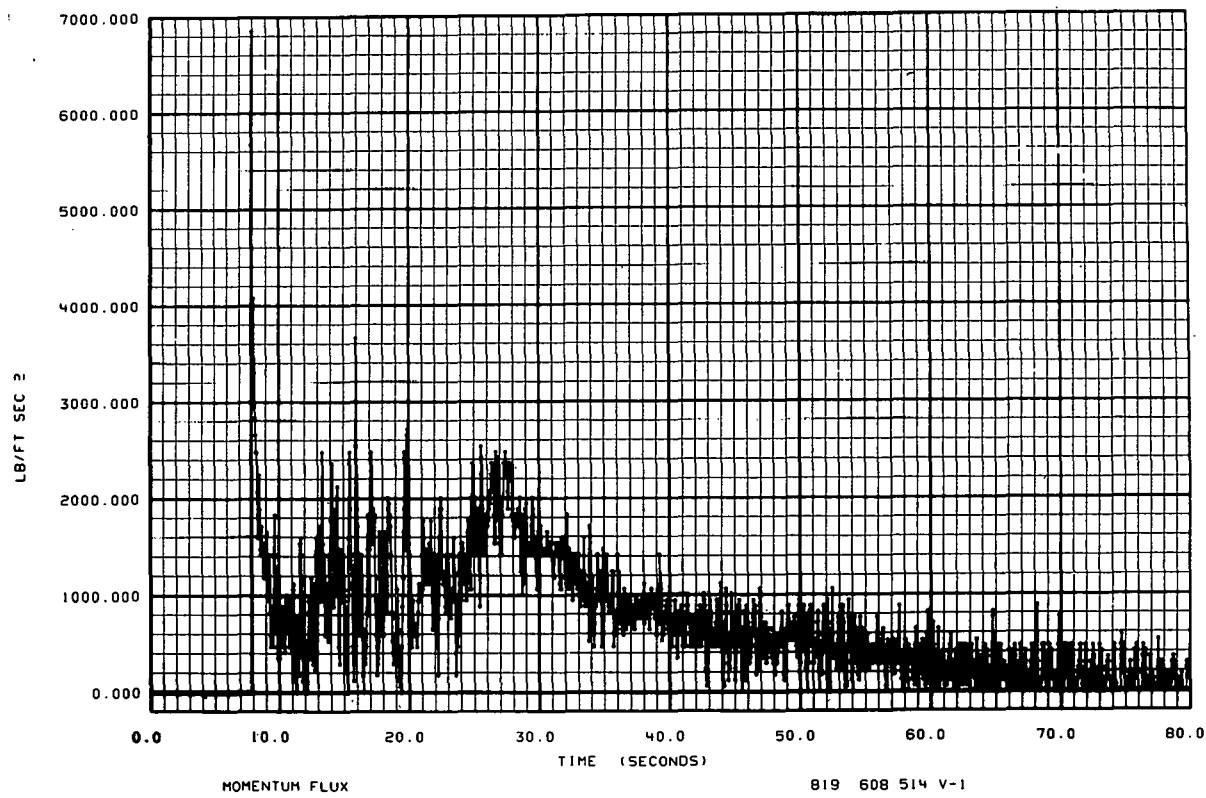
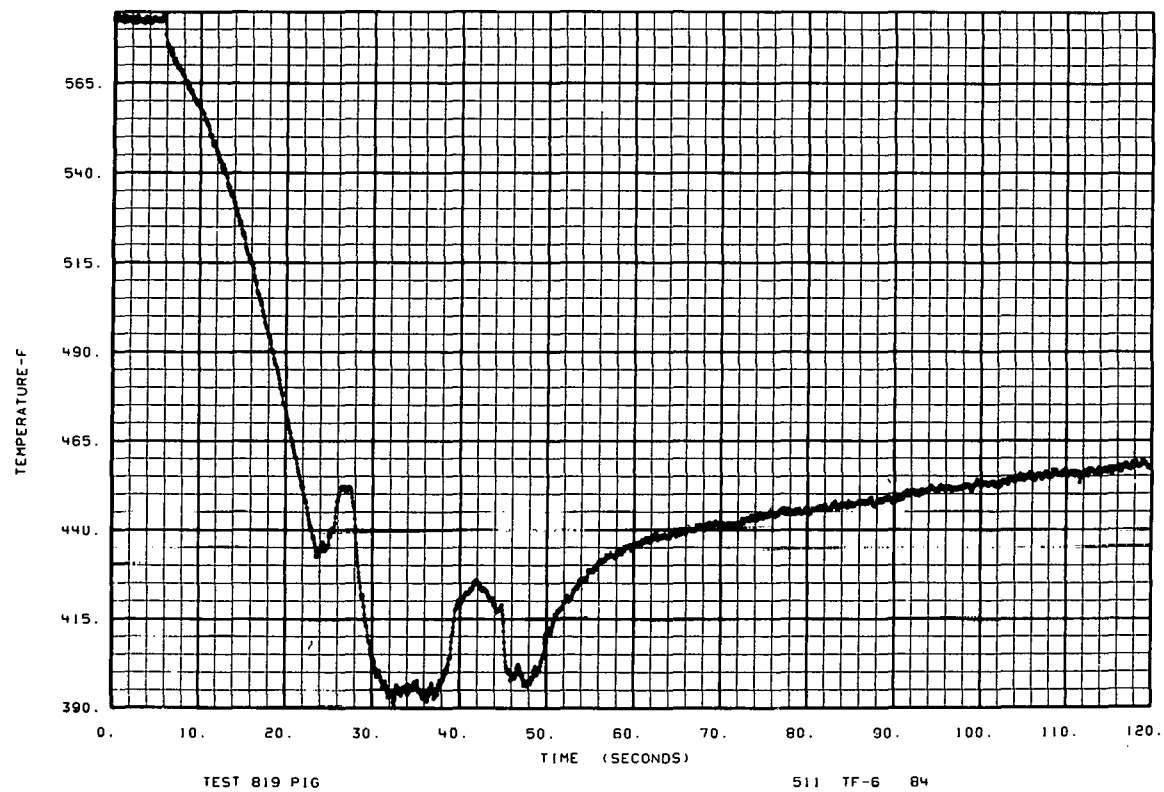


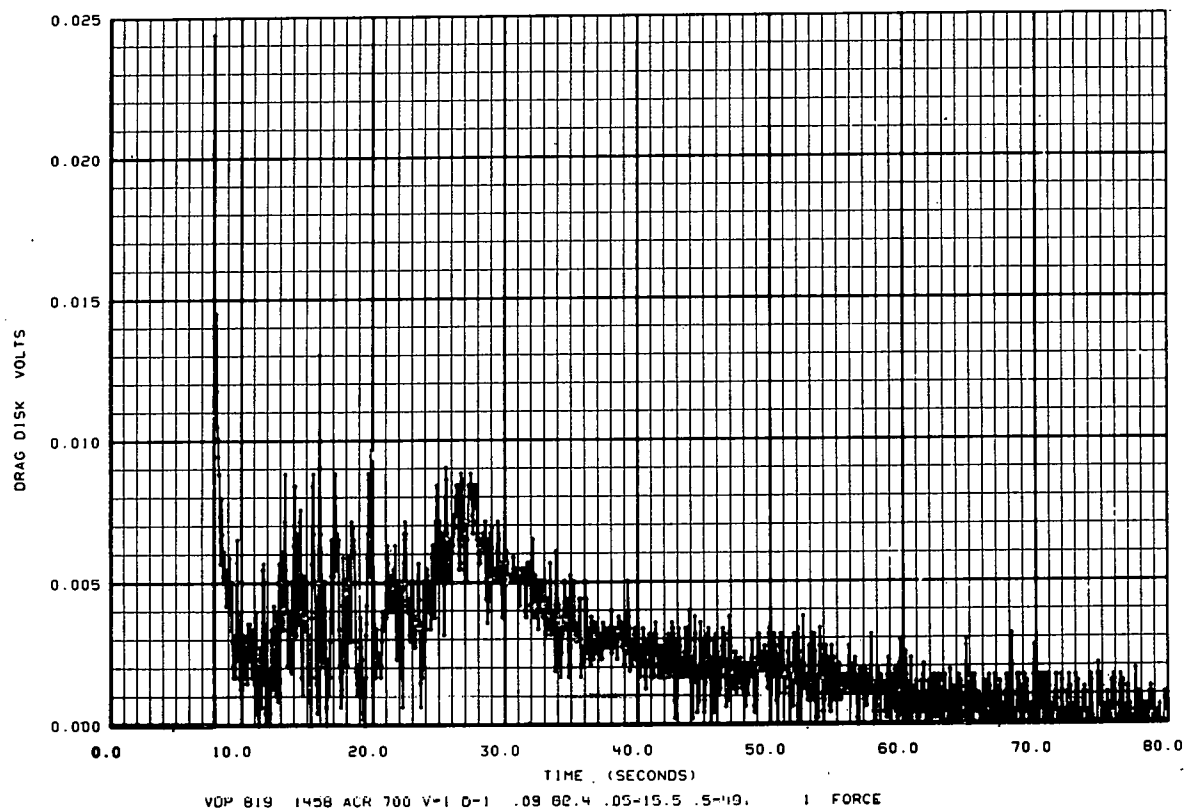
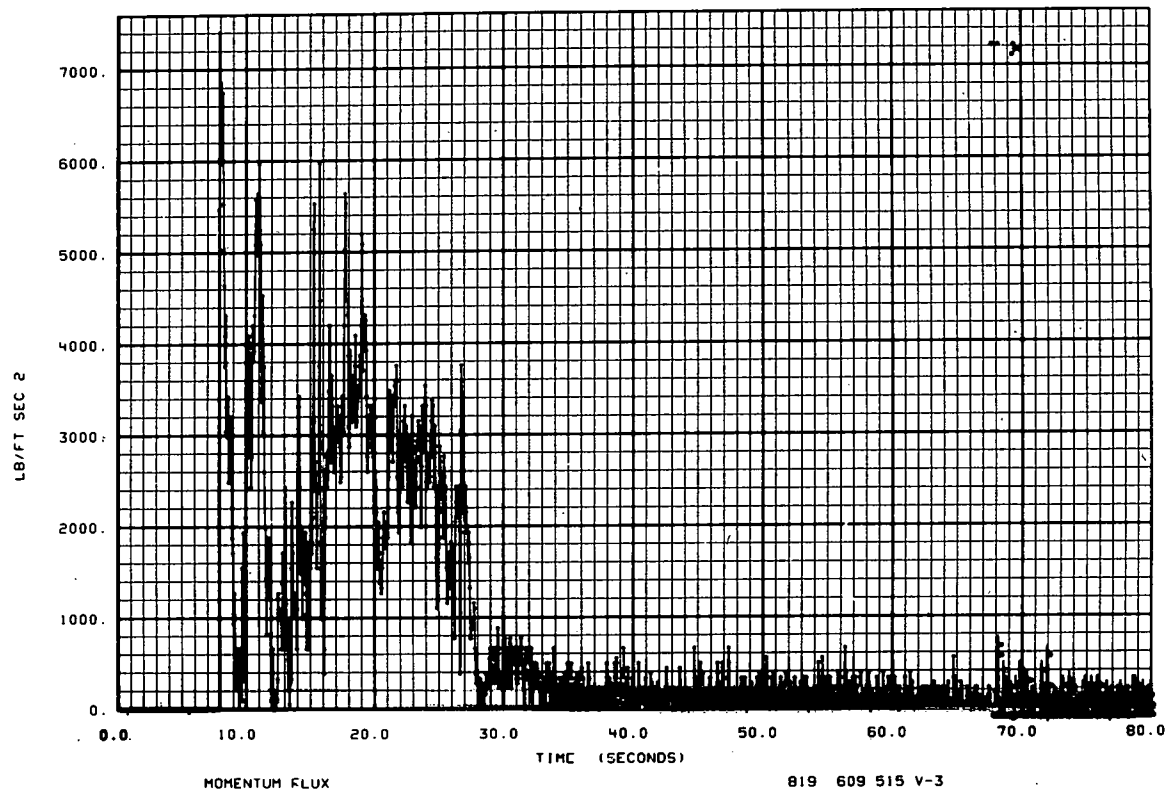


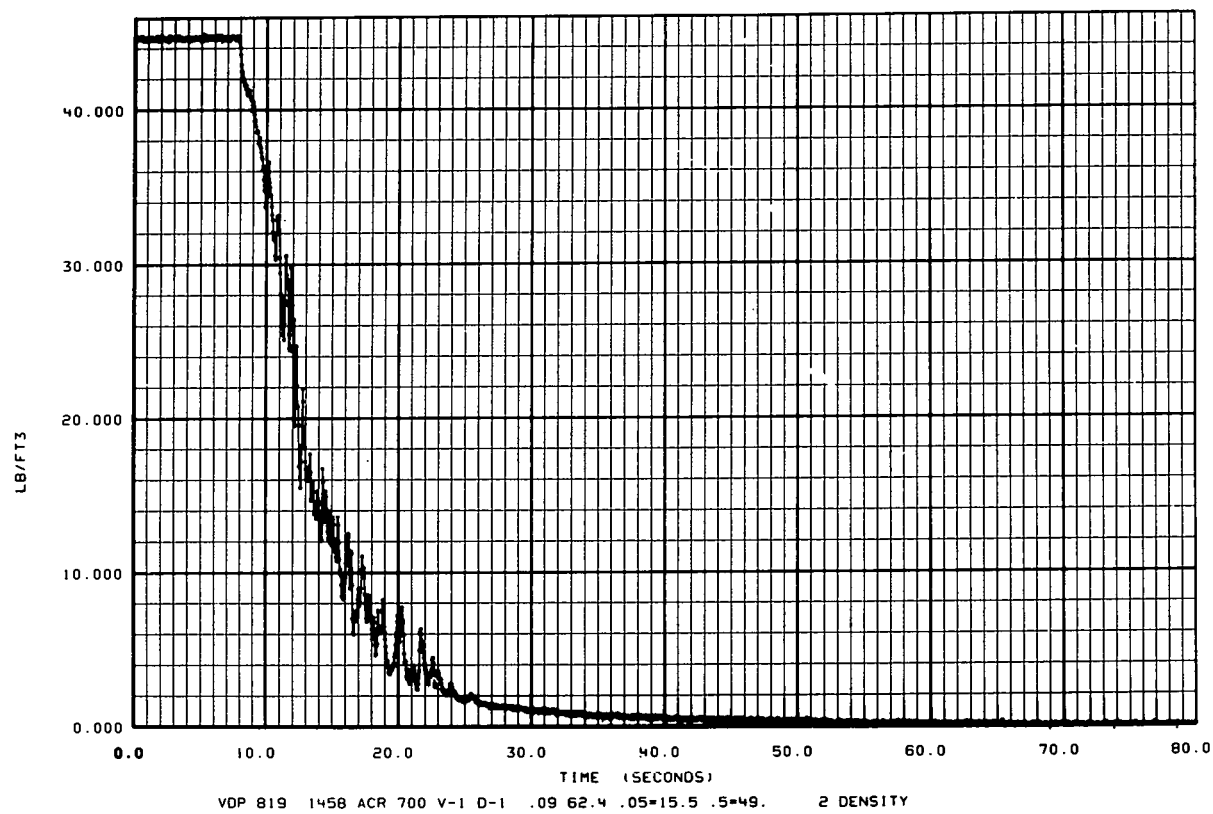




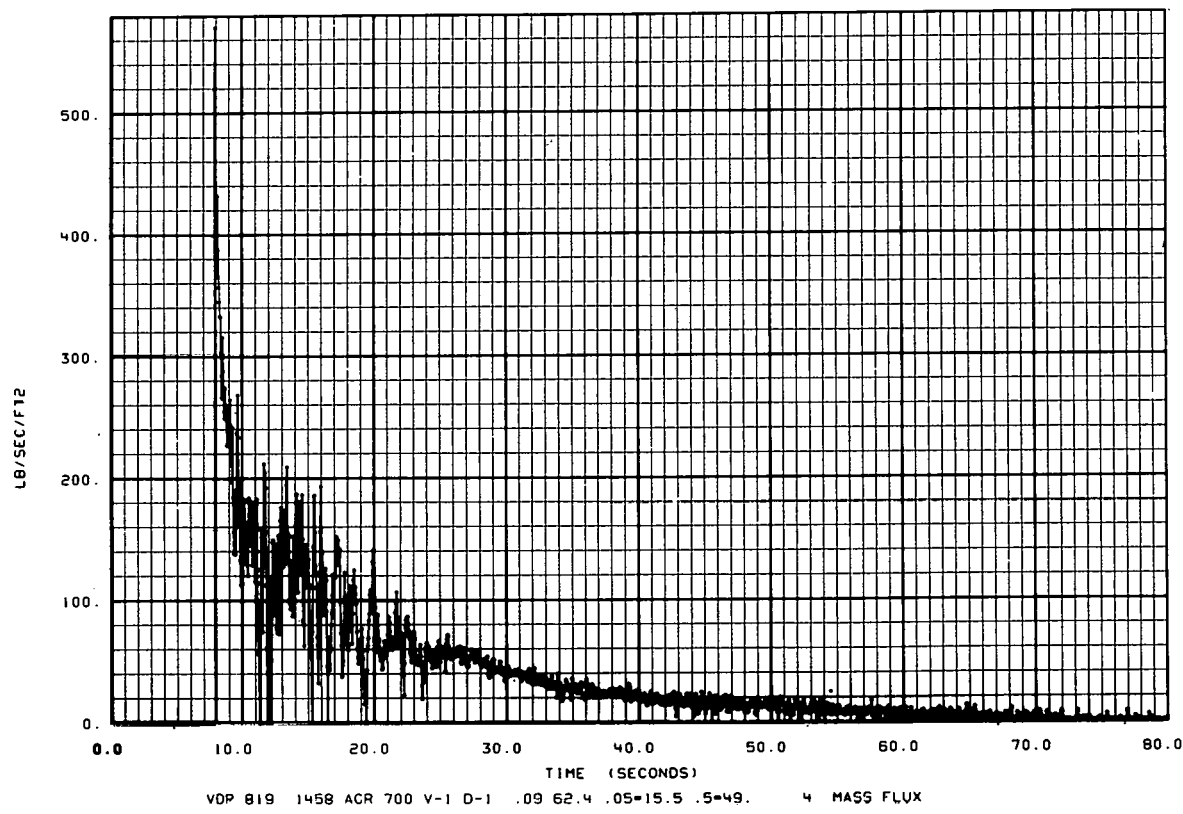




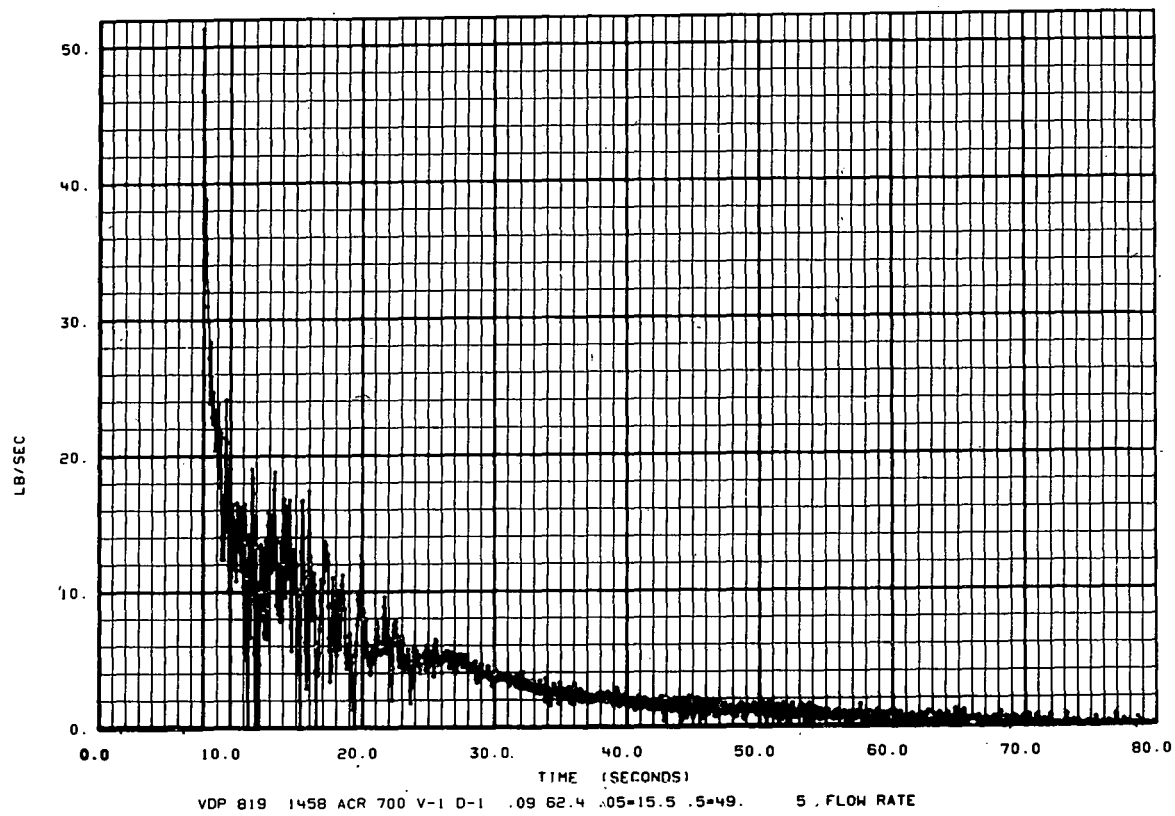




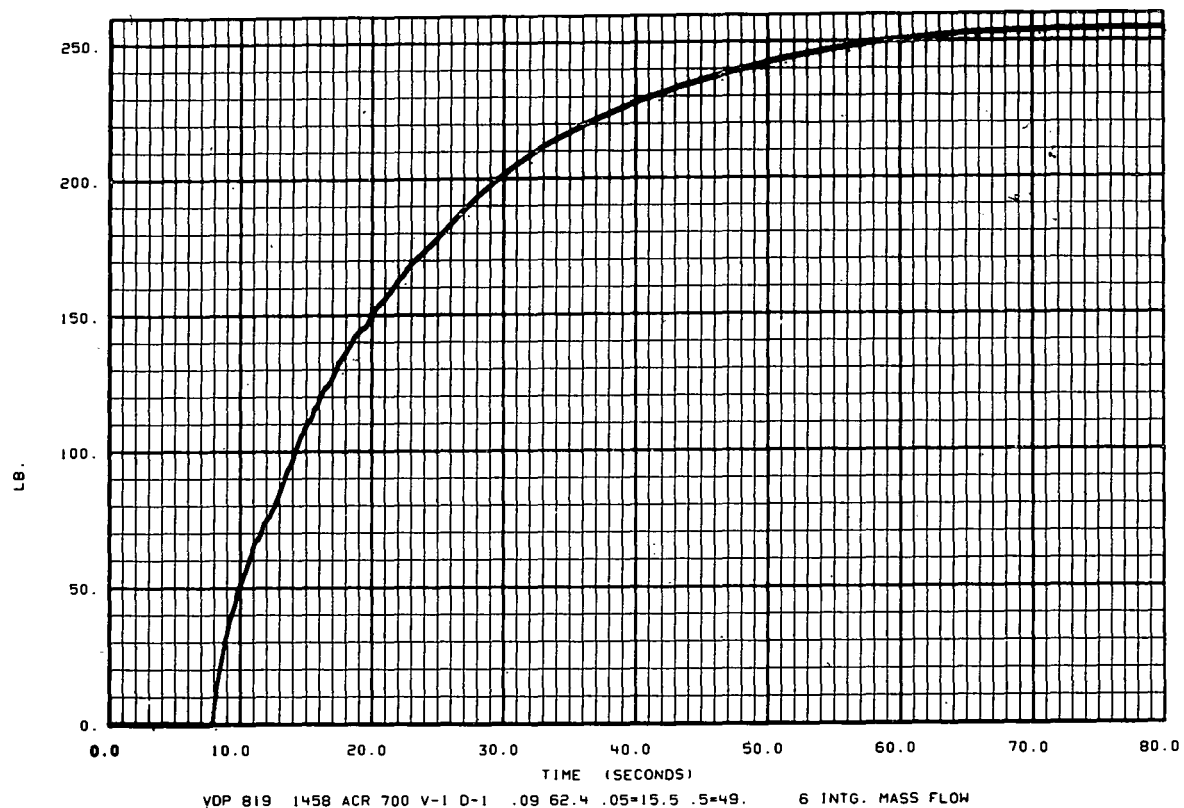
3



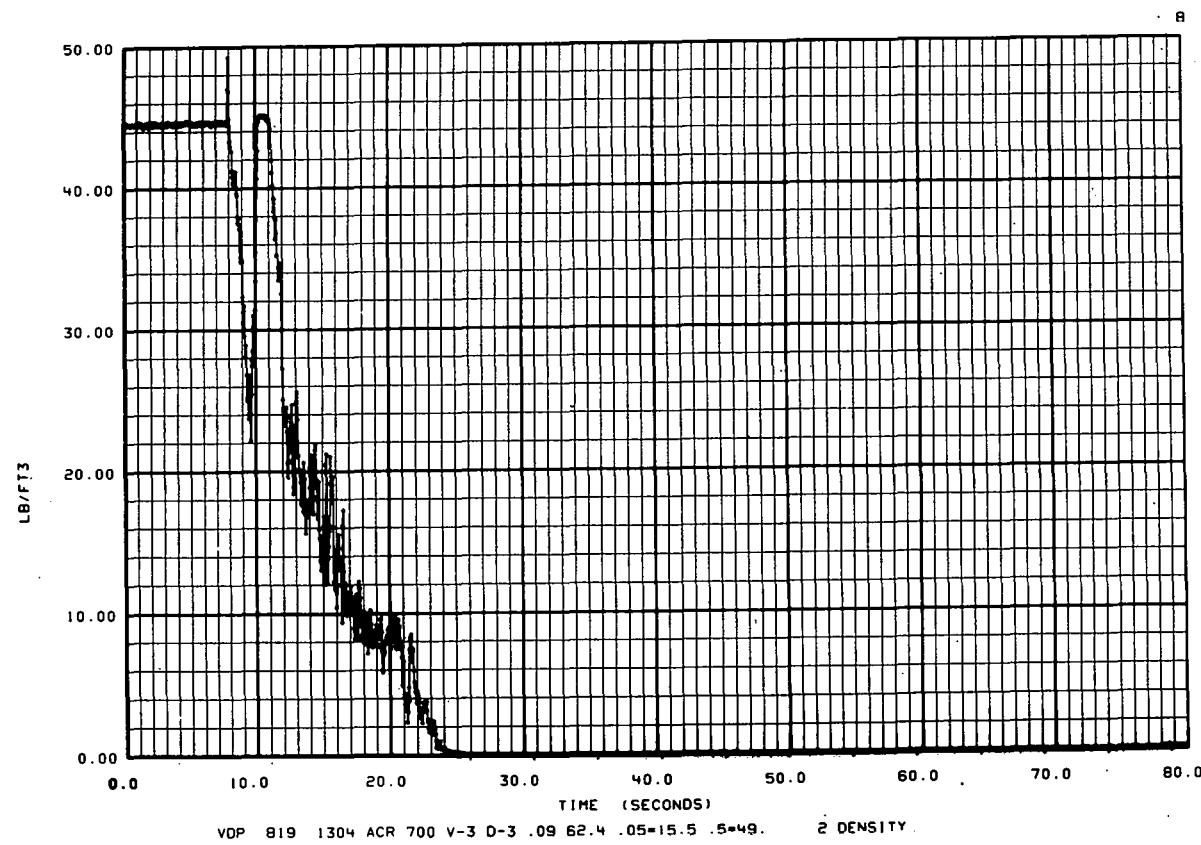
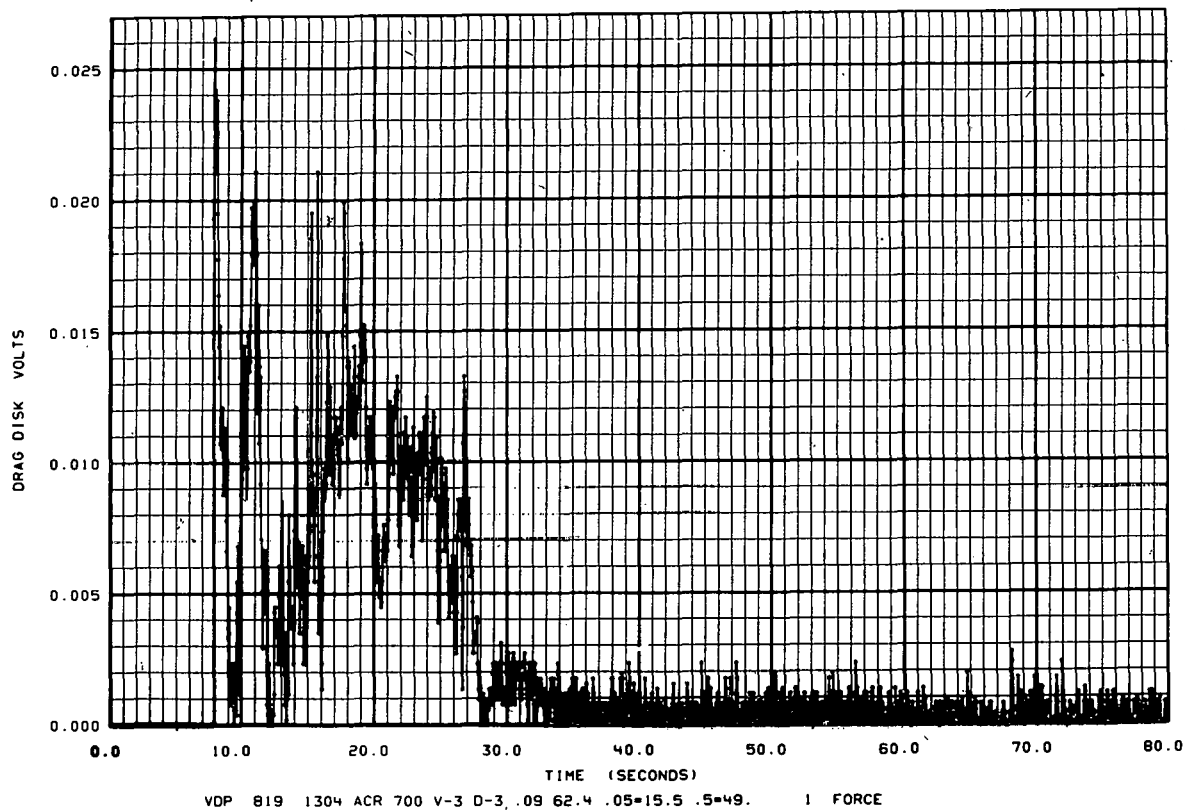
5

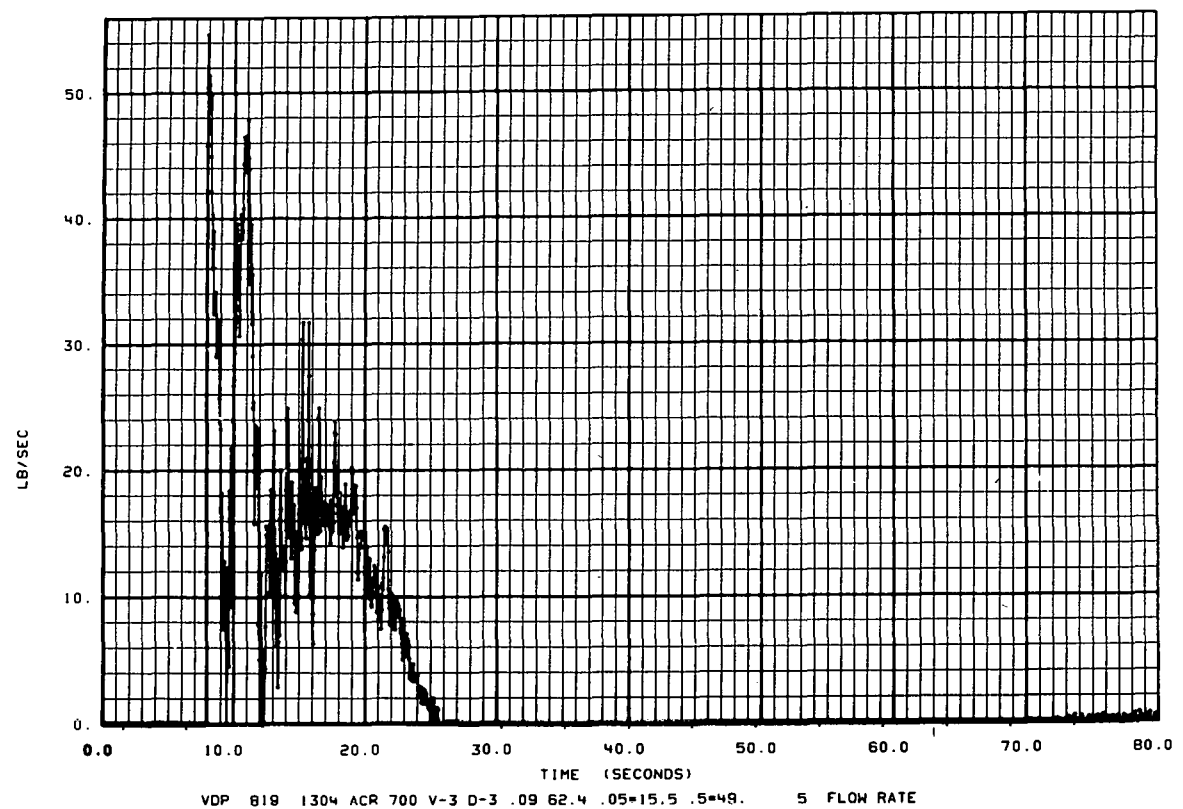
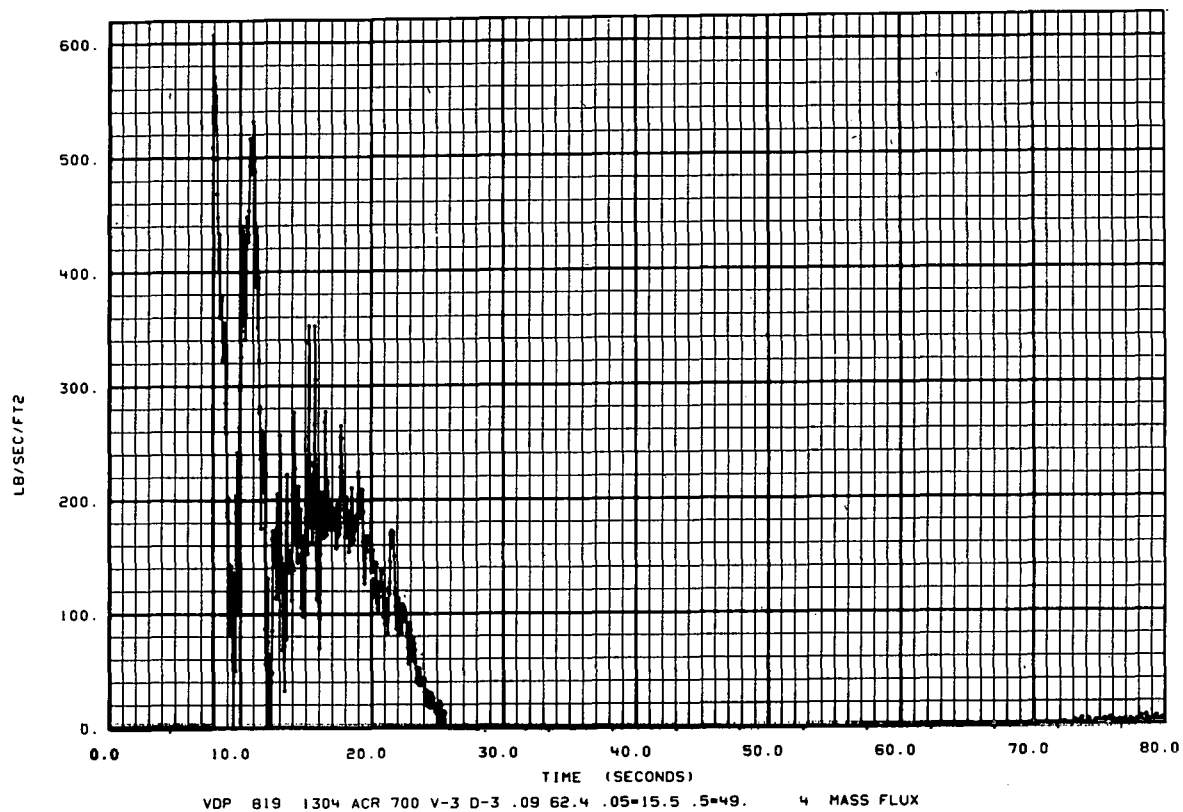


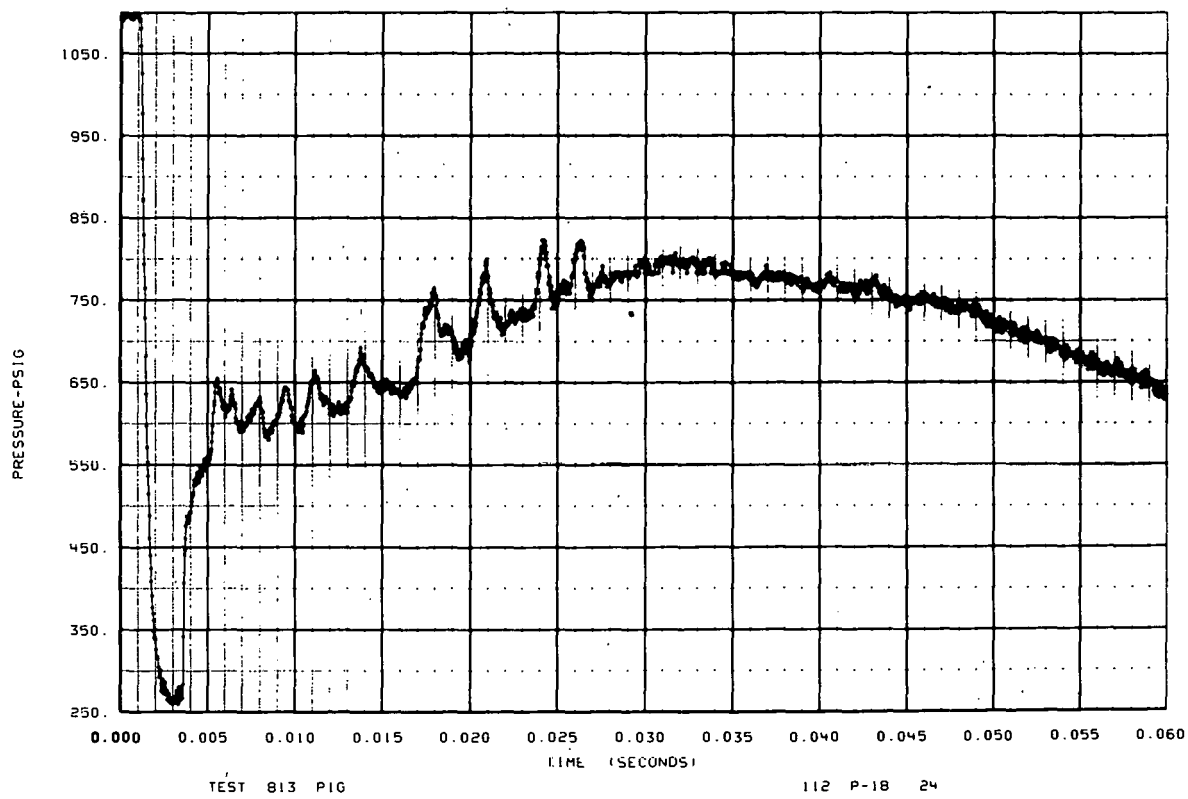
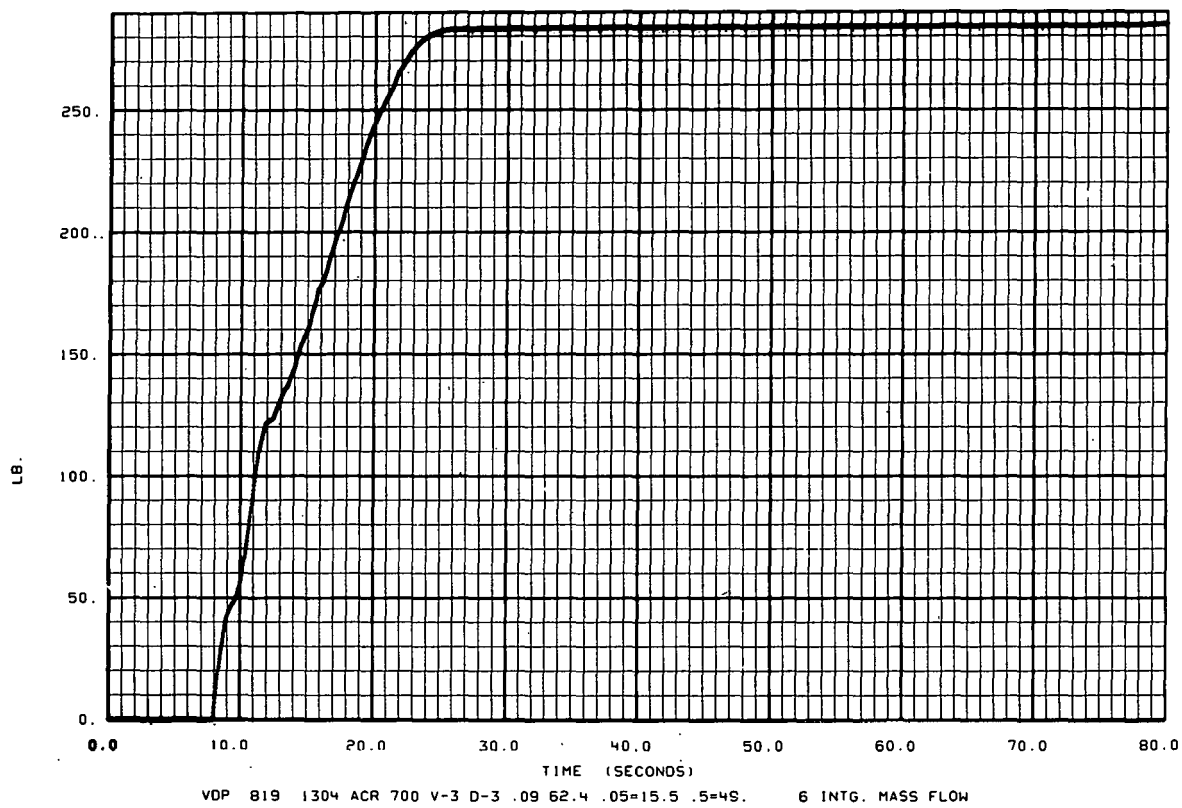
6

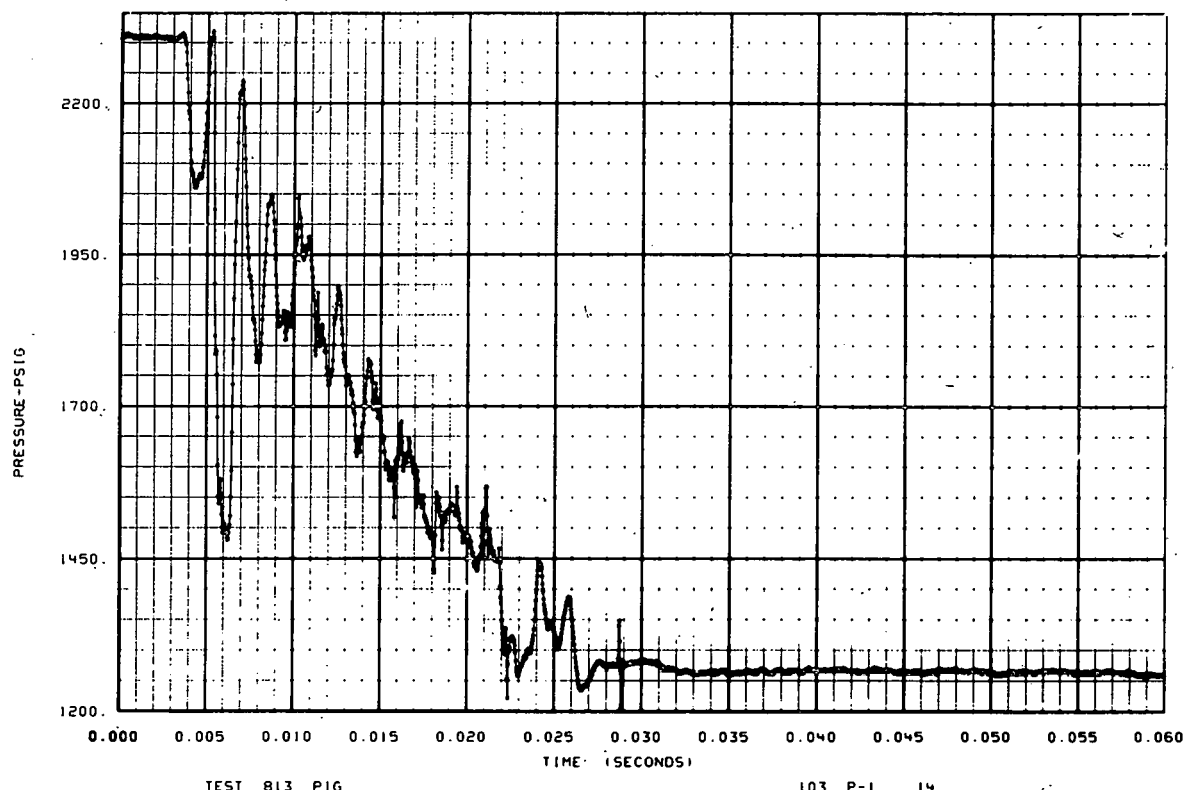
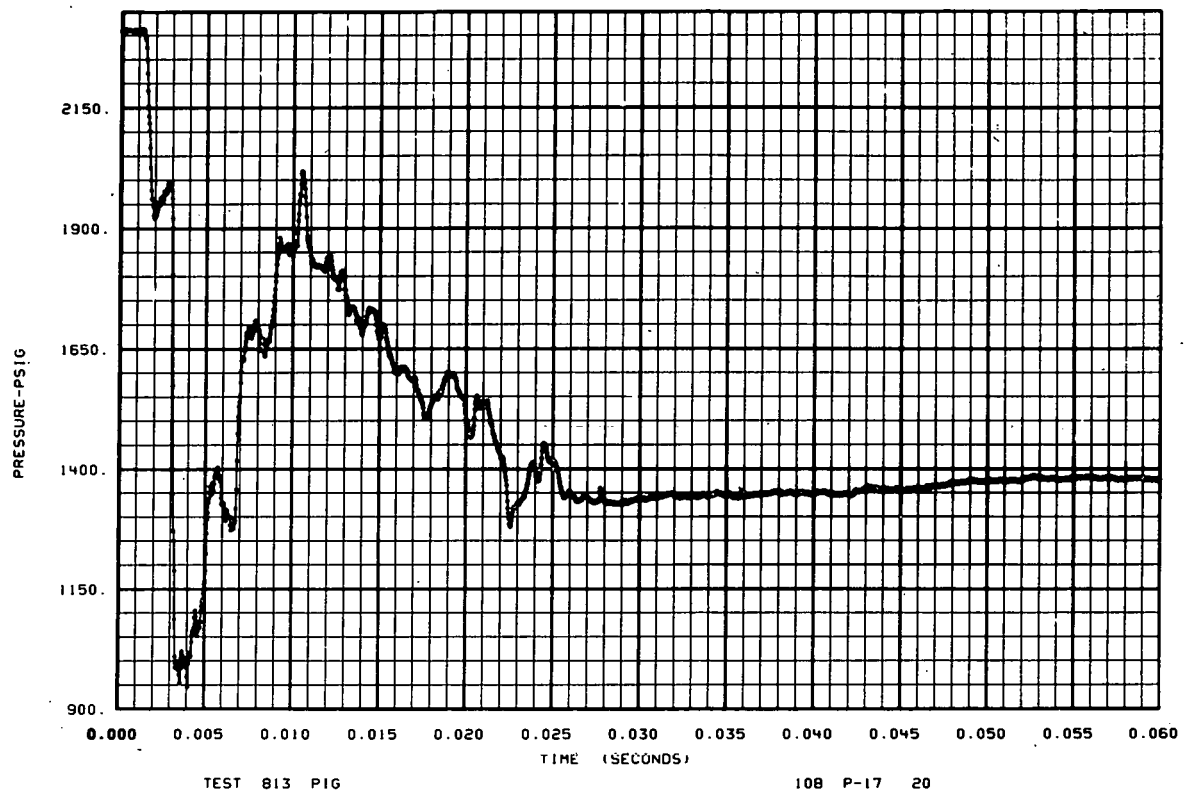


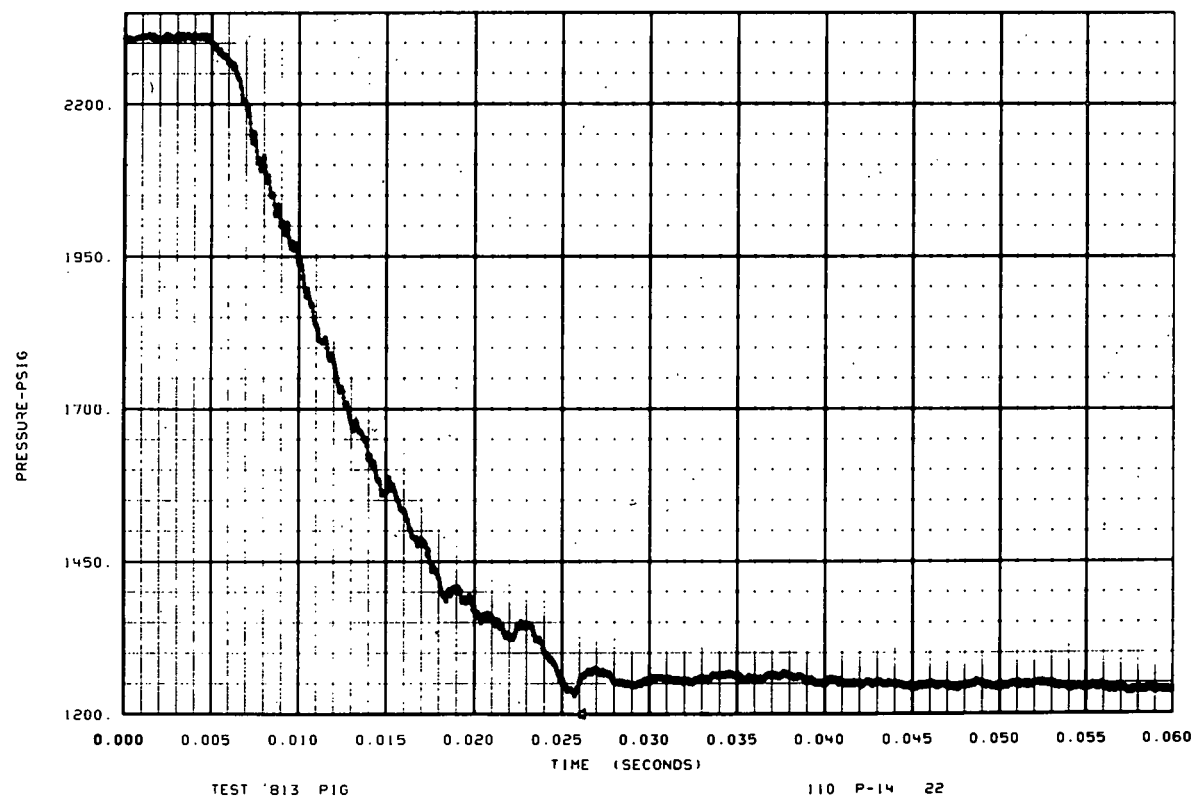
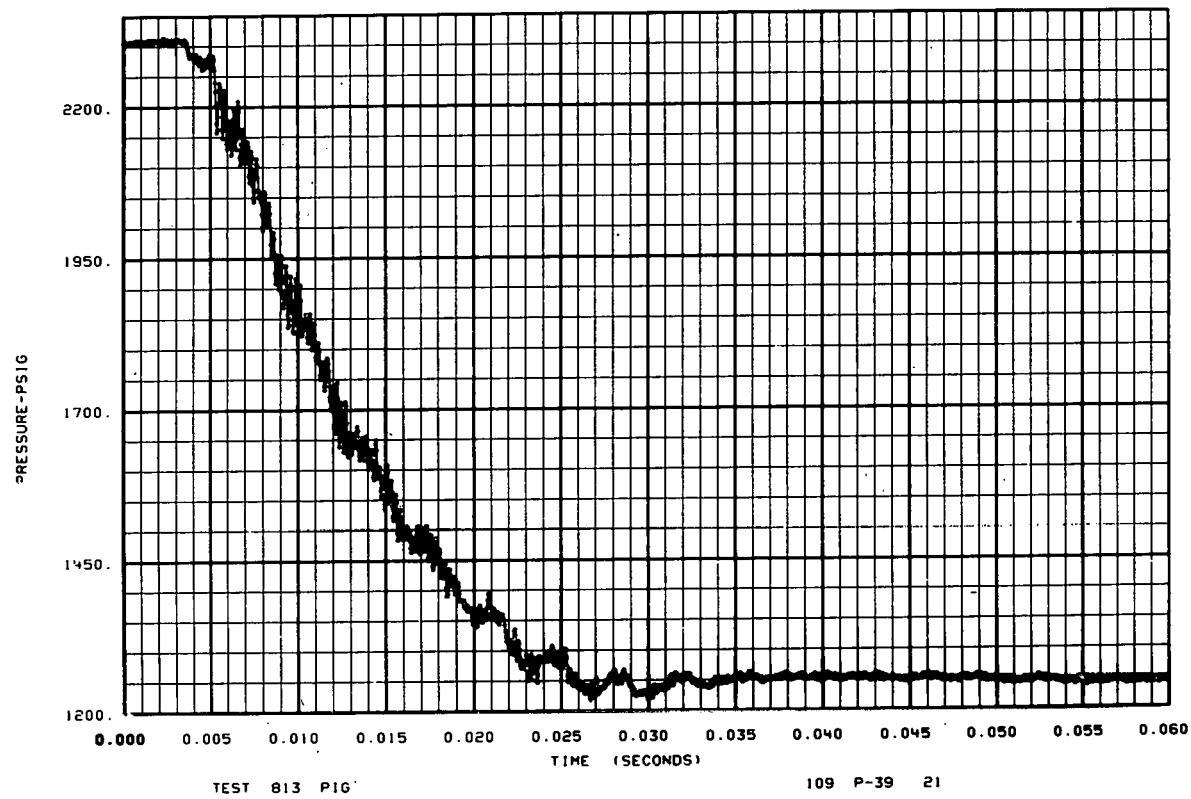
7

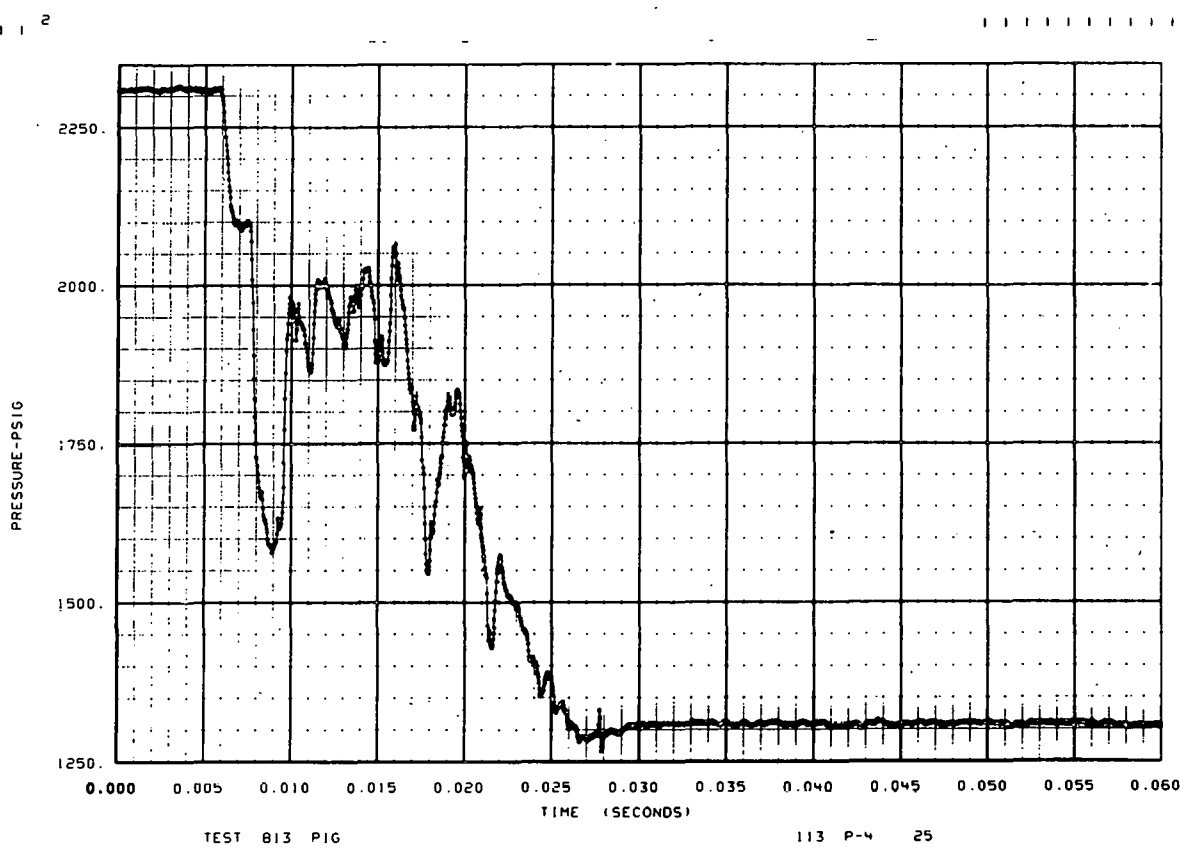
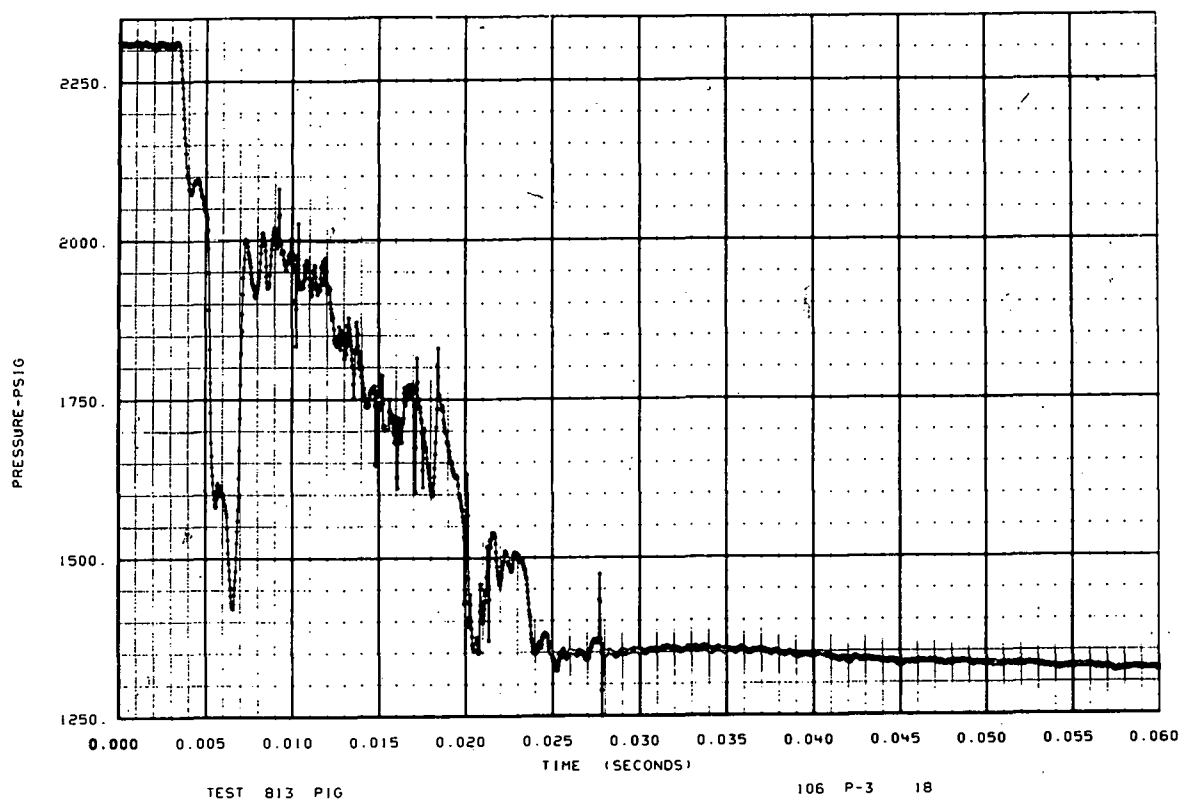




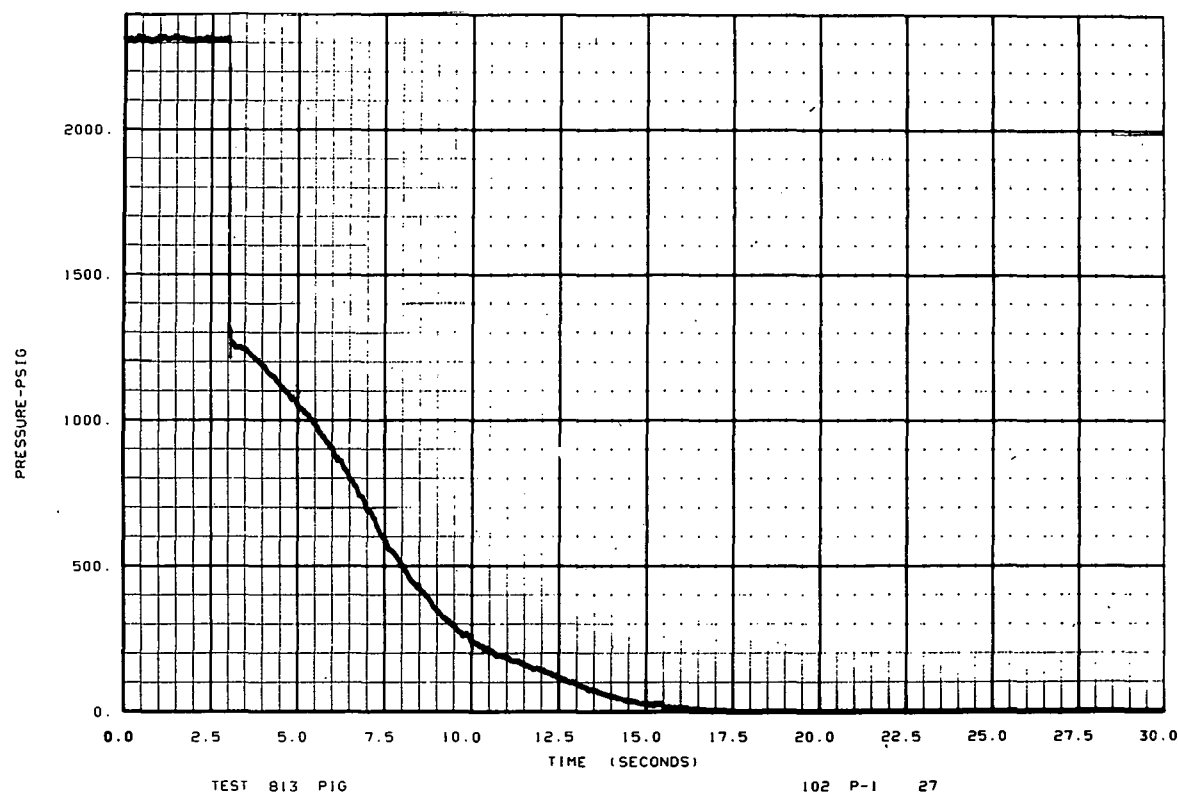
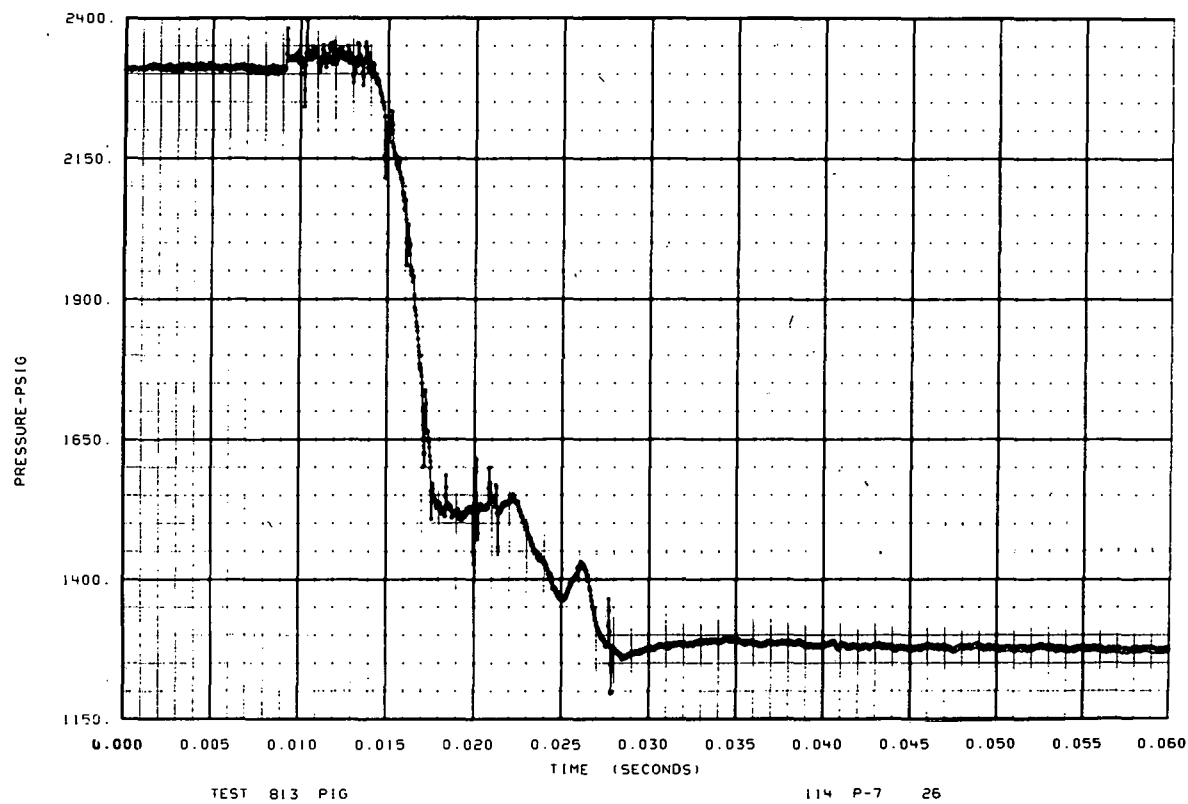


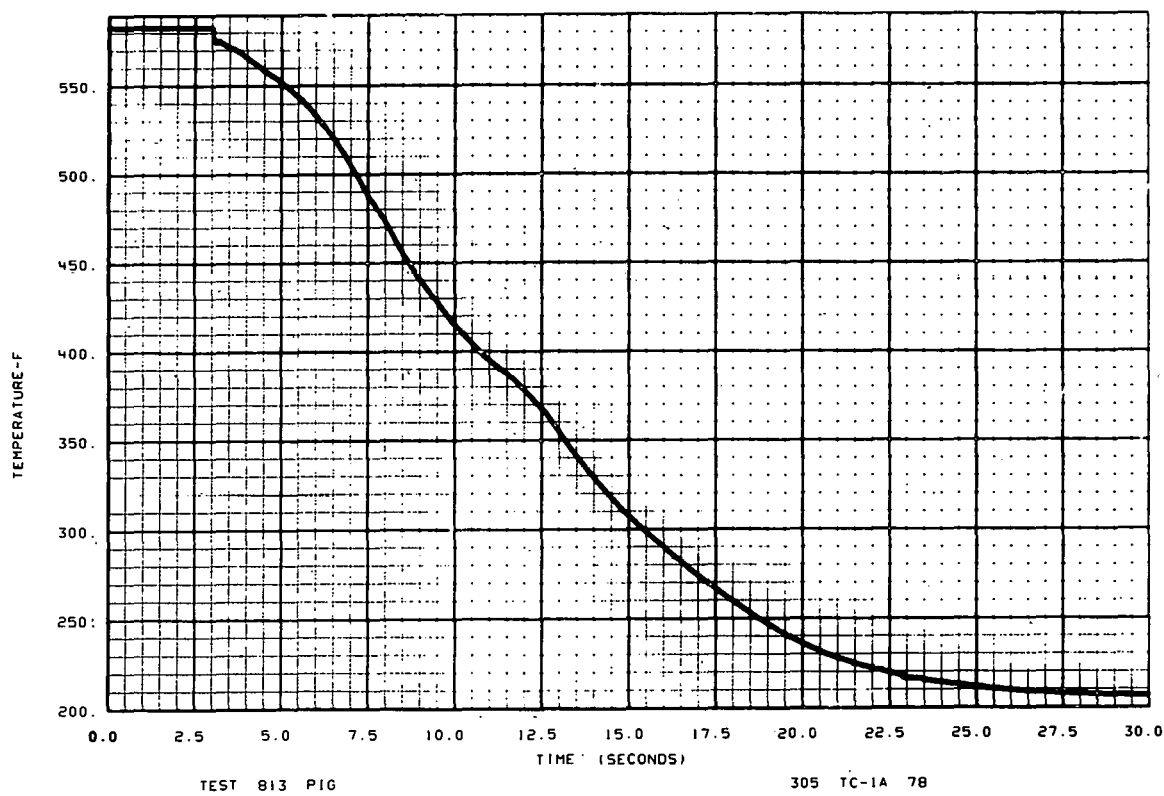
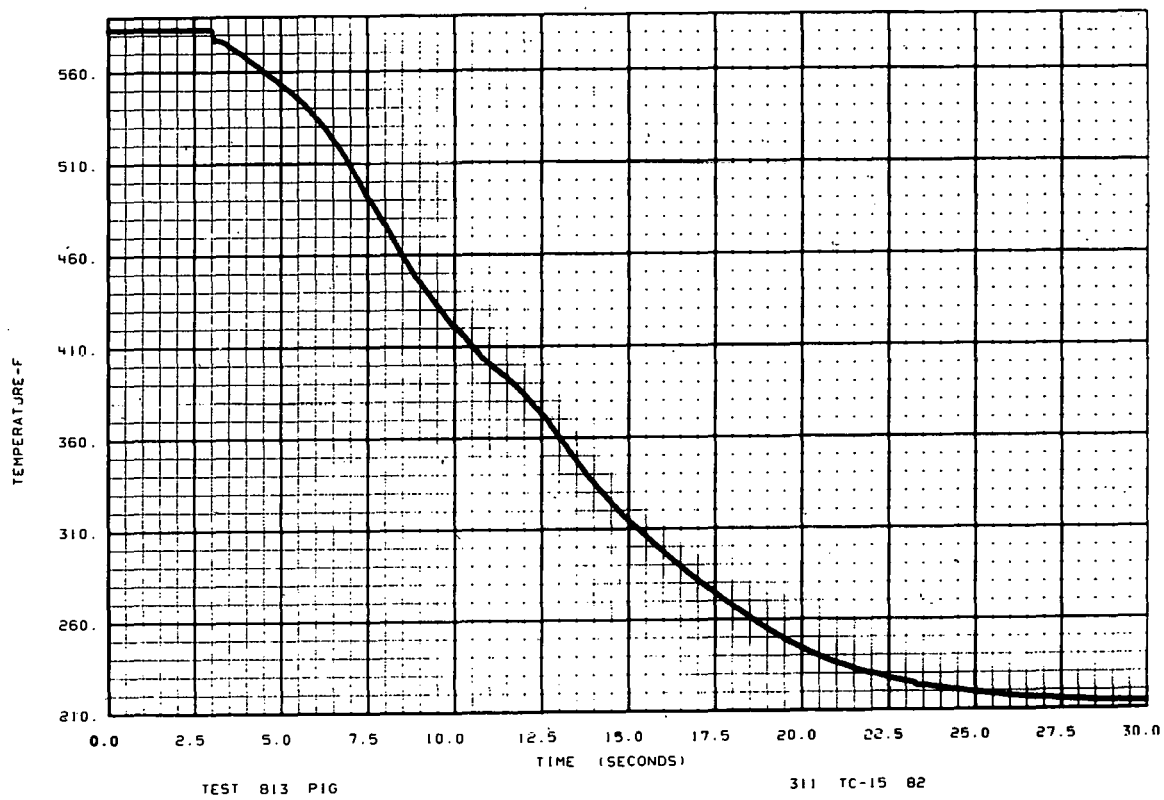


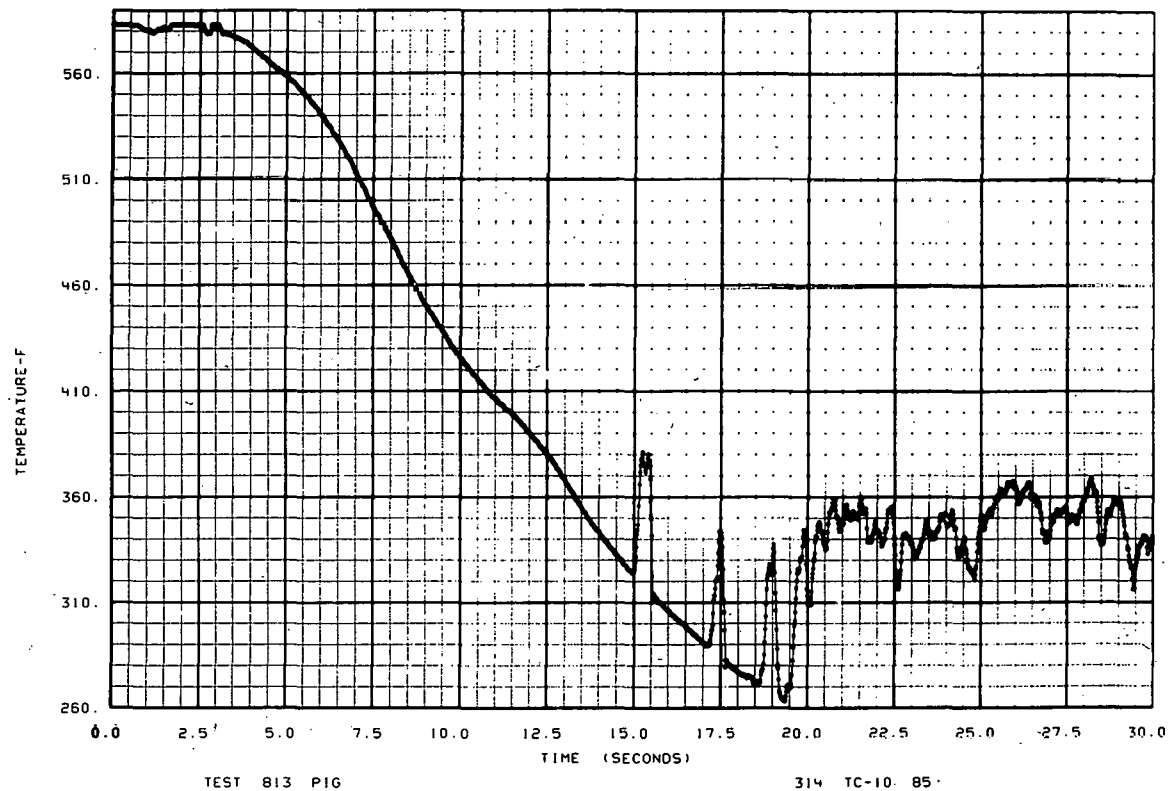


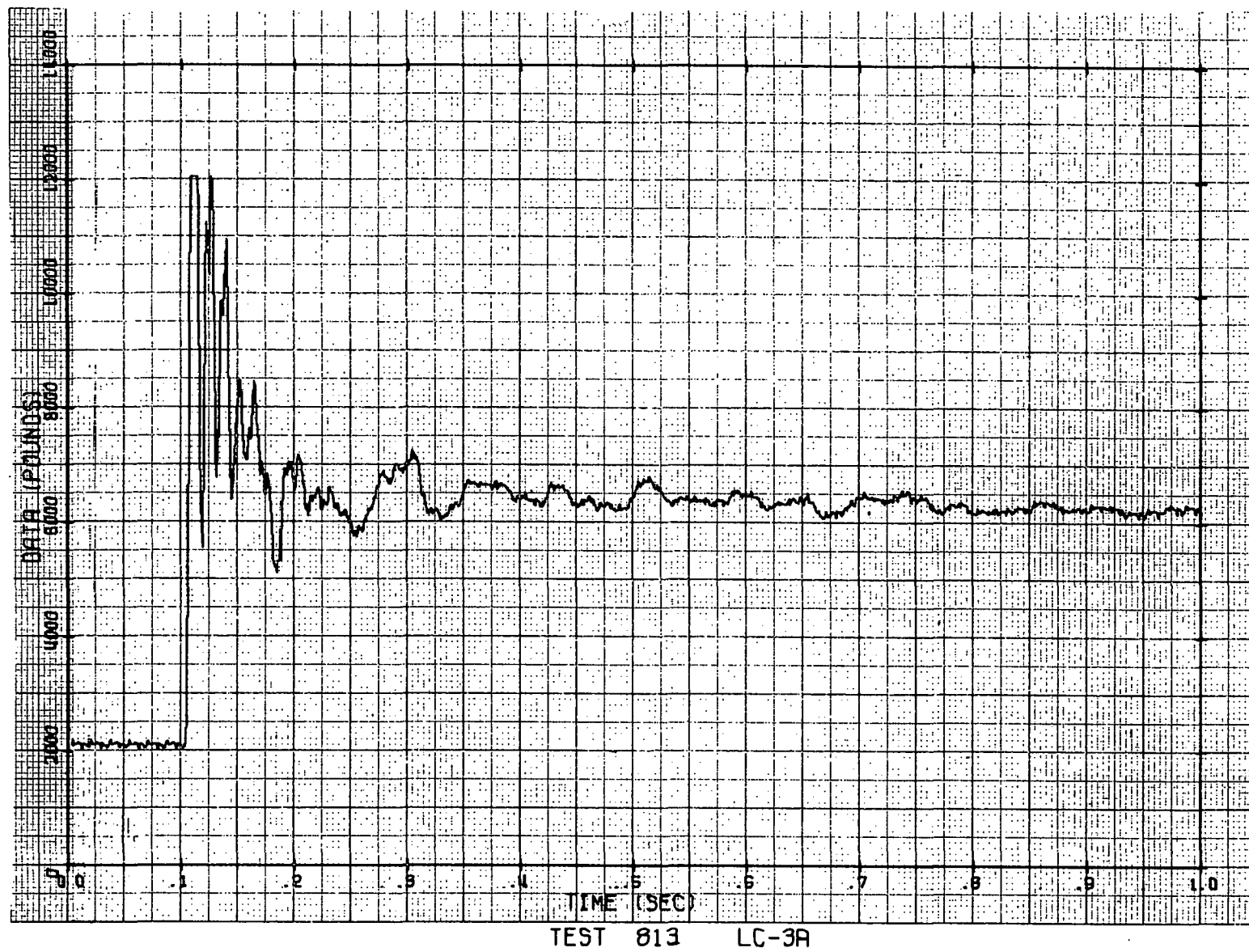


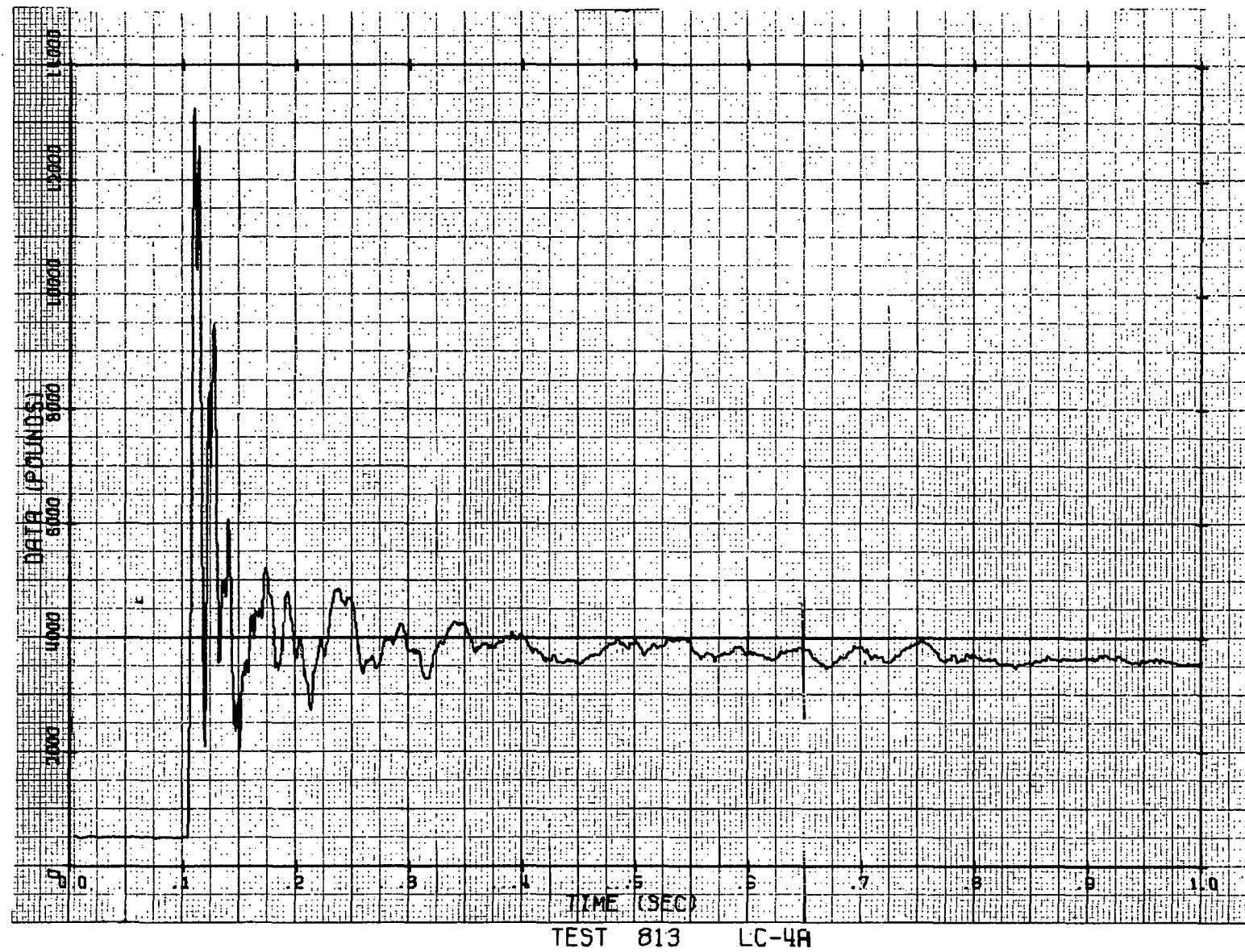
2

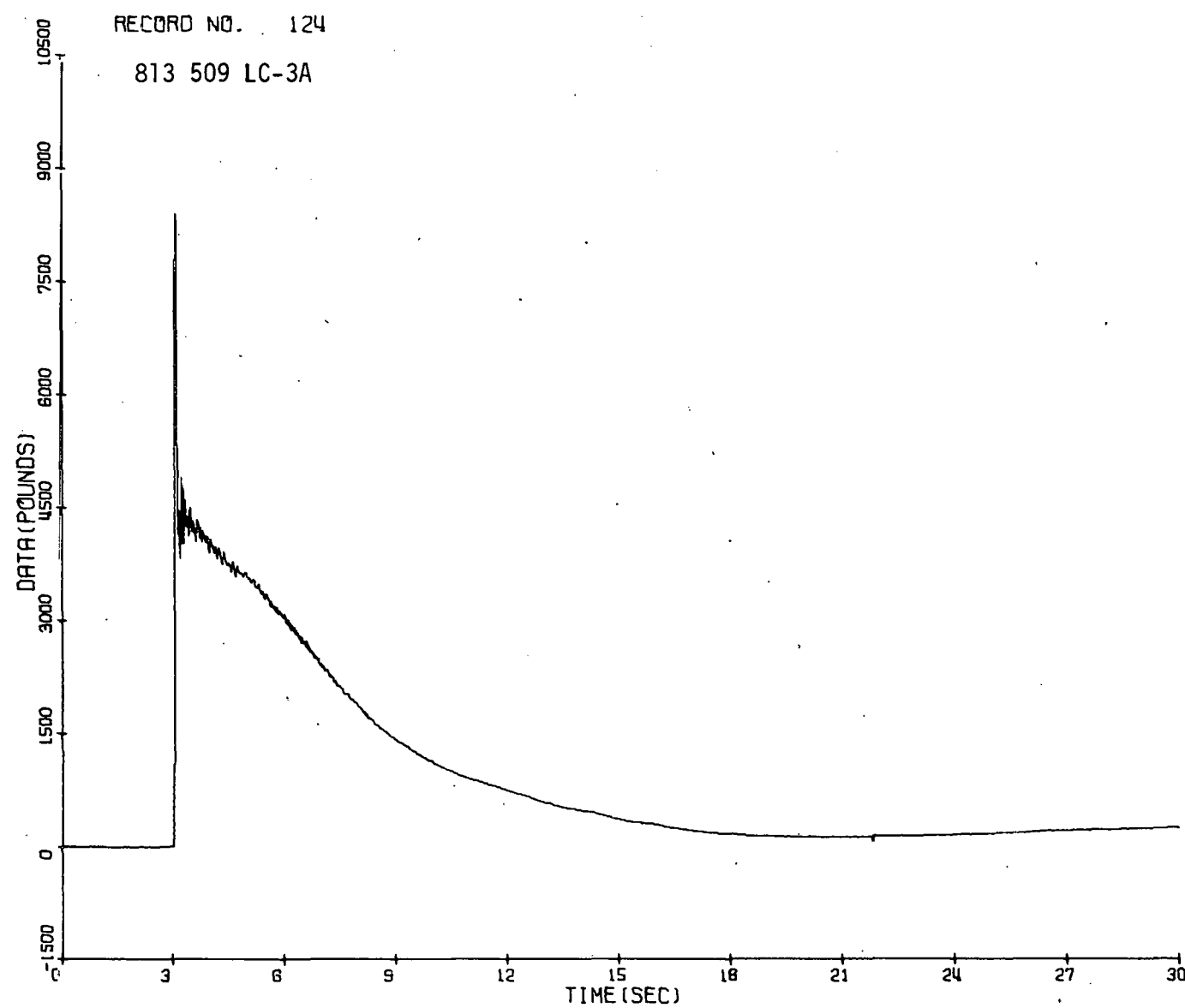






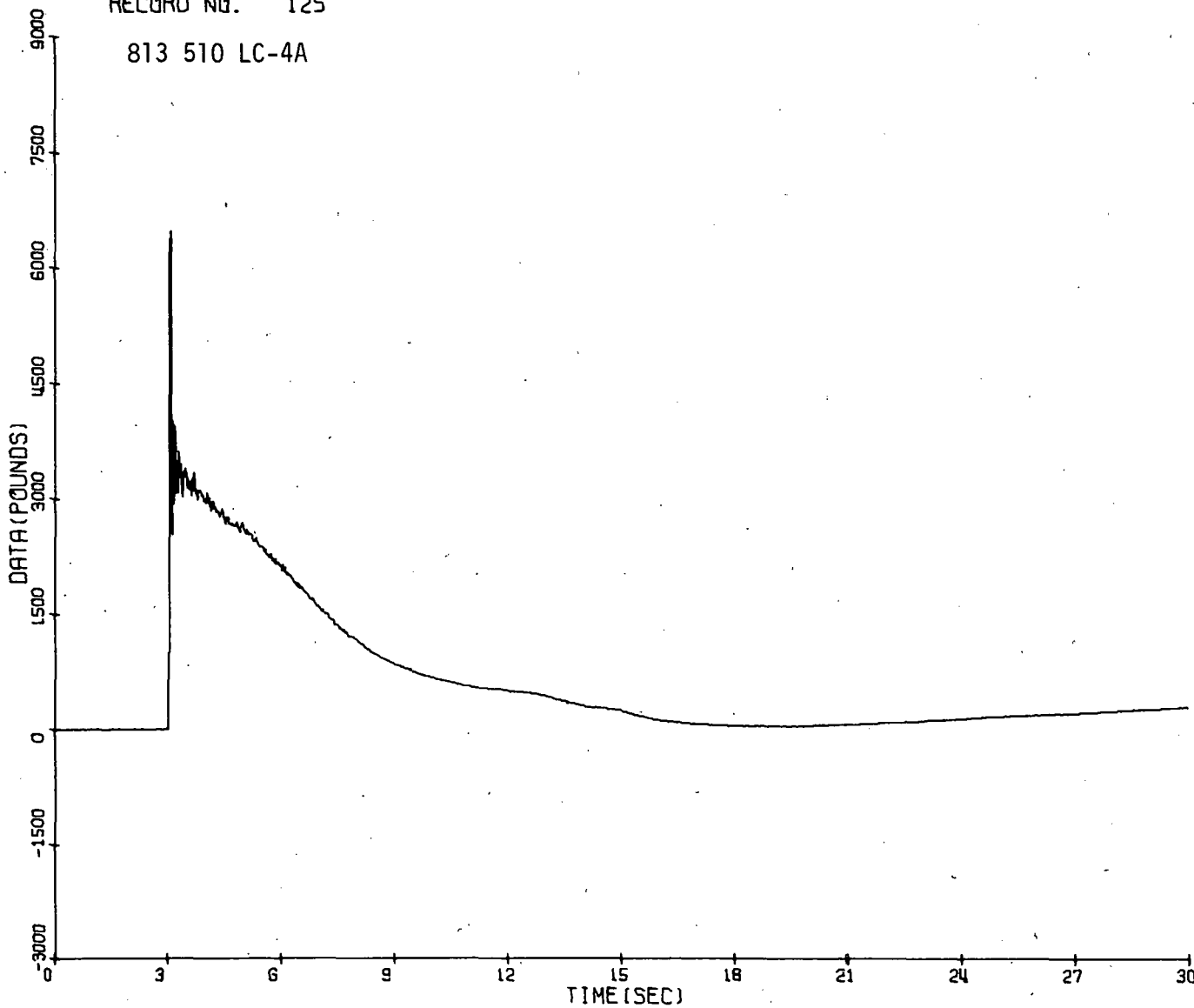


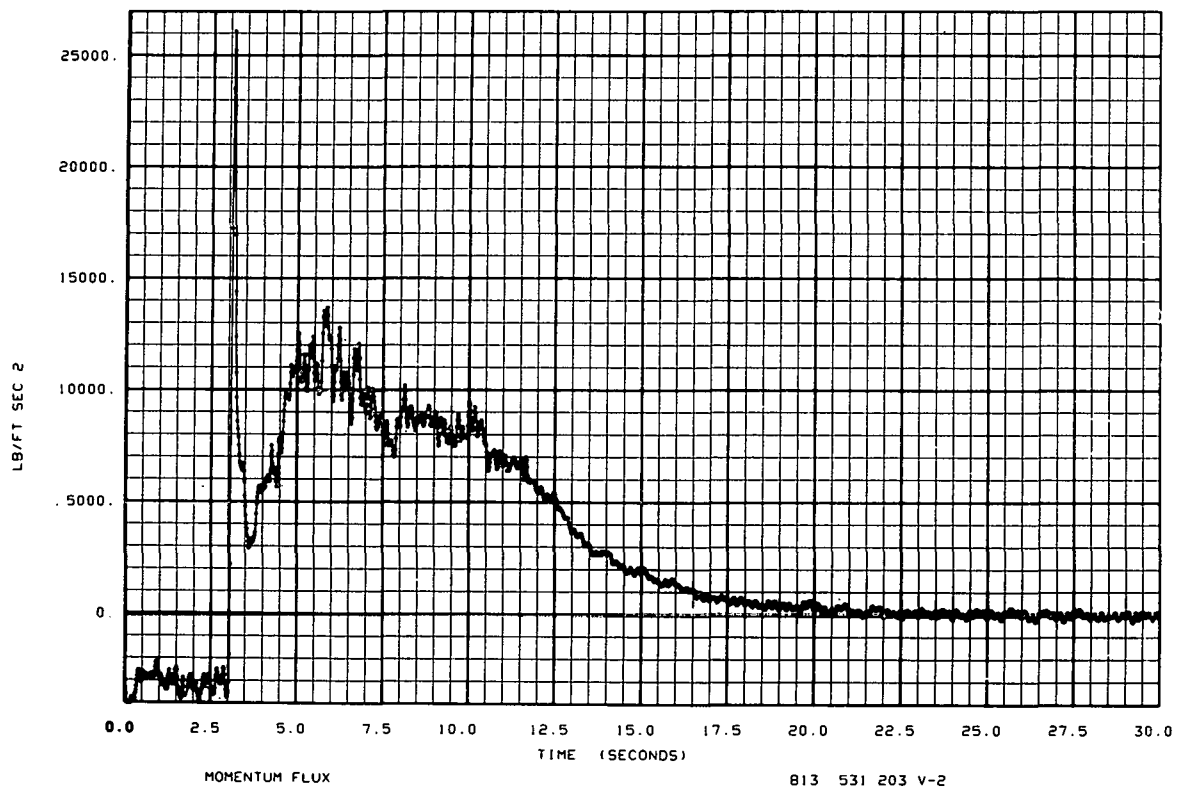
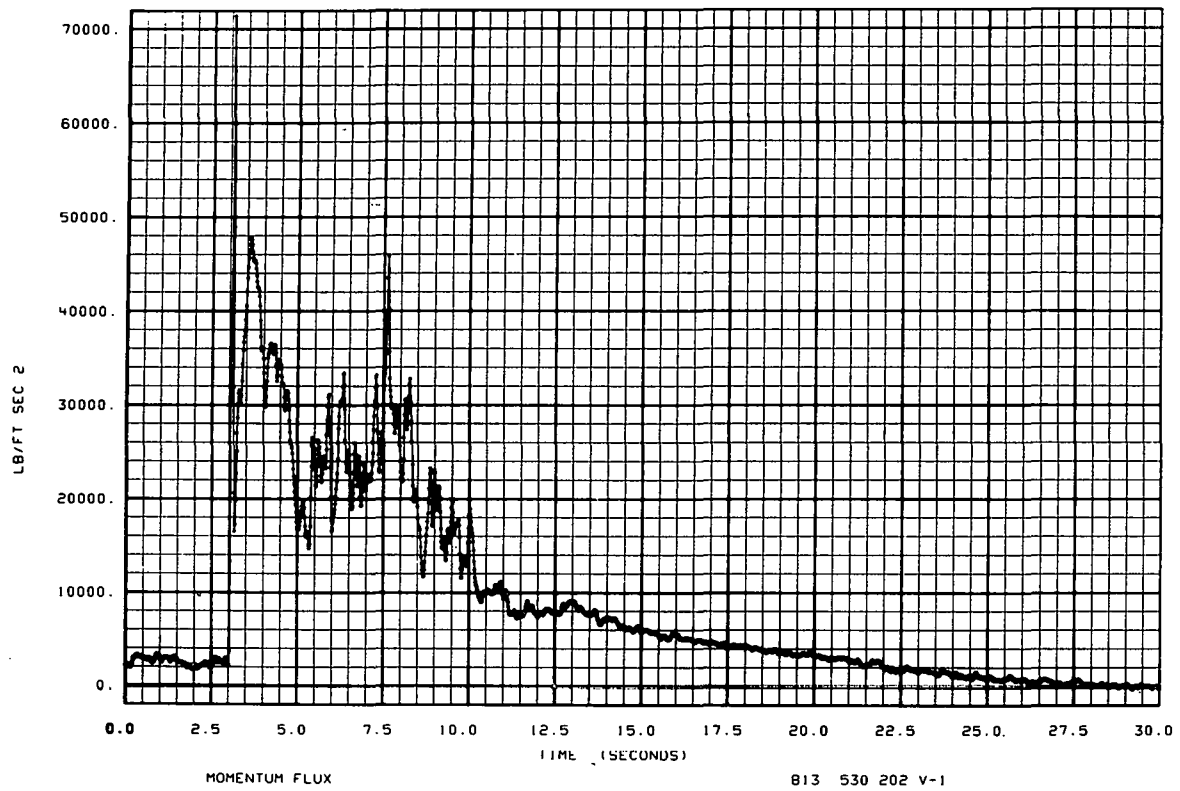


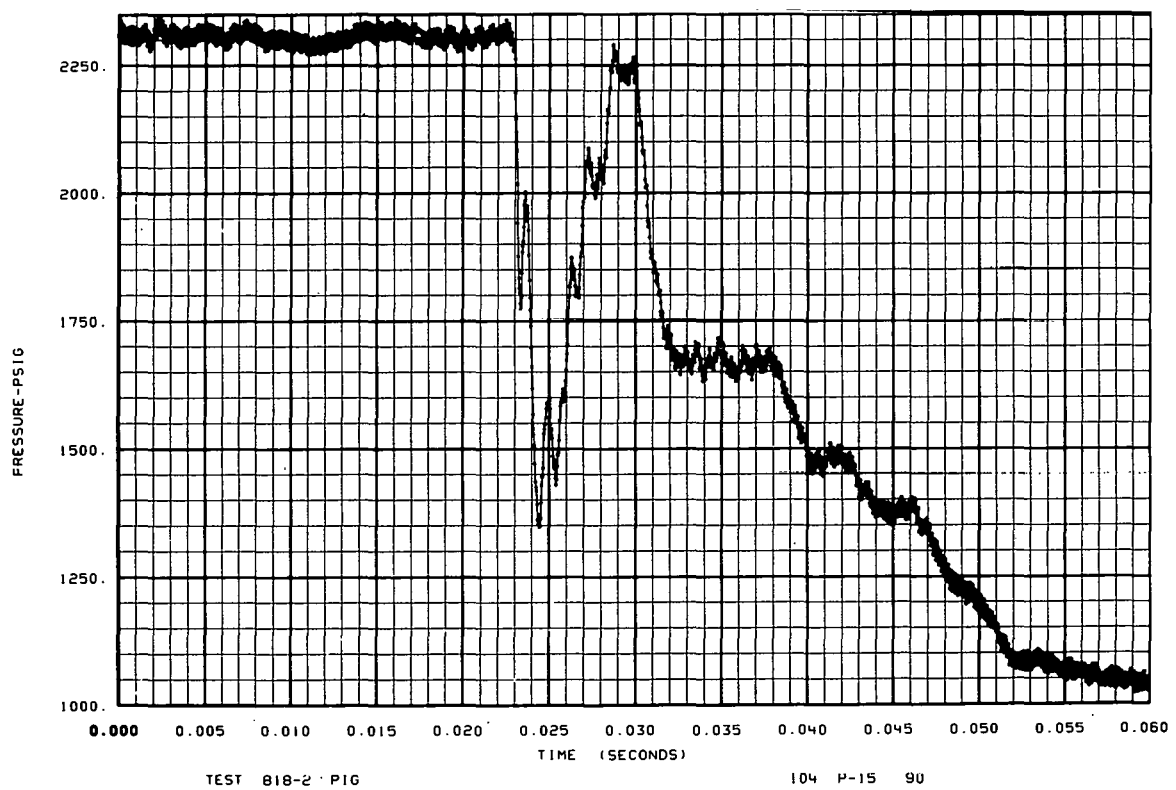
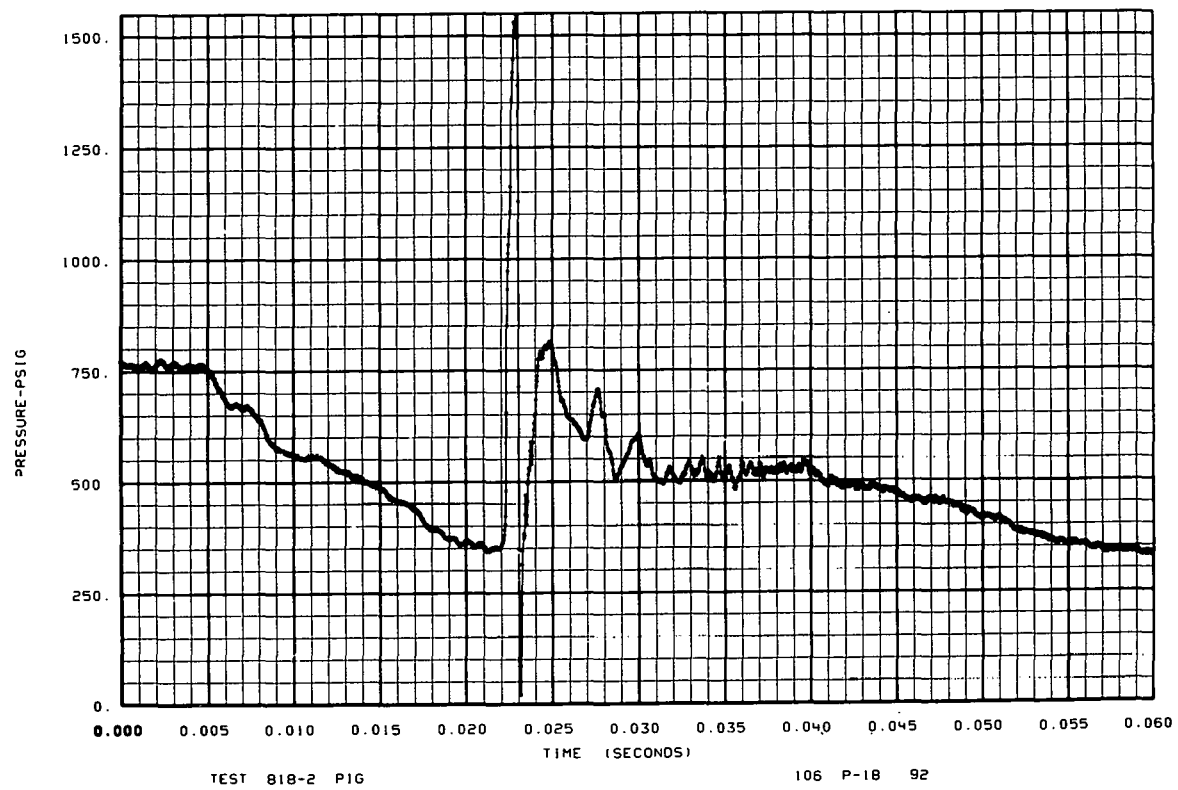


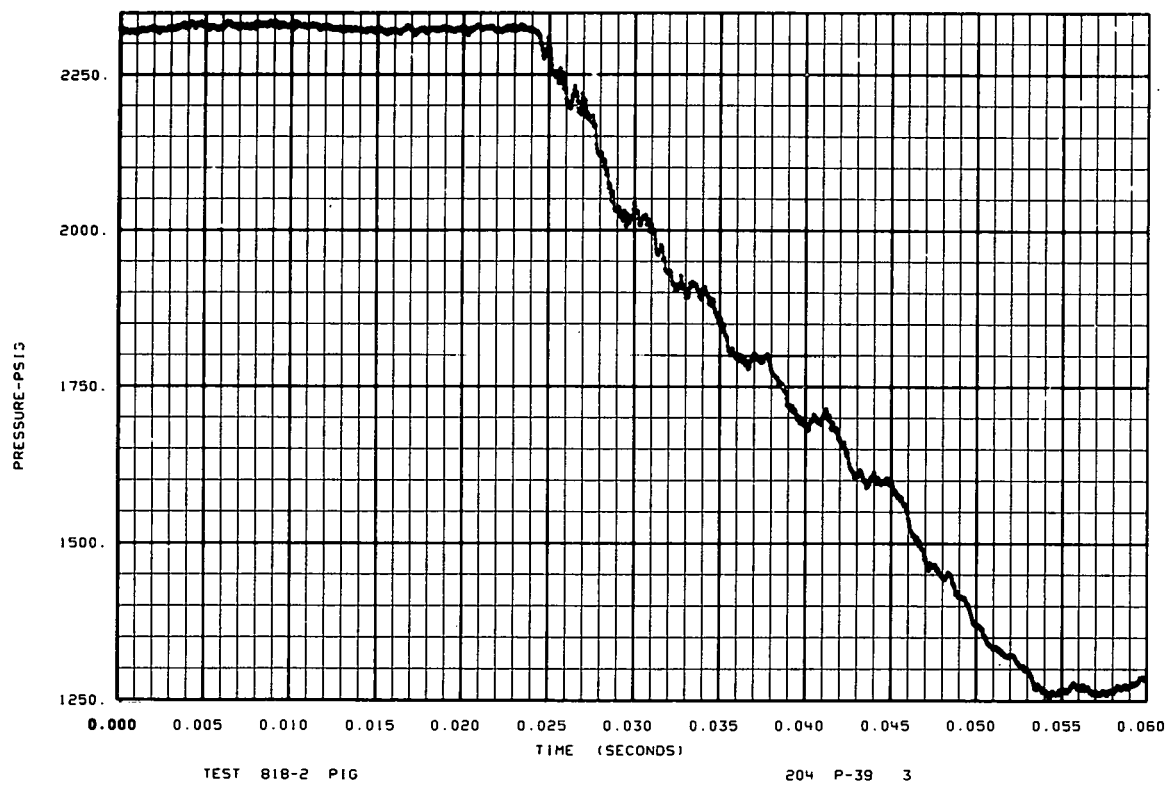
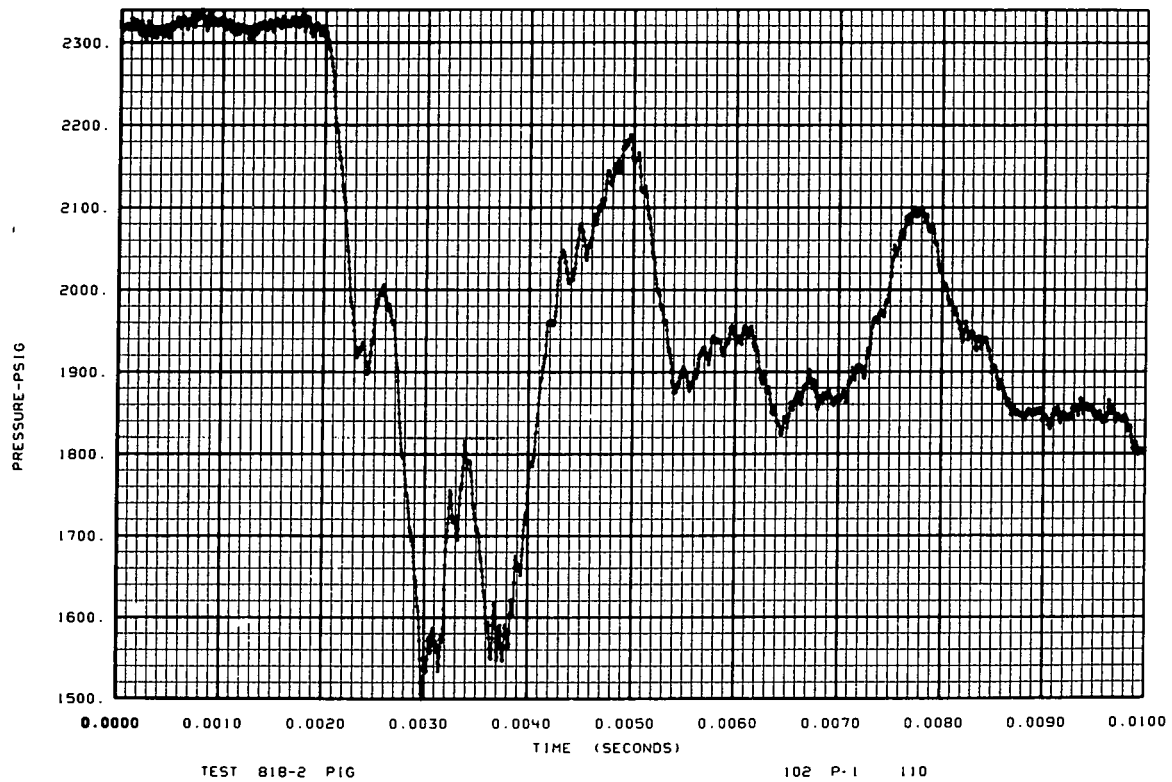
RECORD NO. 125

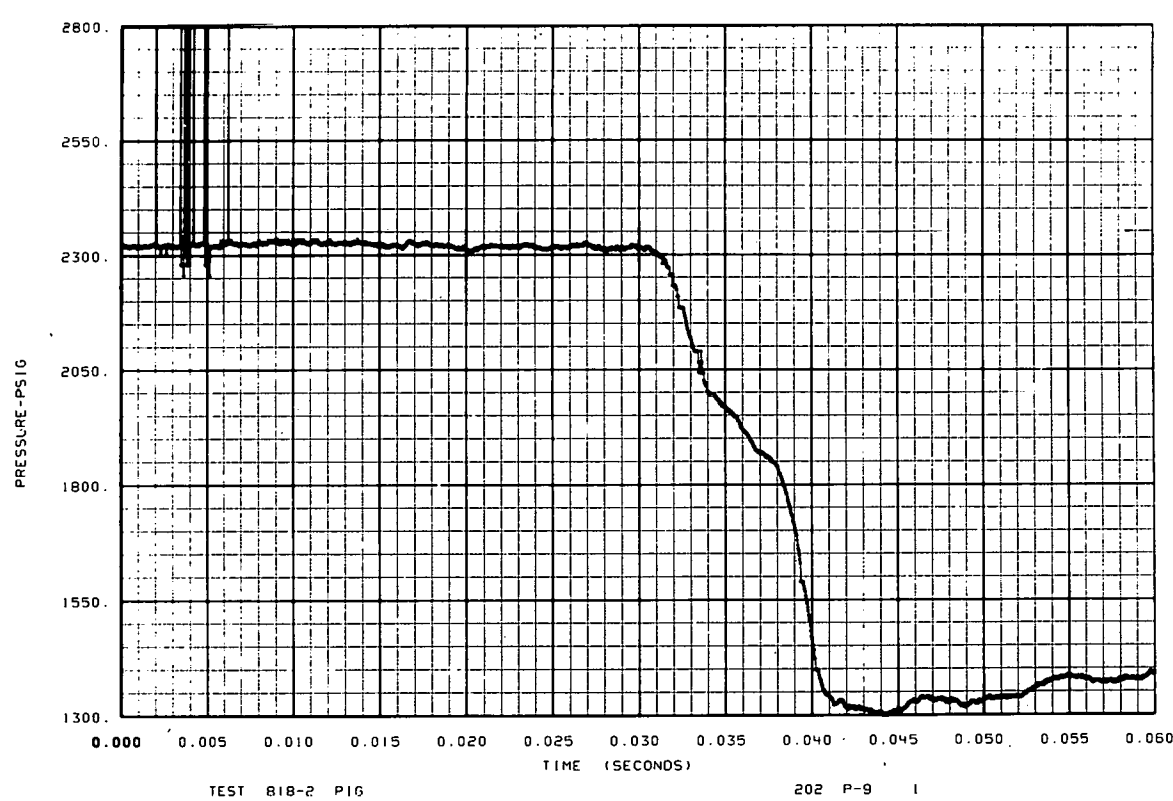
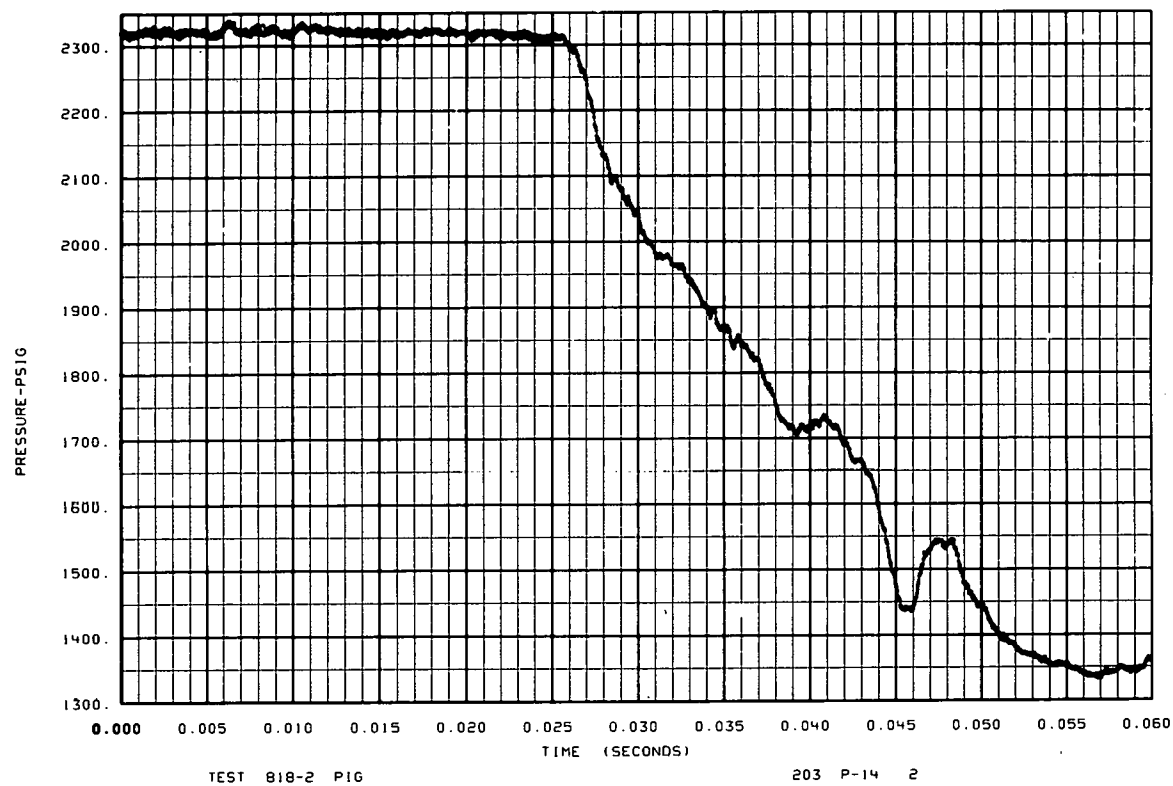
813 510 LC-4A

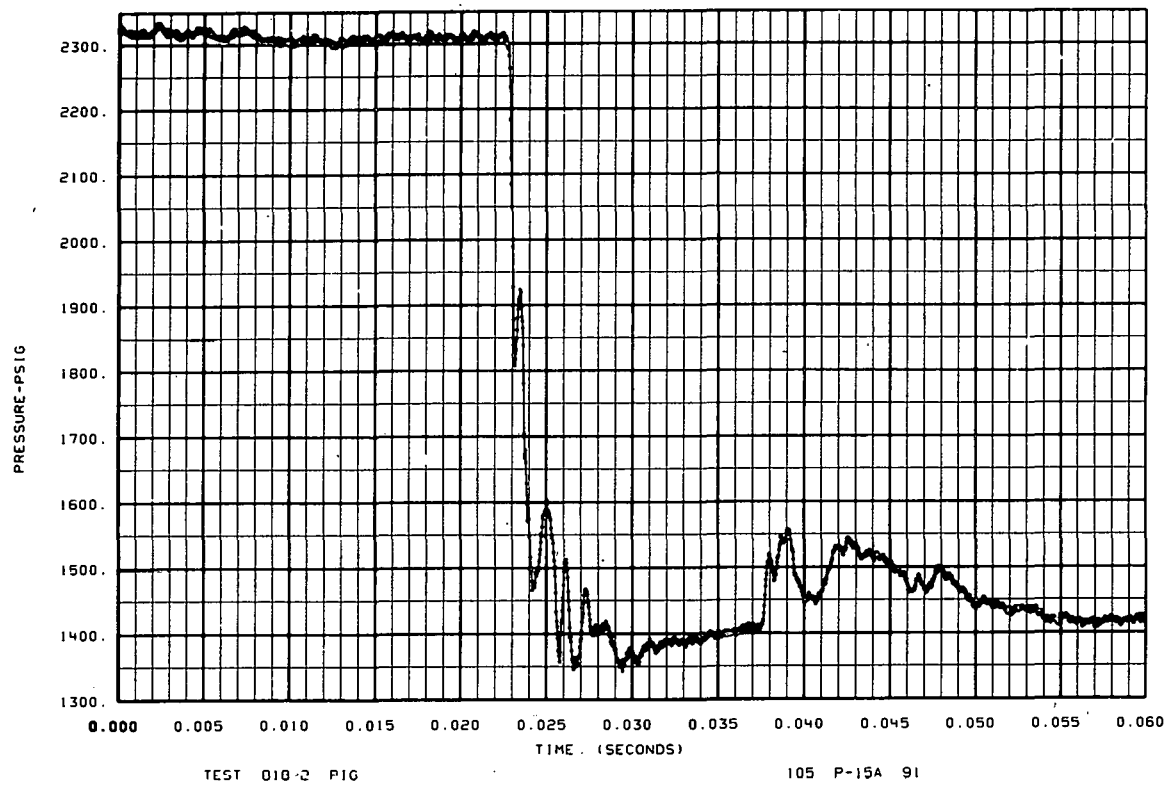
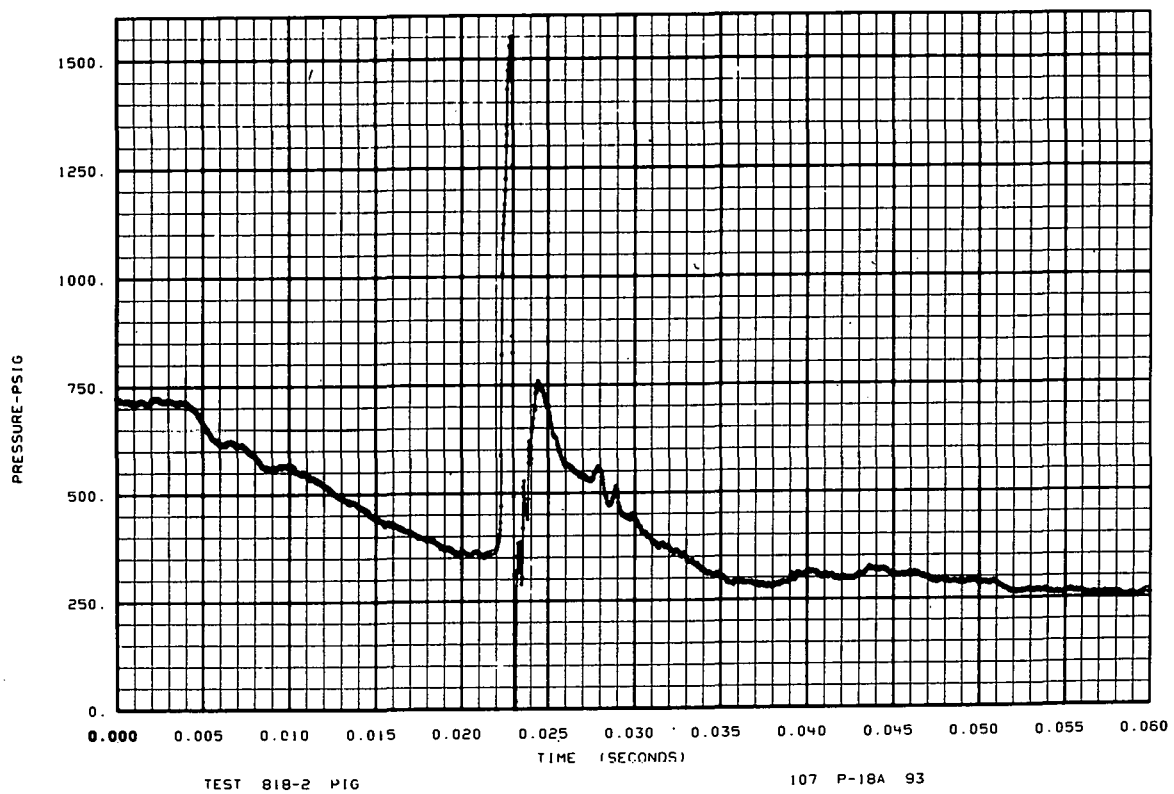


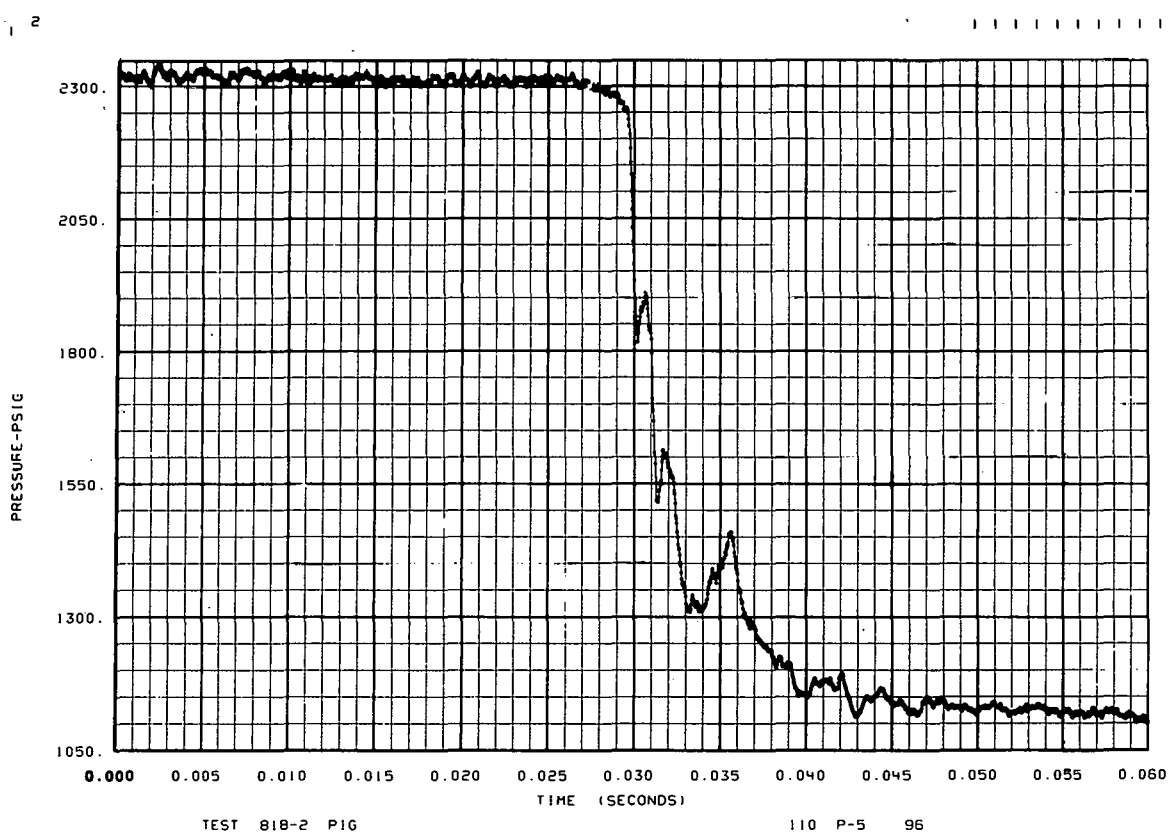
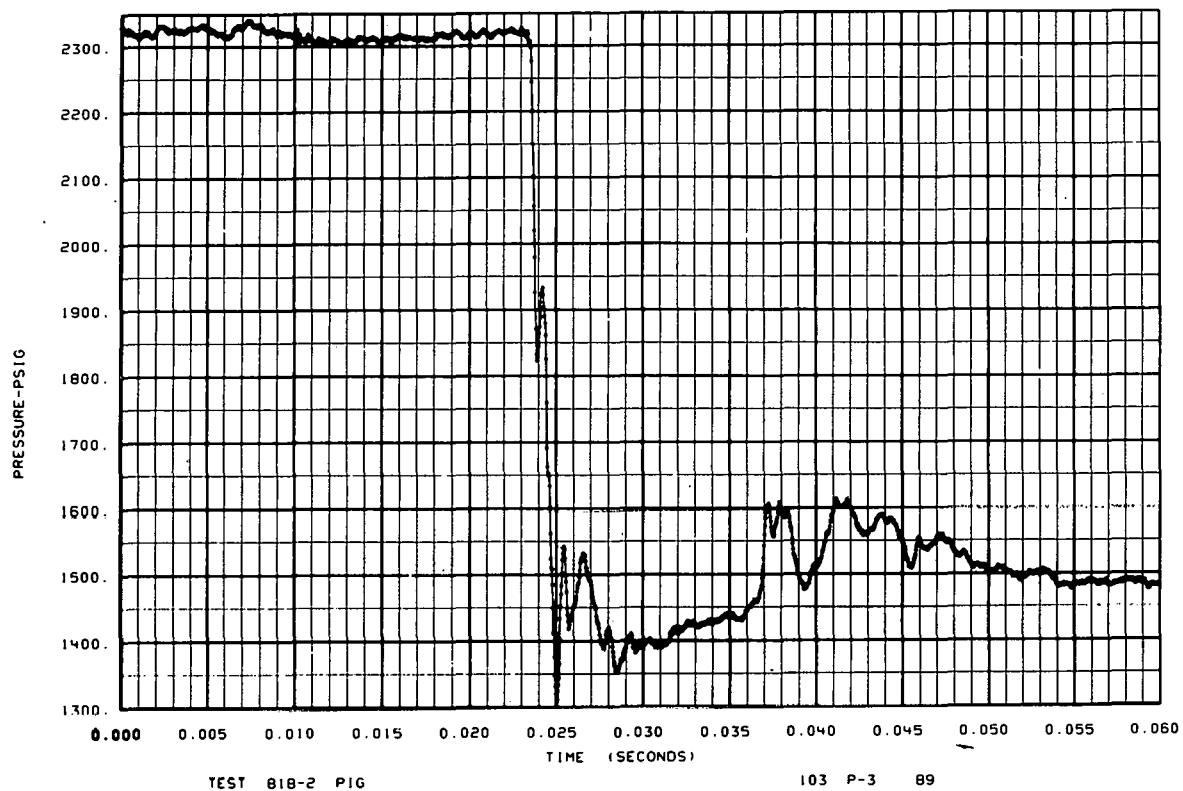


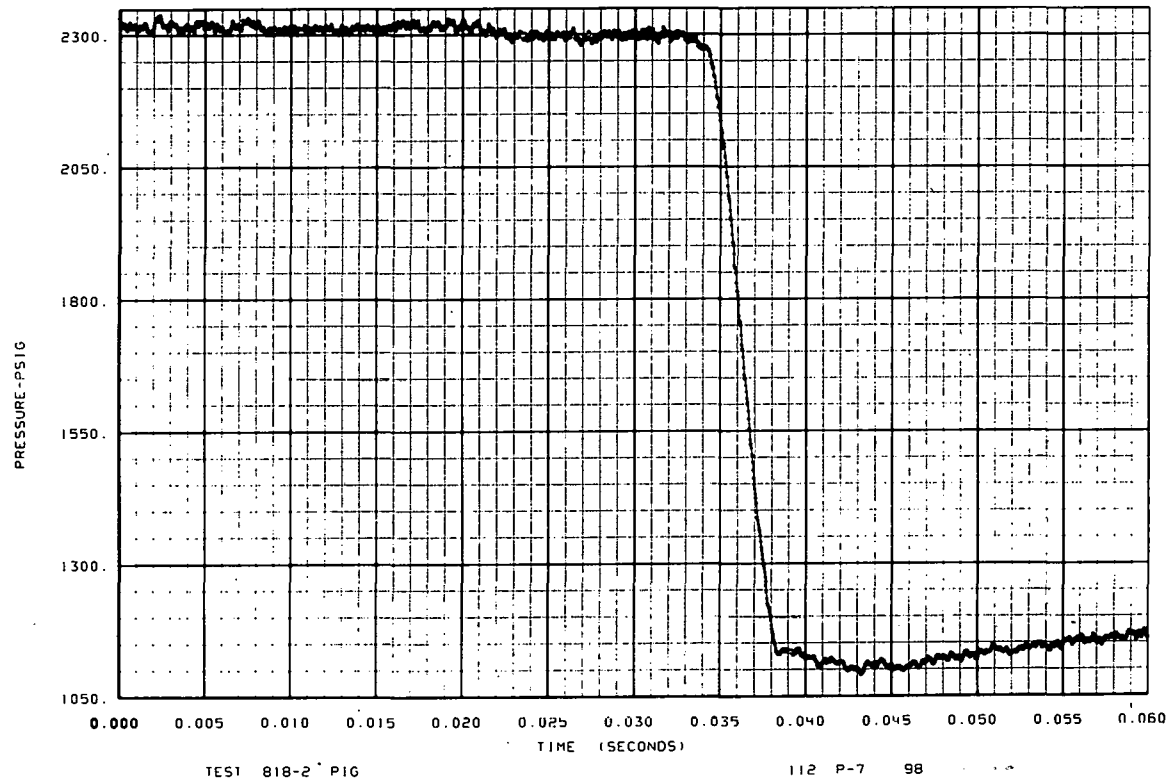
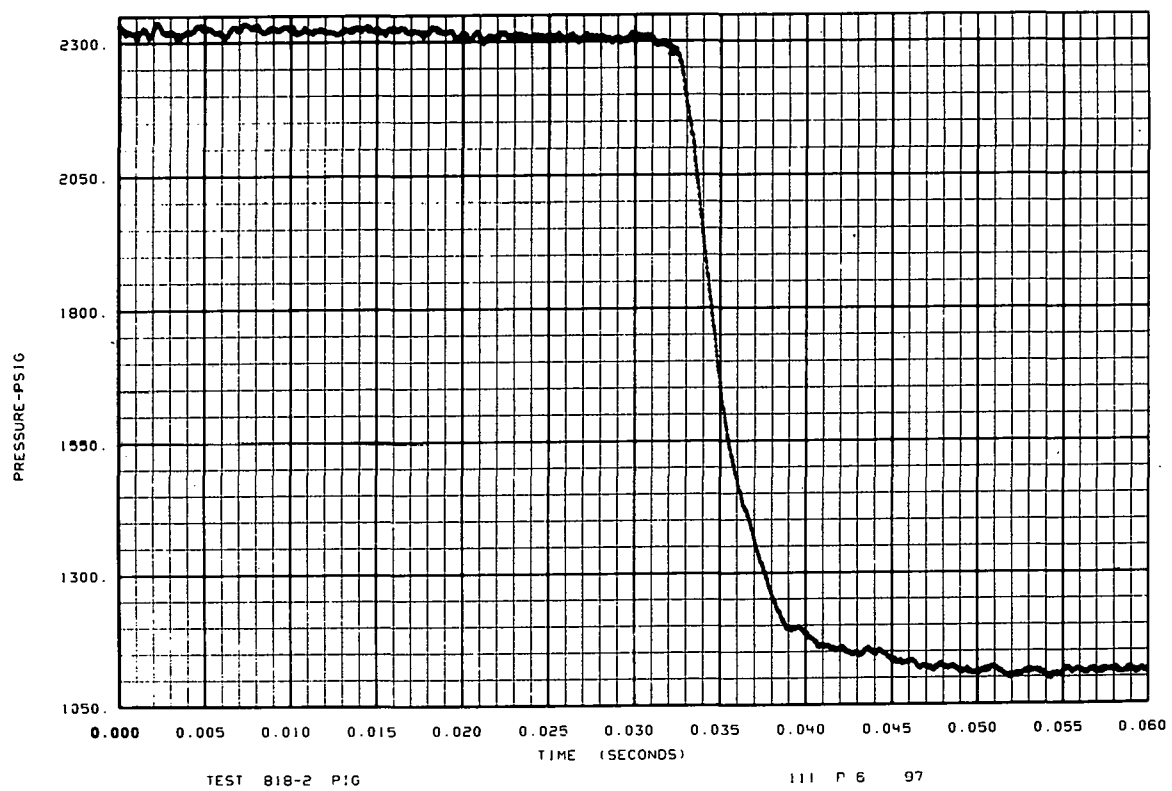


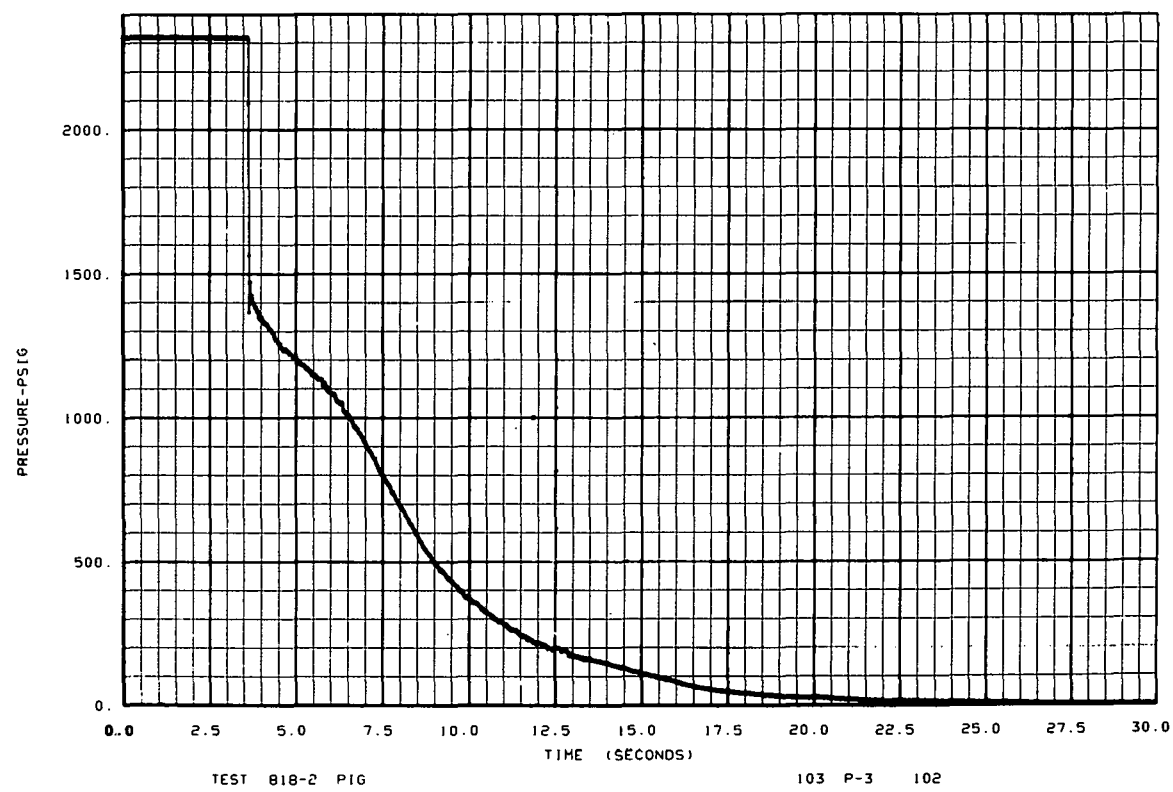
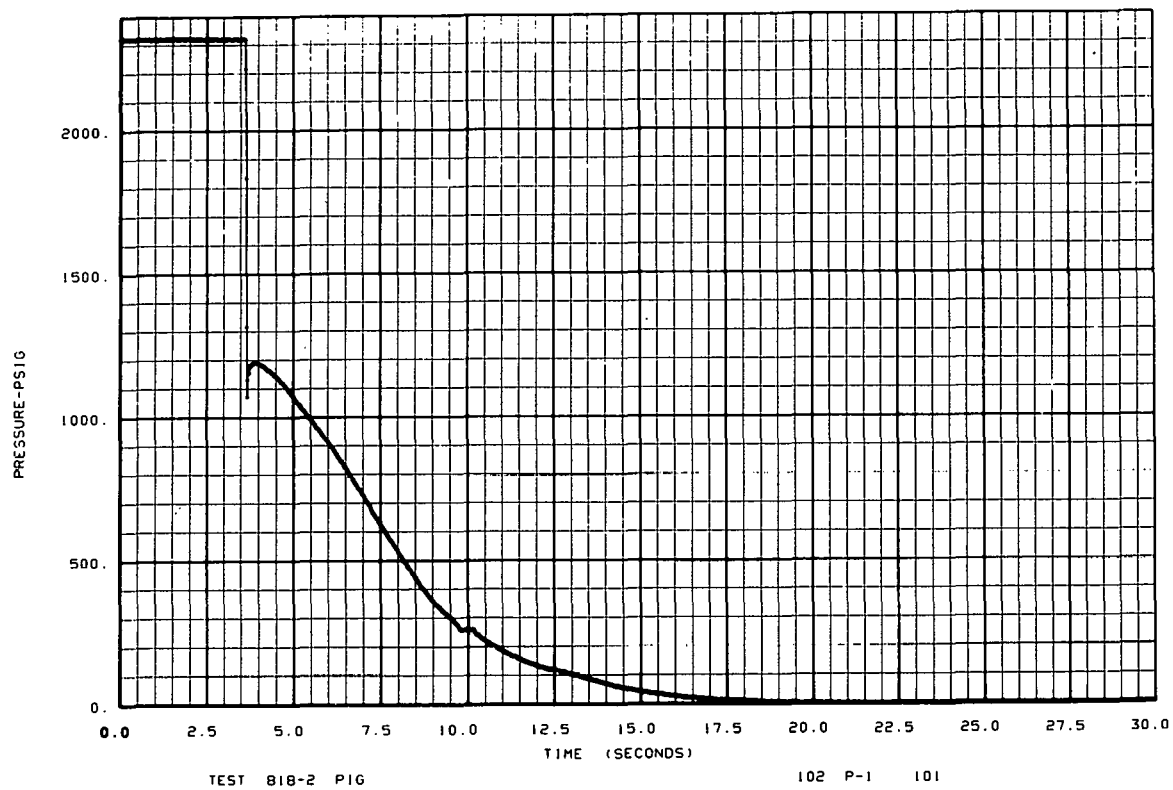


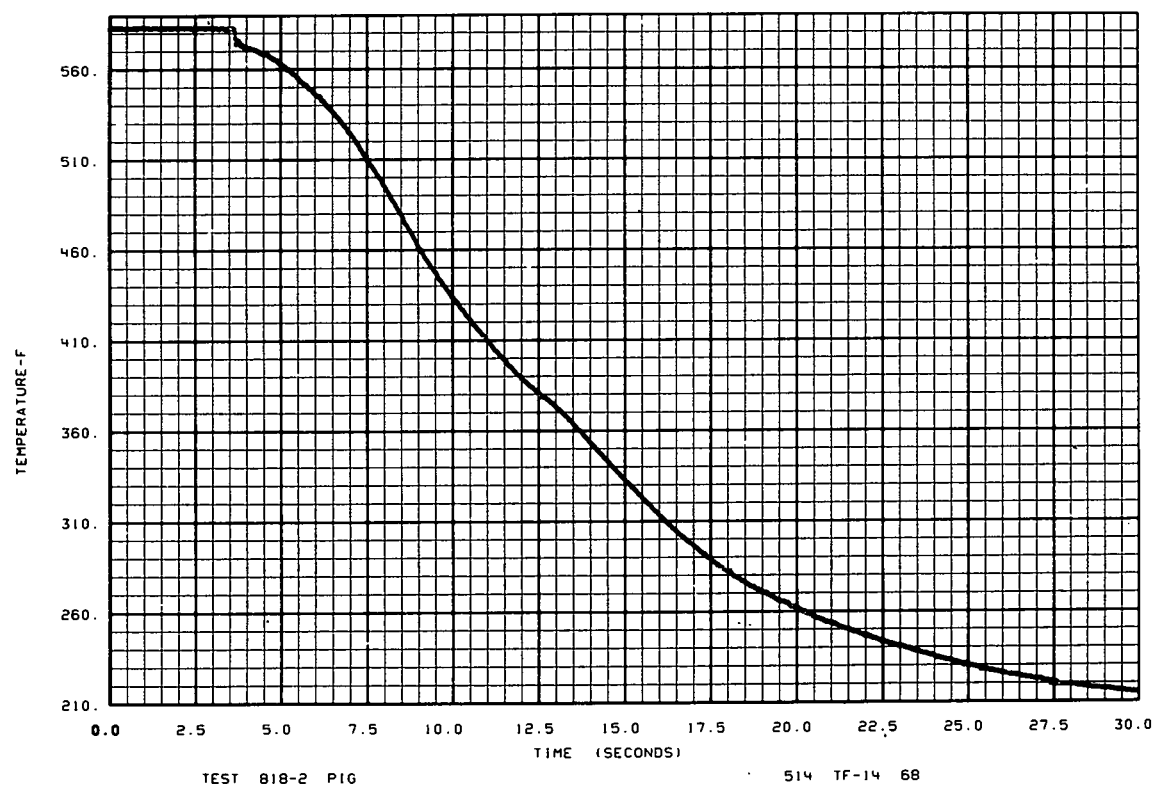
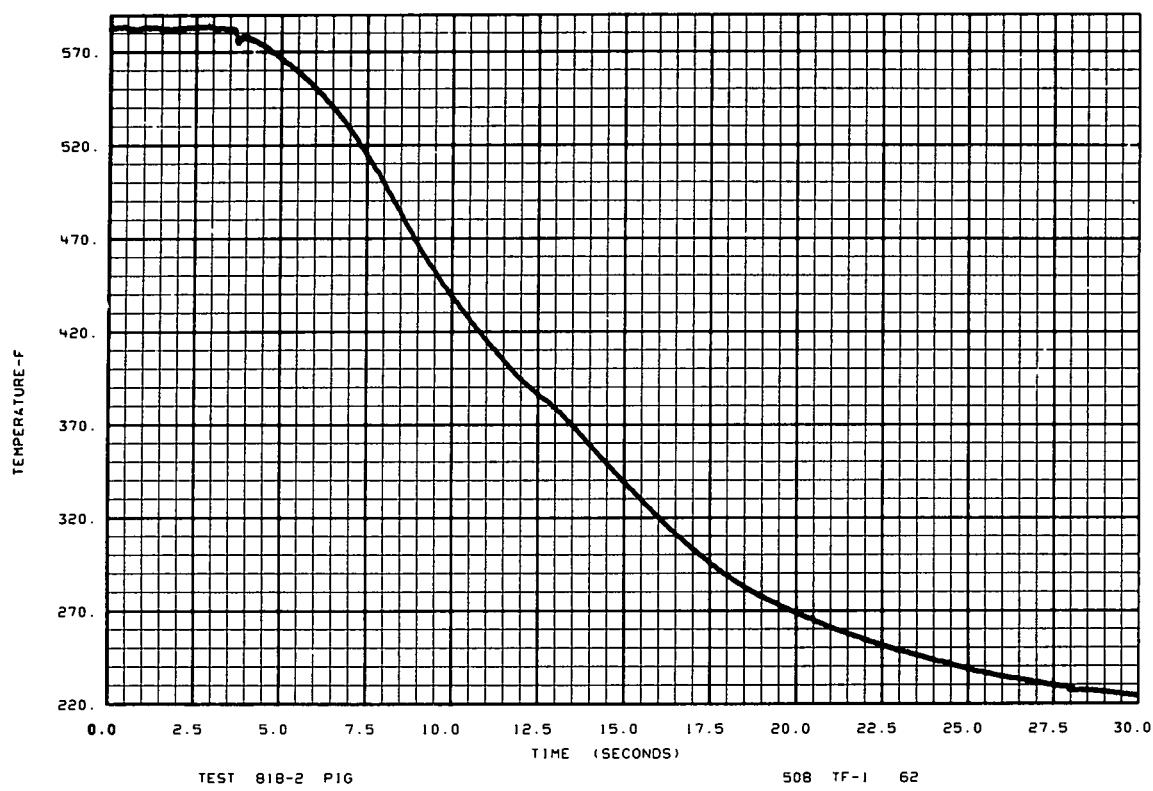


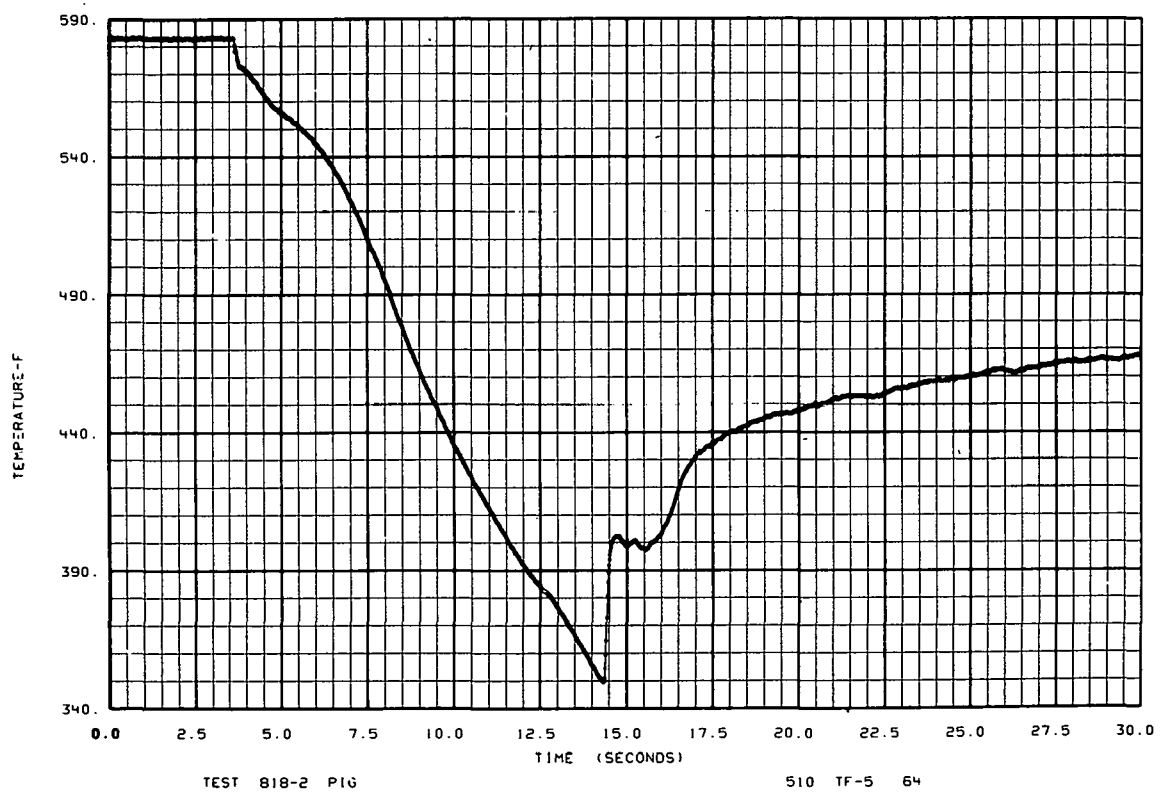
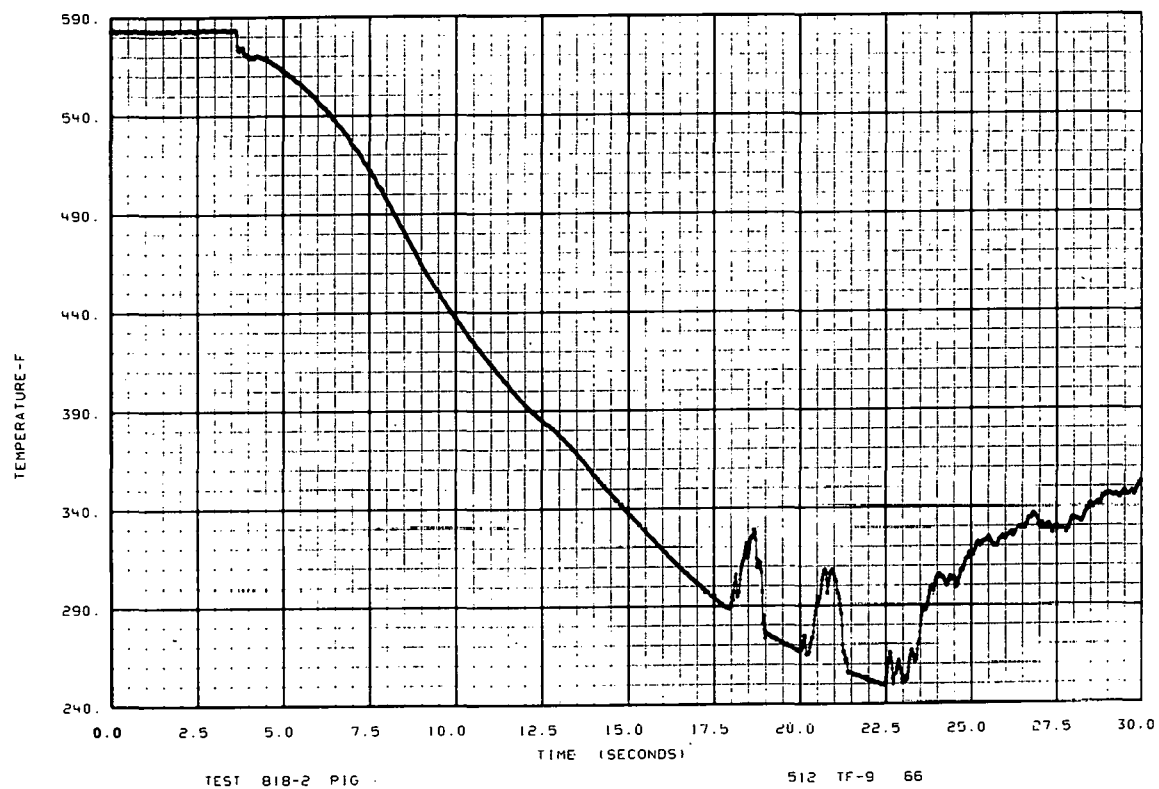


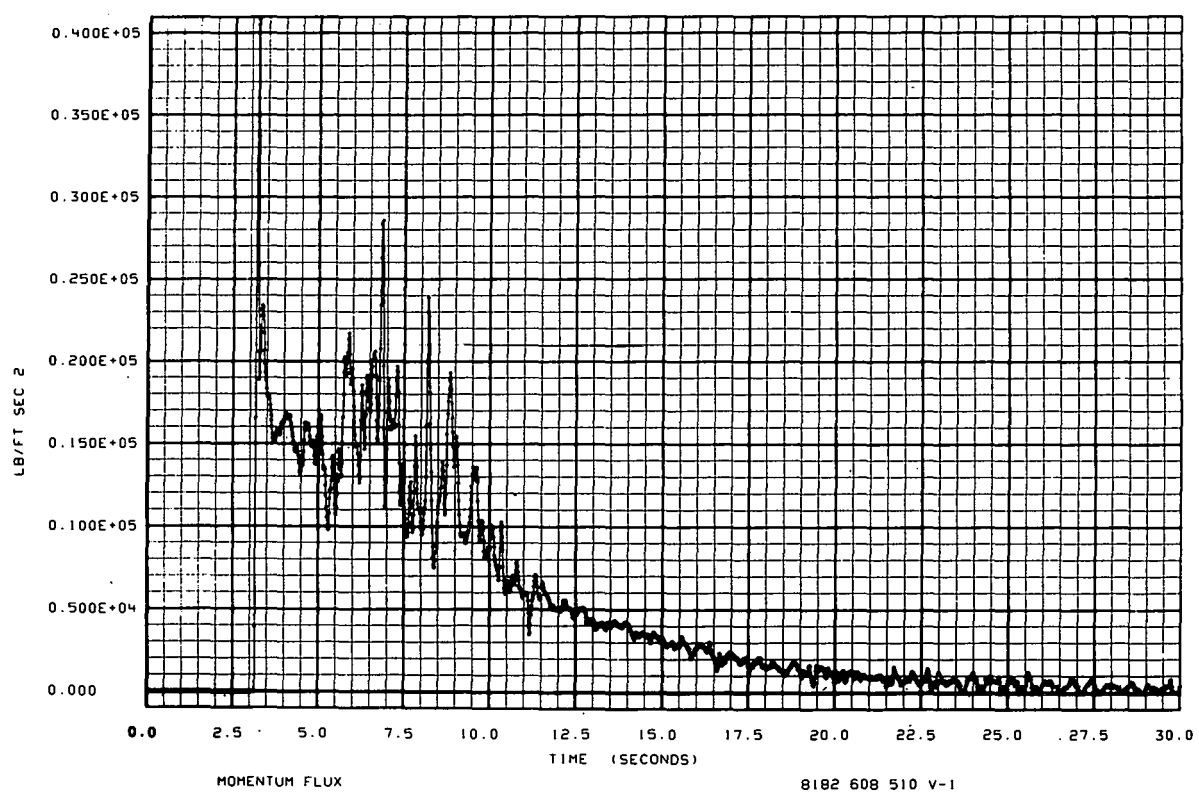
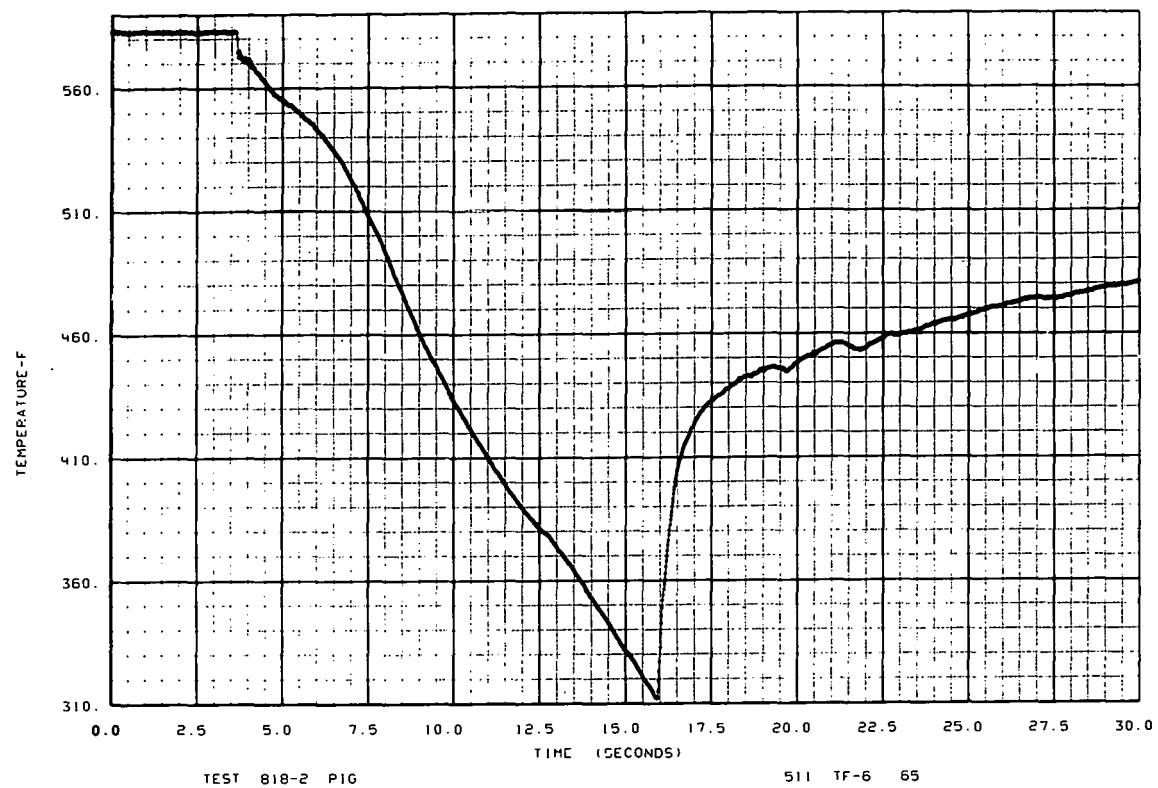


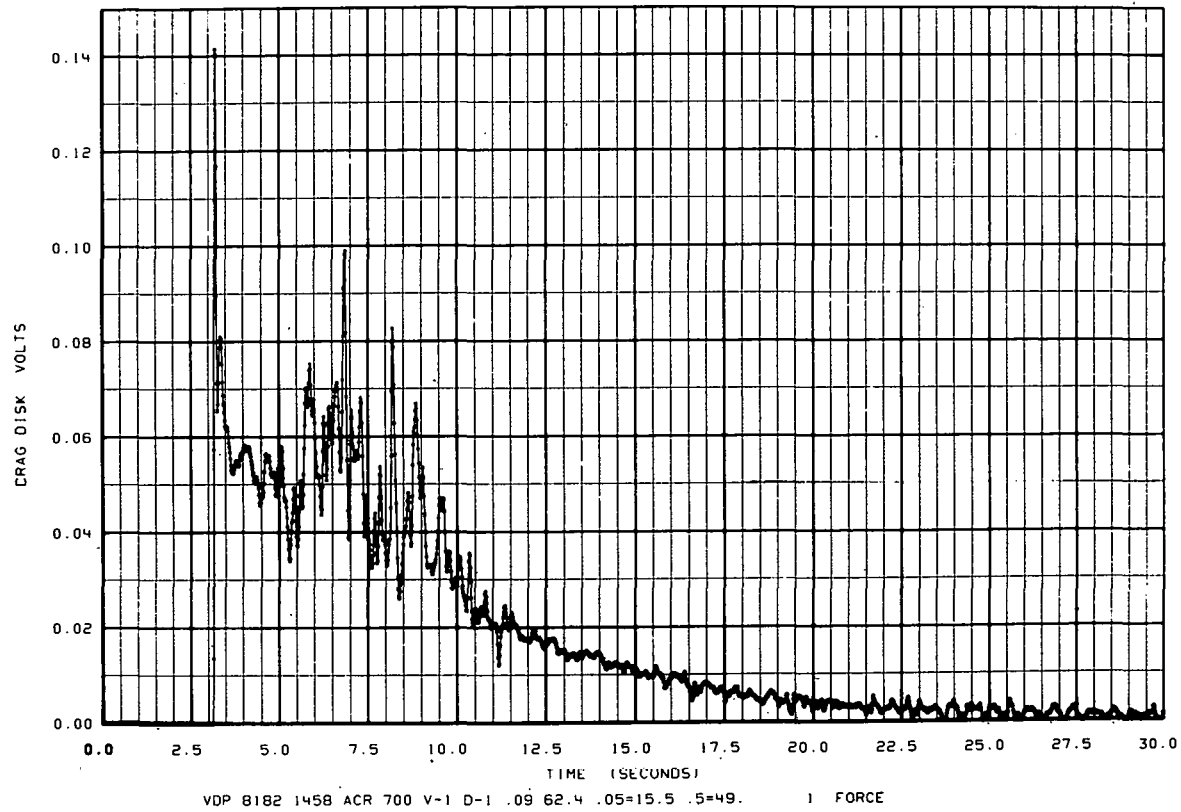
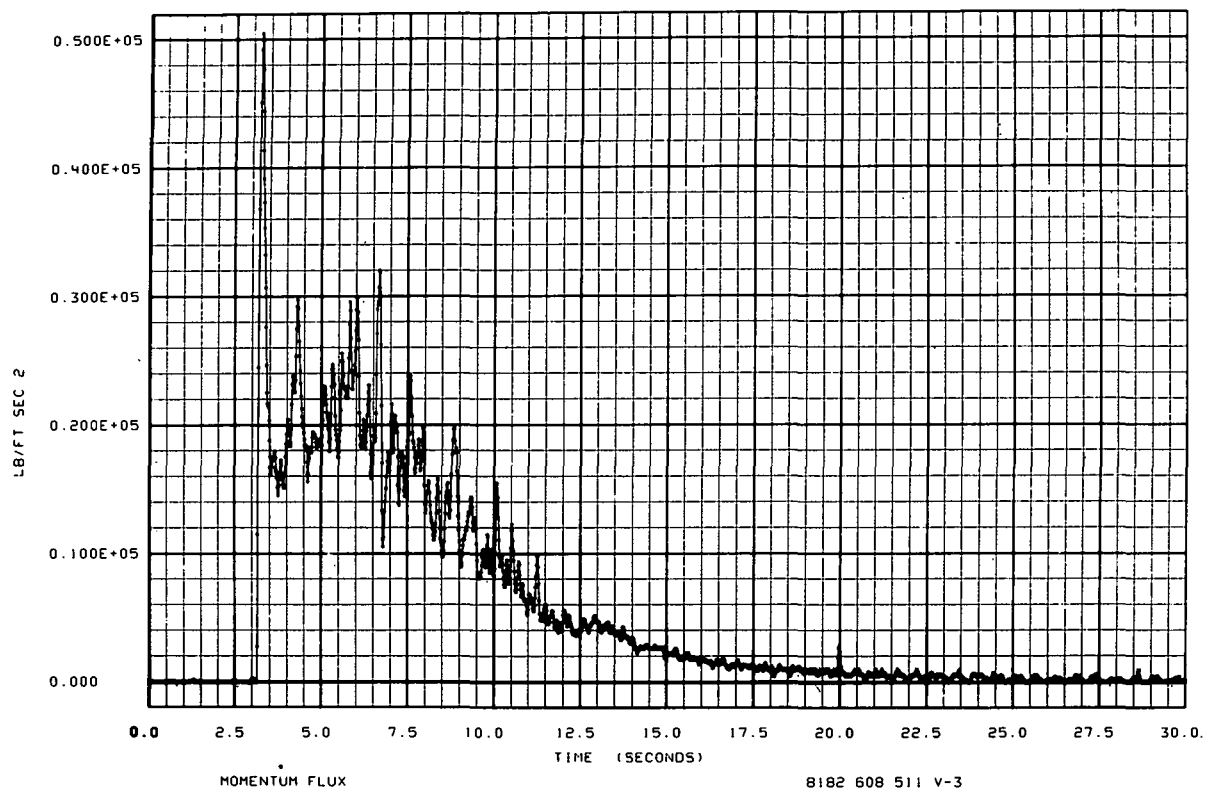


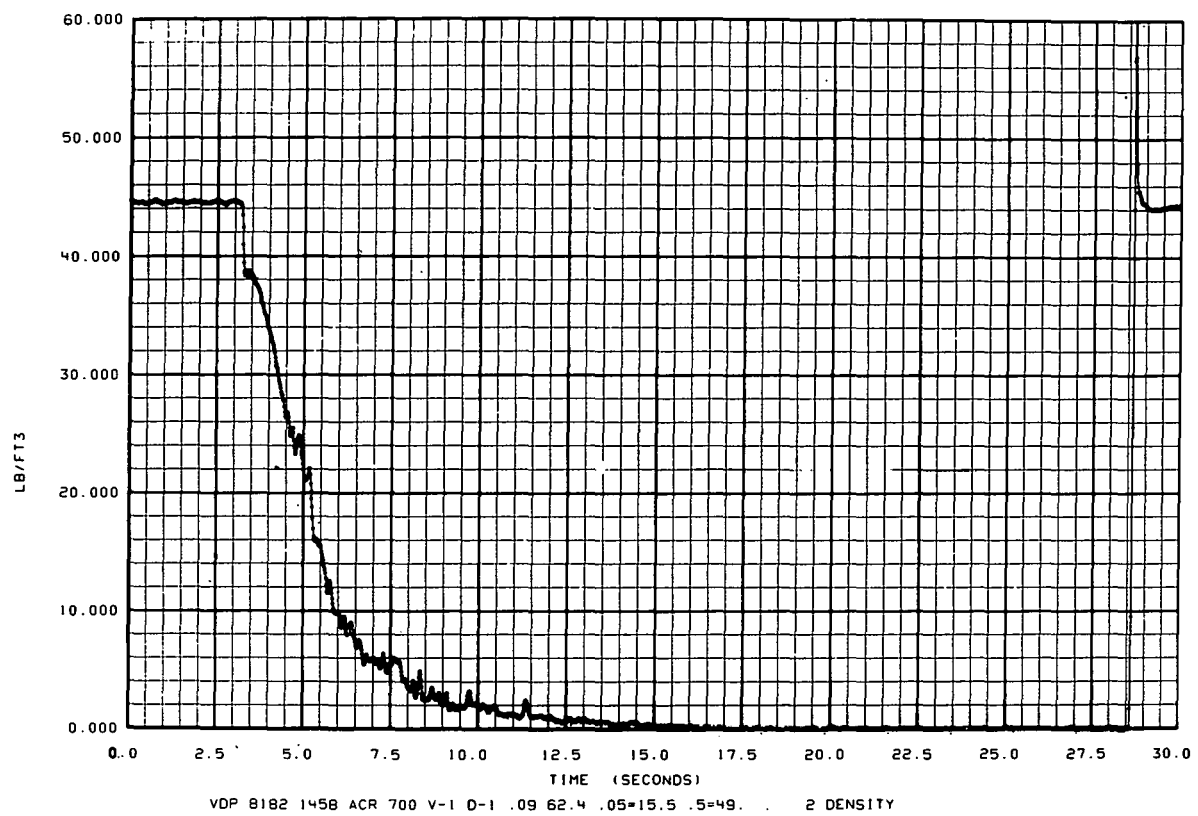




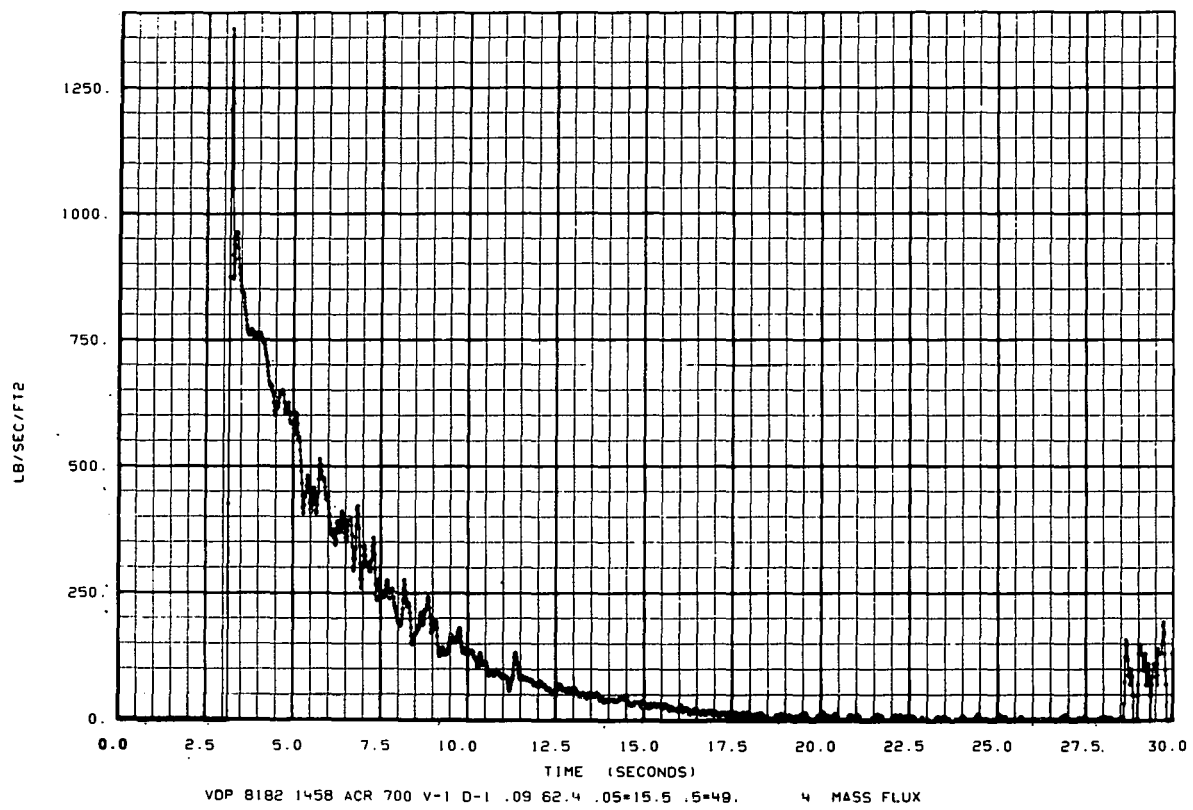




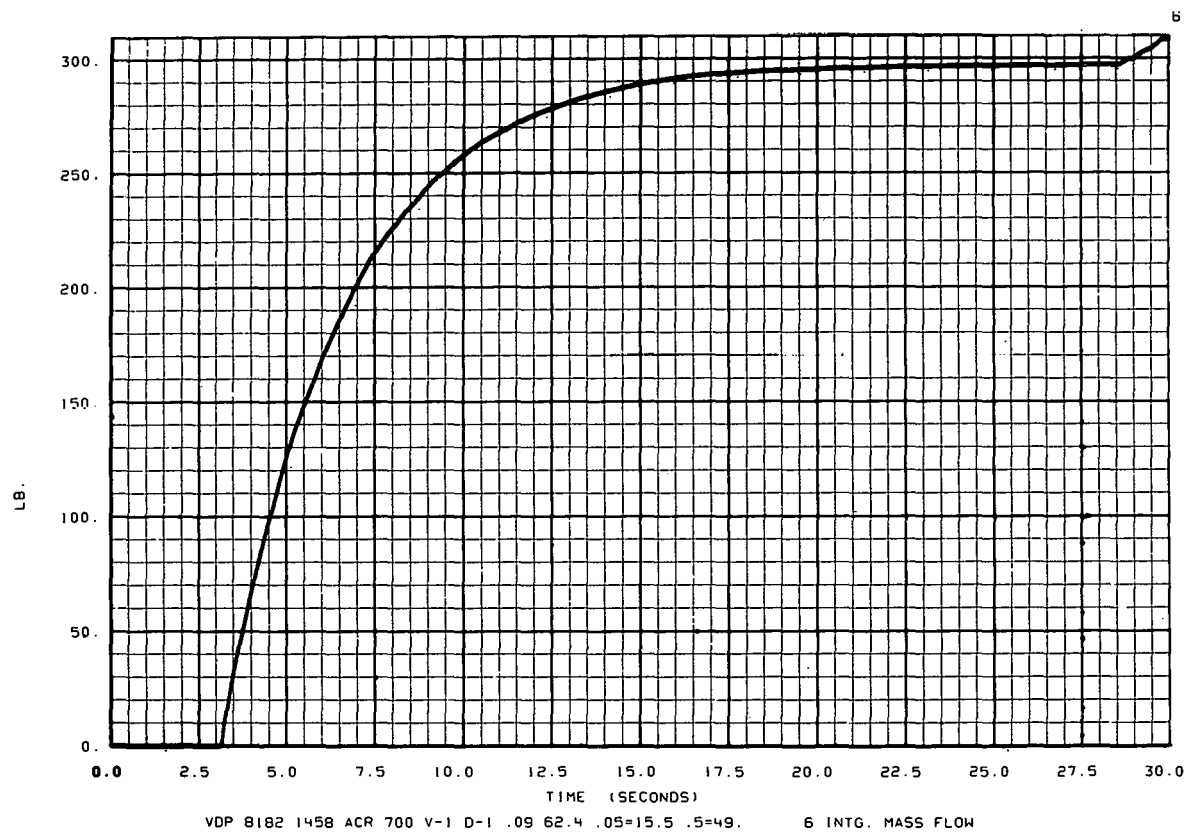
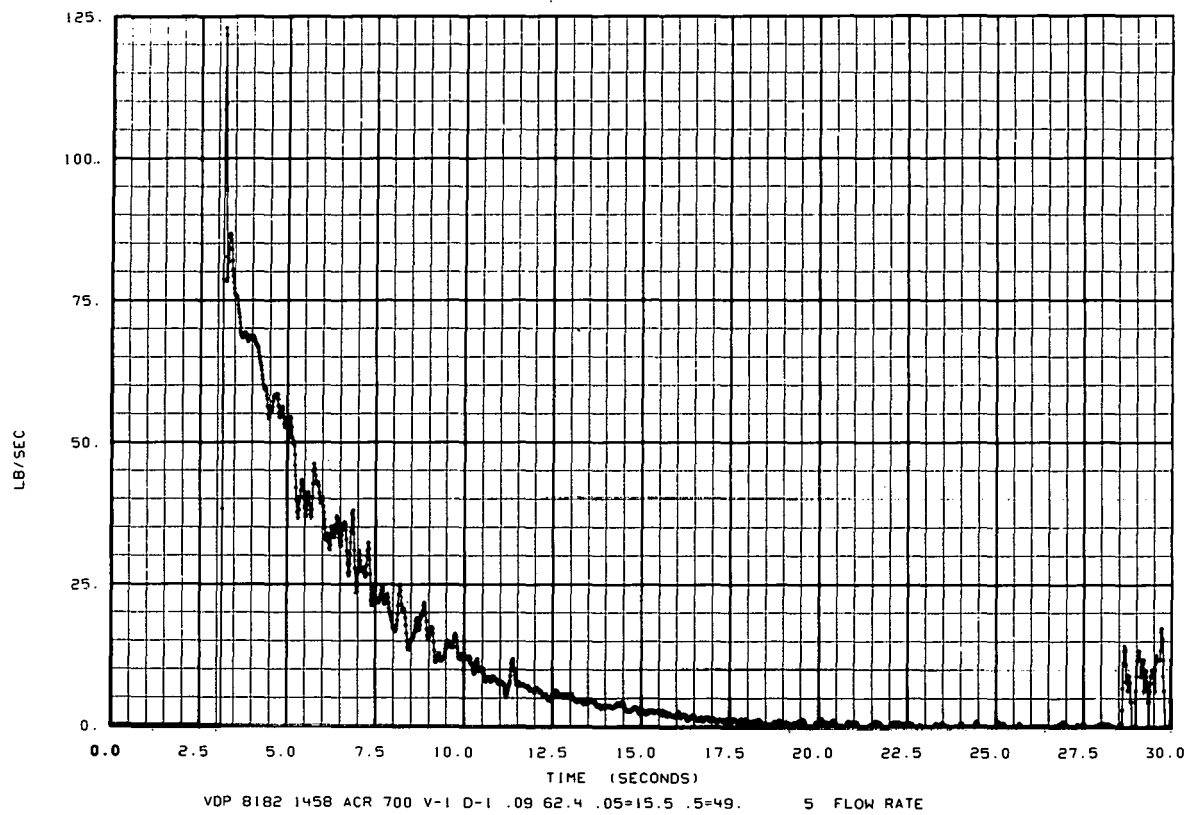


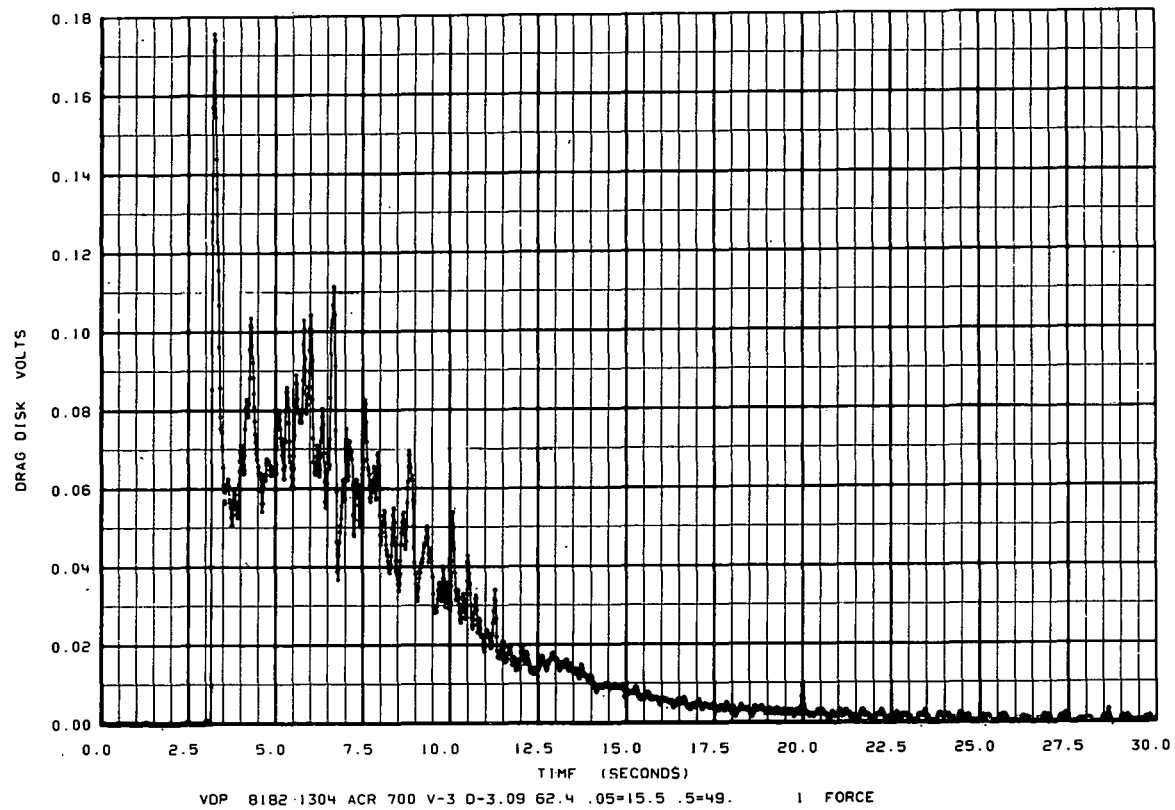


3

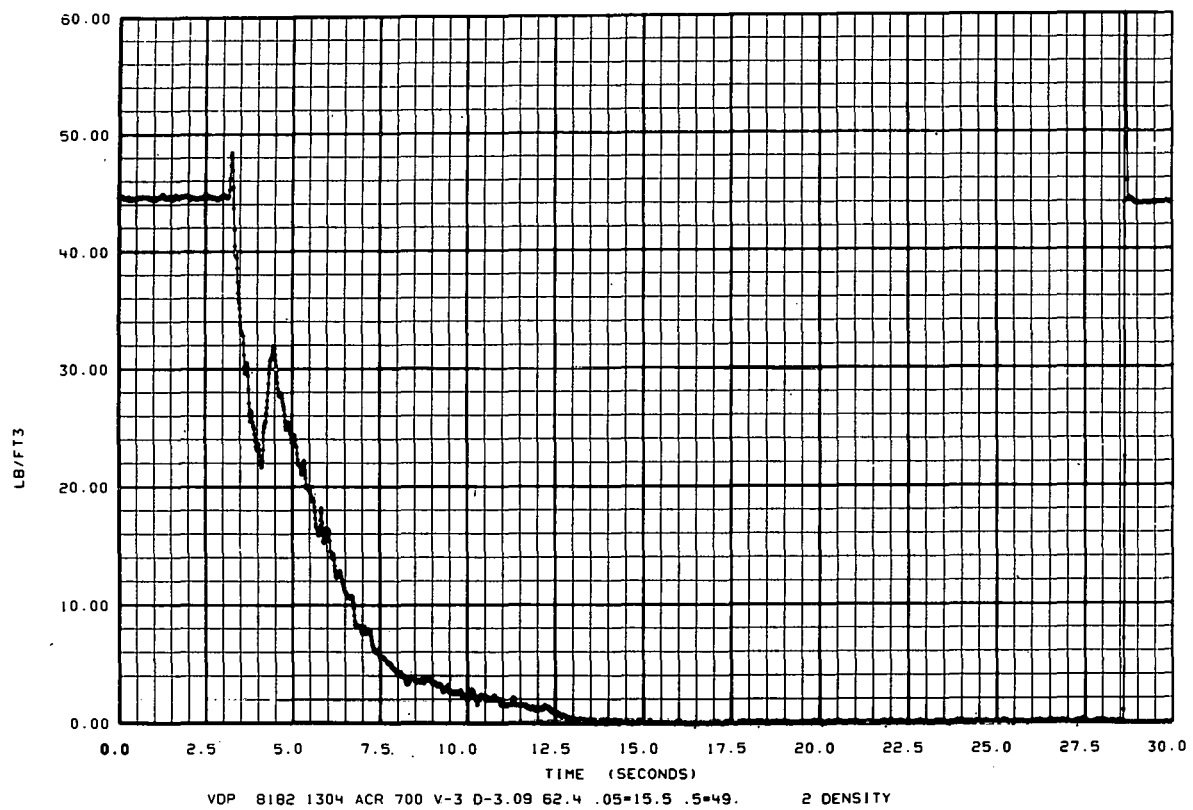


5

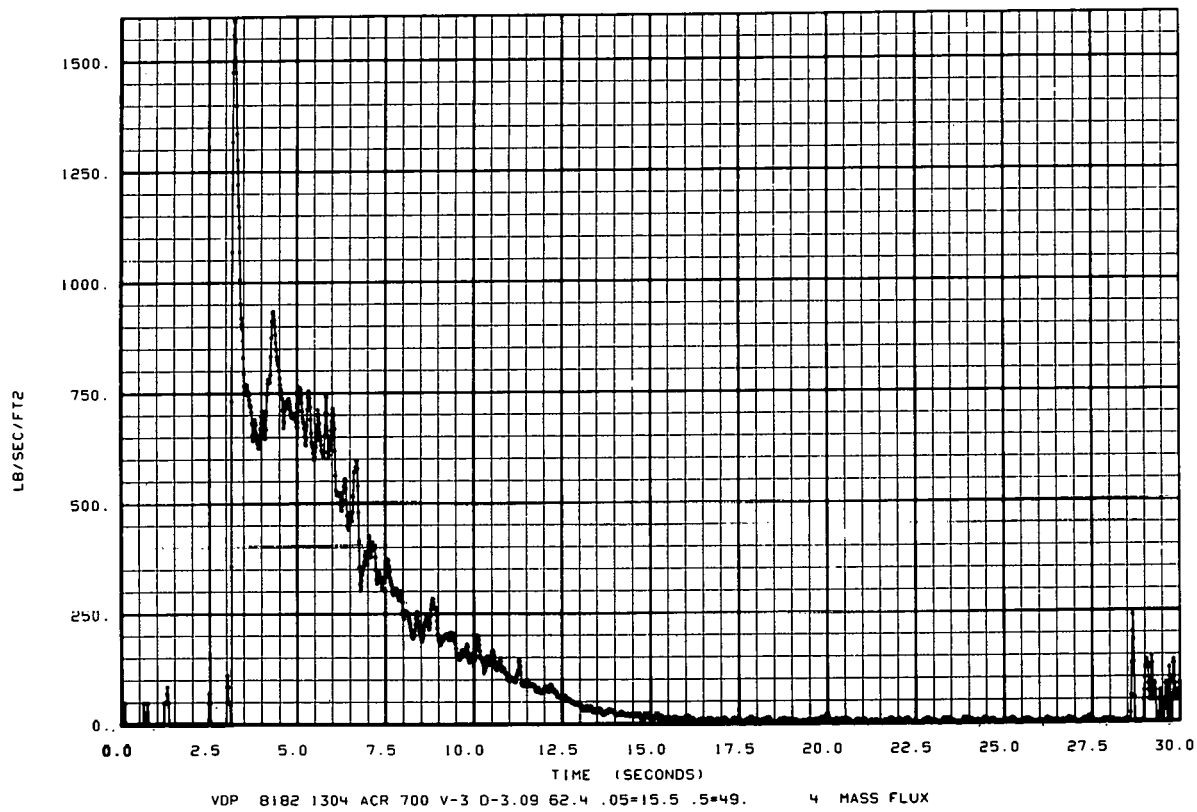




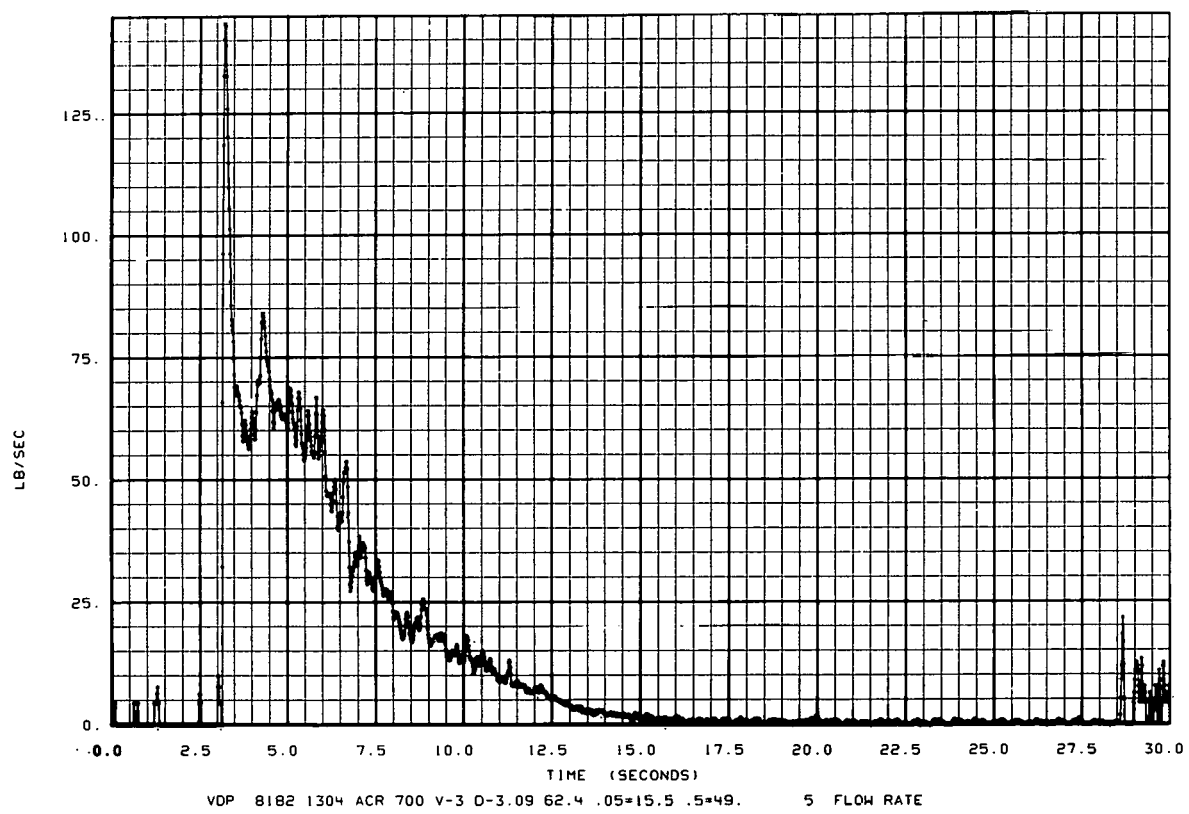
8



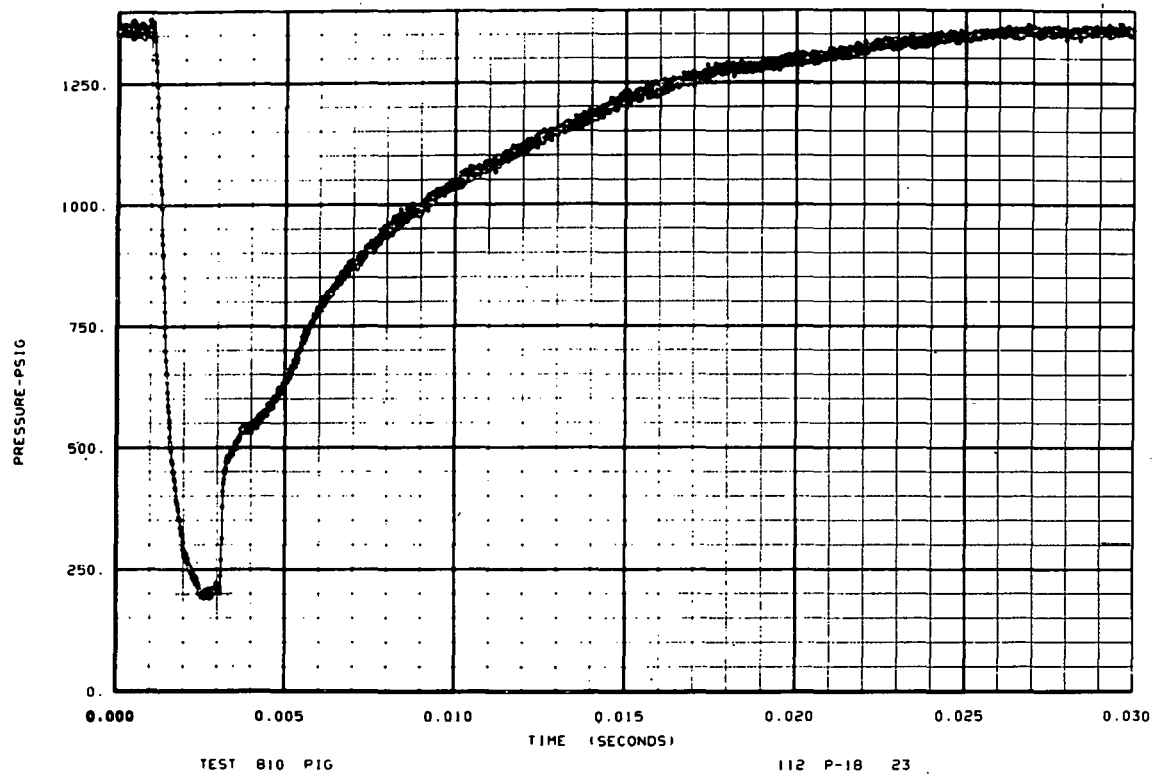
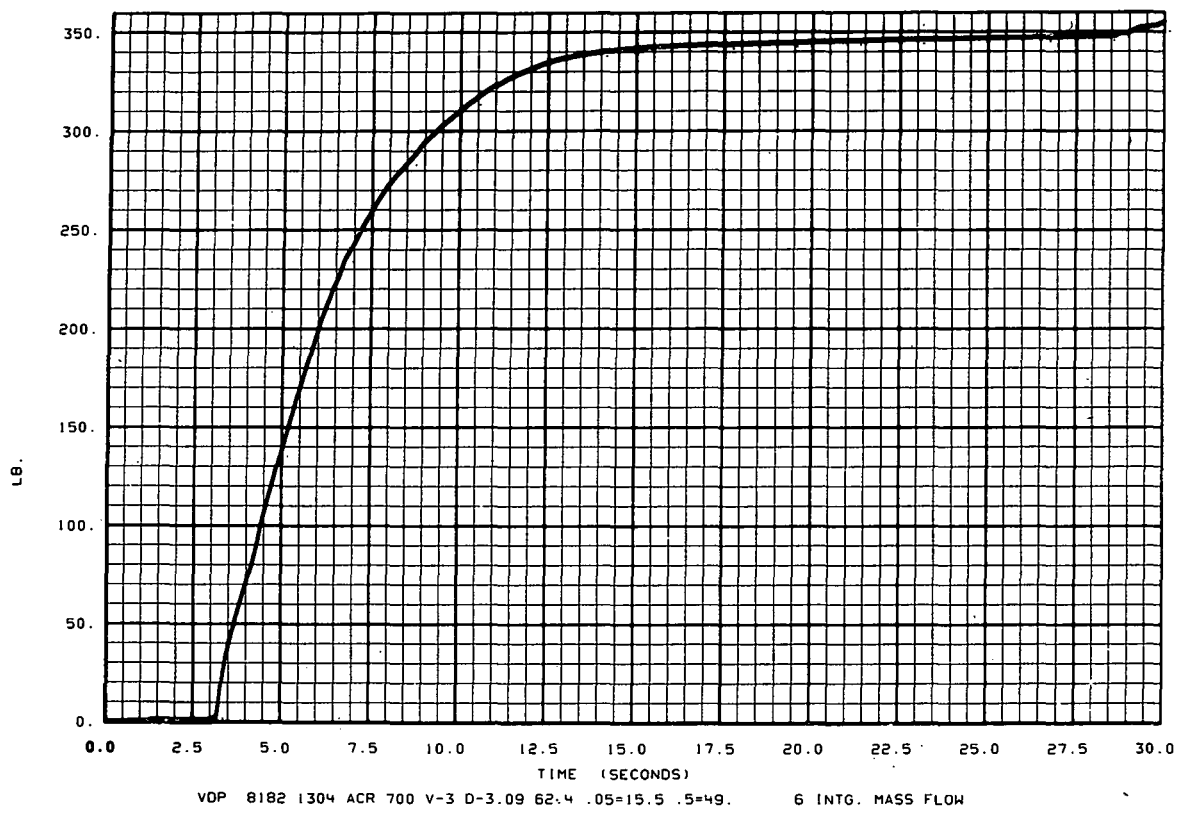
9

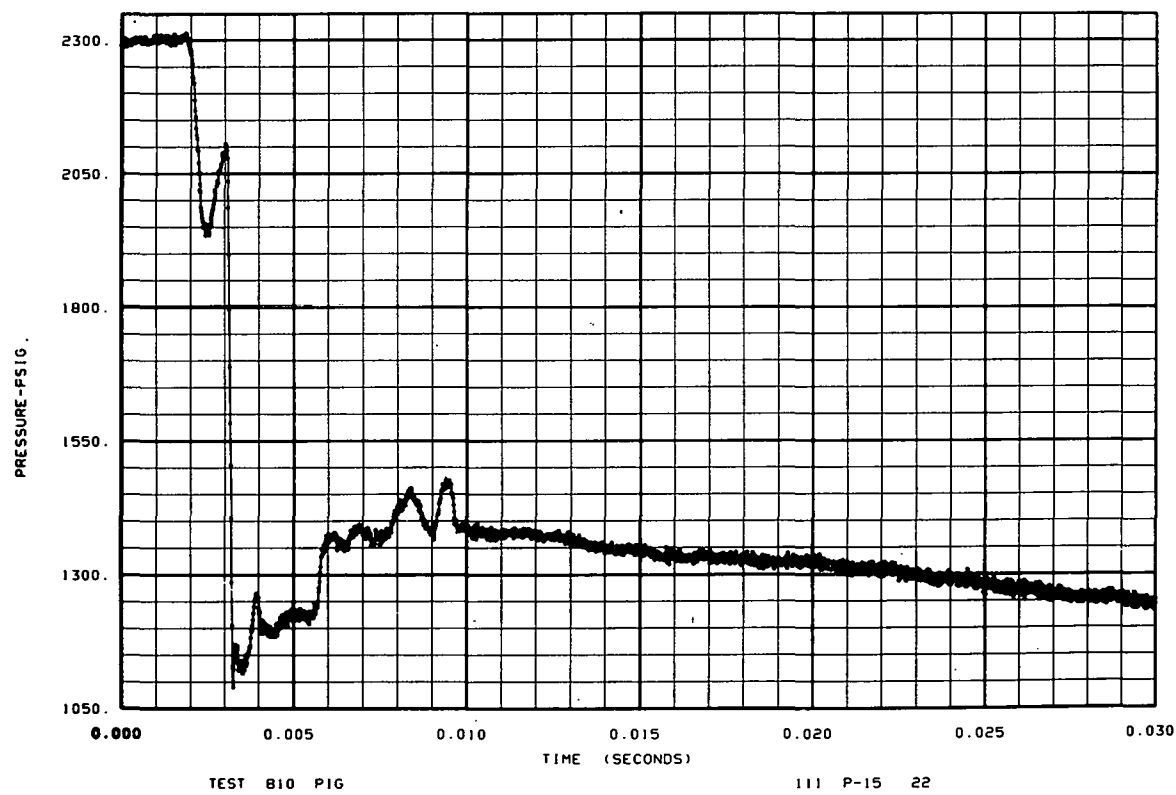
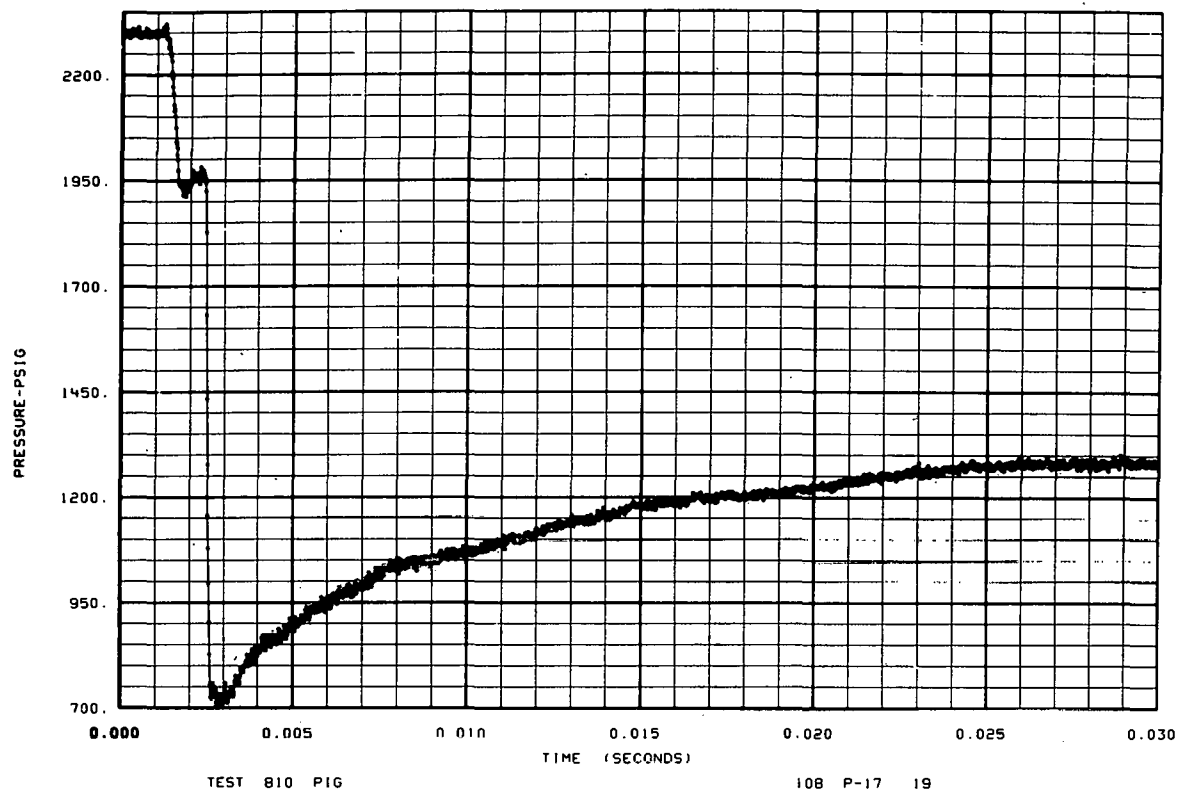


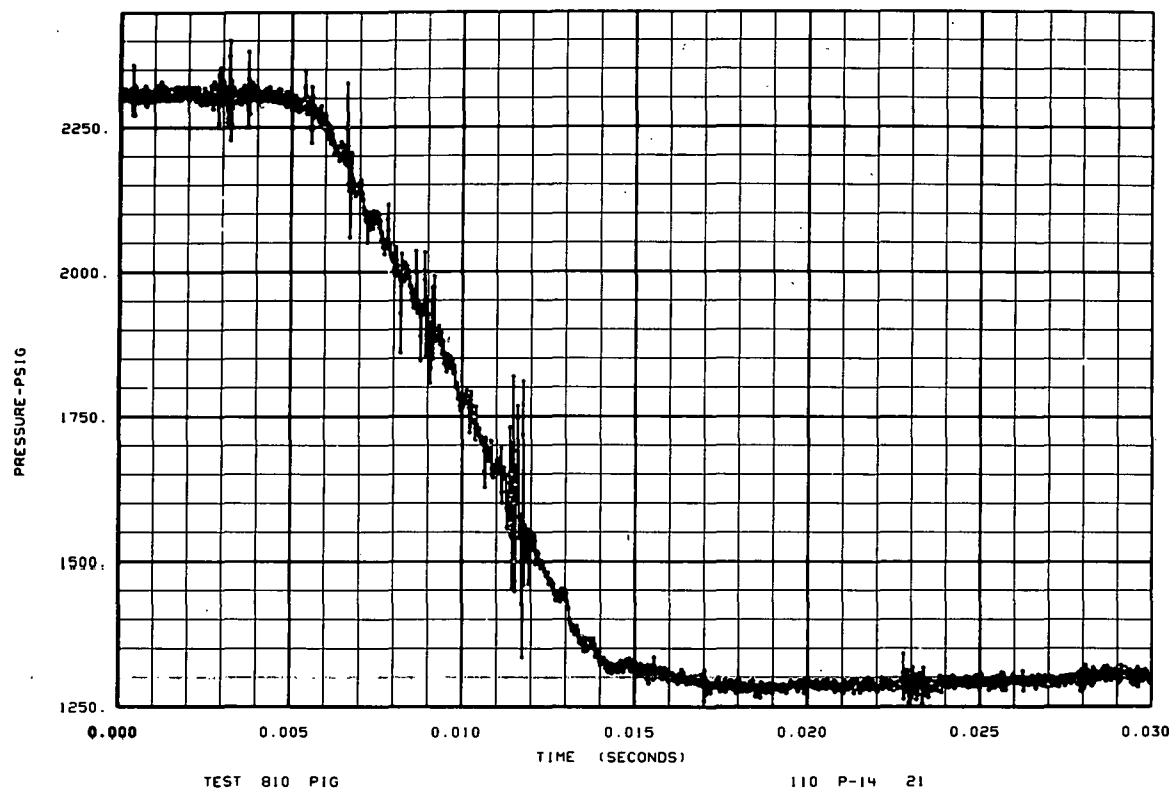
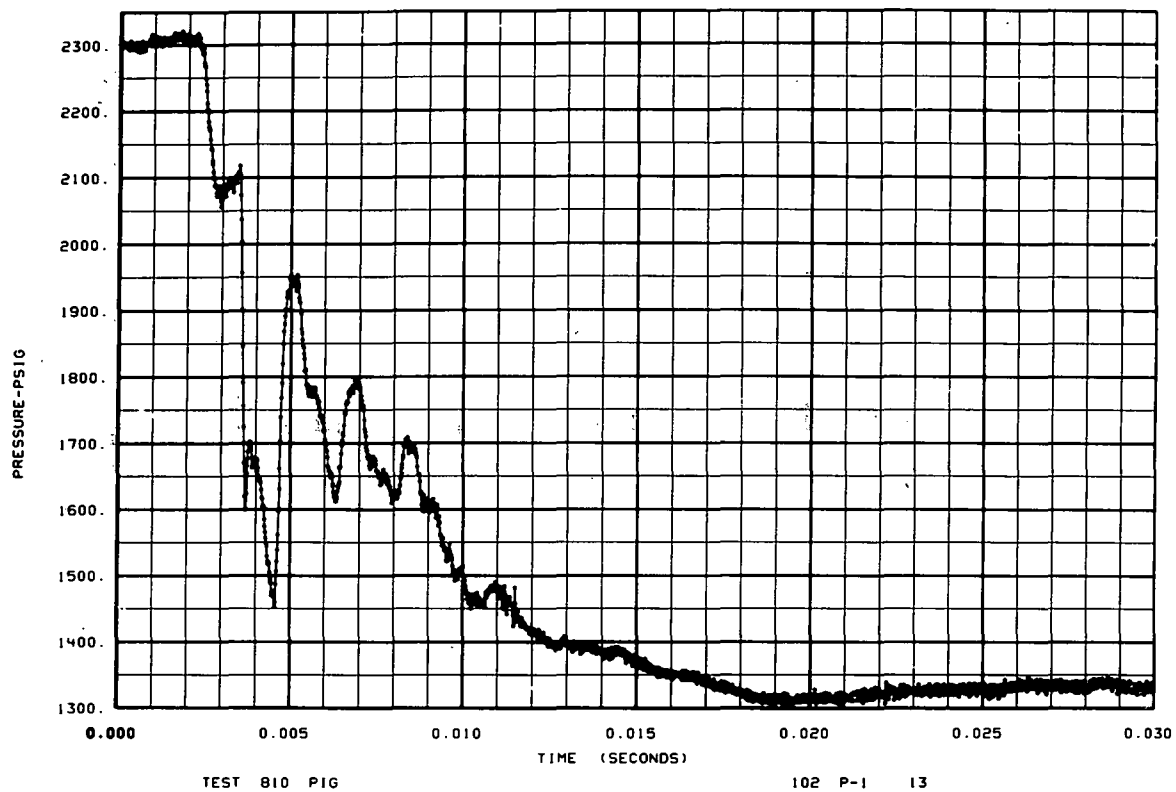
11

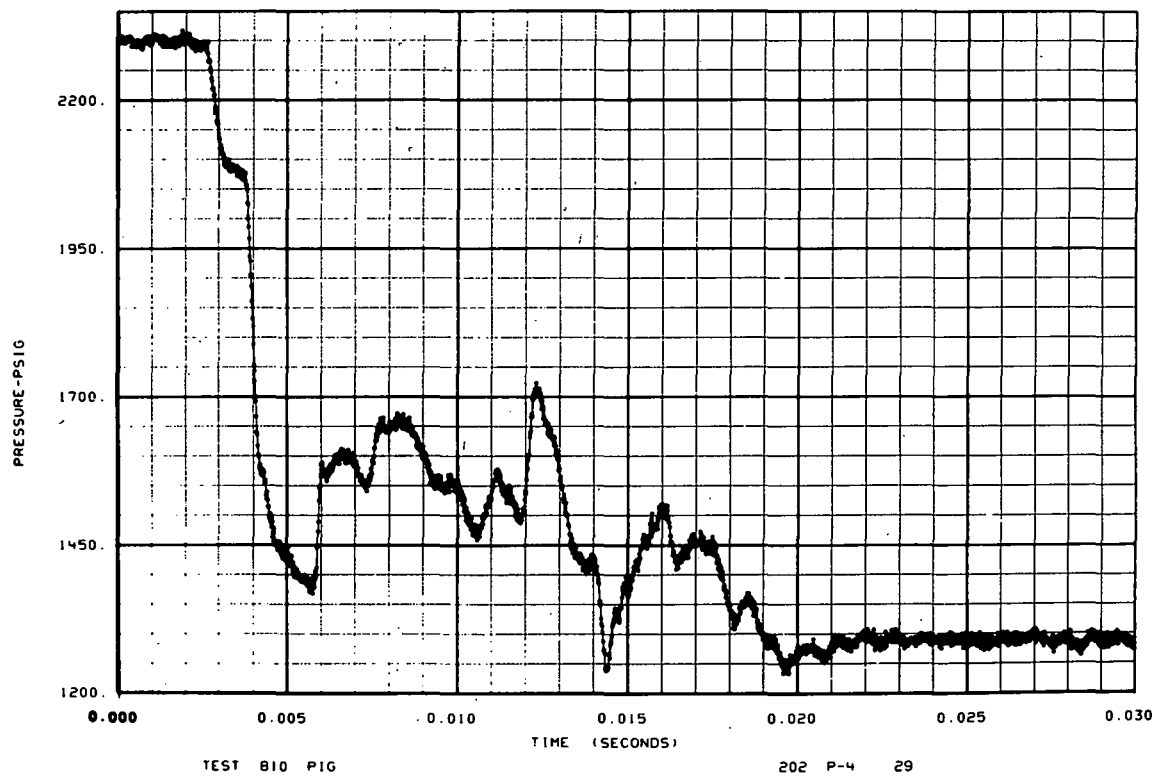
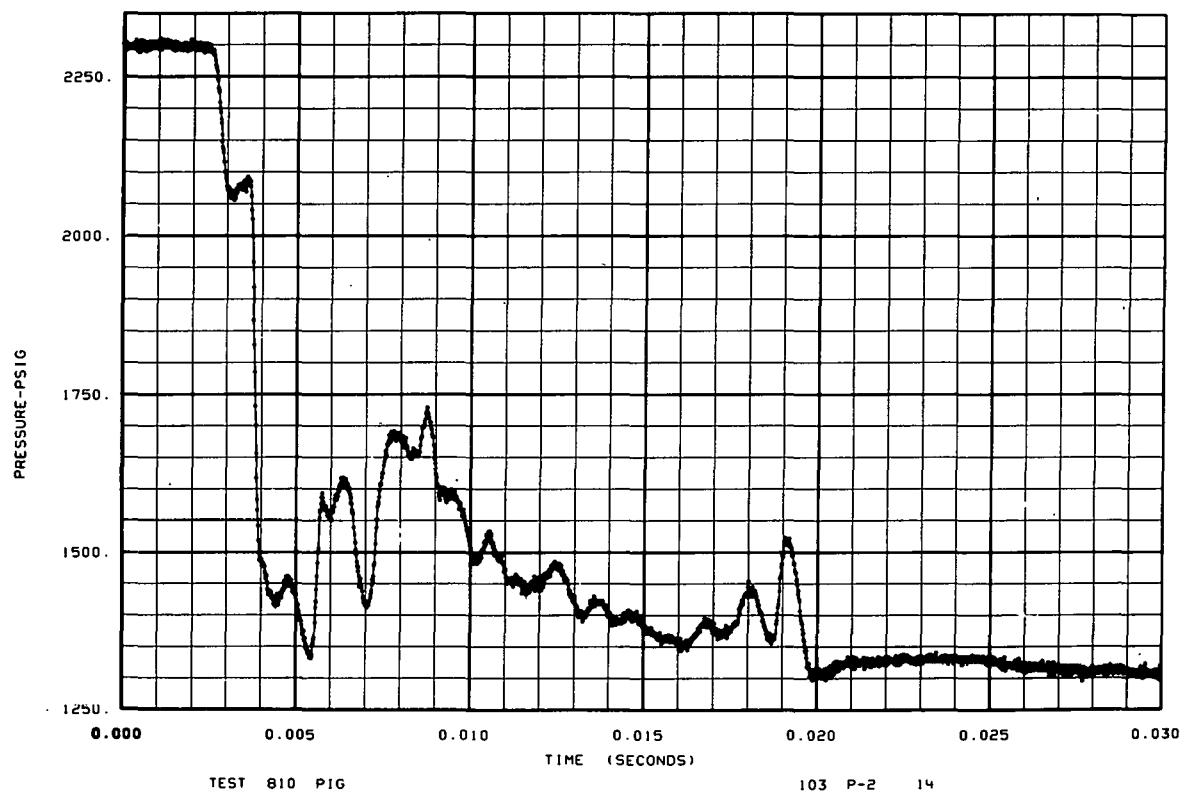


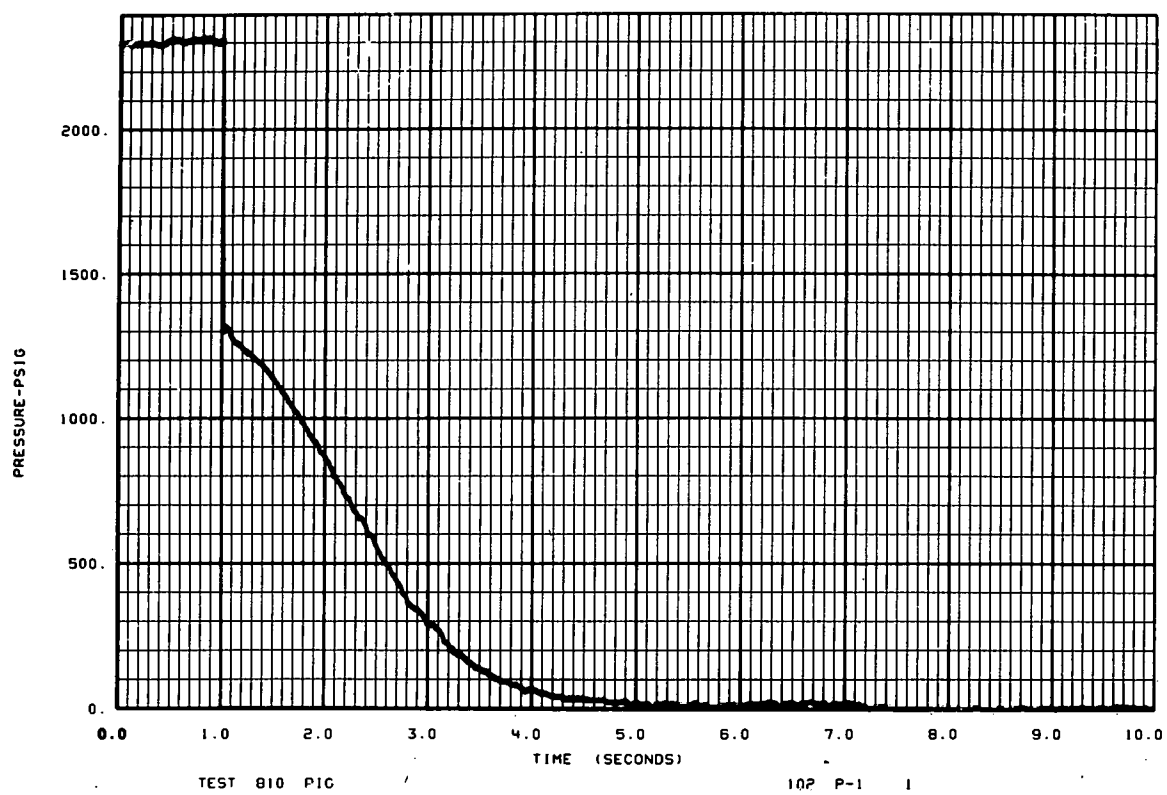
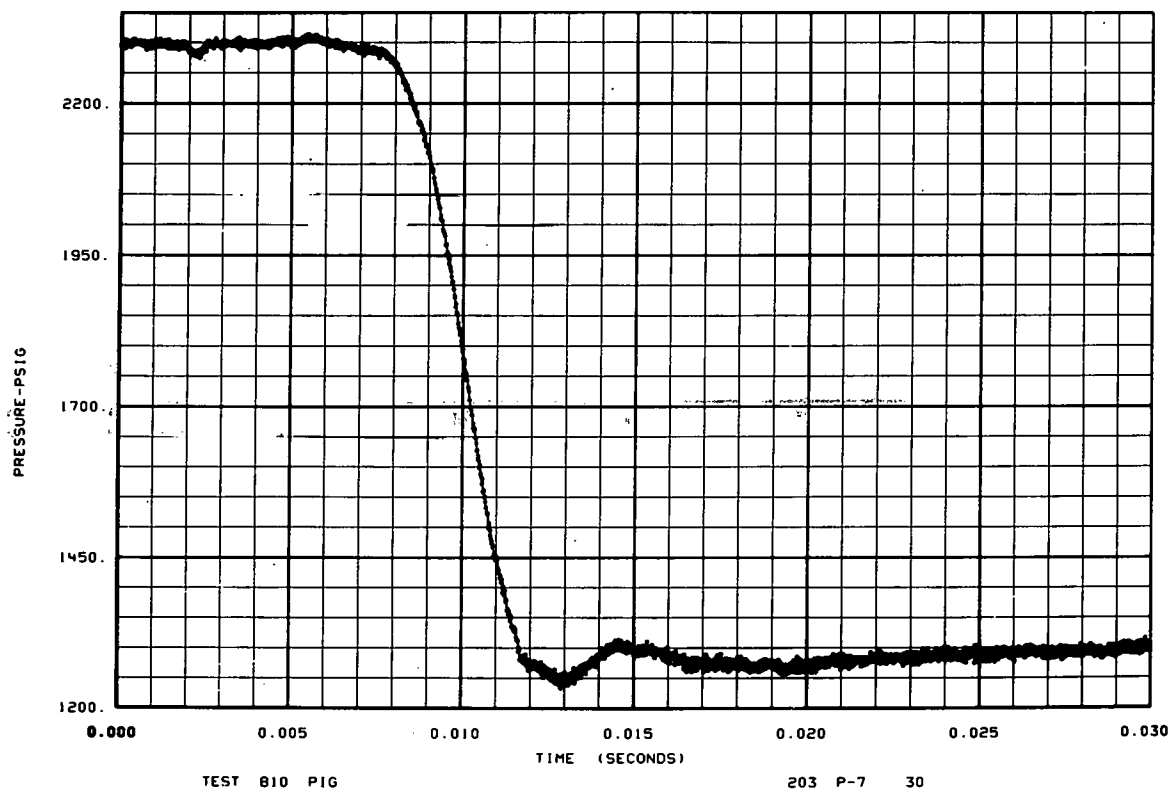
12

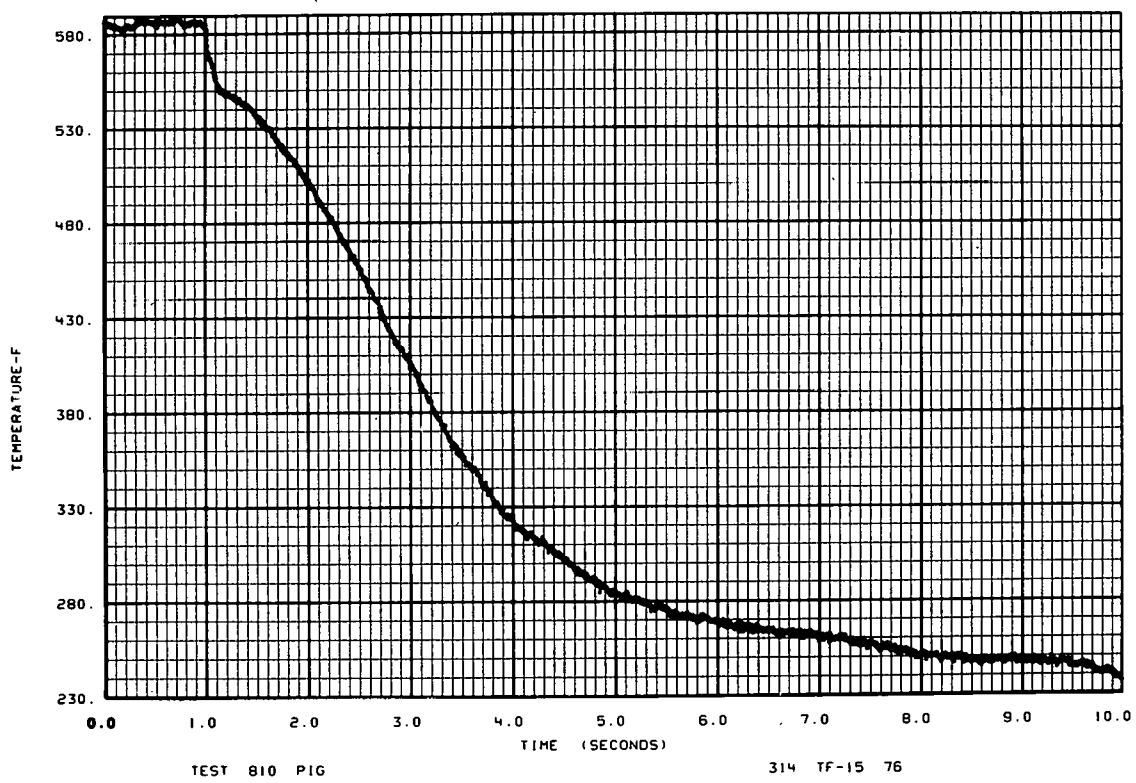
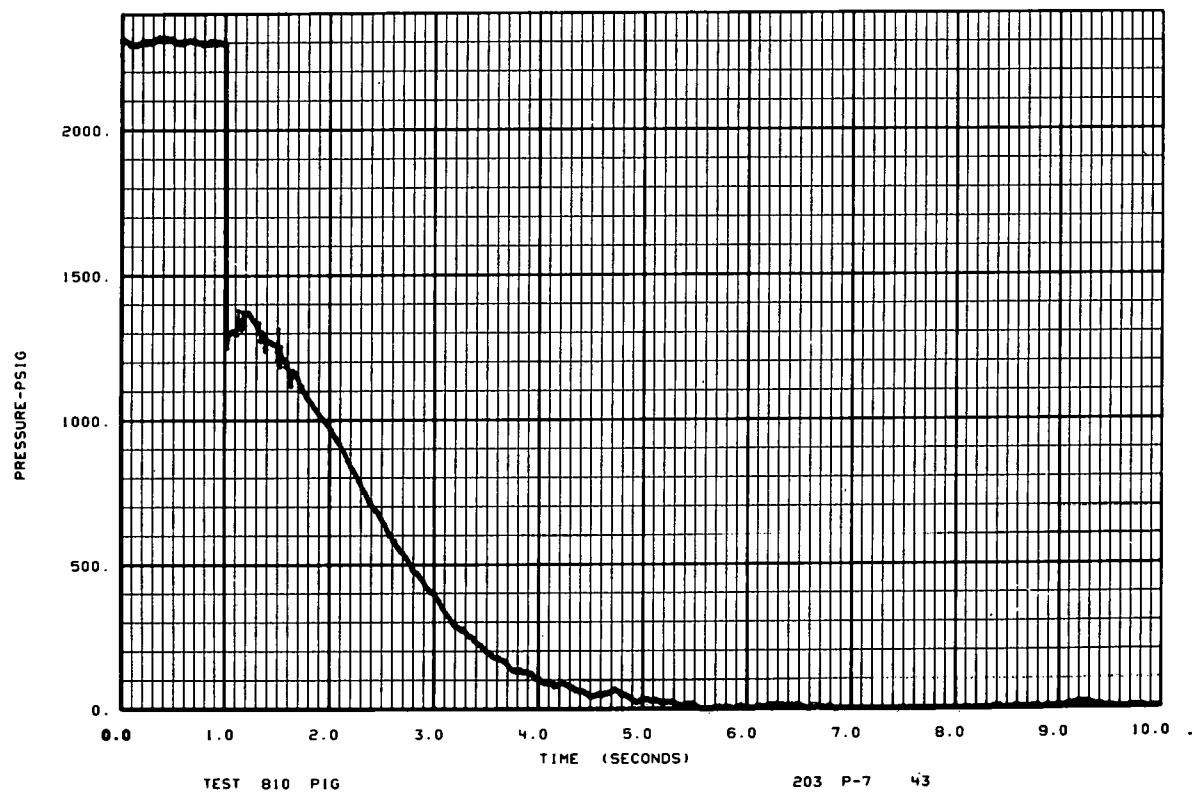


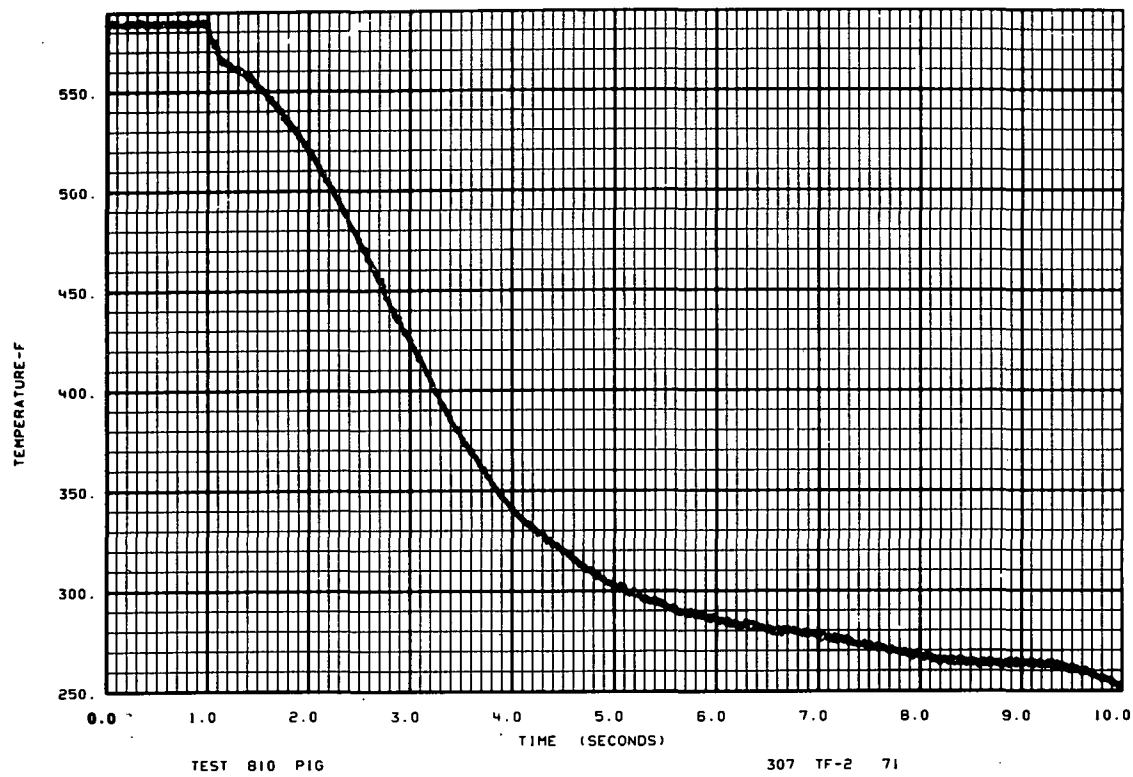
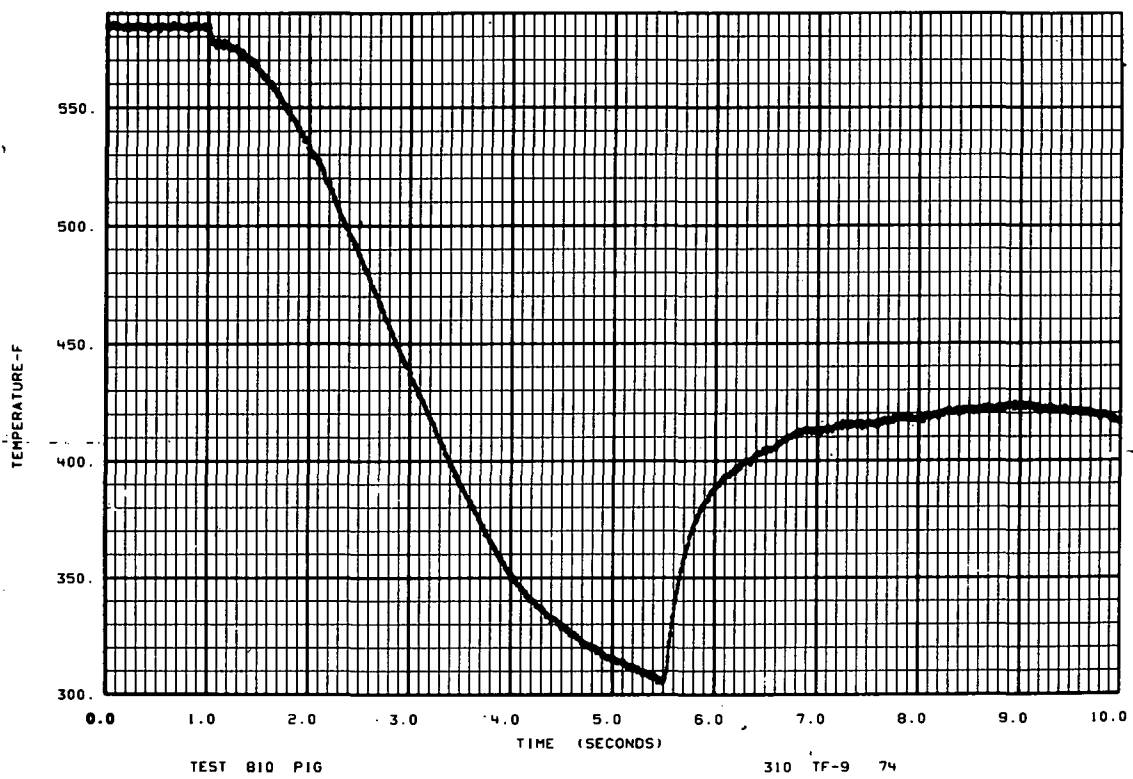


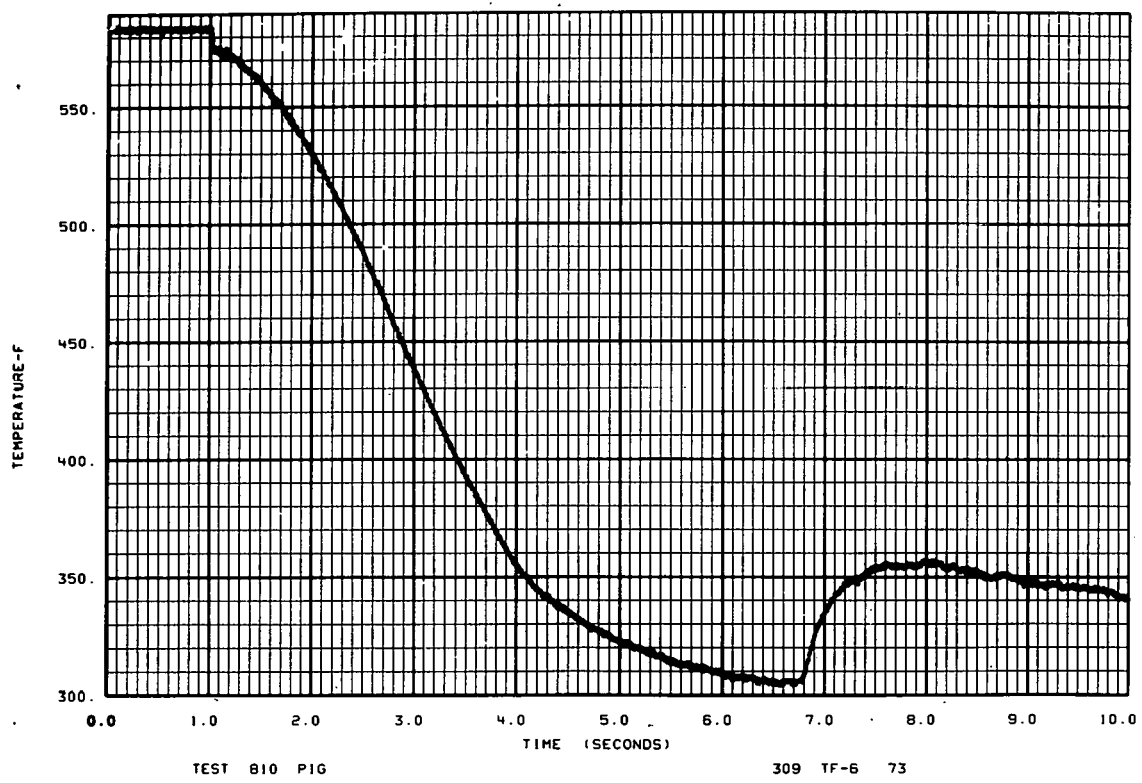
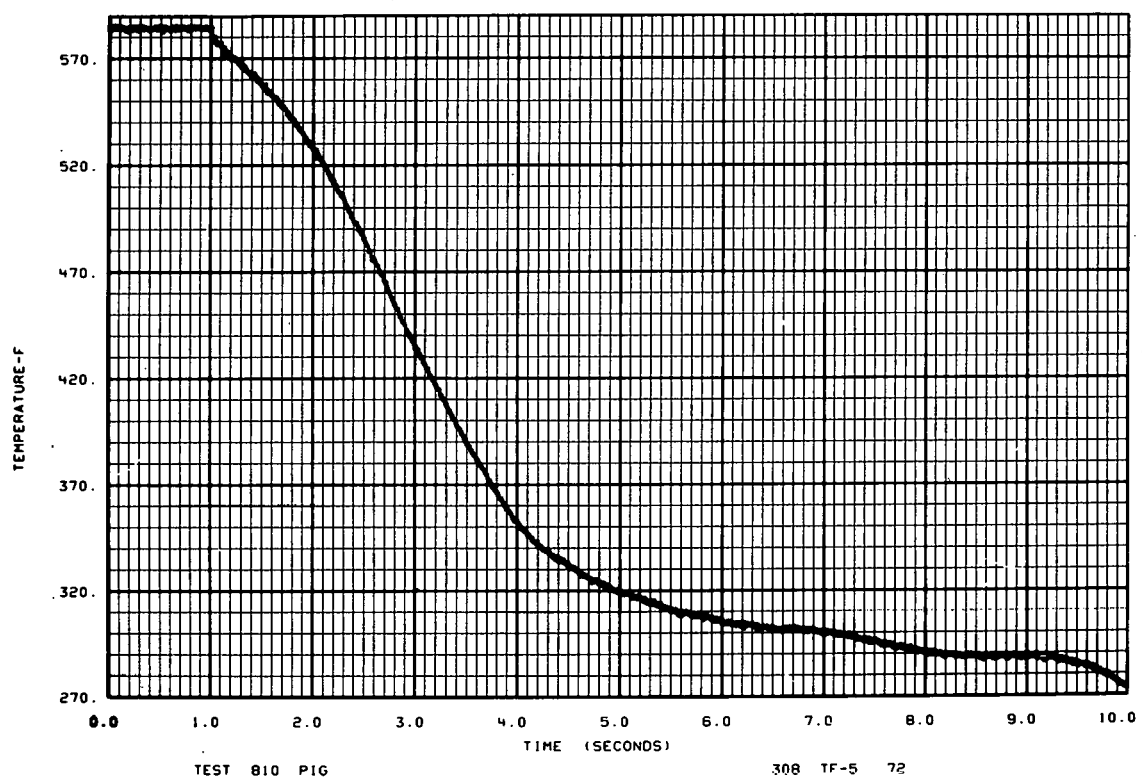


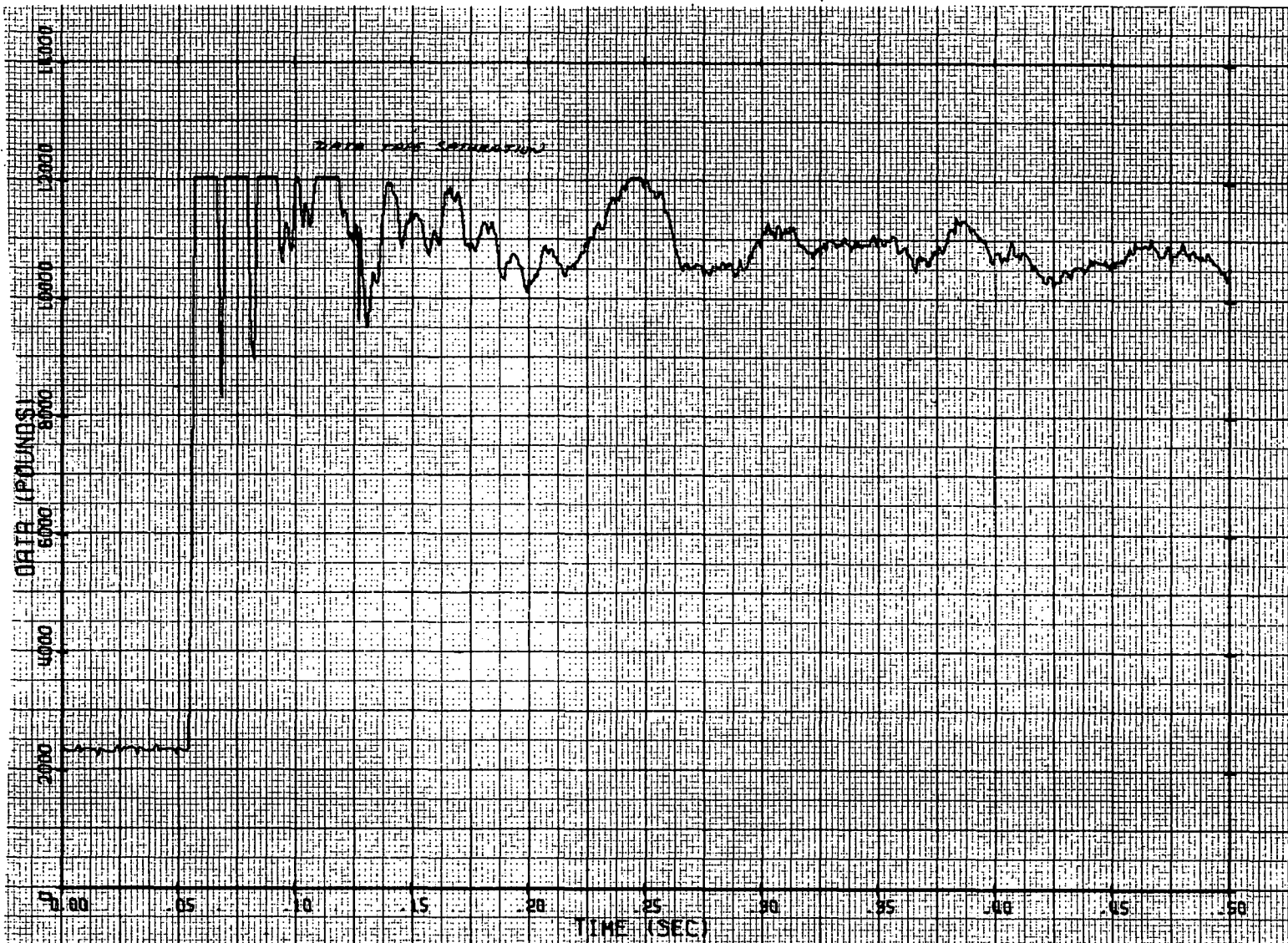


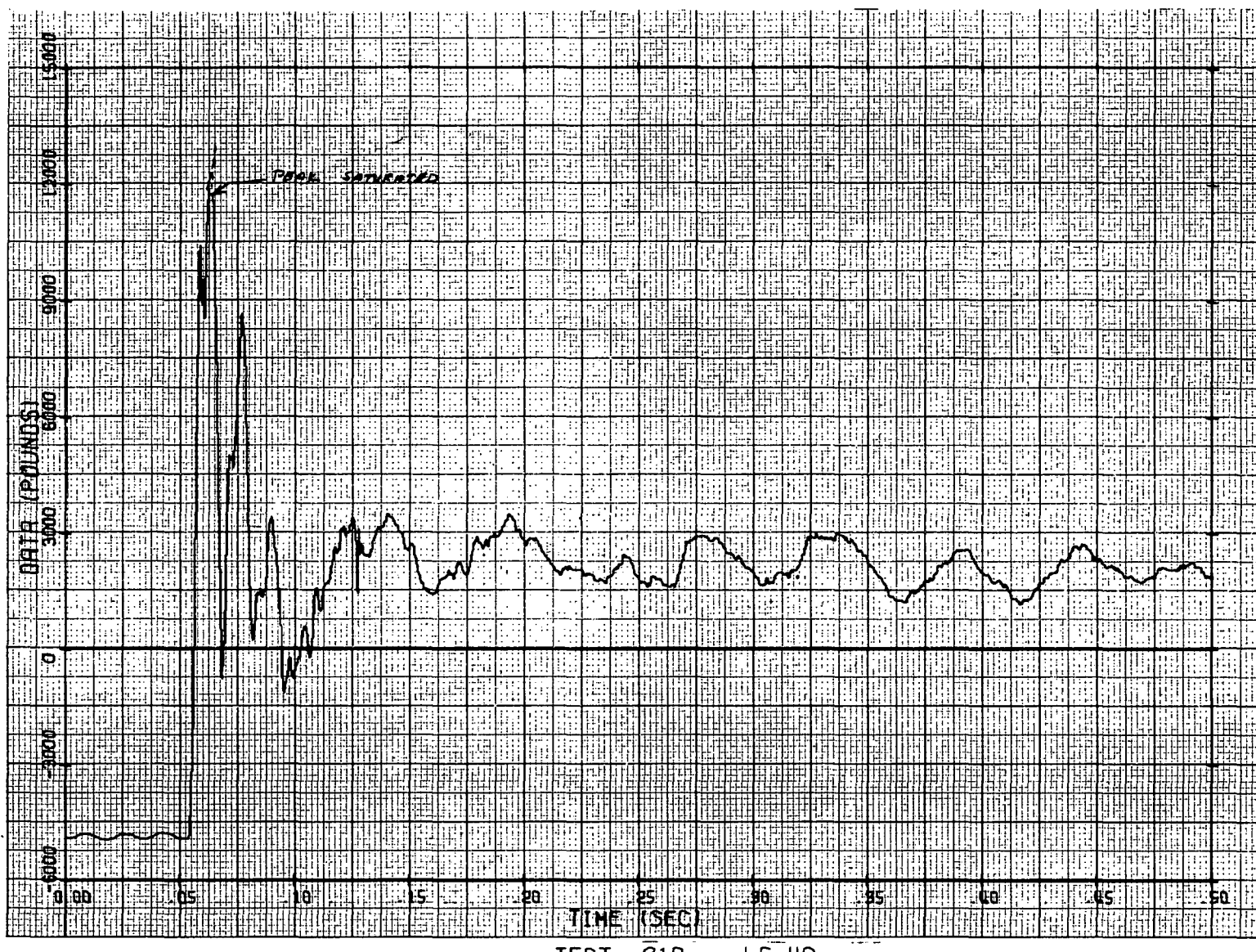




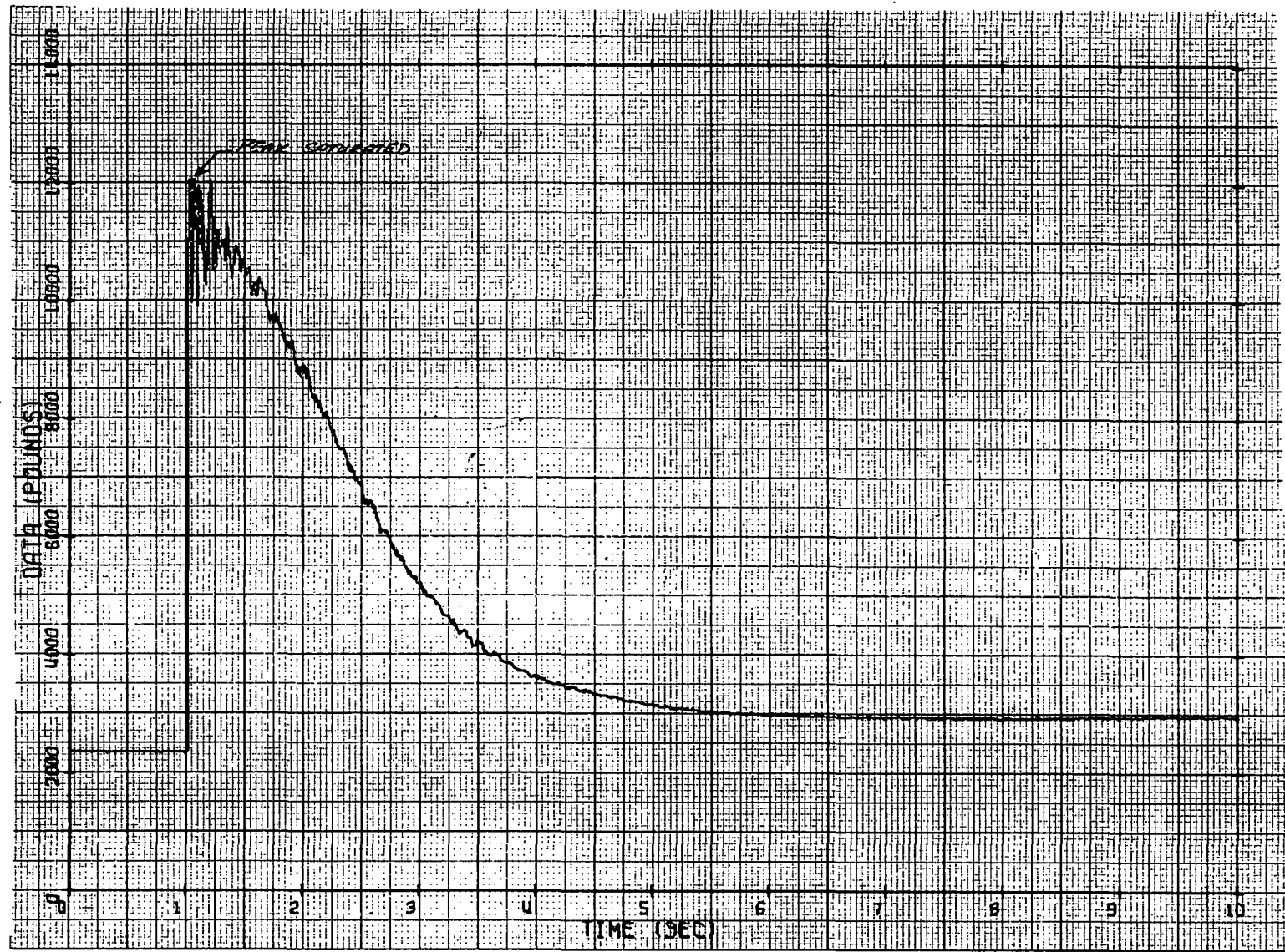


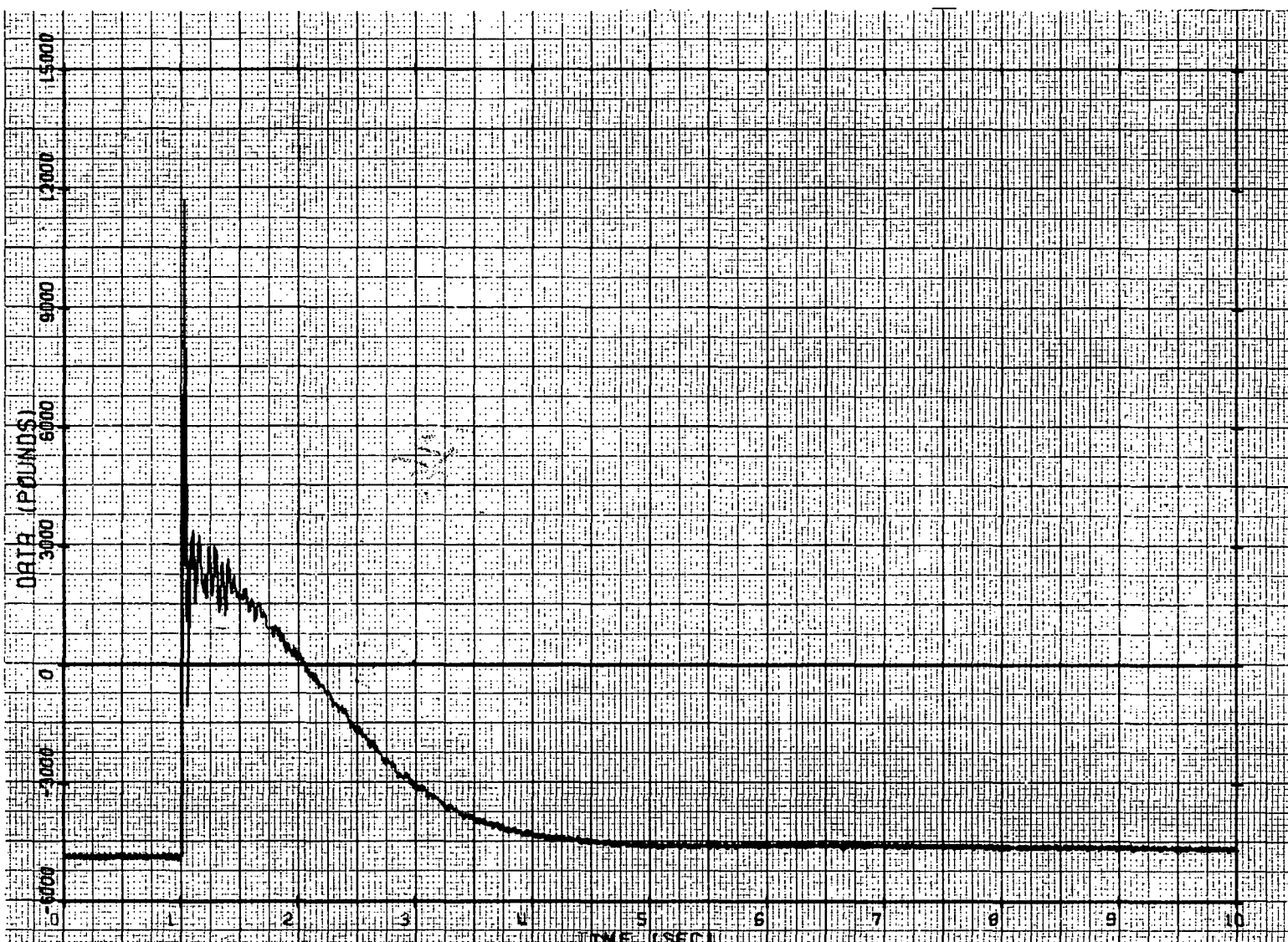


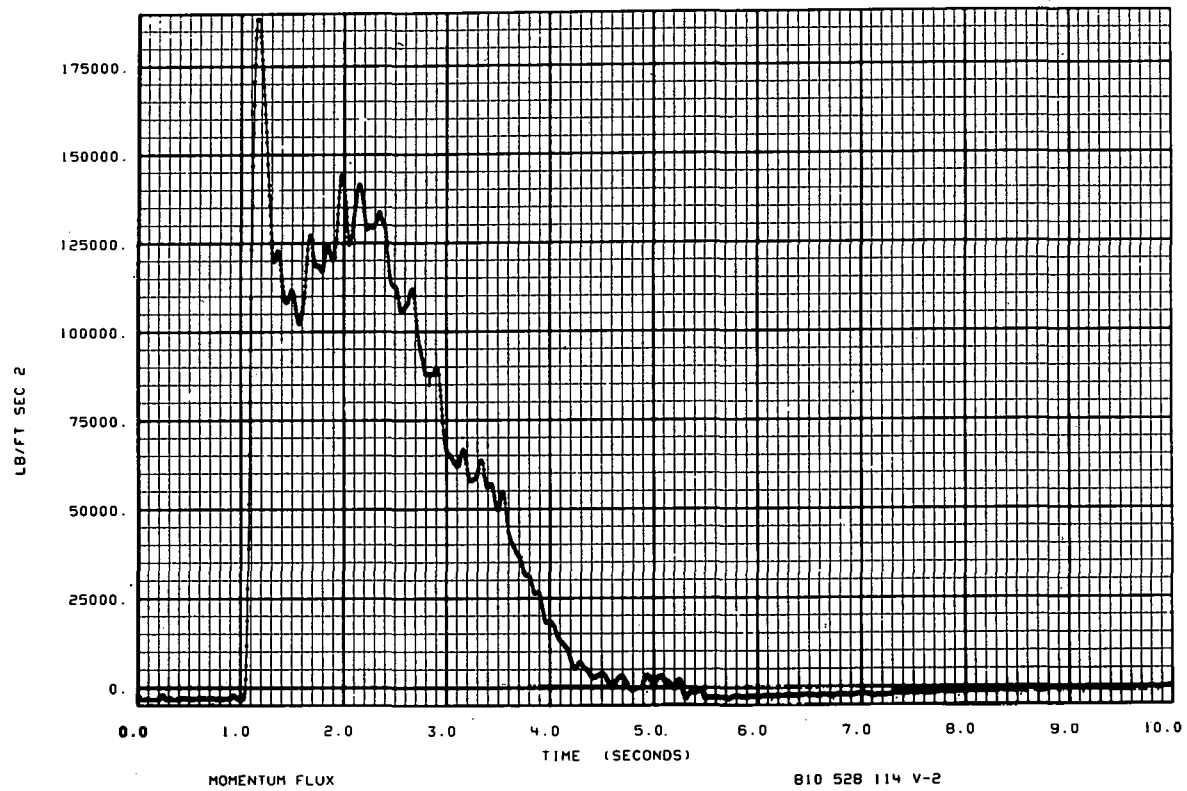
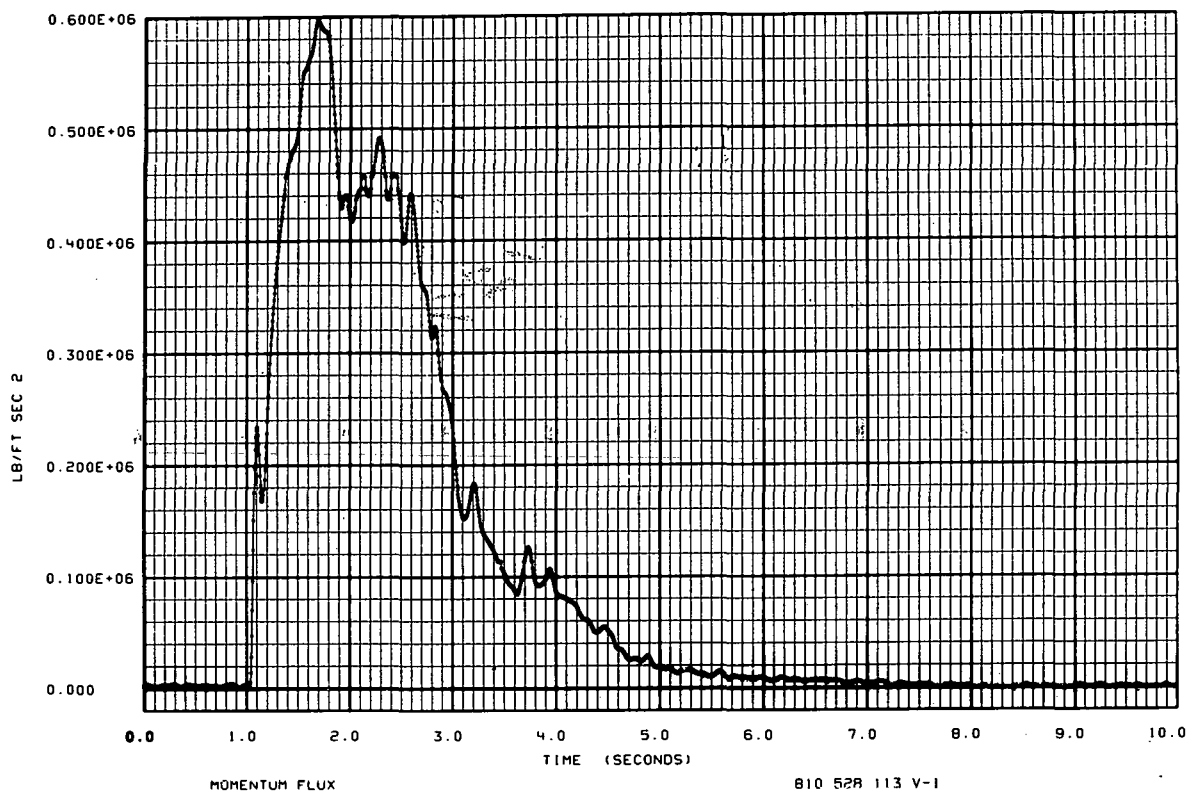


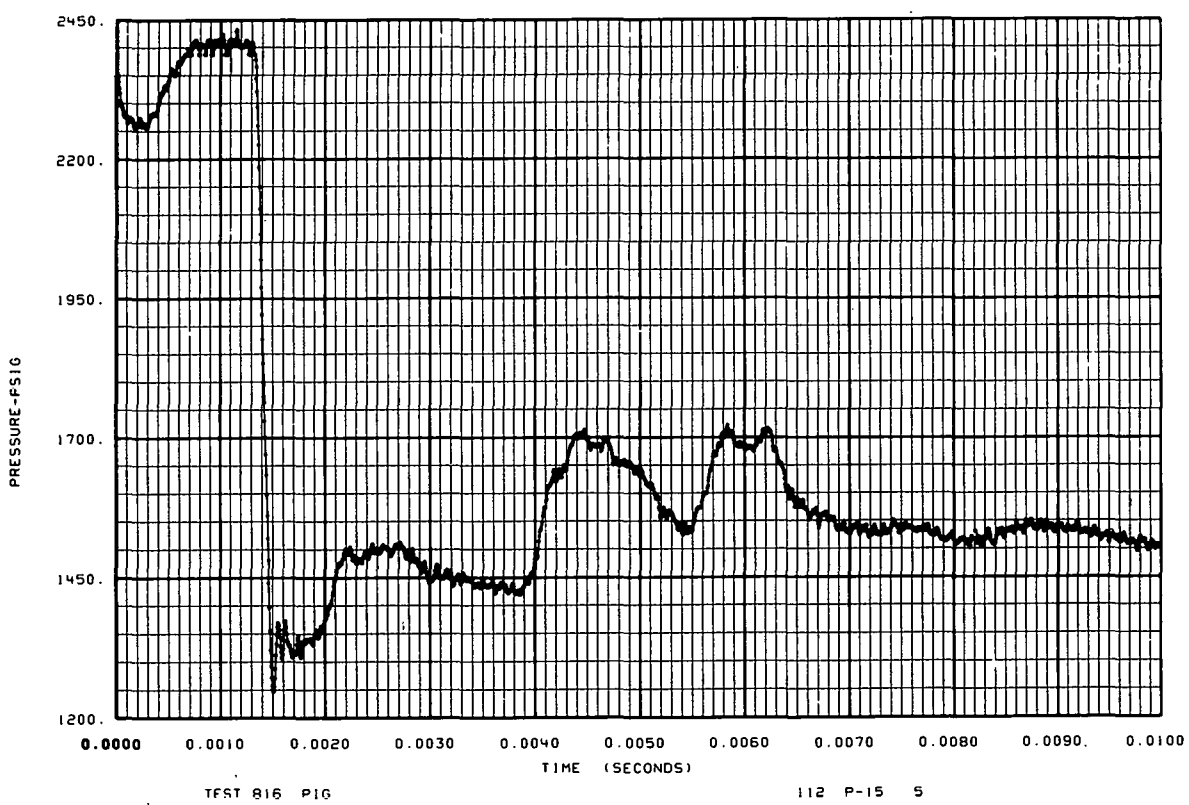
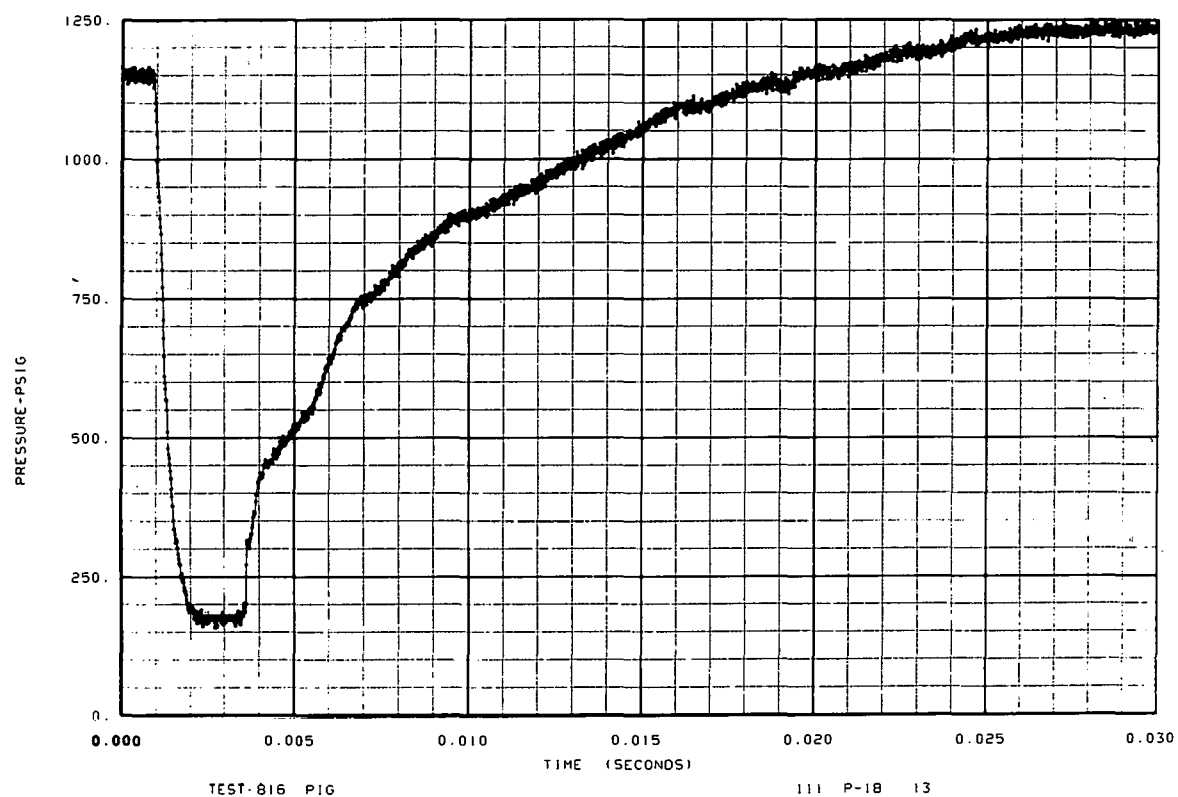


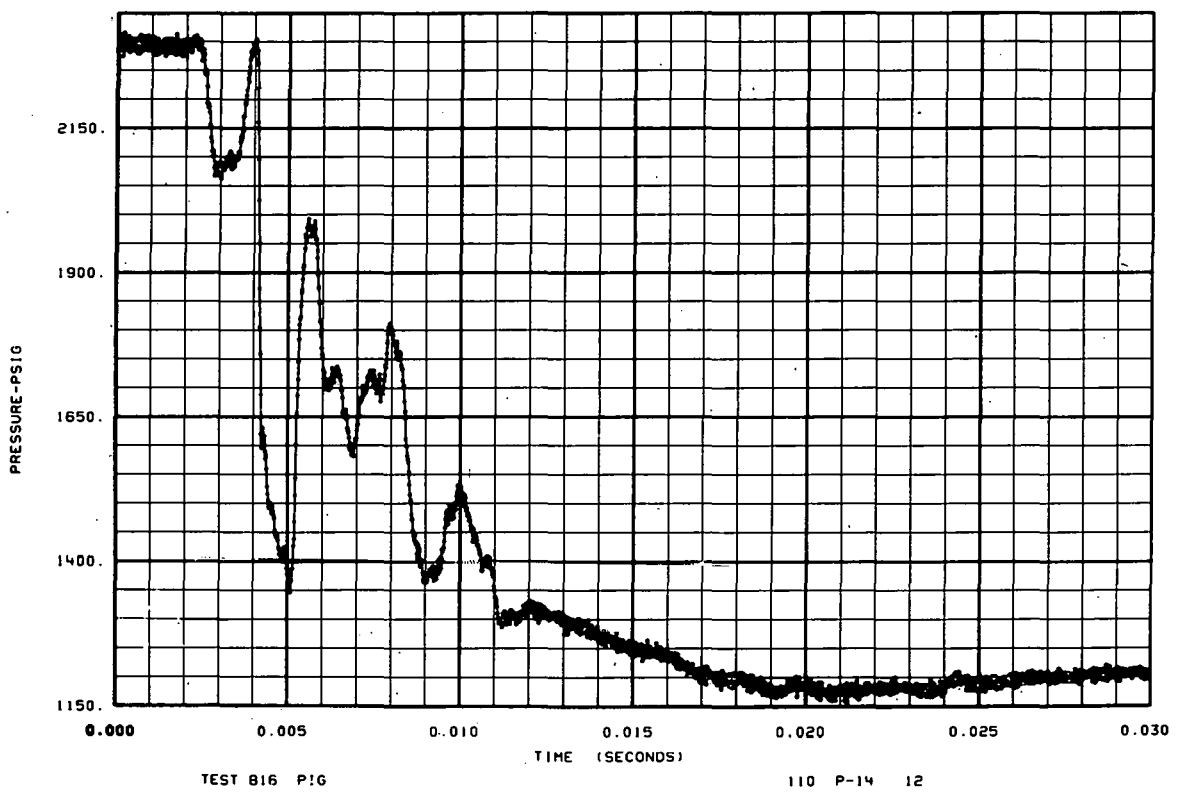
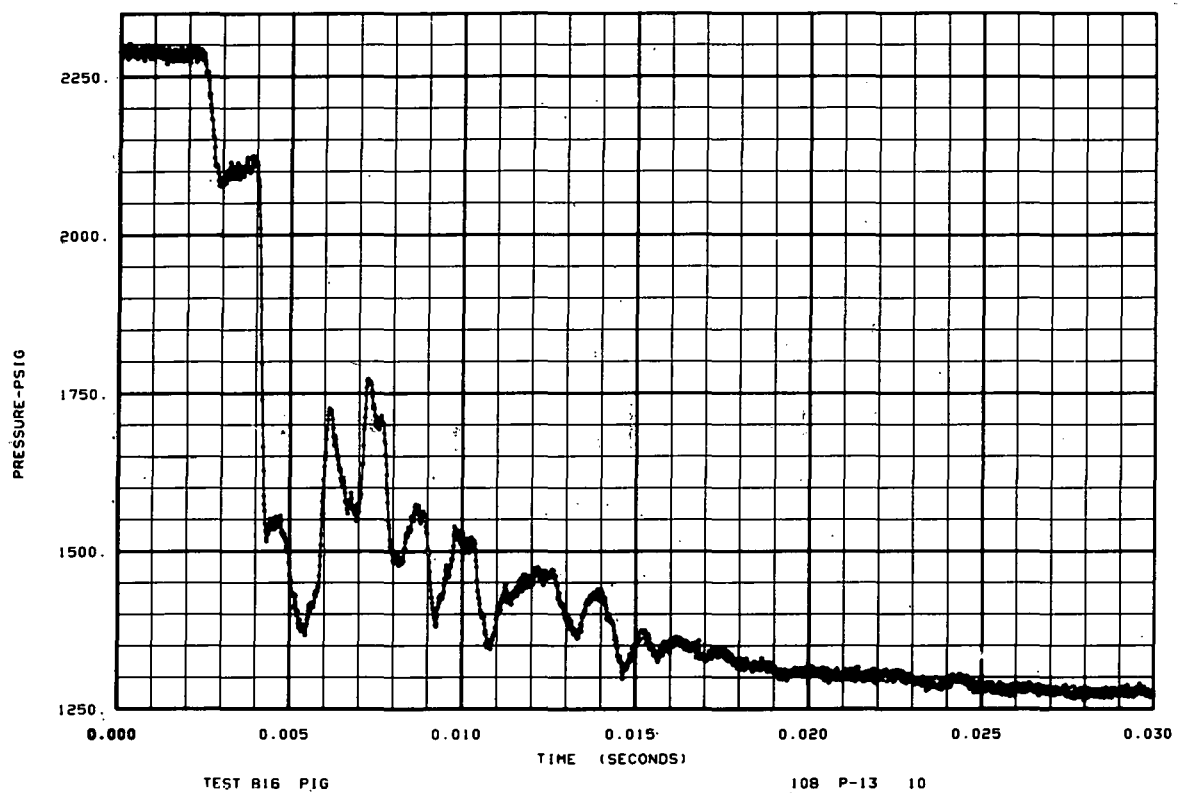
TEST 810. LC-4A

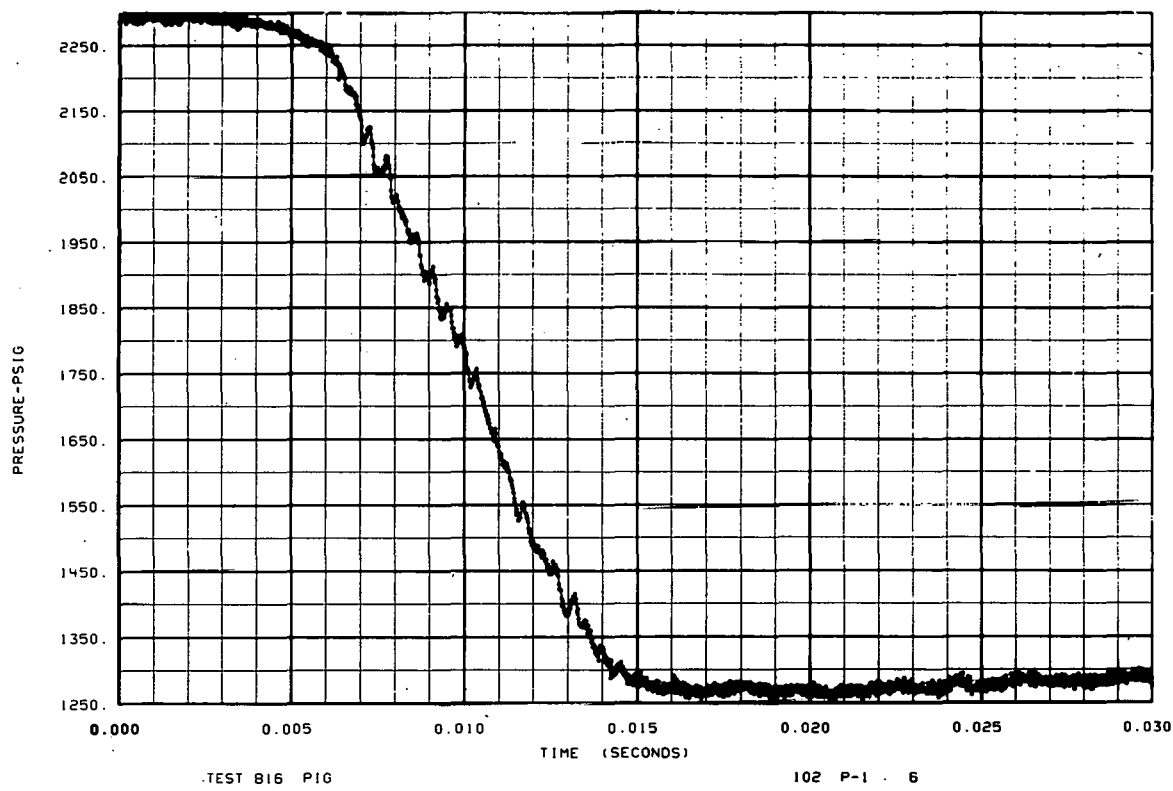
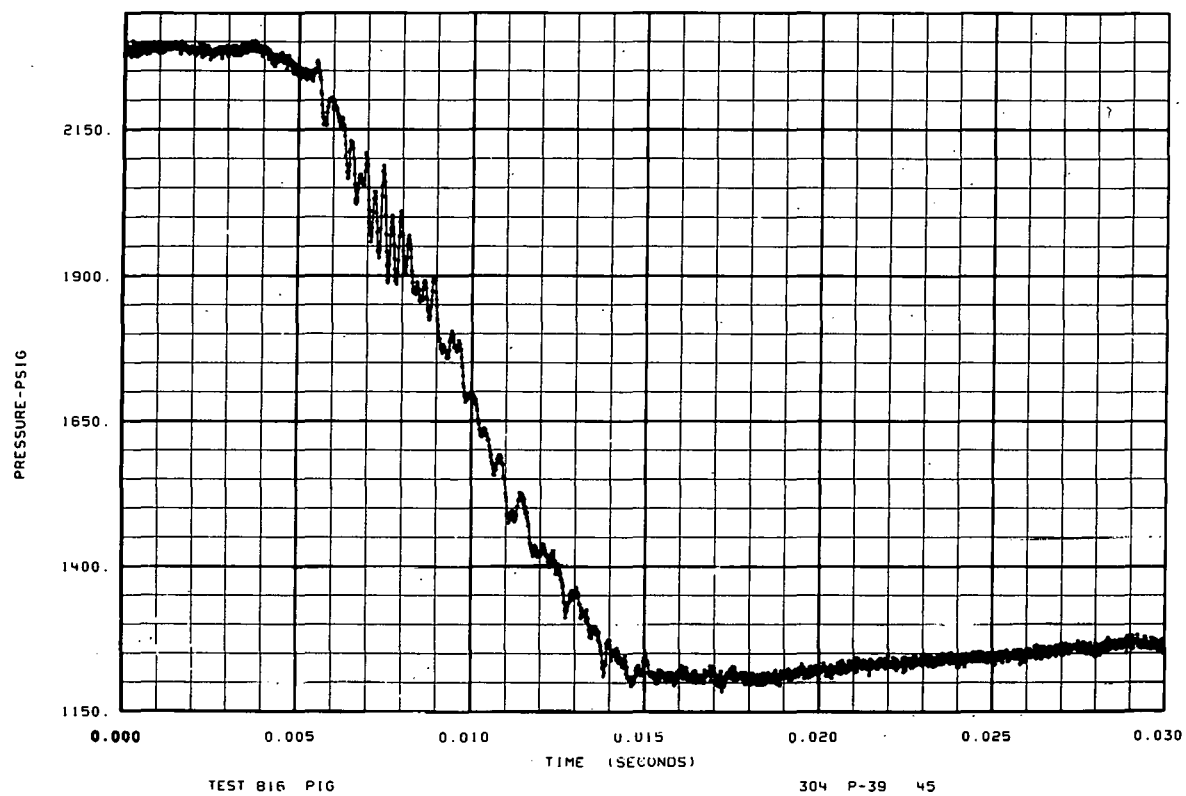


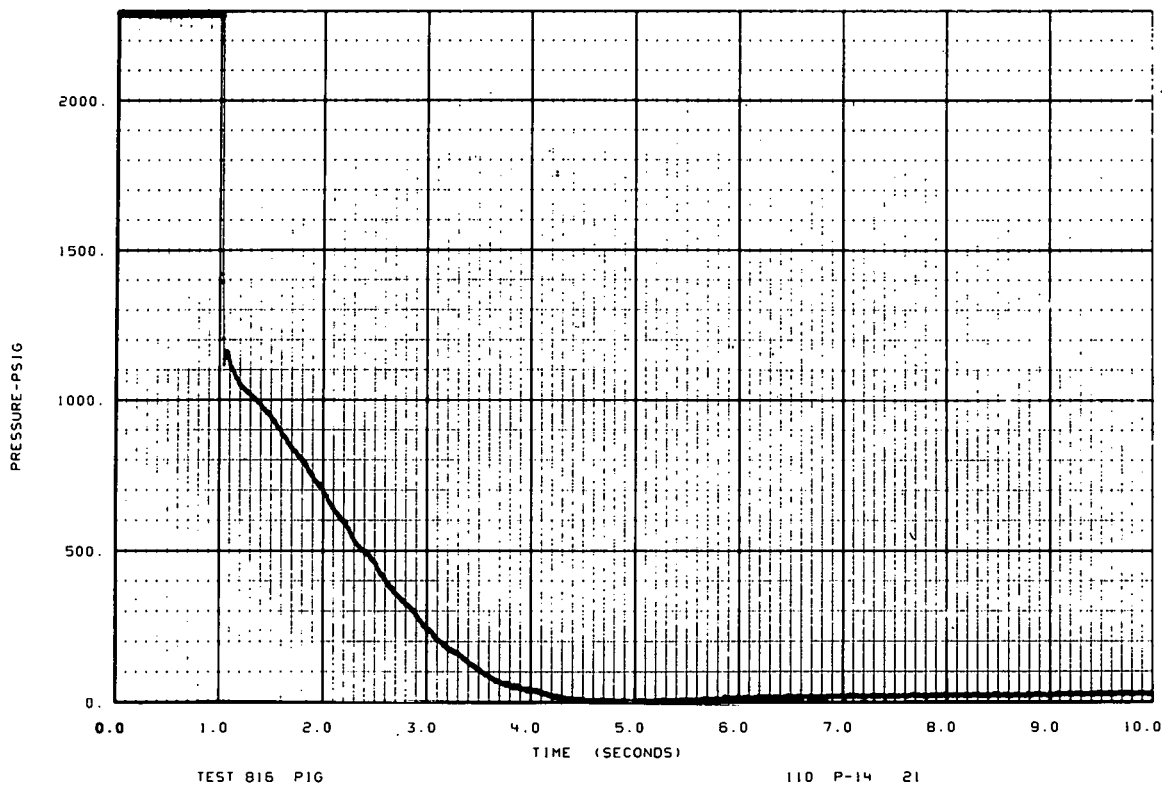
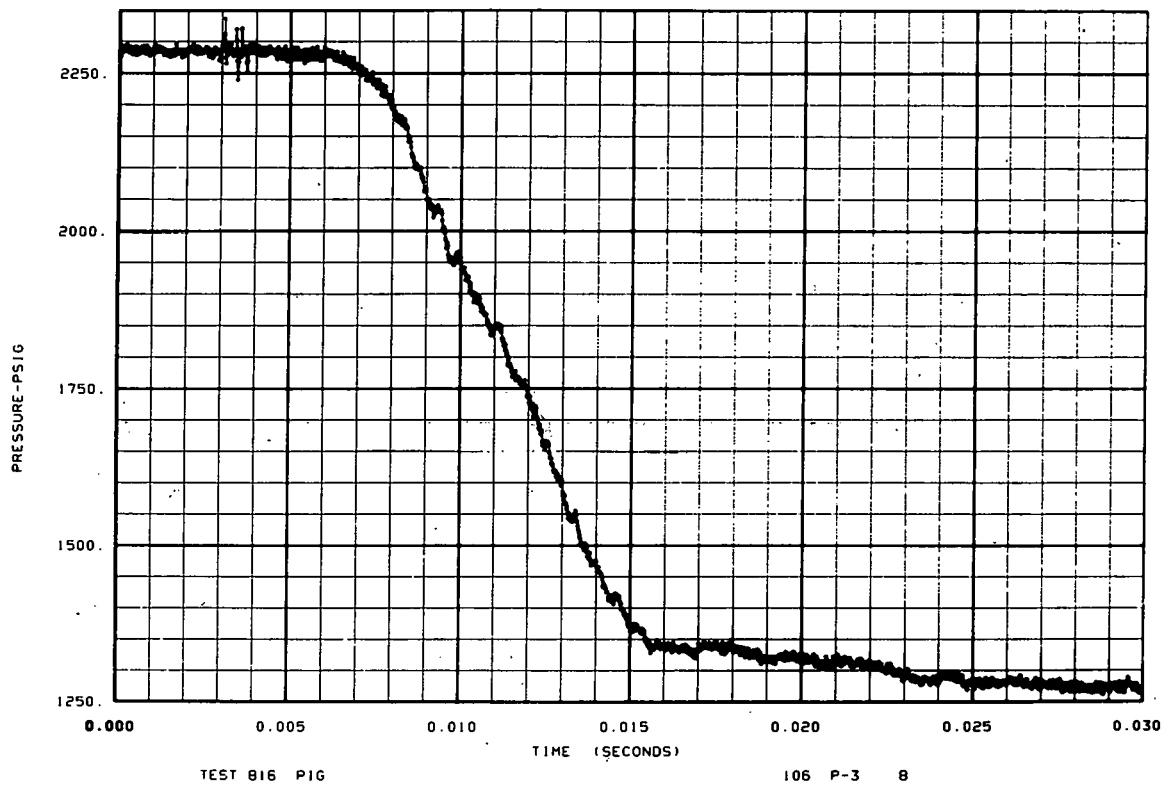


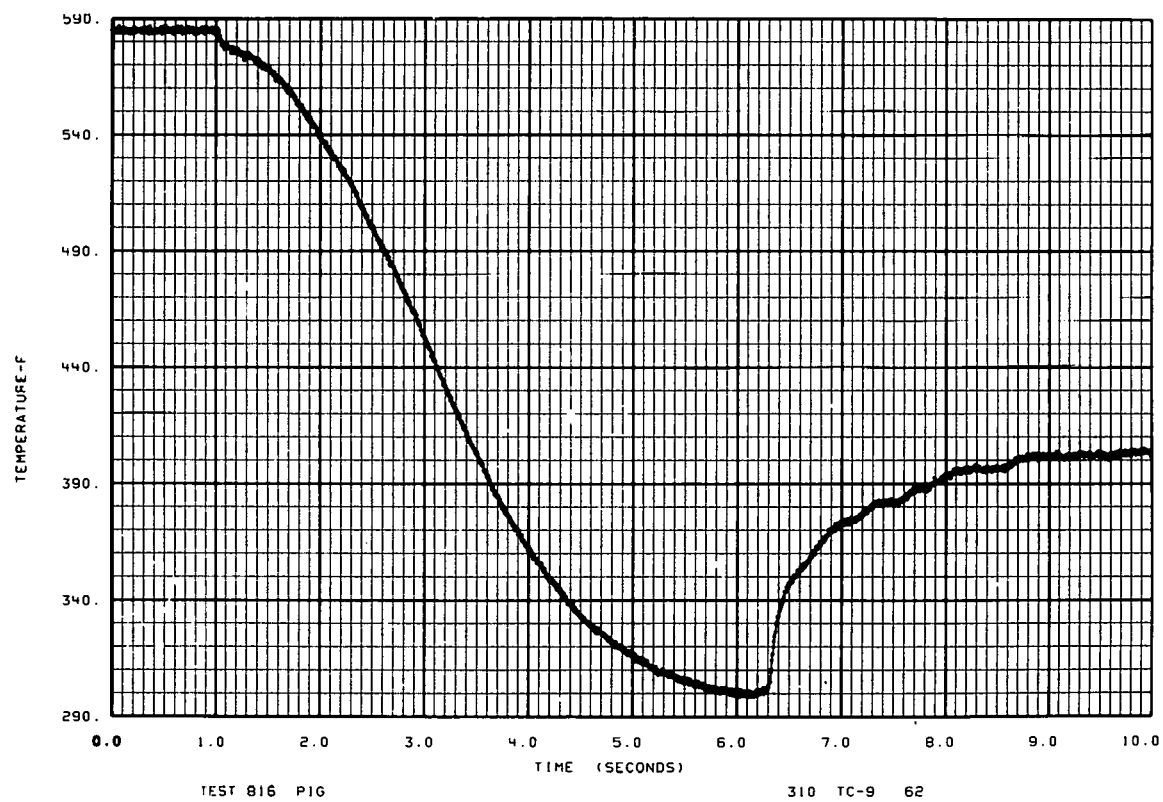
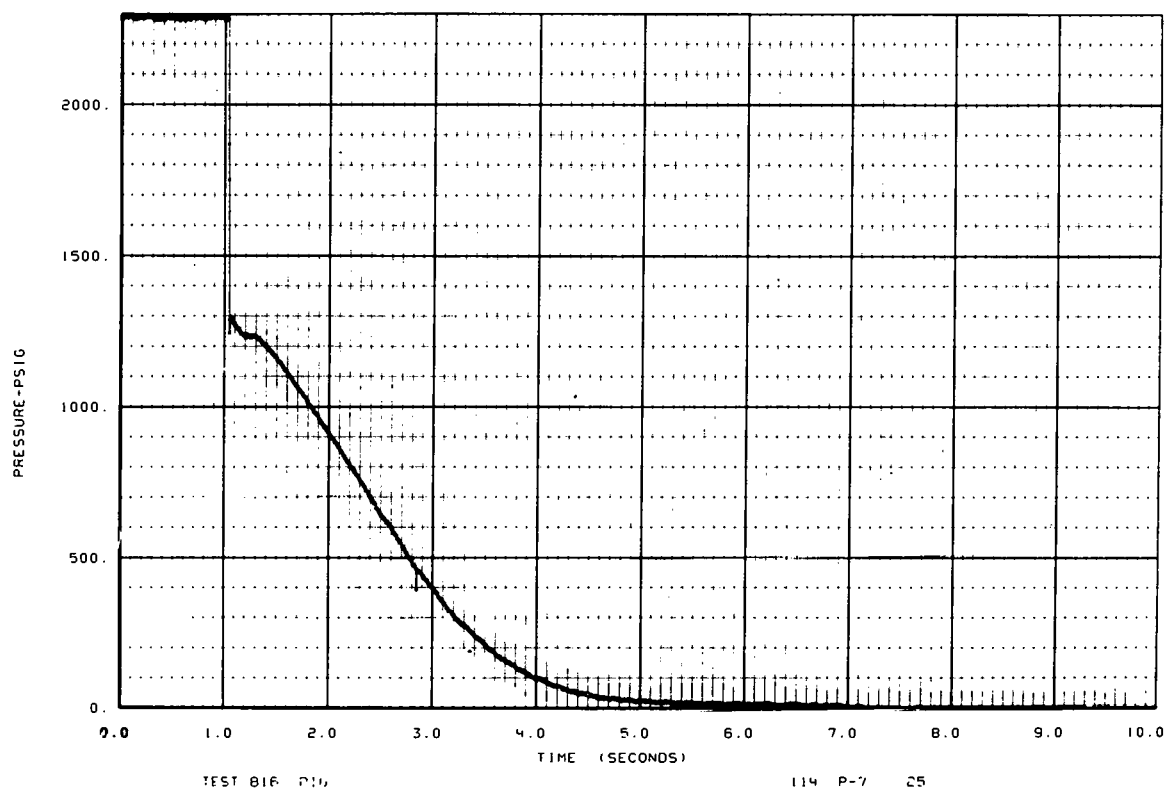


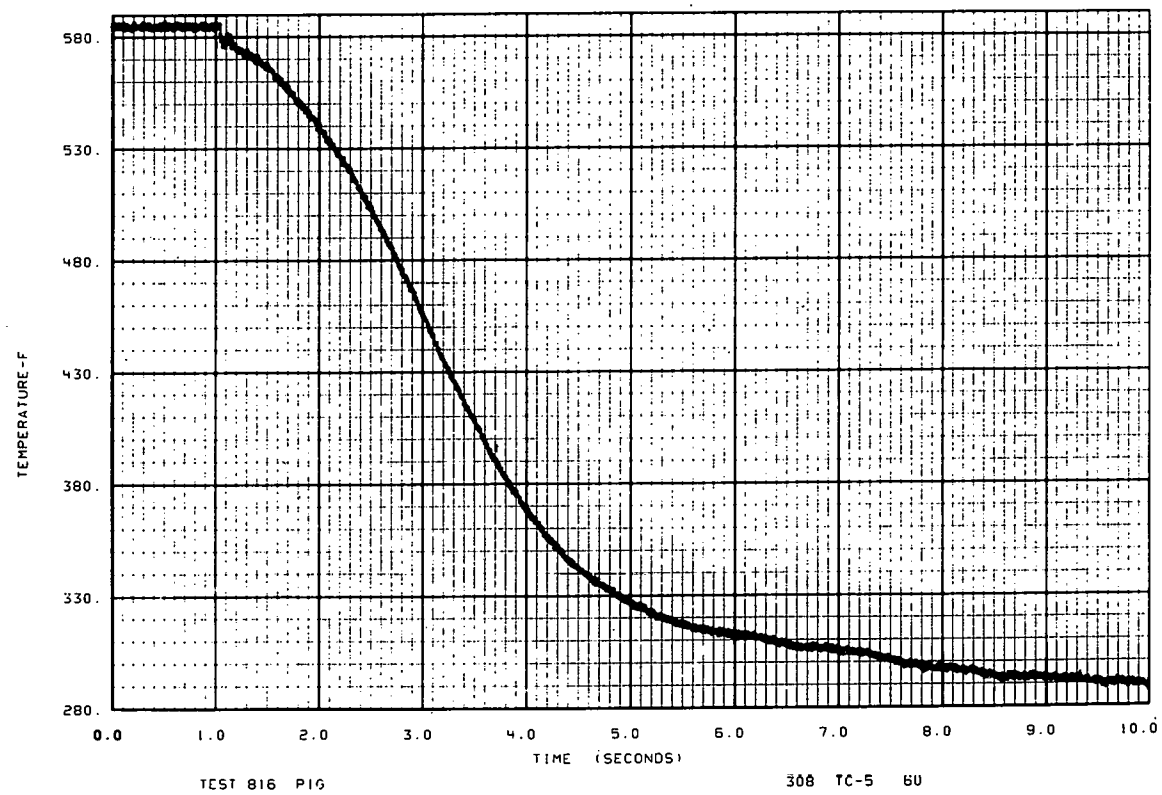
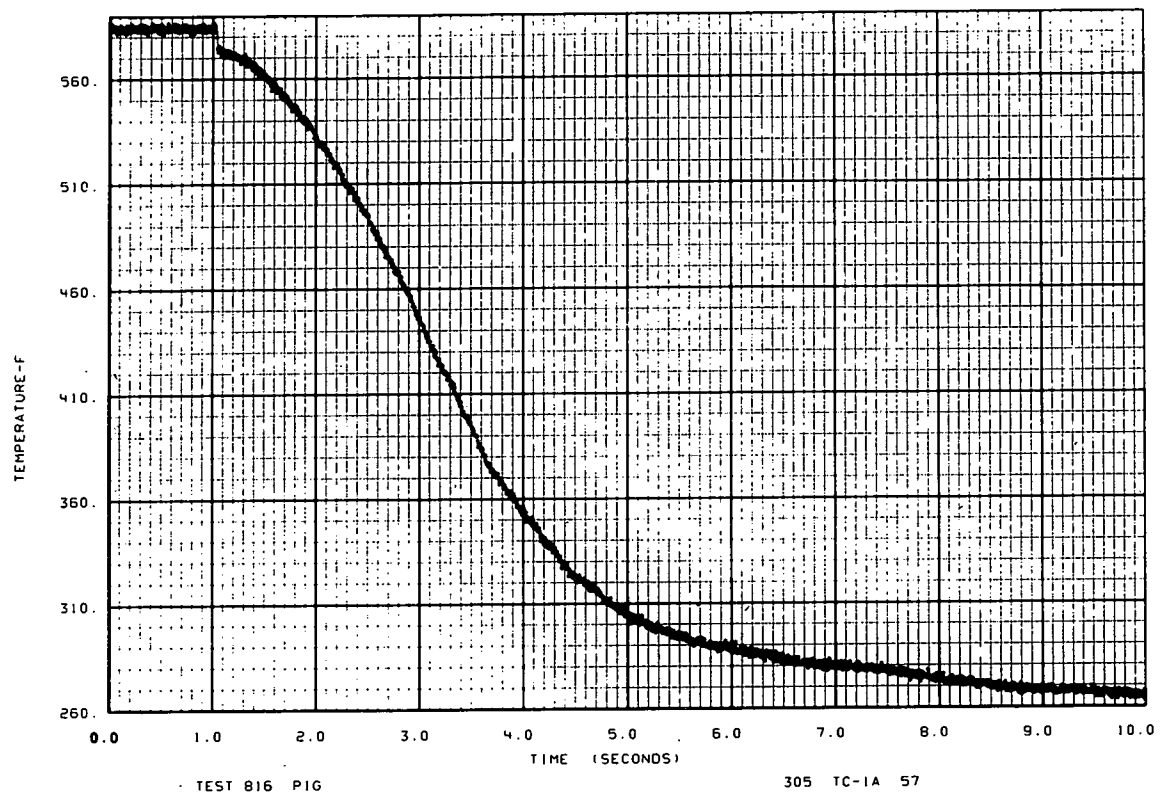


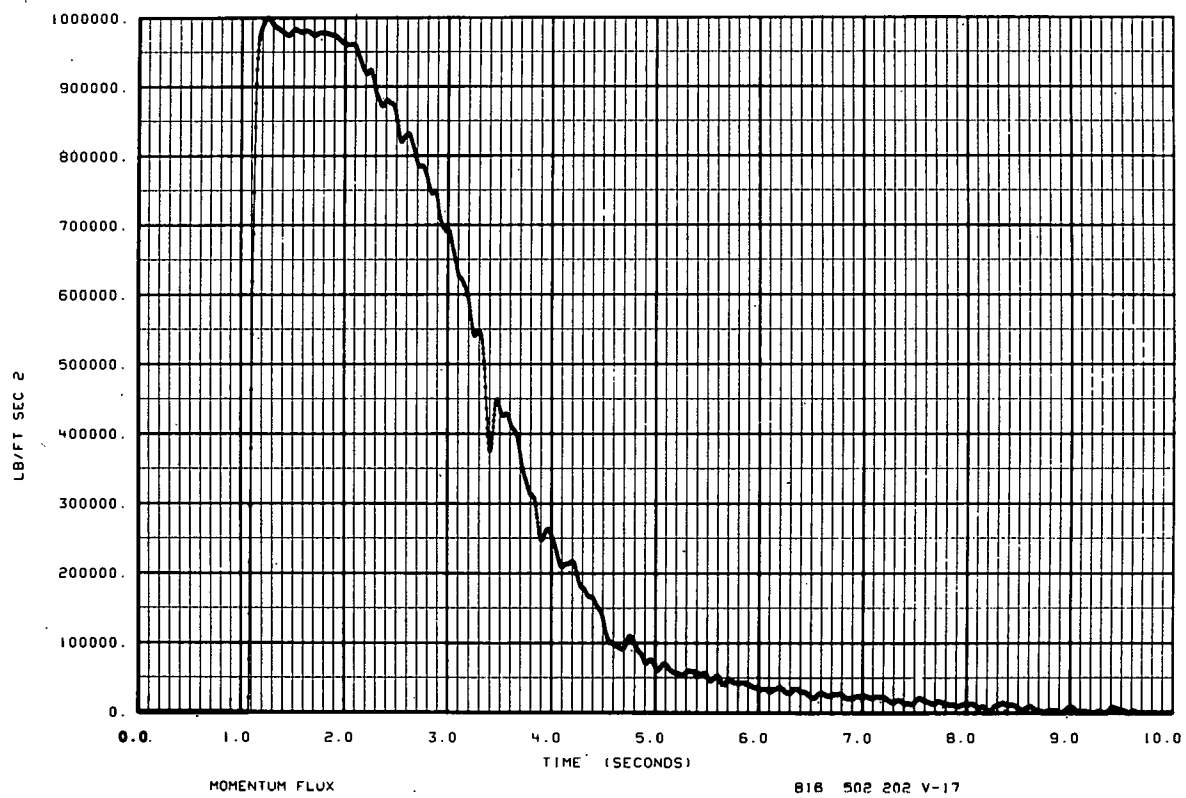
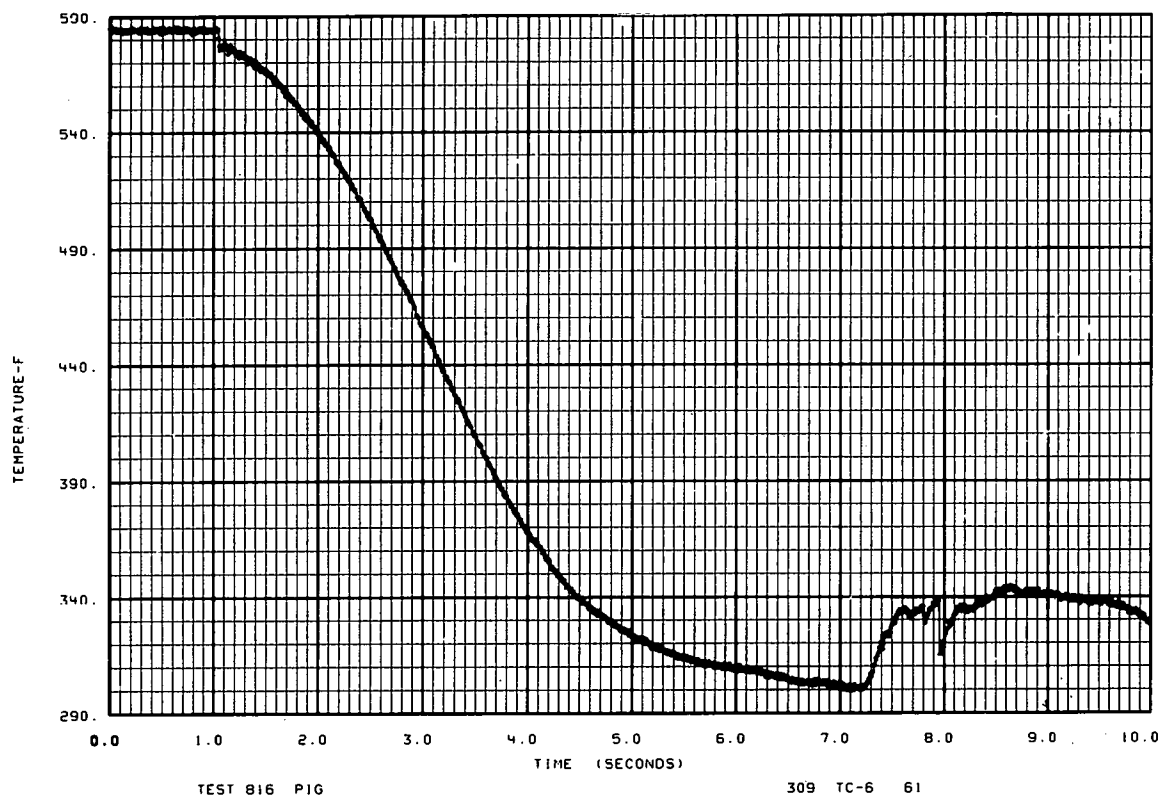


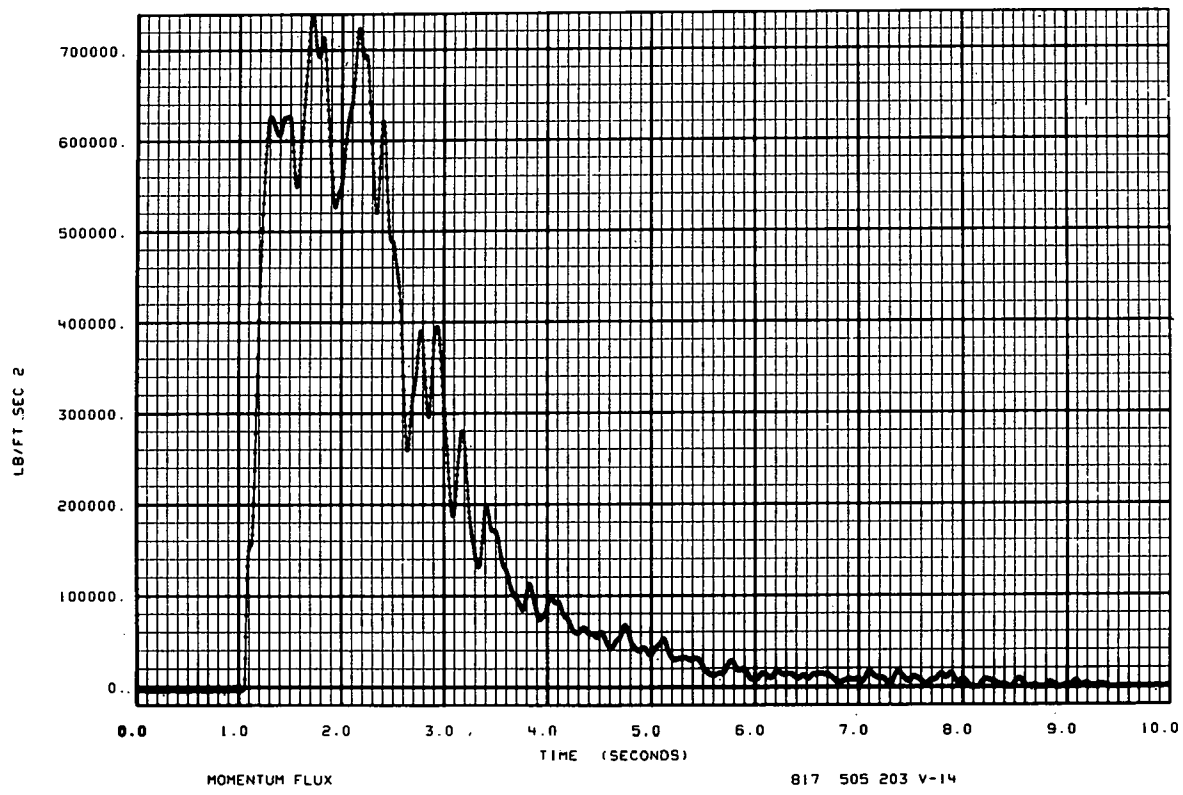
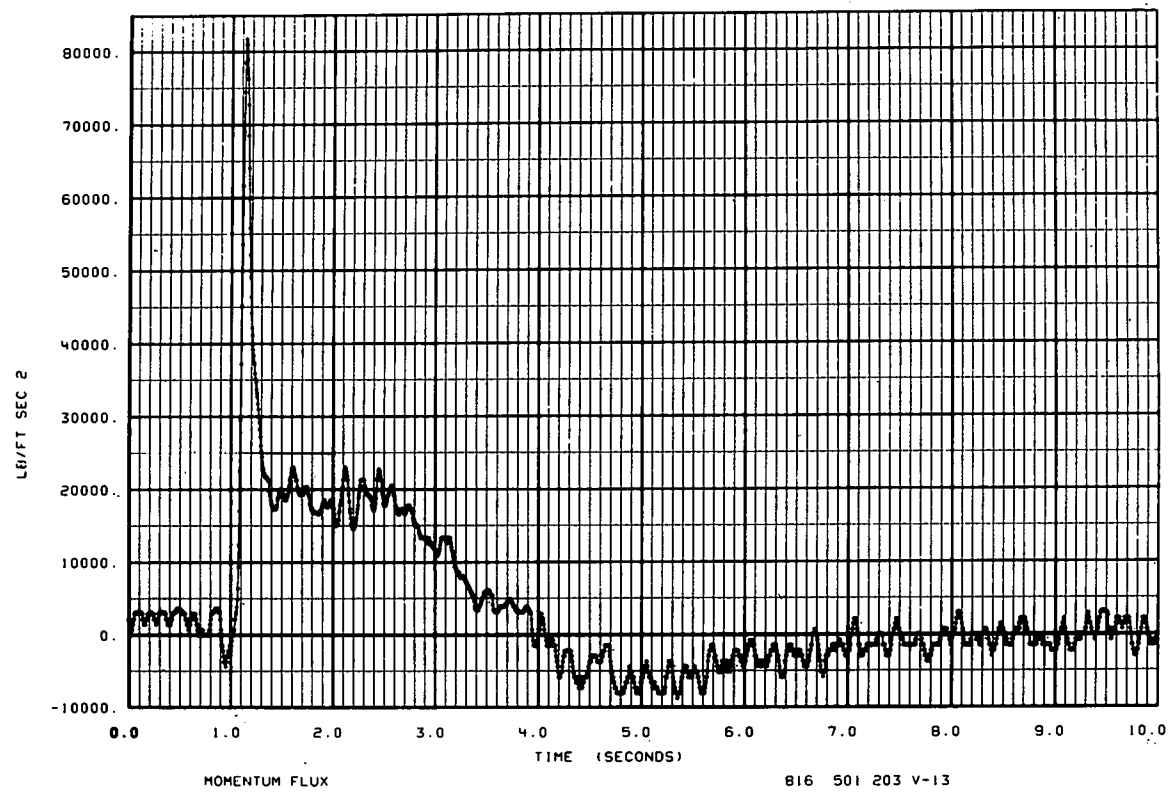


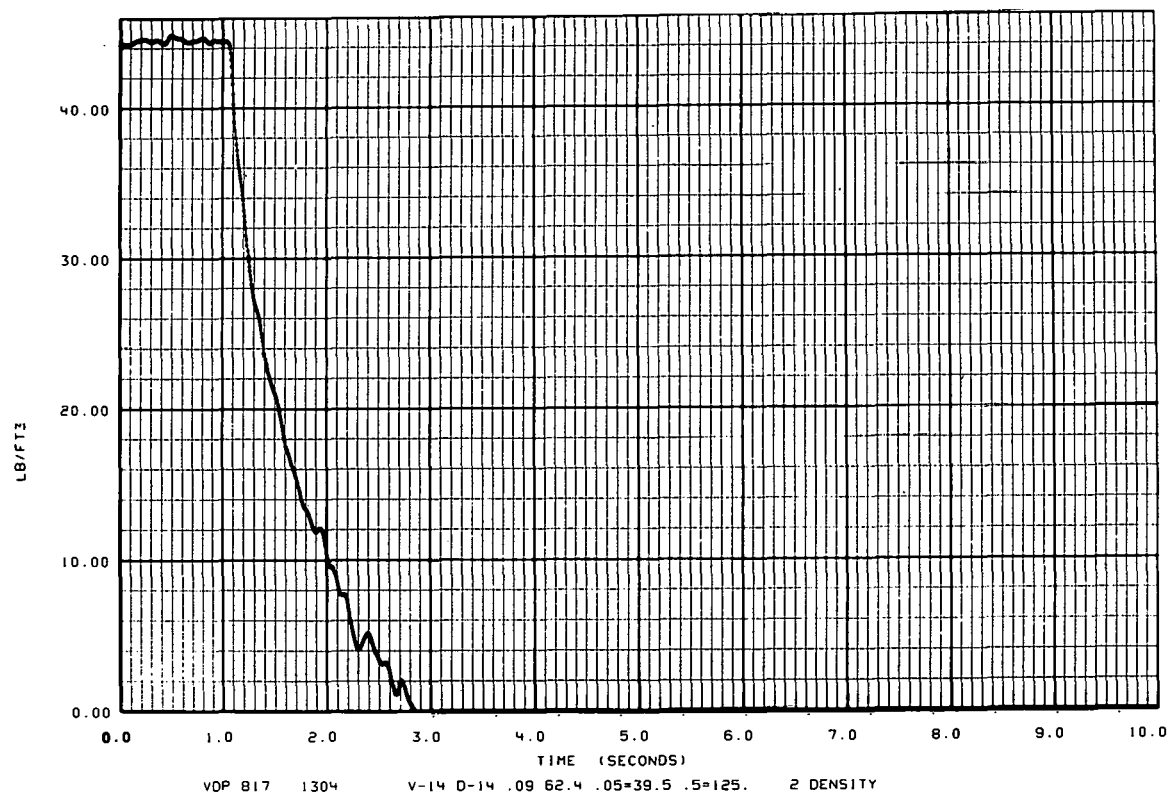
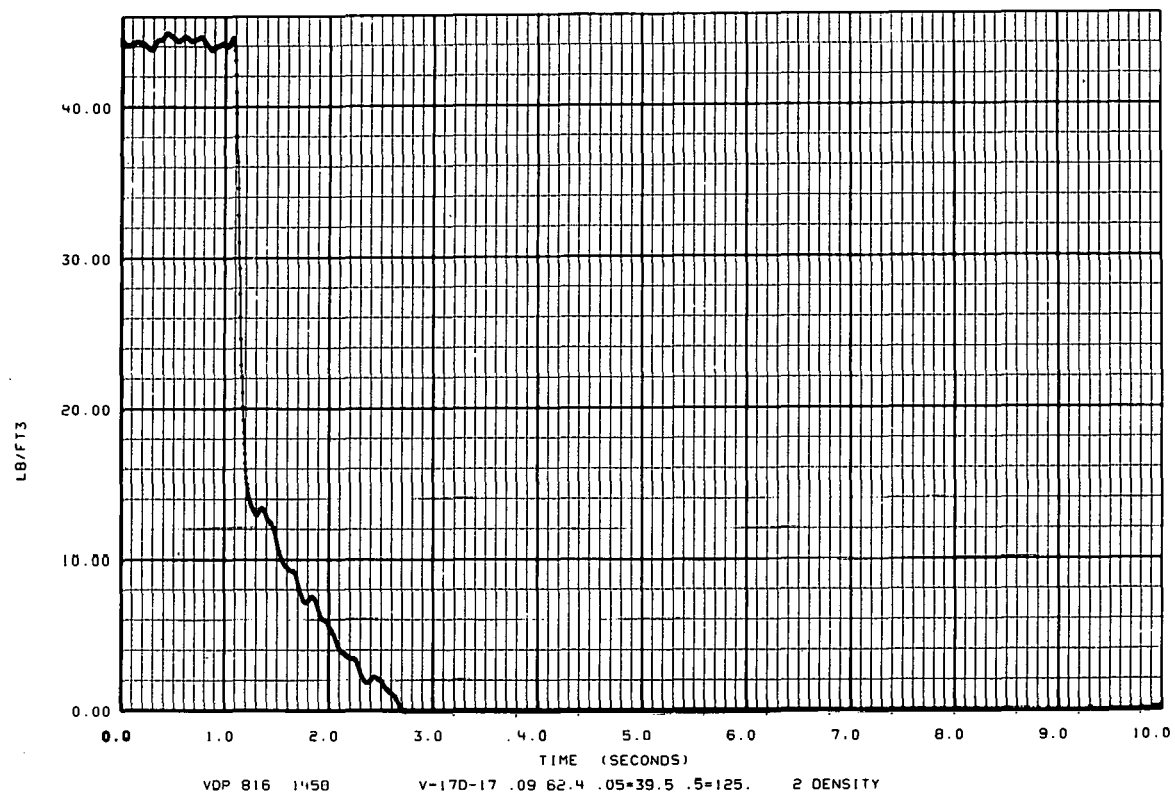


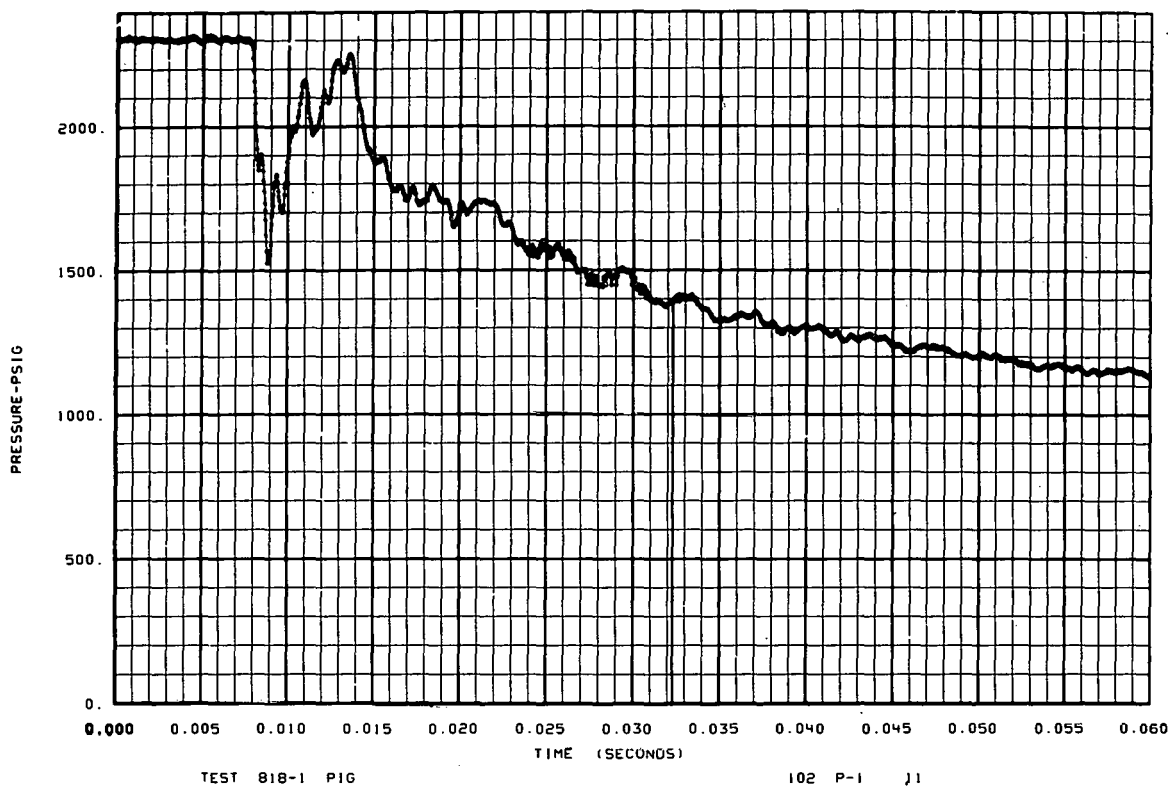
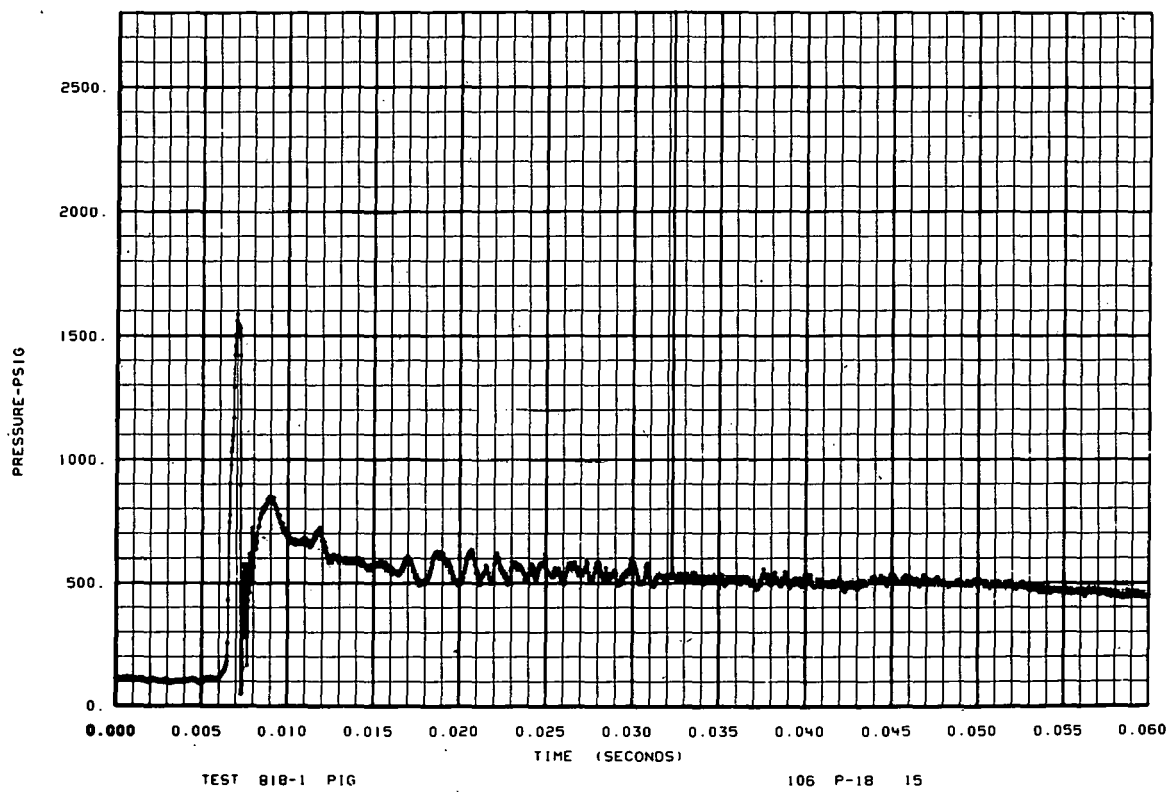


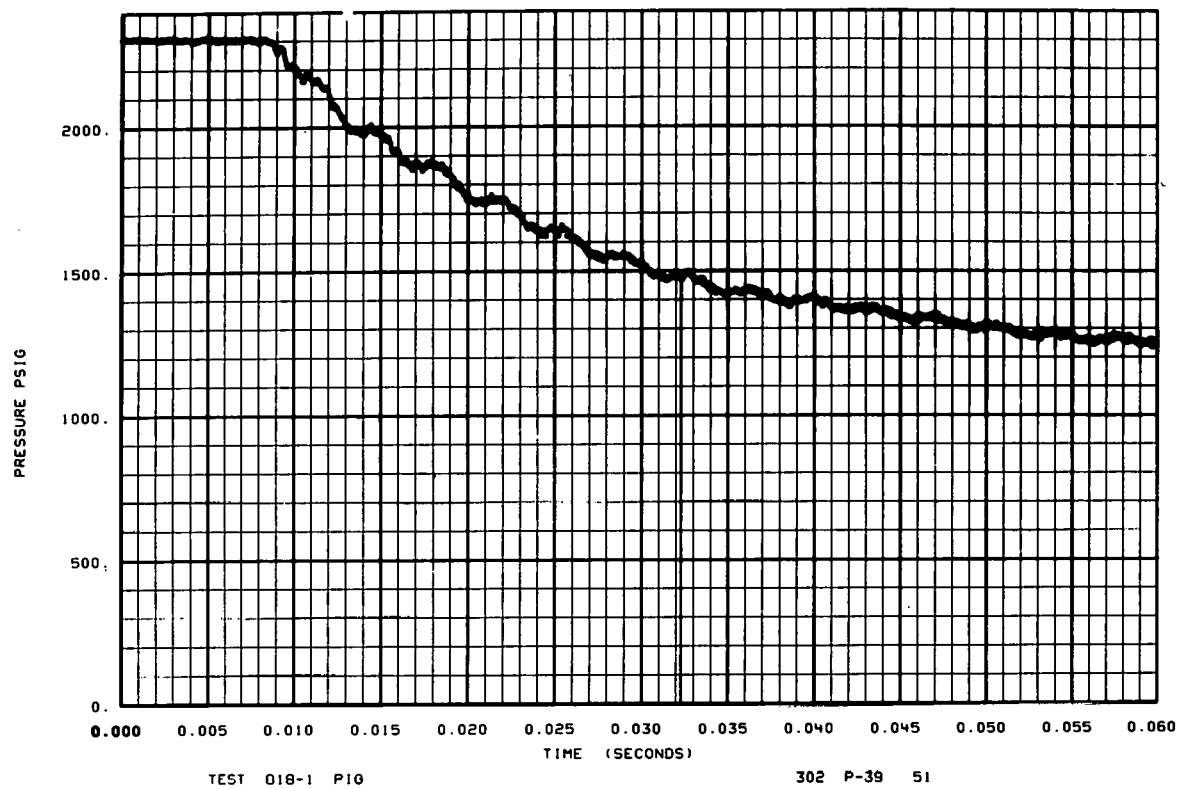




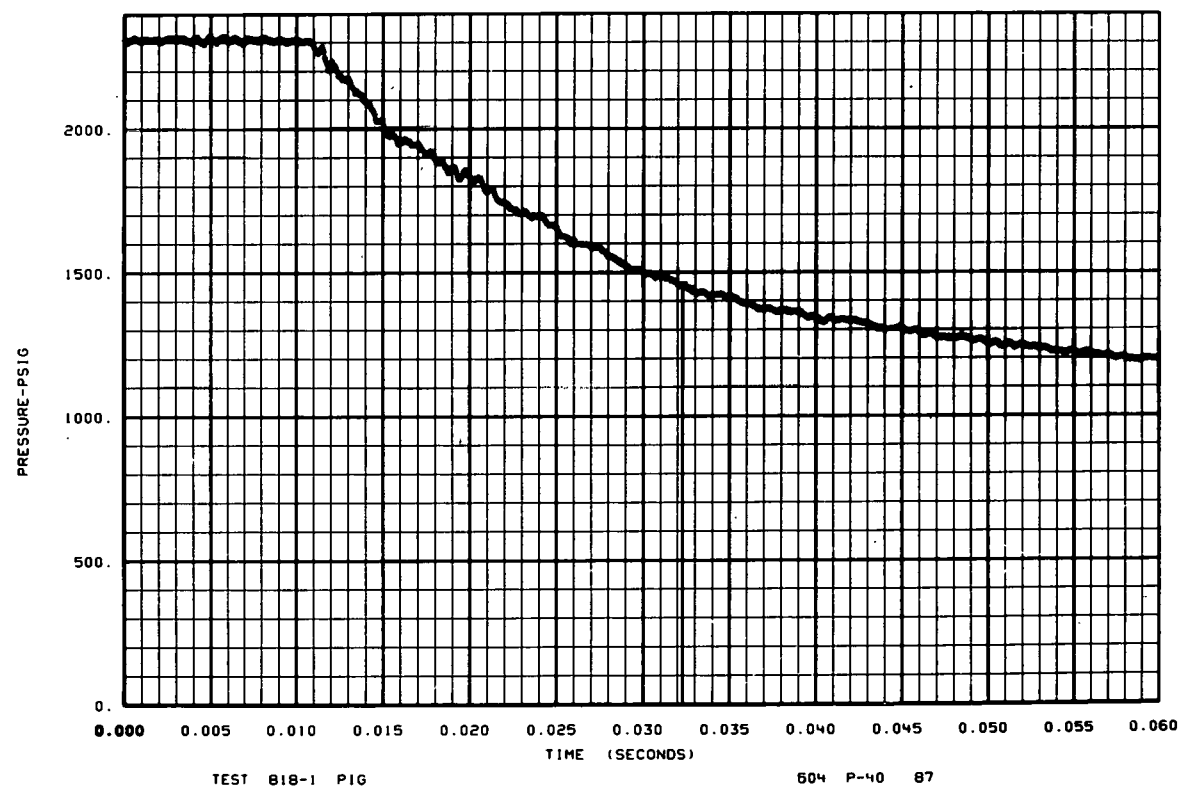


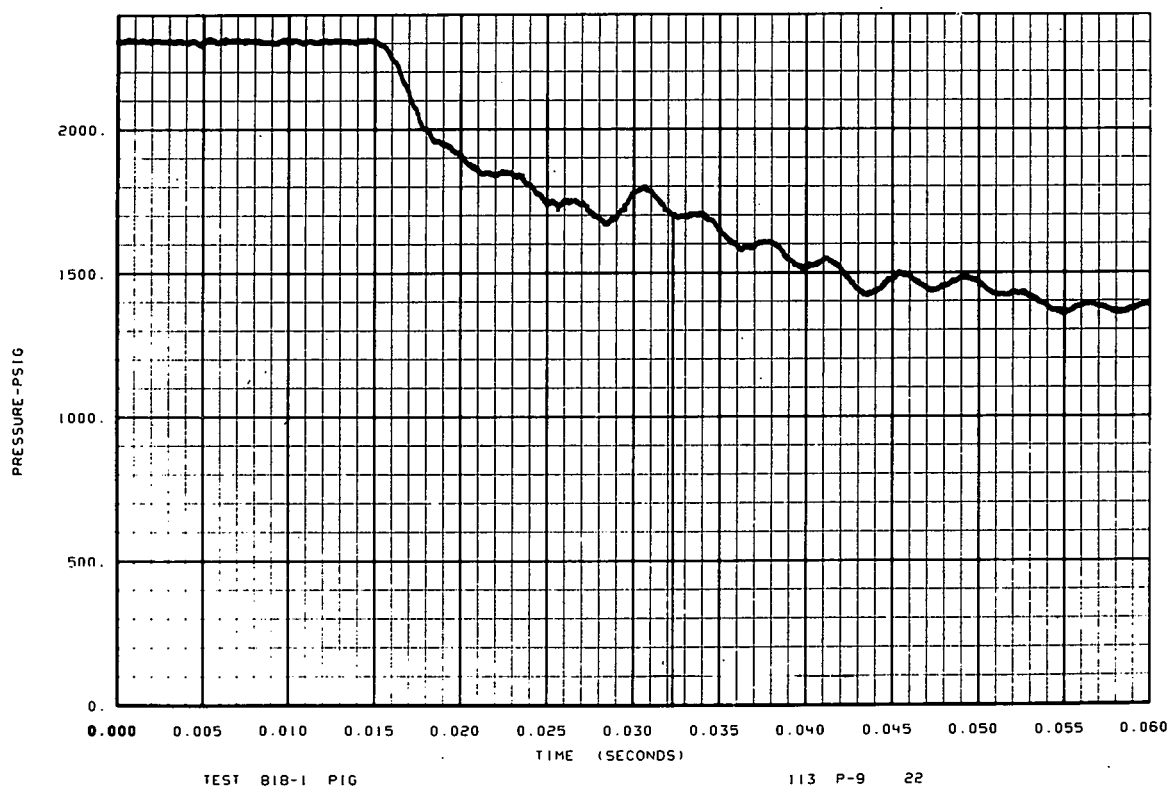
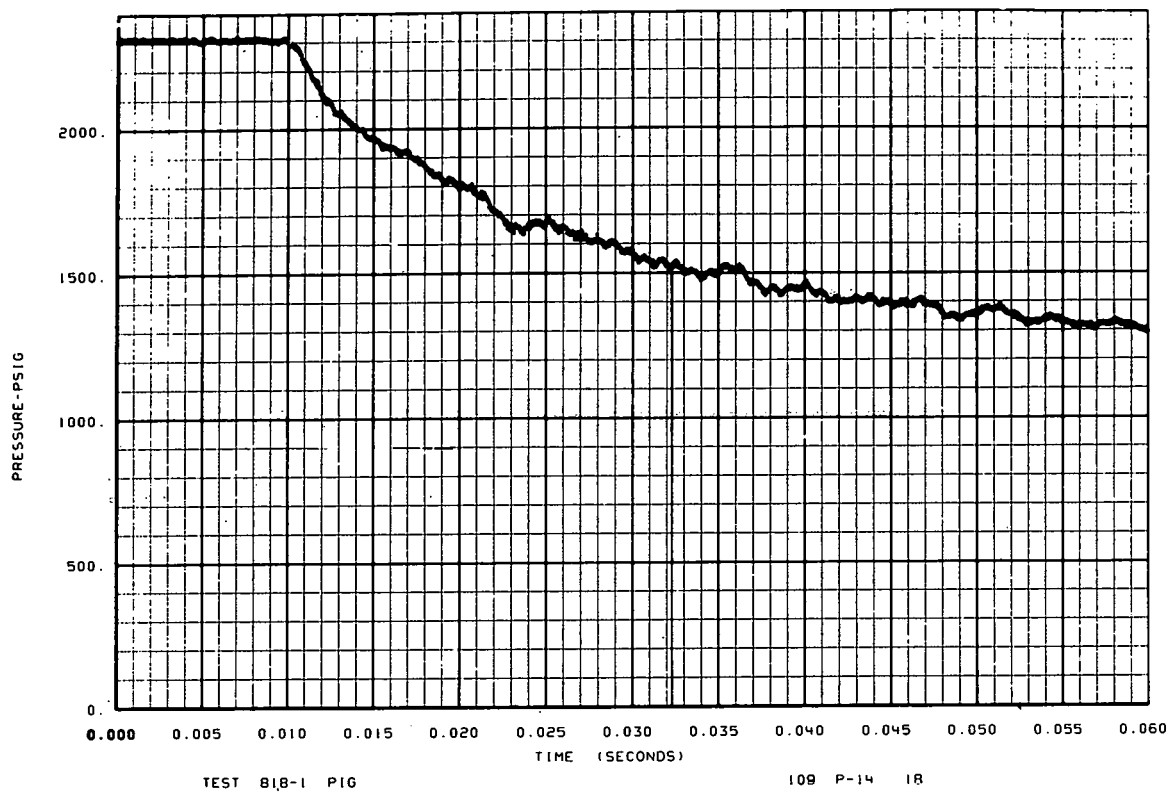


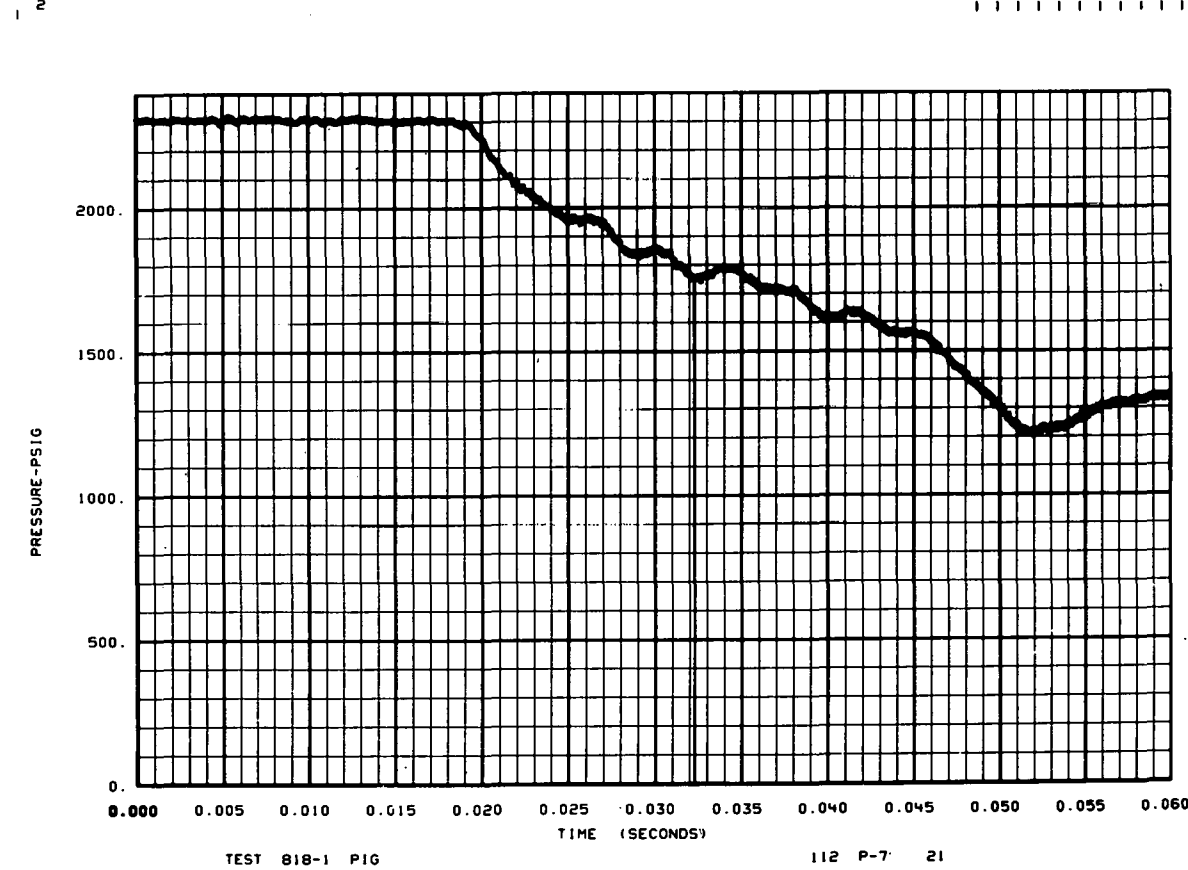
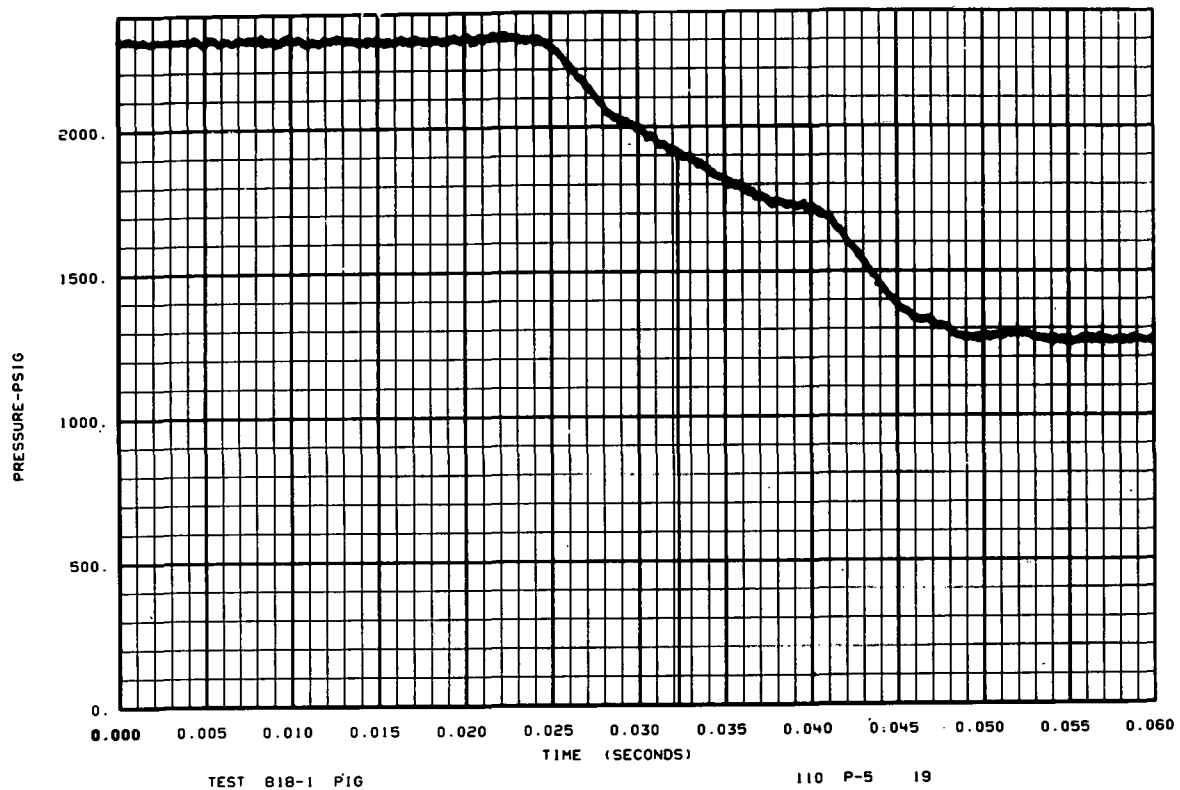


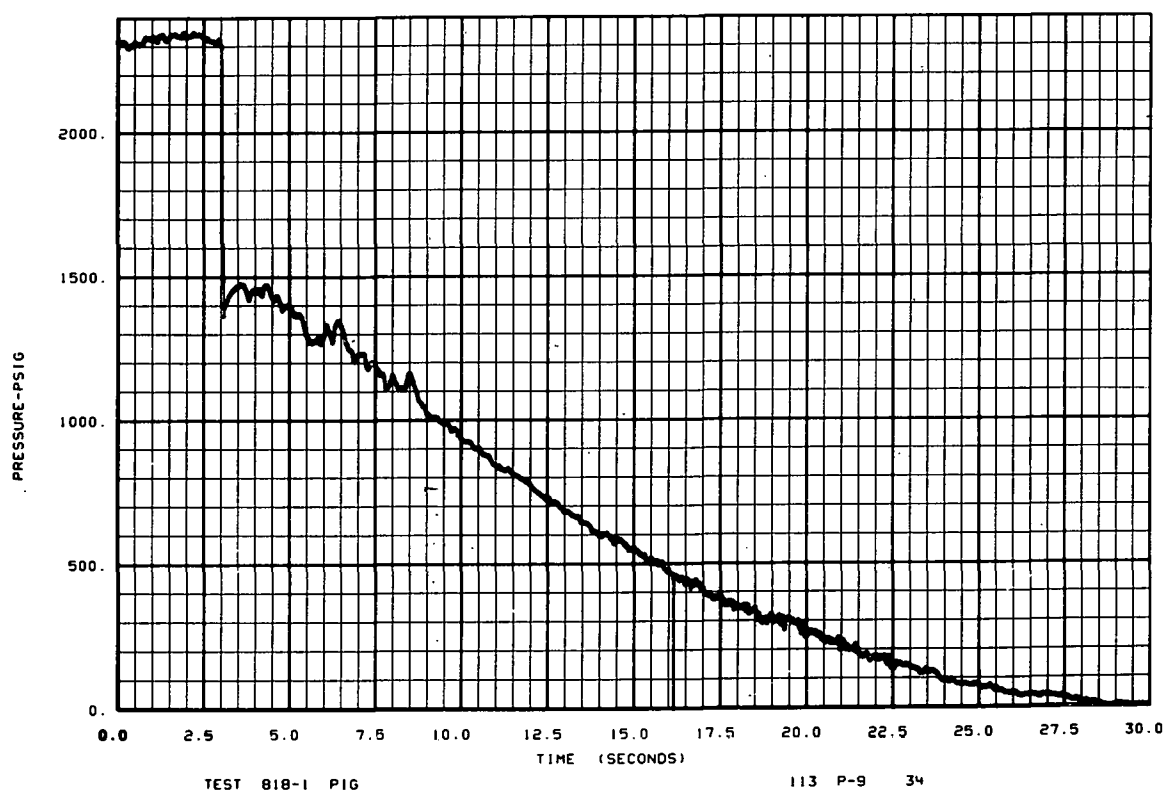
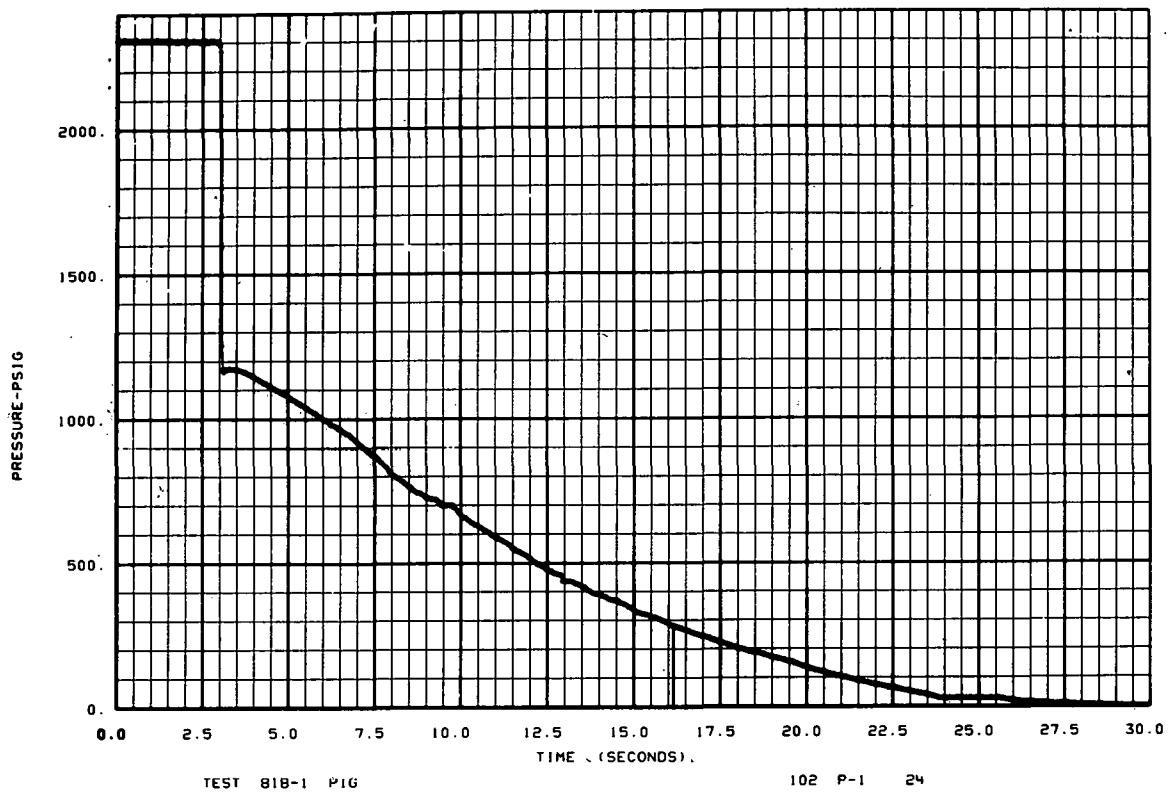


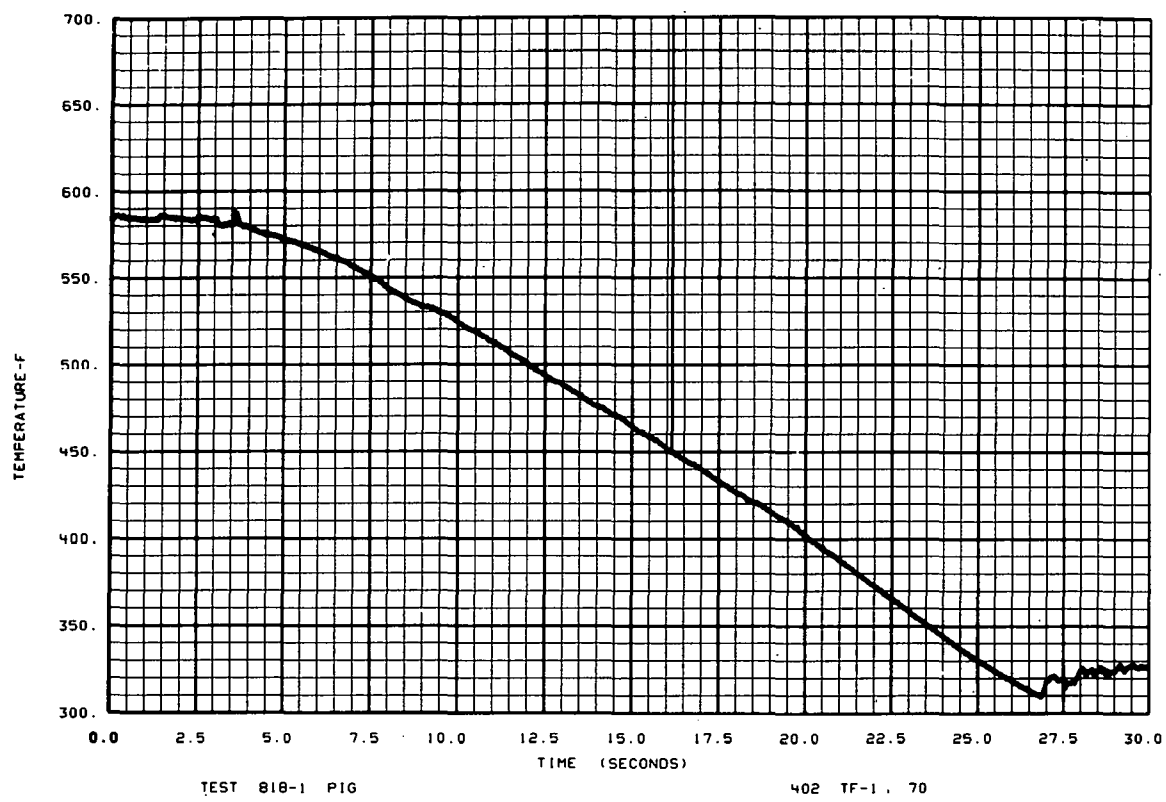
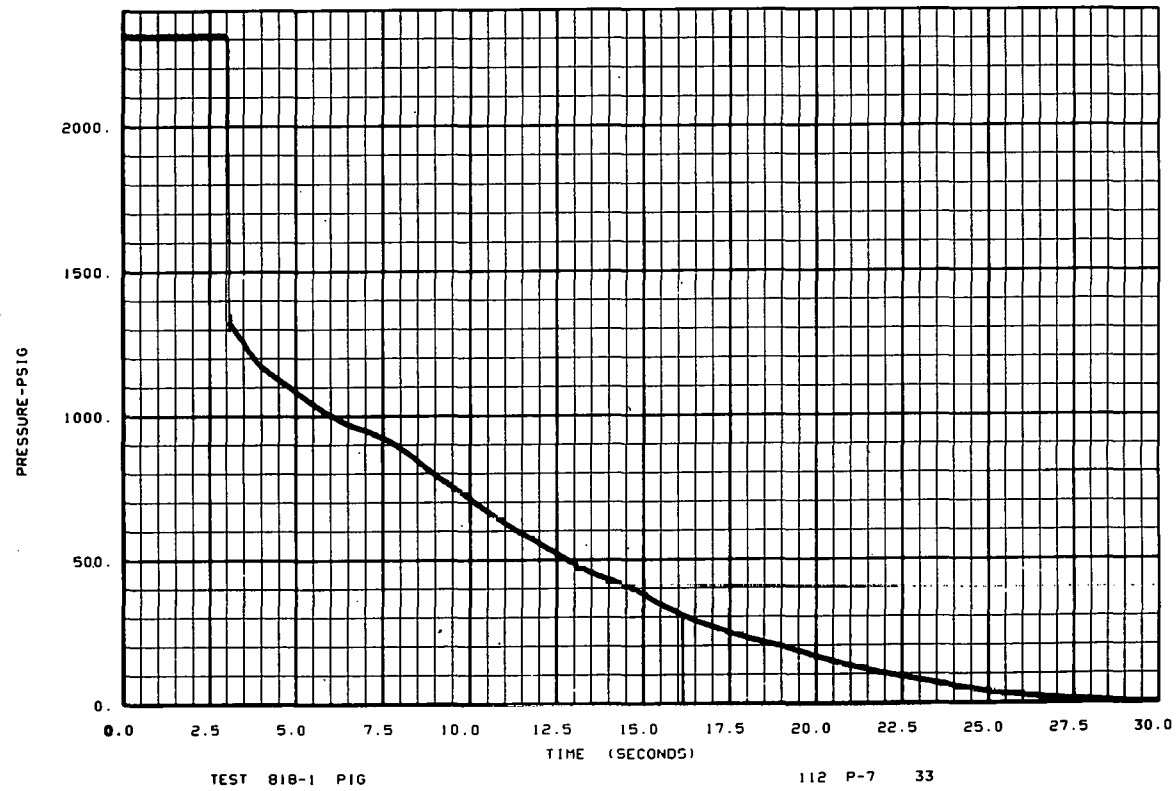
2

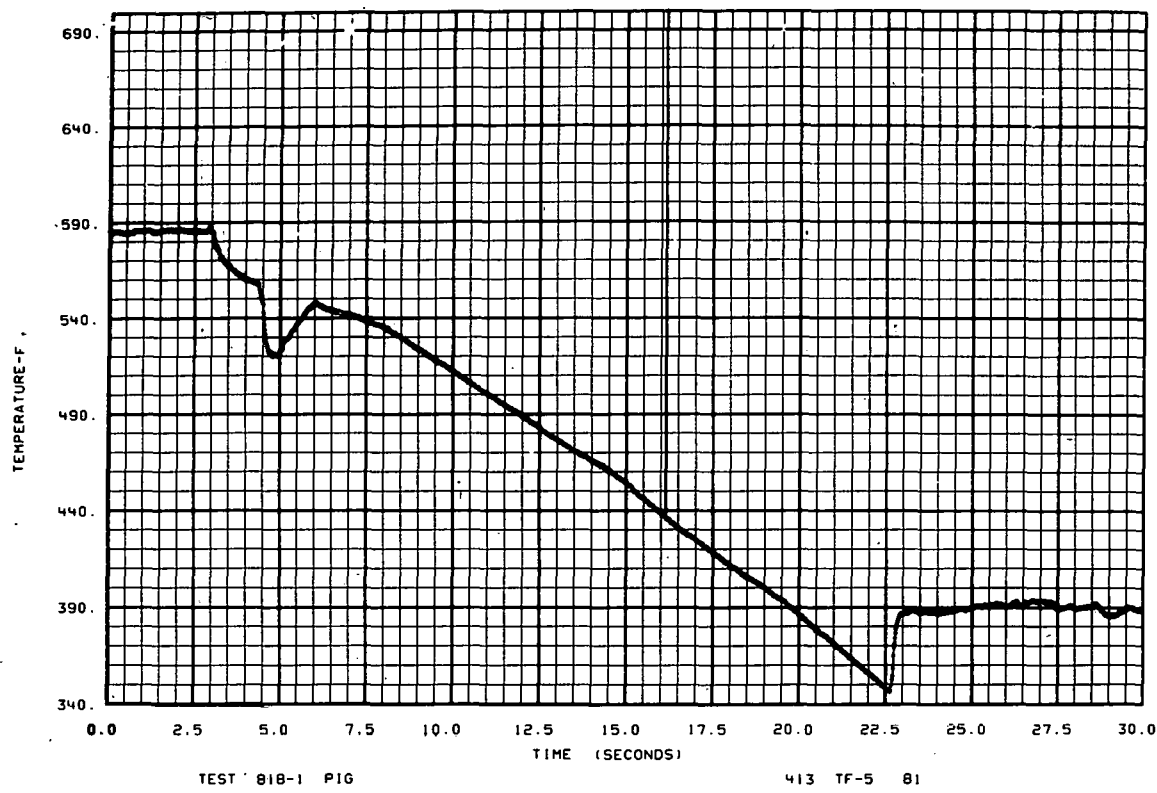


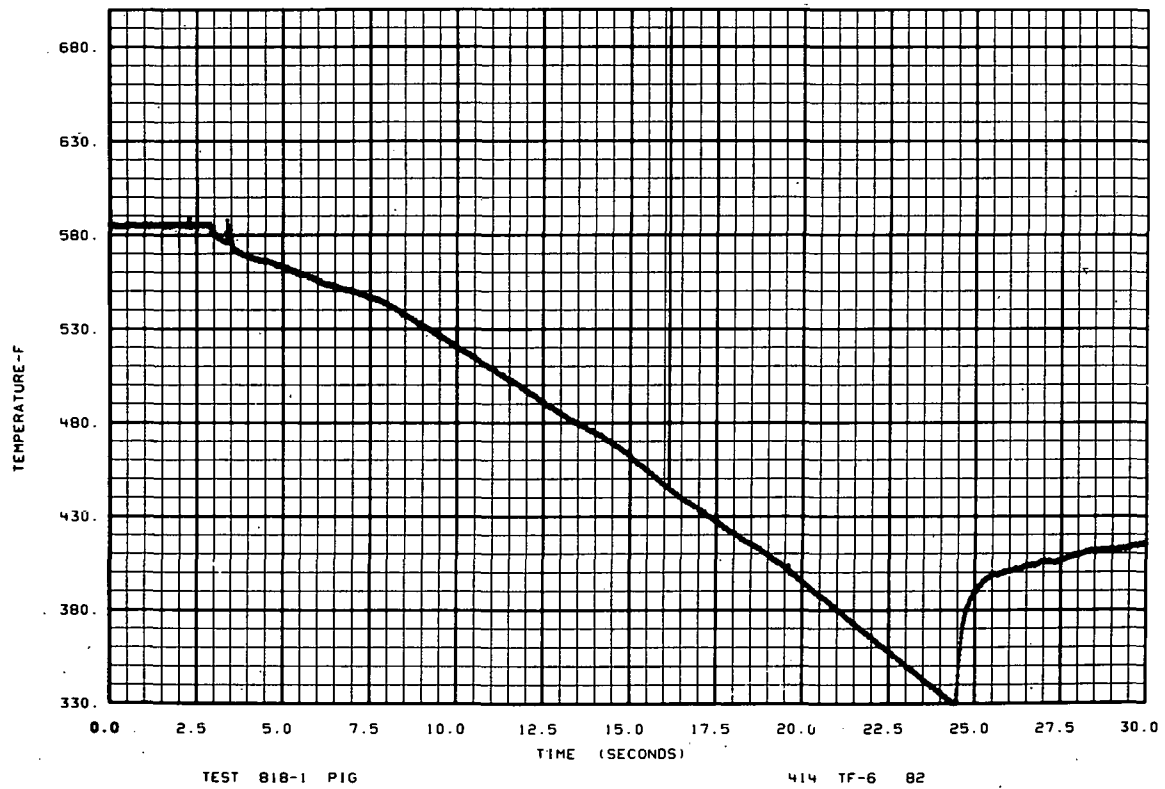




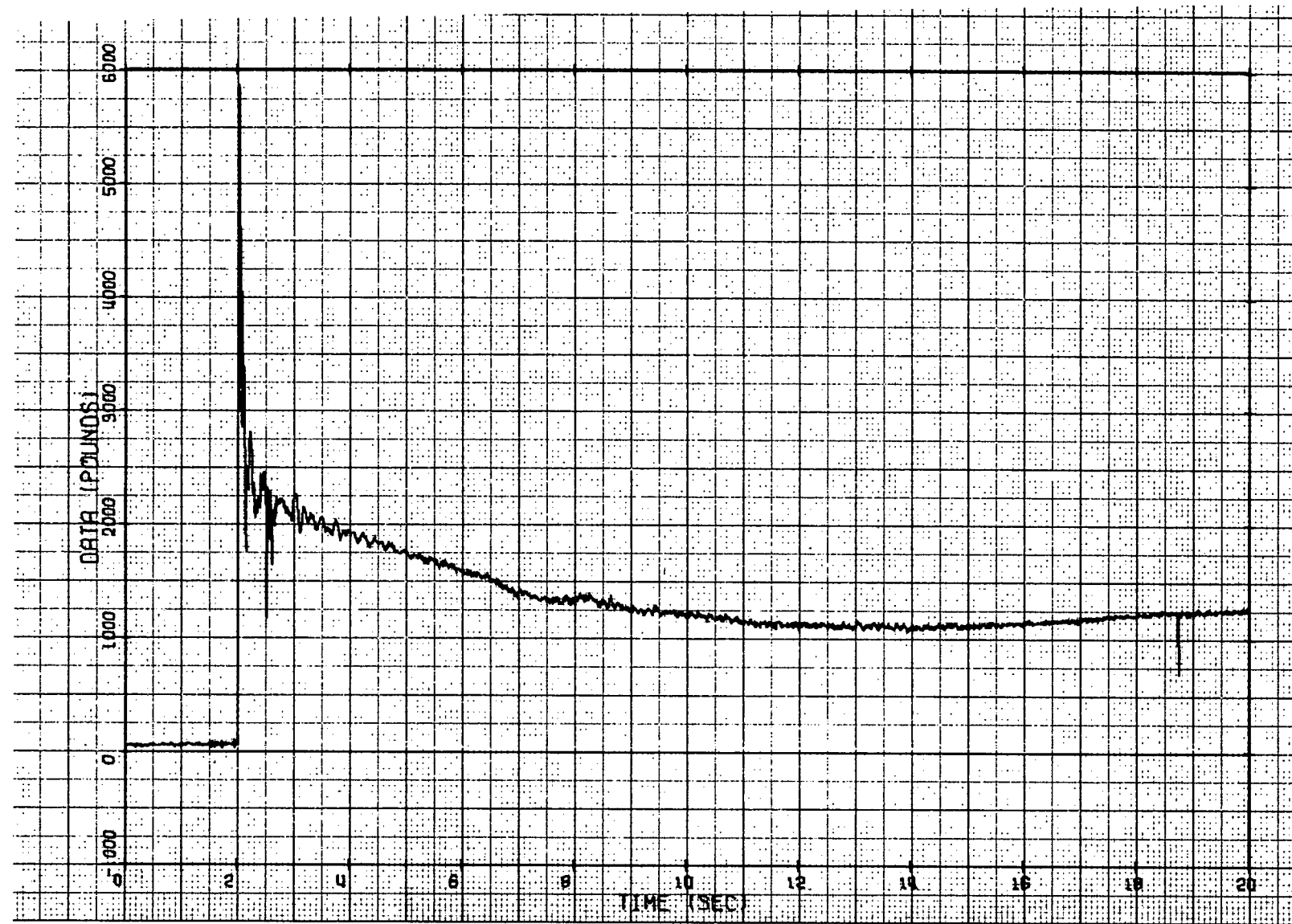








155



TEST 818-1 LC-3A

